Université de Strasbourg

Thèse

présentée à la

FACULTÉ DES SCIENCES DE LA VIE ET DE LA TERRE

pour obtenir le titre de

DOCTEUR DE L'UNIVERSITÉ de STRASBOURG

Domaine : Biologie Moléculaire Végétale

par

Michael Hartmann

Titre du sujet de thèse:

Inhibition and regulation of isoprenoid biosynthetic pathways in plants

Inhibition et régulation des voies de biosynthèse des isoprénoïdes chez les végétaux

Soutenue le **14 septembre 2010** devant la Comission d'Examen :

Thomas J. BACH Université de Strasbourg, Strasbourg	Directeur de thèse
Francis KARST Institut National de la Recherche Agronomique, Colmar	Rapporteur interne
Michael H. WALTER Leibniz-Institut für Pflanzenbiochemie, Halle/Saale (GER)	Rapporteur externe
Benoît ST-PIERRE Université François Rabelais, Tours	Rapporteur externe
Rüdiger HELL Heidelberg Institute for Plant Science, Heidelberg (GER)	Examinateur
Michel ROHMER Université de Strasbourg, Strasbourg	Examinateur

This doctoral thesis has been supported by a full grant of the „Région ALSACE" (Bourse Régionale de Recherche 2005: Convention de thèse **n° d'enregistrement 05/908/702** – HARTMANN Michael).

Table of contents:

Index of Tables and Images

Abbreviations

β-ME	β-mercaptoethanol (2-mercaptoethanol)
λ	wave length
aa	amino acid
AP	ammonium persulfate
A. thaliana	*Arabidopsis thaliana* (thale cress)
ATP	adenosine triphosphate
bp	base pair
BP	band pass
BSA	bovine serum albumin
BY-2	cultivar Bright Yellow - 2 of the tobacco plant
cDNA	complementary DNA
Ci	Curie
cpm	counts per minute
CTAB	cetyl trimethyl ammonium bromide
C-terminal	carboxy-terminus
Da	Dalton
DAPI	4',6-Diamidino-2-phenylindole
DNA	deoxyribonucleic acid
DNase	deoxyribonuclease
dNTP	deoxyribonucleotide triphosphate
DTT	dithiothreitol
EB	ethidium bromide
E. coli	*Escherichia coli*
EDTA	ethylene diamine tetraacetic acid
EGTA	ethylene glycol tetra acetic acid
EST	expressed sequence tag
g	grams
g	relative centrifugal force (RCF)
GFP	green fluorescent protein
HEPES	4-(2-hydroxyethyl)-1-piperazineethanesulfonic acid
His-tag	hexa histidine-tag
HM	High magnification
h	hour
IPTG	isopropyl-beta-D-thiogalactopyranoside
LB	Luria-Bertani

LM	Low magnification
LP	long pass
M	Molar
MCS	multiple cloning site
MES	2-(N-Morpholino)ethanesulfonic Acid
min	minute
mRFP	monomeric Red Fluorescent Protein
mRNA	messenger RNA
MS	Murashige and Skoog
nt	nucleotide
N-terminal	amino-terminus
OD	optical density
o/n	overnight
PAGE	polyacrylamide gel electrophoresis
PBS	Phosphate Buffered Saline
PCR	polymerase chain reaction
PEG	polyethylene glycol
pH	negative decadic logarithm of the proton concentration
pipes	piperazine-N,N'-bis(2-ethanesulfonic acid)
PMSF	phenylmethylsulphonylfluoride
RACE	rapid amplification of cDNA ends
RFP	red fluorescent protein
RNA	ribonucleic acid
RNase	ribonuclease
rpm	rotations per minute
RT	reverse transcription
SDS	sodium dodecyl sulphate
sec	second
TAE	Tris-acetate-EDTA buffer
TBE	Tris-borate-EDTA buffer
TBS	Tris buffered saline
TBY-2	cultivar Bright Yellow - 2 of the tobacco plant
TCA	Trichloroethanoic acid
TE	Tris-EDTA buffer
TEMED	N,N,N',N'-Tetramethylethylenediamine
Tris	(hydroxymethyl)methylamine
U	unit (enzyme activity)

UTRs	untranslated regions
UV	Ultra Violet
V	Volts
wt	wild type

One-letter code Three-letter code, Amino acid			
A Ala, Alanine	**E** Glu, Glutamic acid	**L** Leu, Leucine	**S** Ser, Serine
R Arg, Arginine	**Q** Gln, Glutamine	**K** Lys, Lysine	**T** Thr, Threonine
N Asn, Asparagine	**G** Gly, Glycine	**M** Met, Methionine	**W** Trp, Tryptophan
D Asp, Aspartic acid	**H** His, Histidine	**F** Phe, Phenylalanine	**Y** Tyr, Tyrosine
C Cys, Cysteine	**I** Ile, Isoleucine	**P** Pro, Proline	**V** Val, Valine

Table 1: Standard amino acid abbreviations

Step	Enzyme[a]	Proposed acronym	Other acronyms	*E. coli* gene	*Arabidopsis* gene	*Arabidopsis* mutants[b]	Unified name
1	1-Deoxy-D-xylulose 5-phosphate synthase (EC 2.2.1.7)	DXS		*dxs*	*DXS* (At4g15560)	*cla1* [12] Line 1055 [38] *chs5* [27] *lvr111* [28]	*dxs-1* *dxs-2* *dxs-3* *dxs-4*
2	1-Deoxy-D-xylylose 5-phosphate reductoisomerase (EC 1.1.1.267)	DXR		*ispC* (also known as *yaeM* or *dxr*)	*DXR* (At5g62790)	Line 4036 [38]	*dxr-1*
3	2-*C*-Methyl-D-erythritol 4-phosphate cytidylyltransferase (EC 2.7.7.60)	MCT	MECT, CMS	*ispD* (also known as *ygbP*)	*MCT* (At2g02500)	*ispD-1* [26] *ispD-2* [26] Line GT0946 [38]	*mct-1* *mct-2* *mct-3*
4	4-(Cytidine 5′-diphospho)-2-*C*-methyl-D-erythritol kinase (EC 2.7.1.148)	CMK	CMEK	*ispE* (also known as *ychB*)	*CMK* (At2g26930)	*ispE-1* [26]	*cmk-1*
5	2-*C*-Methyl-D-erythritol 2,4-cyclodiphosphate synthase (EC 4.6.1.12)	MDS	MECPS, MECS, MCS	*ispF* (also known as *ygbB*)	*MDS* (At1g63970)	*ispF-1* [39]	*mds-1*
6	4-Hydroxy-3-methylbut-2-enyl diphosphate synthase (EC 1.17.4.3)	HDS		*ispG* (also known as *gcpE*)	*HDS* (At5g60600)	*clb4-1* [17] *clb4-2* [17] *csb3* [18]	*hds-1* *hds-2* *hds-3*
7	4-Hydroxy-3-methylbut-2-enyl diphosphate reductase (EC 1.17.1.2)	HDR	IDS	*ispH* (also known as *lytB*)	*HDR* (At4g34350)	*ispH-1* [15] *clb6* [30]	*hdr-1* *hdr-2*

[a]Named according to the Nomenclature Committee of the International Union of Biochemistry and Molecular Biology (IUBMB).
[b]Original literature reference in brackets.

Table 2. The biochemical steps of the MEP pathway and the standardized names for *Arabidopsis* genes and mutant lines proposed herein (taken from Phillips et al., 2008)

1 Introduction

1.1 Isoprenoids

1.1.1 Isoprenoids – a diverse class of metabolites

Isoprenoids, also referred to as "terpenoids", represent the largest class of natural metabolites and are ubiquitiously found in all living organisms. These lipidic compounds are particularly abundant in plants, where they have been extensively studied in the past. New isoprenoids are dicovered every year, and as a result, the number of individual compounds described in the literature has doubled every decade since the 1970s with over 45000 isoprenoids identified to date (Devon and Scott, 1972; Glasby, 1982; Connolly and Hill, 1991; Buckingham, 2004). There are countless research papers, reviews and books focusing on various aspects of isoprenoid biosynthesis, function and regulation in microorganisms and plants (for reviews see: (Croteau, 1987; McGarvey and Croteau, 1995; Lichtenthaler et al., 1997a; Sacchettini and Poulter, 1997; Rohmer, 1999; Kuzuyama, 2002; Rodríguez-Concepción and Boronat, 2002; Rohmer, 2003; Bouvier et al., 2005; Chemler et al., 2006; Rodríguez-Concepción, 2006; Ai-Xia et al., 2007; Bohlmann and Keeling, 2008; Ganjewala et al., 2009).

Isoprenoids show the highest diversity in structure and function of all plant metabolites and are implicated in nearly all fundamental processes of plant growth, development, primary and secondary metabolism (Croteau et al., 2000; Chappell, 2002). They are essential components of the plant light harvesting complexes (phytol-containing chlorophylls, carotenoids), structural components of membranes (phytosterols), act as electron carriers in cell respiration (ubiquinones) and photosynthesis (plastoquinone, phylloquinone), are involved in subcellular targeting (prenylated proteins) and in the regulation of growth and development (phytohormones: cytokinins, brassinosteroids, gibberelins, abscisic acid) (Bouvier et al., 2005) (Figure 1).

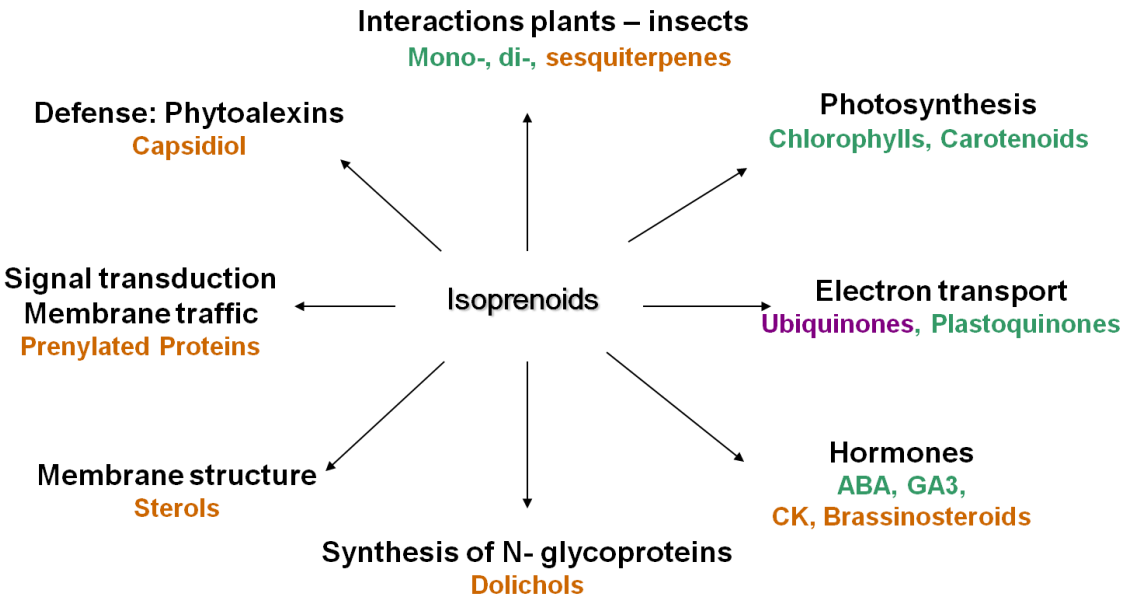

Figure 1. Isoprenoids have various functions in plants.
Examples are highlighted in different colors depending on the compartment where they are synthesized. Color code represents the biosynthetic origin of the isoprenoids: **Orange:** cytosol/endoplasmic reticulum; **green:** plastid; **purple:** mitochondria (for further explanation see text and refer to Figure 6. Simplified scheme of plant terpenoid biosynthesis and compartimentation).

In addition, plants synthesize a large array of unique and often species-specific secondary metabolites with numerous ecological functions, e.g. in plant defense and communication (Ai-Xia et al., 2007). Some isoprenoids can act as attractants for pollinators and seed-dispersers (Pichersky and Gershenzon, 2002; Shuttleworth and Johnson, 2009). Other isoprenoids are emitted as volatiles after damage to a tissue and can be recognized by natural enemies of the attacking herbivore (Ozawa et al., 2000) or by undamaged, neighboring plants, which then induce direct and indirect defense responses (allelochemical compounds) (Paschold et al., 2006; Gershenzon and Dudareva, 2007). Furthermore, many plants synthesize isoprenoids as part of their constitutive or induced defense. For example, phytoalexins, such as gossypol (cotton) or capsidiol (tobacco) are synthesized in reponse to a fungal or pathogen attack (Harborne, 1990; Croteau et al., 2000; Ai-Xia et al., 2007).

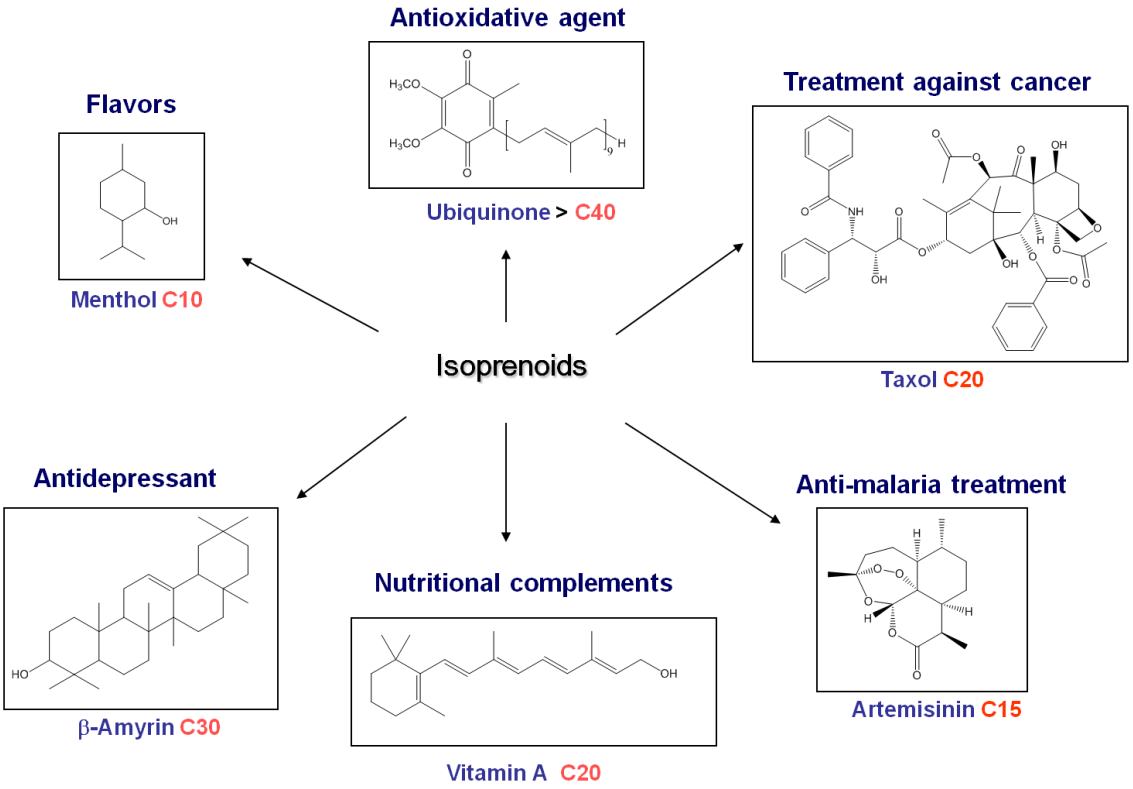

Figure 2. Examples of isoprenoids/terpenoids that are industrially used and have found applications as pharmaceuticals or food complements.

In recent years, plant terpene metabolism has become economically very attractive, as many isoprenoids have nutritional and medical value and are used as pharmaceuticals (anti-cancer agent: Taxol; anti-malarial compund: Artemisinin), flavors (the monoterpenoid menthol), pigments, fragrances, vitamins (A,D,E and K) polymers (rubber) or as complements for potential hydrocarbon biofuels (Bohlmann and Keeling, 2008; Schwab et al., 2008). The availibility of these compounds from their natural source is often very limited and there are many approaches to develop knowledge and tools to genetically engineer the pathways for isoprenoid biosynthesis in microorganisms and plants (Degenhardt et al., 2003; Maury et al., 2005; Kirby and Keasling, 2009). Especially the pharmaceutical industry is increasingly interested in identifying lead compounds in so-called "medicinal plants" , particularly focusing on potential, alternative antiviral and antimicrobial agents (Rodrigues Goulart et al., 2004; Astani et al., 2009).

1.1.2 Biosynthesis of isoprenoids in plants

Despite the immense structural variety of terpenoids, all known (plant) terpenoids are assembeld from only two isomeric, five-carbon (C5) precursors, dimethylallyl diphosphate (DMADP or DMAPP) and isopentyl-diphosphate (IDP or IPP) (Cane, 1999; Dewick, 2002; Kuzuyama, 2002; Bouvier et al., 2005), also referred to as "isoprene units"(Wallach, 1914; Ruzicka, 1953).

For almost four decades, it was assumed that the MVA (Mevalonate) pathway, described in the 1950s in animals and yeast by Konrad Bloch (1959) and Feodor Lynen (1958), was the exclusive pathway for the biosynthesis of IPP and DMAPP in all organisms (Chappell, 1995; McGarvey and Croteau, 1995). However, several results obtained over the past few decades by feeding experiments with labelled precursors in different organisms, were inconsistent with the general biosynthetic scheme of the MVA pathway (Cane et al., 1981; Flesch and Rohmer, 1988; Zhou and White, 1991; Rohmer et al., 1993; Broers, 1994; Schwarz, 1994) and provided the first evidence for the existence of a mevalonate-independent pathway (reviewed in: (Lichtenthaler et al., 1997a; Lichtenthaler, 1999; Rodríguez-Concepción and Boronat, 2002; Rohmer, 2003), that operates in eubacteria (Rohmer et al., 1993; Broers, 1994; Rohmer et al., 1996), algae (Schwender et al., 1996; Disch et al., 1998b) and higher plants (Schwarz, 1994; Arigoni et al., 1997; Lichtenthaler et al., 1997b; Schwender et al., 1997; Lichtenthaler, 1999). Today this long overlooked alternative pathway for the formation of IPP and DMAPP is also known as the 1-deoxy-D-xylulose-5-phosphate (DXP: the first intermediate of the pathway) or 2*C*-methyl-D-erithrytol-4-phosphate pathway (MEP: "considered as the first committed precursor of plastid isoprenoids") (Rohmer, 2003; Eisenreich et al., 2004; Rodríguez-Concepción, 2006).

1.1.3 Plants have evolved two different pathways for the synthesis of isoprenoids

In higher plants, the synthesis of IPP and DMAPP is accomplished through two different routes, the cytosolic mevalonate pathway (MVA) and the plastidial (MEP) pathway.

The MVA pathway supplies the biosynthetic precursors for isoprenoids in the majority of eucaryotes (all mammals), the archea, some eubacteria, fungi and the cytosol/mitochondria of some algae and higher plants. It can be found in several important human parasites, such as *Trypanosoma* and *Leishmania* (Goldstein and Brown, 1990). In humans, the MVA pathway operates alone and produces a variety of critical end-products, including cholesterol, steroid hormones, dolichols and the prenyl moiety of cancer-associated cell signaling proteins like RAS (Edwards and Ericsson, 1999; Veillard and Mach, 2002; Buhaescu and Izzedine, 2007). In plants, the cytosolic IPP provided by the MVA pathway serves as precursor for the synthesis of sterols, brassinosteroids, polyprenols, dolichols and most sesquiterpenes and to some extent as a substrate for protein prenylation. Moreover, cytosolic IPP

is imported into the mitochondria, where it serves as precursor for ubiquinone (Disch et al., 1998a; Chappell, 2002; Ai-Xia et al., 2007).

The alternative pathway (or MEP-pathway) for the synthesis of isoprenoids occurs in eubacteria, cyanobacteria, certain fungi and the plastids of phototrophic algae and plants (Rodríguez-Concepción and Boronat, 2002; Eisenreich et al., 2004). In plants, the precursors, provided by plastidial MEP pathway are used for the biosynthesis of essential isoprenoids of the photosynthetic apparatus such as carotenoids, the phytol-sidechain of chlorophyll, plastoquinone, as well as for isoprene, tocopherols, phylloquinones and the phytohormones ABA and gibberellin (Figure 3). In addition to these ubiquitous coumpounds in plants, the MEP pathway is the route for the biosynthesis of the vast majority of plant terpenoids, including countless secondary metabolites with defensive, allelopathic or signalling properties (Croteau et al., 2000; Rodríguez-Concepción and Boronat, 2002; Ai-Xia et al., 2007).

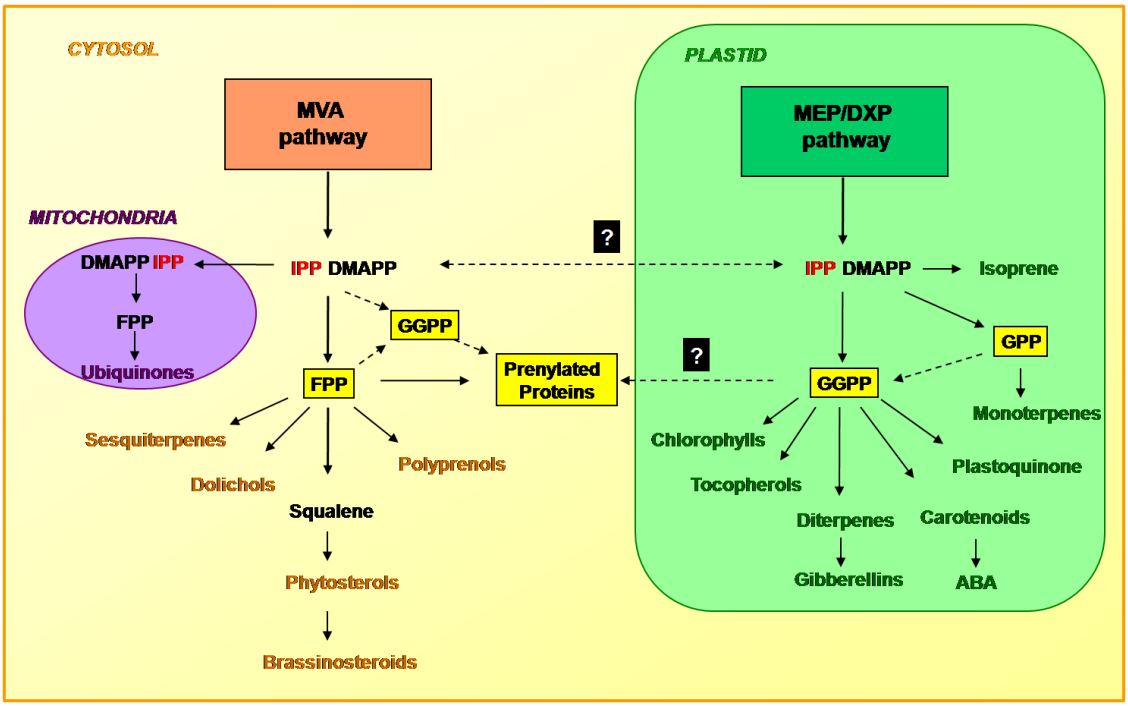

Figure 3: Compartmentation of isoprenoid biosythesis in plant cells.

In plants, the universal isoprenoid precursors IPP and DMAPP can be produced by two pathways operating in different subcellular compartments, the cytosolic MVA pathway and the plastidial MEP pathway. IPP and DMAPP are used for the biosynthesis of bigger prenyl diphosphates, like GPP, FPP and GGPP that serve as building blocks for the different classes of isoprenoids produced by plants. As a general rule, monoterpenoids, diterpenoids and tetraterpenoids derive from isoprenyldiphosphates (IPP and DMAPP) synthesized by the MEP pathway, whereas sesquiterpenes, dolichols, polyprenols and phytosterols are thought to originate from IPP and DMAPP of the MVA pathway. However, there are notable exceptions to this rule and it has been shown that some sesquiterpenes are derived from IPP and DMAPP of plastidial origin (Adam et al., 1999; Dudareva et al., 2005). In addition, a novel pathway for the biosynthesis of sesquiterpenes from a putatively plastidial Z,Z-farnesyl-pyrophosphate has recently reported in the wild tomato, *Solanum habrochaites* (Sallaud et al., 2009). The presence of GGPP in the cytosol as a substrate for the prenylation of proteins has been considered by Bouvier *et al.* (2005). Abbreviations: ABA, abscisic acid; IPP, isopentenyl diphosphate; DMAPP, dimethylallyl diphosphate; FPP, farnesyl diphosphate; GPP, geranyl diphosphate; GGPP, geranylgeranyl diphosphate.

IPP and DMAPP are synthesized by both pathways. The cytosolic mevalonate pathway takes six enzymatic steps to synthesize IPP starting from acetyl-CoA. An IPP isomerase then converts IPP to its more reactive allylic ester DMAPP, thereby maintaining a balance between both isomers.
The plastidial MEP pathway on the other hand consists of seven enzymatic reactions that transform glyceraldehyde-3-phosphate and pyruvic acid directly to IPP and DMAPP with a ratio of about 5:1 (Rohdich et al., 2002). Both molecules can additionally be interconverted by an IPP isomerase.

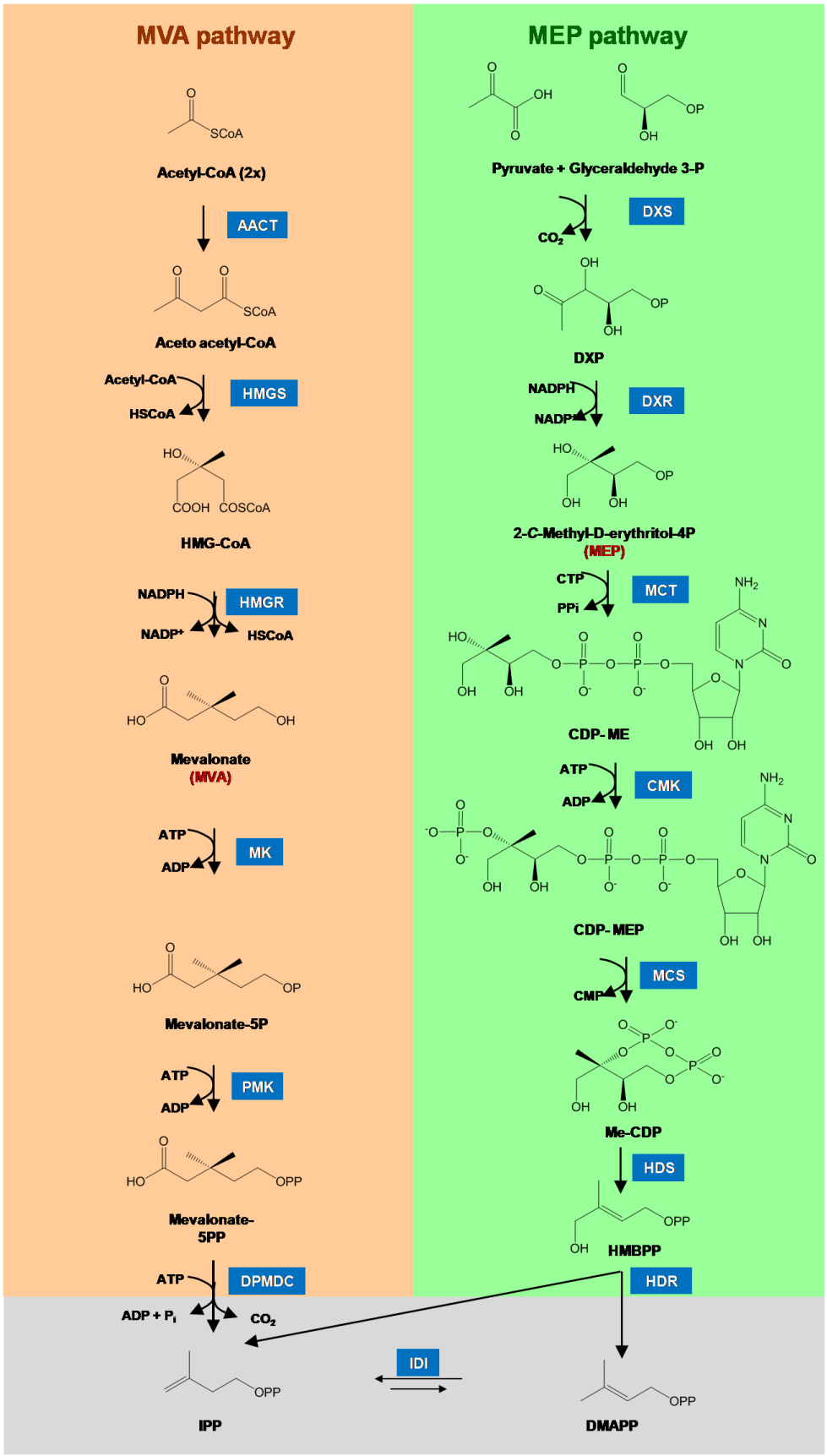

Figure 4: Enzymatic steps of the cytosolic MVA and plastidial MEP pathways for the biosynthesis of IPP and DMAPP in plants (modified from Bouvier et al., 2005).

MVA (mevalonate) pathway: ***Enzyme abbreviations*****:** AACT, Actetoacetyl-CoA thiolase; DPMDC, 5-diphosphomevalonate decarboxylase; HMGR, 3-hydroxy-3-methylglutaryl-CoA reductase; HMGS, 3-hydroxy-3-methylglutaryl-CoA synthase; MK, mevalonate kinase; PMK, 5-phosphomevalonate kinase. ***Substrate abbreviations:*** ADP, adenosine-diphosphate; ATP, adenosine-triphosphate; DMAPP, dimethylallyl diphosphate; IPP isopentenyl diphosphate NADP+, nicotinamide adenine dinucleotide phosphate; NADPH, nicotinamide adenine dinucleotide phosphate (reduced form). **DXP (1-deoxy-D-xylulose-5-phopshate) pathway:** ***Enzyme abbreviations:*** DXS, 1-deoxy-D-xylulose-5-phosphate synthase; DXR, 1-deoxy-D-xylulose-5-phosphate reductoisomerase; MCT, 2-C-methyl-D-erythritol-4-phosphate cytidyltransferase; CMK, 4-(cytidine 50-diphospho)-2-C-methyl-D-erythritol kinase; MCS, 2-C-methyl-D-erythritol-2,4-cyclodiphosphate synthase; HDS, 1-hydroxy-2-methyl-2-(E)-butenyl-4-diphosphate synthase; HDR, 1-hydroxy-2-methyl-2-(E)-butenyl-4-diphosphate reductase. ***Substrate abbreviations*****:** CDP-ME, 4-(cytidine 5-diphospho)-2-C-methyl-D-erythritol; CDP-MEP, 2-phospho-4-(cytidine 5-diphospho)-2-C-methyl-D-erythritol; CTP, cytidine 5-triphosphate; DXP, 1-deoxy-D-xylulose-5-phosphate; HMBPP, 1-hydroxy-2-methyl-2-(E)-butenyl 4-phosphate; MECPP, 2-C-methyl-D-erythritol-2,4-cyclodiphosphate. *Additional downstream enzymes*: IDI, IPP-DMAPP isomerase.

a) The cytosolic MVA pathway

The MVA pathway starts with the successive condensation of three molecules of acetyl-CoA, leading to the formation of HMG-CoA. These reactions are catalyzed by acetoacetyl thiolase (AACT) and HMG-CoA synthase (HMGS), respectively. HMG-CoA then is reduced to mevalonate by HMG-CoA reductase (HMGR). Next, the mevalonate is phosphorylated in two sequential steps to diphosphomevalonate (catalyzed by mevalonate kinase and phosphomevalonate kinase, respectively), which is then decarboxylated to form the universal precursor isopentenyl diphosphate (IPP) (Figure 4). IPP can be isomerized to DMAPP (and to some extent *vice versa*) by isopentenyl diphosphate isomerase (IDI), an enzyme apparently ubiquitous in all living organisms (Gershenzon and Kreis, 1999).

The conversion of HMG-CoA to mevalonate is considered as the rate-limiting step of the MVA pathway for several reasons. First of all, the expression of HMGR is known to be well-regulated on the transcriptional and post-transcriptional level in plants (Enjuto et al., 1994; Bach, 1995; Enjuto et al., 1995; Re et al., 1995; Learned and Connolly, 1997; Leivar et al., 2005). Second, upregulation of its activity in plants (e.g. by overexpression), led to increased levels of (phyto-)sterols, which constitute the largest group of MVA-derived isoprenoids, further confirming the rate-limiting role of HMGR in the flux regulation of the MVA pathway (Bach, 1986; Chappell, 1995; Schaller et al., 1995; Harker et al., 2003; Enfissi et al., 2005; Hey et al., 2006). In *Arabidopsis thaliana*, HMGR is encoded by two genes, *HMG1* and *HMG2*. Double knock-out of these genes led to male gametophytic lethality and demonstrated the essentiality of the MVA pathway in plants (Suzuki et al., 2009).

In animals, the MVA pathway is mainly used to synthesize the precursors for the biosynthesis of cholesterol and the prenylation of Ras proteins. As HMGR can be specifically inhibited by statins and derivatives, these have valuable medical applications as anti-cancer drugs or cholesterol-lowering agents for the prevention of cardio-vascular diseases (Liao and Laufs, 2005; Sebti, 2005).

Since its discovery over half a century ago, the MVA pathway has been well studied by molecular genetics and biochemical approaches and all of its genes have been identified and characterized in different species.

b) The plastidial MEP pathway

The alternative pathway (or MEP-pathway) for the synthesis of isoprenoids occurs in eubacteria, cyanobacteria, algae and plant chloroplasts. The discovery of the early steps of MEP pathway by Rohmer and colleagues was a "side-product" of the studies focusing on the biosynthesis of hopanoids (bacterial triterpenoids/ sterol suurogate) in bacteria, using radioactively labelled precursors (Flesch and Rohmer 1988; Rohmer, 1993; Rohmer et al., 1993). In 1994, first indices for the existence of the MEP pathway in plants came from labeling experiments with ^{13}C-Glucose performed on Gingko embryos, resulting in gingkolides with a diterpenoid labeling pattern in accordance with the biosynthesis of bacterial isoprenoids discovered independently shortly before (Schwarz, 1994; Schwarz and Arigoni, 1999). In 1996, the first reaction steps of the alternative pathway were described by Rohmer et *al.* in *E.coli*, followed by the rapid identification of the first gene of the pathway in *E.coli* (Sprenger et al., 1997; Lois et al., 1998) and in peppermint (Lange et al., 1998). Further studies confirmed the presence of the MEP pathway in cyanobacteria, algae and plants (Eisenreich et al., 2001; Rodríguez-Concepción and Boronat, 2002; Rohmer, 2003; Eisenreich et al., 2004; Bouvier et al., 2005), as well as in some apicomplexean parasites like the malaria parasite *Plasmodium falciparum* (Jomaa et al., 1999).

In the last decade, all enzymes of the MEP-pathway and the genes coding for have been identified in *E.coli* and several eucaryotic organisms, including the universal model plant, *Arabidopsis thaliana* (Rodríguez-Concepción, 2006; Hunter, 2007). Interestingly, despite the existence of a plastidial genome, all enzymes of the MEP pathway characterized to date, are encoded by nuclear genes and have to be imported into the plastid after their expression, which is mediated by N-terminal transit peptides of varying length (Araki et al., 2000; Lois et al., 2000; Rodríguez-Concepción et al., 2001; Carretero-Paulet et al., 2002; Querol et al., 2002).

The first step of the MEP pathway is the formation of 1-deoxy-D-xylulose 5-phosphate (DXP or DOXP) after condensation of pyruvate and D-glyceraldehyde 3-phosphate. This step is catalyzed by deoxyxylulose 5-phosphate synthase (DXS) (Sprenger et al., 1997; Lois et al., 1998), an enzyme that has been extensively studied in recent years, including its partial crystallization (Xiang et al., 2007). DXS needs thiamine pyrophosphate (TPP) and divalent cations (Mn^{2+} or Mg^{2+}) as cofactors (Sprenger et al., 1997; Lange et al., 1998; Lois et al., 1998). Interestingly, DXP is also a precursor for the biosynthesis of thiamine (vitamin B_1) and pyridoxal (vitamin B_6) in *E.coli* (Himmeldirk et al., 1996). DXP also serves as precursor for thiamine in the chloroplasts of higher plants (Julliard and Douce,

1991). However, only recently, evidence has been found for a DXS-independent pathway for the synthesis of pyridoxal in plants and several bacteria (Tambasco-Studart et al., 2005; Fitzpatrick et al., 2007). DXP can be formed from its free alcohol, 1-deoxy-D-xylulose (DX). An *Arabidopsis thaliana* mutant, bearing a defective *DXS* gene (*cla1*) (Mandel et al., 1996) shows an albino phenotype with impaired chlorophyll and carotenoid accumulation, that can be restored after external feeding with DX (Estévez et al., 2000). In bacteria, DX can be synthesized from pyruvate and D-glyceraldehyde by a subunit of pyruvate dehydrogenase (Yokota and Sasajima, 1984, , 1986), an enzyme that can also be found in the plastids and mitochondria of plants (Tovar-Méndez et al., 2003). A cytosolic kinase able to catalyze the phosphorylation of DX to DXP in *Arabidopsis thaliana* has recently been described by Hemmerlin *et al.* (2006).

The second step of the MEP pathway involves an intramolecular rearrangement of DXP, leading to a methylerythrose intermediate that is then reduced to yield 2-*C*-methyl-D-erythritol-4-phosphate (MEP), the first pathway product that shows the characteristic, isoprenoid C5 skeleton structure. As DXP also serves as intermediate for the biosynthesis of thiamine and pyridoxol in *E.coli*, MEP is generally considered as the first committed precursor of isporenoids synthesized via the alternative pathway (Takahashi et al., 1998; Lange and Croteau, 1999; Schwender et al., 1999). The enzyme catalyzing this NADPH-dependent reaction is DXP reductoisomerase (DXR). It has been well characterized in the past years, including its crystallization from bacteria, and has been studied in presence of cofactors and various inhibitors like the antibiotic Fosmidomycin (Takahashi et al., 1998; Jomaa et al., 1999; Reuter et al., 2002; Yajima et al., 2002; Steinbacher et al., 2003; Proteau, 2004; Yajima et al., 2004; Lauw et al., 2008). Similarly to DXP, MEP can also be synthesized from its corresponding, unphosphorylated alcohol 2-C-methyl-D-erythritol (ME), when added to the growth medium (Duvold et al., 1997; Fontana et al., 2001). However, unlike in bacteria, ME proved to be toxic in complementation assays with plant cells (Hemmerlin et al., 2003).

After the synthesis of MEP, 5 subsequent steps are needed for the formation of IPP and its isomer, DMAPP (Figure 4):

MEP first reacts with CTP, producing 4-diphosphocytidyl-2-*C*-methyl-D-erythritol (CDP-ME) in an CDP-ME synthase-catalyzed reaction (also: MCT-2-*C*-methyl-D-erythritol-4-phosphate cytidyltransferase (Rohdich et al., 1999; Kuzuyama et al., 2000c; Gabrielsen et al., 2006). CDP-ME then is phosphorylated by CDP-ME-Kinase (in an ATP-dependent reaction) yielding 4-diphosphocytidyl-2-*C*-methyl-D-erythritol-2-phosphate (CDP-MEP) (Lüttgen et al., 2000; Rohdich et al., 2000).

ME-ccP-Synthase (MDS) catalyzes the conversion of CDP-MEP to ME-ccP (2-*C*-methyl-D-erythritol-2,4-cyclodiphosphate) by eliminating CMP (Herz et al., 2000; Takagi et al., 2000). After reduction of ME-ccP to 1-hydroxy-2-methyl-2-(*E*)-butenyl-4-diphosphate (HMBPP) by HDS (HMBPP synthase), HMBPP is then used by HDR (1-hydroxy-2-methyl-2-(*E*)-butenyl-4-diphosphate reductase to produce

a mixture of IPP and DMAPP with a ratio of about 5 to 1 (Rohdich et al., 2002). HDR is sometimes also referred to as IDS (IPP/DMAPP-Synthase).

As for the MVA pathway, IPP and DMAPP can be interconverted by a plastidial isoform of isopentenyl/dimethylallyl diphosphate isomerase (IDI), which seems to play an essential role for the biosynthesis of higher isoprenoids by regulating the ratio of the two isomeric C5 precursors in the plastids and the cytosol (Wille et al., 2004).

DXS, the first enzyme of the pathway is the only known enzyme of the MEP pathway, which is encoded by more than one genes in *Arabidopsis thaliana* (Araki et al., 2000; Walter et al., 2002) and early studies suggested that most genes of the MEP pathway were present as single copy genes in the genomes of plants. Multiple *DXS*-like genes have been reported from monocots and dicots (Cordoba et al., 2009), including *Zea mays* (Walter et al., 2000), *Medicago trunculata* (Walter et al., 2002), *Oryza sativa* (Kim et al., 2005), *Picea abies* (Phillips et al., 2007), *Gingko biloba* (Kim et al., 2006) and *Pinus densiflora* (Kim et al., 2009). Depending on the plant species, two to three different DXS types could be detected that showed similar expression patterns. For instance, DXS type-1 expression strongly ressembles to *DXS/CLA1* from *Arabidopsis* and transcripts are particularly abundant in photosynthetic tissues, whereas the transcripts of the DXS type-2 gene were, for example, found to accumulate in the roots of maize, rice, barley and medigaco in response to colonization by mycorrhizal fungi (Walter et al., 2000; Walter et al., 2002). Multiple copies for other MEP pathway enzymes have also been reported for DXR in *Hevea brasiliensis* (Seetang-Nun et al., 2008) and for HDR in *Gingko biloba* and *Pinus taeda* (Kim et al., 2008). However, the specific functions and expression patterns of these different DXR and HDR isogenes are largely unknown until today.

The MEP pathway seems to be modulated at multiple levels, including transcriptional and post-transcriptional regulation (for review: (Rodríguez-Concepción, 2006; Cordoba et al., 2009)). The analyses of transcript levels in *Arabidopsis thaliana* seedlings showed that the expression of all MEP pathway enzymes was induced upon exposure to light. The same phenomenon was observed at early stages of leaf development in *Arabidopsis* seedlings (Carretero-Paulet et al., 2002; Guevara-Garciá et al., 2005; Hsieh et al., 2008). These data correlated with the observation that the expression of all MEP pathway enzymes in *Arabidopsis* was following a circadian rhythm, reaching the highest transcript levels just before dawn (Cordoba et al., 2009).

Especially the two first enzymes of the MEP pathway, DXS and DXR, are generally considered as key-enzymes/control-points in the flux-regulation of the MEP pathway.

In bacteria, several studies showed that the biosynthesis of isoprenoids is limited by the activity of DXS (Harker and Bramley, 1999; Kuzuyama et al., 2000a). In plants, transgene-mediated overexpression of DXS in *Arabidopsis* (Estévez et al., 2001) and tomato (Enfissi et al., 2005) was correlated with a significant increase of MEP-derived isoprenoids, also suggesting a limiting role for DXS in the plastidial MEP pathway.

In bacteria however, DXR-overexpression did not increase the levels of isoprenoid precursors (Miller et al., 2000). Although DXR expression was for example not upregulated during the accumulation of carotenoids (lycopene) in ripening tomato fruits (Rodríguez-Concepción et al., 2001), its overexpression in transgenic peppermint plants resulted in an increased production of monoterpenes (essential oils) in green leaf tissue (Mahmoud and Croteau, 2001). In addition, more recent studies showed that nuclear and transplastomic overexpression of DXR in *Arabidopsis* and tobacco plants led to an overall increase of total chlorophylls and carotenoids, among other significant isoprenoid end-products (Hasunuma et al., 2008).

Interestingly, the gene encoding IDI1 from *Arabidopsis*, the plastid-targeted isozyme of IPP/DMAPP isomerase, shows a positive correlation with the MVA pathway, indicating a possible role of this enzyme in the regulation of C5 precursor levels in the plastid (Wille et al., 2004).

Furthermore, studies with mutants have suggested that the MEP pathway may be controlled at the post-transcriptional level by changes in the metabolic flux (e.g., the ratio of its precursors or end-products). For instance, DXS and HDR proteins were shown to accumulate in several MEP pathway mutants, despite the fact that the transcript levels were considerably reduced (Lois et al., 2000; Rodríguez-Concepción et al., 2001; Wolfertz et al., 2004; Guevara-Garciá et al., 2005).

More detailled results concerning the regulatory expression networks of the MEP pathway may come in the future by integrated/genetic approaches looking at the expression profiles of genes involved in isoprenoid biosynthesis. In this context, the analysis of data from DNA microarrays obtained from plants treated under different conditions will allow a closer look on both isoprenoid pathways and contribute to a better understanding of various aspects, like for example the crosstalk between both pathways at the transcriptional level (Wille et al., 2004).

c) Crosstalk between both pathways in plants

In higher plants, both pathways are involved in the biosynthesis of isoprenoids. Despite the physical compartmentation of these biosynthetic routes - the MVA pathway operates in the cytosol and the mitochondria, whereas the MEP pathway is located in the plastids, there is no absolute separation between the pathways, and a bidirectional exchange of precursors and intermediates has been observed under certain conditions. This exchange is also referred to as “crosstalk”.

First indications for a crosstalk between the plastidial and cytosolic pathways came from several studies using feeding experiments with labeled sugars (^{13}C-glucose) or pathway intermediates (1-deoxy-D-xylulose) and subsequent analysis of isoprenoid end-products by NMR spectroscopy (Jeffrey et al., 1991). These experiments and the resulting labeling patterns of downstream metabolites allowed to shed light on the biosynthetic origins of a considerable number of plant terpenoids. Among those,

some terpenoids were built from derivatives of both pathways, which implied that intermediates cross the boundary between the compartments.

For example, Arigoni *et al.* (1997) provided evidence for the incorporation of labelled 1-deoxy-D-xylulose into cytosolic sitosterol in a cell culture of *Cataranthus roseus*. In a similar way, Adam *et al.* (1999) were able to demonstrate the contribution of the nonmevalonate pathway to the biosynthesis of sesquiterpenes of chamomile (*Matricaria recutita*), thus confirming earlier observations that certain sterols and sesquiterpenoids are not exclusively formed by IPP and DMAPP derived from the MVA pathway, but could be assembled from precursors of the MEP pathway (Schwender et al., 1996; Piel et al., 1998), or as a cooperation of both pathways (Adam et al., 1998). Only recently Skorupinska-Tudek *et al*. (2008) have been able to estimate the respective contributions of both pathways to the biosynthesis of dolichols in *Coluria geoides* hairy root cultures, after *in vivo*-labeling with ^{13}C-glucose and showed that up to 50% of the isoprene units were derived from the MEP pathway.

Further proof for a crosstalk came from experiments conducted in tobacco BY-2 cells, where growth inhibition by the statin mevinolin (inhibiting HMGR) could be complemented with exogenously applied 1-deoxy-D-xylulose (DX). In addition, incorporation studies, using radiolabeled DX demonstrated, that sterols were synthesized from IPP and DMAPP provided by the MEP pathway, in the presence of mevinolin (Hemmerlin et al., 2003).

These results confirm several studies which indicate that the transport of terpenoid precursors (IPP, GPP and GGPP) may occur preferentially in an unidirectional manner, from the plastid to the cytosol. This transport might be mediated by a hypothetical plastidial proton symport system (Bick and Lange, 2003), but until today, no such transporter has been identified.

However, there are also examples for a transport of intermediates from the cytosol to the plastids. Nagata *et al.* (2002) were able to partially complement the *Arabidopsis thaliana* albino mutant *cla1-1*, a null mutant of the first enzyme of the plastidial MEP pathway, by feeding exogenous mevalonic acid. These results correlate very well with the observation that an inhibition of the MEP pathway by fosmidomyin (inhibitor of DXR) could be partially overcome by feeding tobacco BY-2 cells with mevalonic acid (Hemmerlin et al., 2003).

Nevertheless, in *Arabidopsis* for example, specific inhibition of the MVA pathway by mevinolin (MVA, inhibiting HMGR) or the MEP pathway by fosmidomycin (FOS, inhibiting DXR) or oxoclomazone (OXO, inhibiting DXS) led to a developmental block very early at the seedling stage (Rodríguez-Concepción, 2004; Hemmerlin et al., 2006), suggesting that one of the limiting factors for the crosstalk may be the action of specific membrane transporters (Laule et al., 2003).

Clearly, the complex interactions between both pathways still bear many secrets. As an example, experiments with transplastomic tobacco plants overexpressing DXR from *Synechosystis* showed the that among various isoprenoids analyzed, the highest increase concerned sitosterol, which is usually synthesized by the cytosolic MVA pathway (Hasunuma et al., 2008).

1.1.4 Biosynthesis of higher isoprenoids

As mentioned above, IPP and DMAPP are the basic building blocks for all isoprenoids. Subsequent addition of IPP (C5) to DMAPP (C5) by prenyl transferases leads to the production of geranyl diphosphate (GDP, C10), farnesyl diphosphate (FPP, C15) and geranylgeranyl diphosphate (GGPP, C20) (Takahashi and Koyama, 2006). These bigger building blocks then serve as precursors for monoterpenoids (C10), sesquiterpenoids (C15) and diterpenoids (C20), whereas hemiterpenes (C5), the simplest known isoprenoids, can be directly synthesized from DMAPP (Miller et al., 2001). The formation of all these classes of terpenoids is catalyzed by different terpene synthases (Bohlmann et al., 1998; Christianson, 2006; Tholl, 2006). Triterpenoids (C30) and tetraterpenoids (C40) are formed by pairwise condensation of FPP (C15) and GGPP (C20) units, whereas the considerably bigger polyterpenoids (e.x. rubber: up to 30000 units) are synthesized by condensation of an undefined number of C5 precursors (Ai-Xia et al., 2007).

In order to build the different classes of regular, irregular terpenoids and their derivatives and conjugates, these basic prenyl diphosphate precursors can additionally undergo multiple modifications (e.g., oxidation, reduction, isomerizations, cyclizations) through the action of terpene-modifying enzymes, such as cytochrome P450 monooxygenases (Bernardt, 2006; Kaspera and Croteau, 2006; Mau and Croteau, 2006).

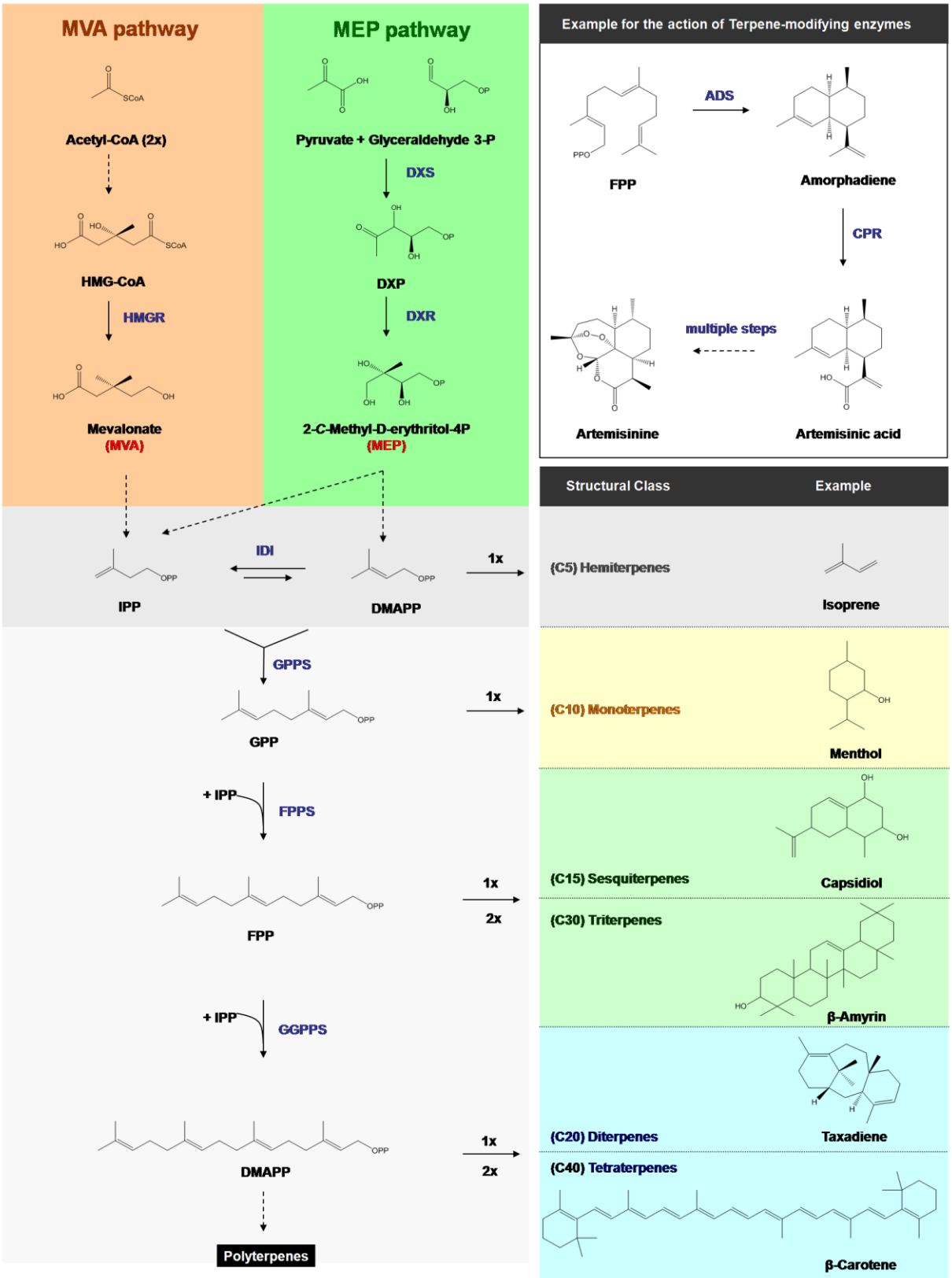

Figure 5: Biosynthesis of various classes of isoprenoids in plants (modified from Kirby and Keasling, 2009).

The cytosolic mevalonate (MVA) and the plastidial methyl-erythritol (MEP) pathway both produce the universal C5-precursors, isopentenyl diphosphate (IPP) and dimethylallyl diphosphate (DMAPP),. The key enzymes of both pathways have been described in detail in Figure 4. Downstream of the compartmentalized pathways, prenyltransferases are responsible for the conversion of IPP and DMAPP to longer chain isoprenoid buidling

blocks, such as the C_{10} geranyldiphosphate (GPP, precursor for monoterpenoid biosynthesis), the C_{15} farnesyl diphosphate (FPP, precursor for sesquiterpene and triterpene biosynthesis, leading to phytosterols) as well as geranylgeranyl diphosphate (GGPP, which serves as precursor for diterpenes, tetraterpenes and the phytol-sidechain of chlorophylls). For each group of prenyl diphosphate precursors one example of a downstream product is given. These conversions are catalyzed by terpene synthases. Further modifications leading to more complex isoprenoids are usually catalyzed by terpene-modifying enzymes, including P450s. One such reaction is schematized for the biosynthesis of taxol, starting from FPP. Multiple enzymatic steps are shown by dashed lines. ADS = amorphadiene synthase; CPR = cytochrome P450 reductase.

1.2 Non-mevalonate pathway as a target for the development of antimicrobial drugs and herbicides

The impact of the various natural compounds synthesized by the MEP pathway on various aspects of human life is steadily increasing, and terpenes isolated from microorganism and plants have already found various applications, e.g. as chemotherapeutic agents in human healthcare. The most prominent example in this context is certainly the sequiterpenoid artemisinin, which is naturally produced in the leaf-trichomes of the annual wormwood (*Artemisia annua*). Artemisinin is at the moment widely considered as the most promising agent for the treatment of the malaria parasite *Plasmodium falciparum*, and many recent approaches are focusing on understanding the exact mechanism of its biosynthesis with the goal to apply this knowledge to microbial and plant metabolic engineering. However, the case artemisinin is also reflecting one of the most important dilemmas in human healthcare: Artemisinin is one of the last efficient treatments that until recently defied the increasing development of resistance against therapeutic agents, which can be observed in the majority of human pathogens (Livermore, 2003; Levy and Marshall, 2004; Fisk et al., 2005; Kokwaro, 2009; Dondorp et al.). Especially the development of multi-drug resistant strains in different pathogens (bacteria, fungi, protozoans as well as their vectors) threatens the therapeutic efficacy of most current treatments that usually involve multiple agents. Therefore, novel drug targets urgently need to be identified in order to develop new strategies and new generations of anti-infective agents.

Although the complete elucidation of the MEP pathway in plants only dates back a few years, much knowledge about the seven identified enzymes of the MEP pathway and the genes encoding them has been gathered in recent years and contributed to a better understanding of the complex regulation of this pathway (for review: (Rohdich et al., 2005; Rodríguez-Concepción, 2006; Hunter, 2007)

On the basis of these data it is possible to deduce that the MEP pathway enzymes are very promising candidates for the development of antimicrobial agents and herbicides, as they possess several properties that are generally considered as highly desirable for a potential drug target (Pucci, 2006):

i. One of the most important features is its **essentiality** for growth and survival of the targeted organism. In the last couple of years, all enzymes of the MEP pathway have been validated either genetically (e.g. by knock-out mutants, random mutagenesis, targeted gene disruption)

and/or chemically (target of a antimicrobial agent/herbicide) as essential for the growth of their vector (Campos et al., 2001; Freiberg et al., 2001; Sauret-Güeto et al., 2003; Hunter, 2007; Eoh et al., 2009)

ii. Another important property is the **selectivity** of the drug target. This aspect is particularly important, considering its future clinical applications. As mentionned before, the MEP/DOXP pathway occurs in the chloroplasts of phototrophic organisms like algae and plants, in most eubacteria and in some pathogenic parasites, but not in animals. Therefore, the enzymes of this pathway can be specifically targeted without the risk of interfering with human isoprenoid biosynthesis. In addition, all enzymes are particularly substrate-specific, and their active sites seem to be highly conserved across species. Consequently, the ongoing, fast characterization of their catalytic properties and three-dimensional structures should make them ideal targets for future approaches like structure-based drug design and further contribute to a decreased toxicity for humans if any (Hunter, 2007; Rohdich et al., 2005).

iii. Ideally, a promising drug target is also **present in many organisms/pathogens.** Enzymes of the MEP pathway are found in all higher plants and in many pathogenic microorganisms, including the causative agents of some of the most important human diseases, malaria (*Plasmodium falciparum*) and tuberculosis (*Mycobacterium tuberculosis*) (Jomaa et al., 1999; Boucher and Doolittle, 2000; Freiberg et al., 2001; Rohdich et al., 2005). As a result, any identified inhibitor of a MEP pathway enzyme could have a broad spectrum of activity across different species.

iv. Finally, the **availability of an *in vitro* assay** will allow a very precise characterization of a targeted enzyme in presence of its potential inhibitors as well as a comparision with existing drugs. Integrated research approaches have provided structural and biochemical data for almost every MEP pathway enzyme, at least in bacteria (Hunter, 2007). The *in vitro*-expression of these enzymes has already revealed pivotal information about their mode of action, e.g. about DXR in presence of its known inhibitor fosmidomycin (Steinbacher et al., 2003; Mac Sweeney et al., 2005). This knowledge about the reactivity of the individual MEP pathway enzymes should allow to specifically design prodrugs (Schlüter et al., 2006) or to develop approaches for the identification of novel effective compounds (Ramsden et al., 2008).

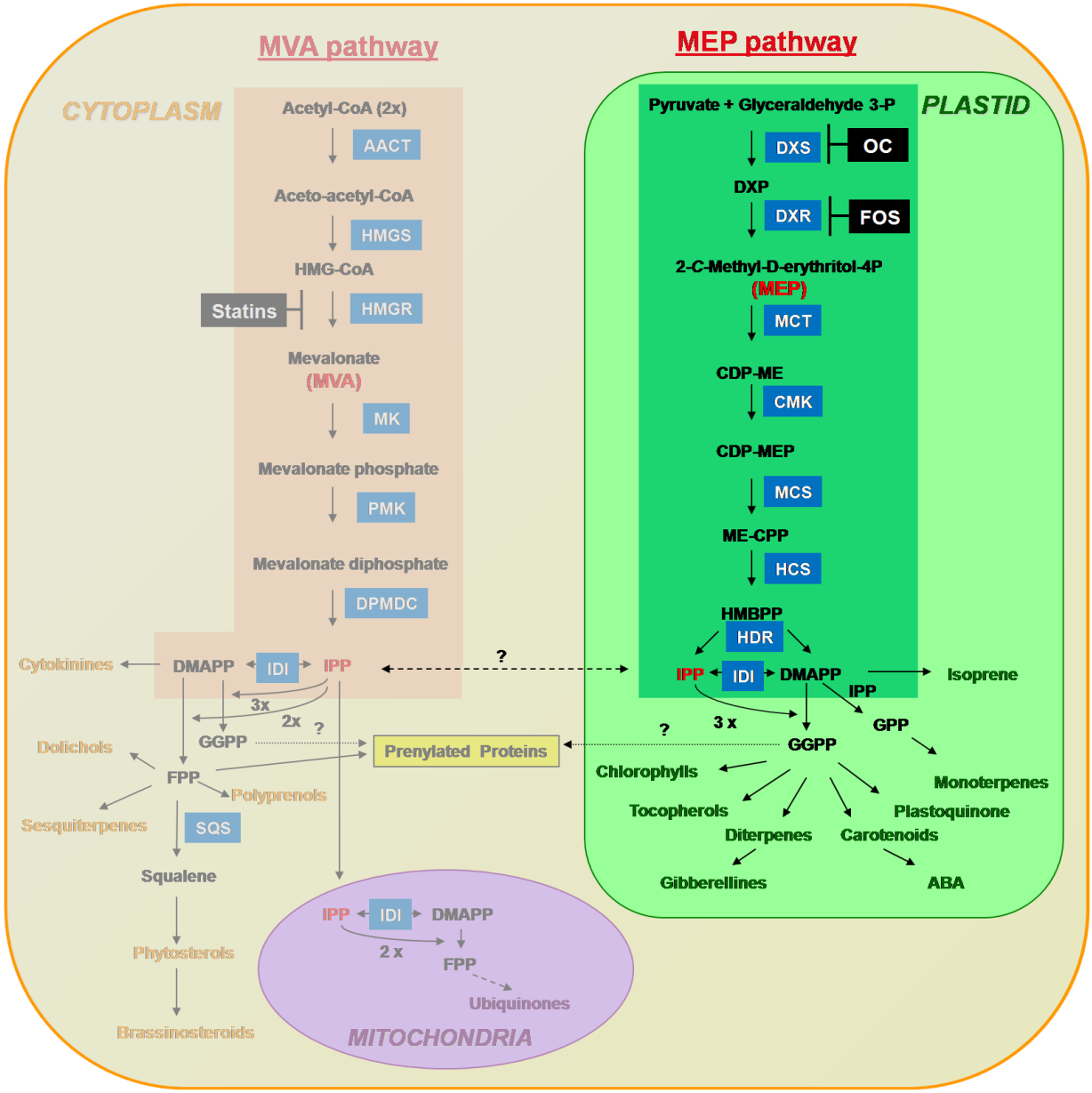

Figure 6. Simplified scheme of plant terpenoid biosynthesis and compartimentation

Abbreviations ABA, abscicic acid; DMAPP, dimethylallyl diphosphate; DXP, 1-deoxy-D-xylulose-5-phosphate; DXR, 1-deoxy-xylulose-5-phosphate reductoisomerase; DXS, 1-deoxy-D-Xylulose-5-phosphate synthase; FPP, farnesyl diphosphate; GGPP, geranylgeranyl diphosphate; GPP, geranyl diphosphate; HMBPP, 1-hydroxy-2-methyl-2-(*E*)-butenyl-4-phosphate; HMG-CoA, 3-hydroxy-3-methylglutaryl-CoA; HMGR, 3-hydroxy-3-methylglutaryl-CoA reductase; IDI, isopentenyl diphosphate isomerase; 1-Hydroxy-2-methyl-2-(E)-butenyl 4-diphosphate reductase; IPP, isopentenyl diphosphate; MEP, 2-C-methyl-D-erythritol-4-phosphate; MVA, mevalonate

1.2.1 Microbial targets (eubacteria)

Due to the availability of whole genome sequences from several hundred mircroorganisms within the last decade, genes encoding for isoprenoid biosynthetic enzymes could be identified in many pathogenic microorganisms by bioinformatic approaches and provided new insights about the distribution of both pathways in the eubacterial kingdom (Rohdich et al., 2005). These data revealed that the majority of eubacteria use almost exclusively the alternative non-mevalonate pathway for the synthesis of their isoprenoids. However, there are several exceptions, notably the gram-positive cocci (e.g. *Streptococcus pneumoniae* or *Staphylococcus aureus*), which utilize enzymes of the MVA pathway (Wilding et al., 2000; Voynova et al., 2004). Remarkably, there are also a few examples for bacteria, whose genomes encode enzymes from both pathways (e.x. *Listeria monocytogenes*) (Boucher and Doolittle, 2000; Begley et al., 2004).

Among the bacteria which synthesize their isoprenoids exclusively via the MEP pathway, there are many important human pathogenes, such as *Mycobacterium tuberculosis* (Bailey et al., 2002; Dhiman et al., 2005; Eoh et al., 2007), the causative agent of tuberculosis, a disease of the respiratory system in mammals, responsible for up to 9 million new infections and 1,6 million new deaths worldwide each year (Mathema et al., 2006; WHO, 2009). Multiple approaches indicate that the MEP pathway is essential for the pathogenicity, as well as for the growth and the survival of *M. tuberculosis*. For instance, the disruption of the *lytB1-dxs2* operon in *M. tuberculosis* has been reported to abolish the bacterial ability to prevent acidification of its phagosome and resulted in diminished intracellular survival of the pathogen (Pethe et al., 2004). This is supported by recent publications demonstrating that several enzymes of the MEP pathway, including DXS, DXR, IspD, IspF and gpcE are essential for the *in vitro* growth and survival of *M.tuberculosis* (Buetow et al., 2007; Eoh et al., 2007; Brown and Parish, 2008; Brown et al., 2010).

For example, it was shown that *M. tuberculosis* DXR mutants created by homologous recombination were not viable, unless a copy of the *DXR* operon was provided on a second vector (Brown and Parish, 2008). This is in agreement with previous results obtained with *E.coli*, where loss-of-function mutants of the MEP pathway could only be rescued after transformation of the mutant cell line with plasmids carrying the corresponding MEP pathway gene (Sauret-Güeto et al., 2003).

Despite the huge amount of efforts put in the development of drug therapies against bacterial pathogens like *M.tuberculosis*, strains of single and multidrug resistant bacteria (MDR-TB) rapidly emerge due to spontaneous genetic mutations (Musser, 1995; Mitchinson, 2005; Zignol et al., 2006) and pose a major thread for public health, especially for immunodeficient patients (WHO, 2009).

1.2.2 Antimalarial targets

Malaria is an infectious disease, which is caused by a single-cell protozoa of the genus *Plasmodium* (*Phylum apicomplexa*). It is transmitted by mosquitos and responsible for more than 1 million casualities per year world-wide, with 300 to 500 million registered infections (Miller et al., 2002; Suh et al., 2004; Thayer, 2005). Among the four different pathogenous *Plasmodium* parasites, *Plasmodium falciparum*, which is causing malaria tropica, is by far the the most dangerous, being responsible for nearly all the mortality observed.

Since 2002, the complete genome sequence of *Plasmodium falciparum* (Gardner et al., 2002) is available and genes of the MEP pathway have been found in the DNA of the apicoplast, a 4-layered non-photosynthetic plastid structure with its own ciruclar DNA (35 kb), that is supposedly derived very early in evolution by secondary endosymbiosis of a green algae (Wilson et al., 1996; Köhler et al., 1997; Maréchal and Cesbron-Delauw, 2001), whereas other publications claim that the secondary endosymbiont may be a red algae (Cavalier-Smith, 1999; Lim and McFadden, 2010). But more importantly, there are no hints for the presence of mevalonate pathway related genes, which makes the apicoplast a very attractive target for the development of antimalarial drugs (Wiesner et al., 2003; Olliaro and Wells, 2009). For instance, fosmidomycin, a known inhibitor of IspC (or DXR; deoxy-reductoisomerase) has a high impact on the growth of *Plasmodium falciparum* in different phases of its complex sexual and asexual life cycle (Jomaa et al., 1999; Cassera et al., 2007).

Another very interesting approach in fighting *Plasmodium* is based on the observation that some intermediates and final products of isoprenoid biosynthesis found in mammals are different from those identified in *Plasmodium falciparum*. Their potential as antimalarial drugs was confirmed, when tested on intraerythrocytic stades of *Plasmodium falciparum*. Several terpenes (farnesol, nerodiol, limonen and others) and S-farnesylthiosalicylic acid had inhibitory effects on the biosynthesis of dolichol and the isoprenic side chain of ubiquinone at µM concentrations (Rodrigues Goulart et al., 2004).

1.2.3 Herbicides

The MEP pathway proves also to be a very promising target for the development of herbicides. As mentioned before, the plastidial MEP pathway provides essential components of the light harvesting complexes, such as the phytol-side chain of chlorophylls or carotenoids (Schwender et al., 1997). The latter also play an important role in photoprotection. In addition, many MEP pathway-derived, secondary metabolites are involved in interactions with other organisms or in the protection against herbivores (Ai-Xia et al., 2007).

Although crosstalk between the cytsolic and plastidial compartments has successfully been shown in several cases (Crosstalk between both pathways in plants), the albino or chlorotic phenotypes observed in mutants or silenced genes of MEP pathway enzymes (Mandel et al., 1996; Araki et al., 2000; Estévez et al., 2000; Page et al., 2004) indicated that MVA-derived IPP was not able to rescue these plants, which may be due to the limited exchange of diphosphate precursors (Kasahara et al., 2002; Nagata et al., 2002).

Consequently, blocking the MEP pathway by mutagenesis or other approaches has dramatic, often lethal effects, as it prevents correct chloroplast function and leads to an embryo-lethal phenotype (Budziszewski et al., 2001). For these reasons, all enzymes of the MEP pathway are potential targets for the development of novel herbicides.

A prominent example of a herbicide acting on the MEP pathway is clomazone [2-(2-chlorobenzyl)-4,4-dimethyl-1,2-isoxazolidin-3-one], which inhibits the enzyme of the first committed step of the MEP pathway, DXS, catalyzing the formation of DXP. Clomazone is a soil-applied herbicide, which acts against weeds and grasses that occur in many crops, such as cotton, tobacco, rice, and soybeans (Vencill, 2002; Yasuor et al., 2008). In susceptible plants, clomazone inhibits the formation of chloroplast-derived isoprenoids (phytol, carotenoids, plastoquinone etc.) and thus prevents correct chloroplast development and pigment accumulation, resulting in a bleaching phenotype (Duke and Paul, 1986; Norman et al., 1990b, , 1990c; Jordan et al., 1998; Hess, 2000). In order to be effective, clomazone first needs to be converted to its bioactive metabolite 5-ketoclomazone (or oxoclomazone), which is accomplished by two P450-mediated metabolizing steps in susceptibe plants (Ferhatoglu et al., 2005; Ferhatoglu and Barrett, 2006).

This is even more interesting, if one considers that clomazone represents the “last line of defense” in the fight against certain weeds (e.x. *Echinochloa phyllopogon*) in rice (*Oryza sativa*) fields, that developped P450-mediated metabolic resistances to multiple herbicides (Fischer et al., 2000; Osuna et al., 2002; Ruiz-Santaella et al., 2006) (Yun et al., 2005; Yasuor et al., 2008) and that should normally be treated by P450 inhibitors (such as malathion, disulfoton or the more specific piperonylbutoxide and 1-aminobenzotriazole).

The question wether the emerging clomazone-resistance in these plants is due to P450-mediated oxidative bioactivation or to alternative mechanisms for the detoxification of clomazone, such as the

conjugation with sugars or glutathione (Norman et al., 1990c; Vencill et al., 1990; ElNaggar et al., 1992), remains still open. This situation is nevertheless alarming (Yasuor et al., 2008; Yasuor et al., 2010) and underlines the need to identify new generations of effective herbicides.

1.3 How to study the effects of potential inhibitors of the MEP pathway?

In the past, different approaches have been used to find possible inhibitors of IPP/DMAPP biosynthesis in plants. For instance, etiolated and greening leaves of barley (*Hordeum vulgare*) have been used in several cases to test the effects of potential pathway inhibitors (e.g. Fosmidomycin) on the formation of chlorophylls and carotenoids (Zeidler et al., 2000). As these leaves contain tissues with high enzymatic activities due to light-induced thylakoid formation during chloroplast differentiation, they represent a nice model system for *in vivo* studies. First indications came from observations that treatment with the commercial herbicide clomazone resulted in a significant decrease of chlorophyll and carotenoid levels in barley leaves (ElNaggar et al., 1992). The same effect was observed years later by Zeidler *et al.* (Zeidler et al., 1998; 2000), who applied Fosmidomycin at 100 µM to greening barley leaves. In addition, these authors were able to demonstrate that the inhibition caused by 10^{-5} M clomazone and its metabolite oxoclomazone can be reversed by exogenous application of 5 mM DXP to barley leaves.

Another approach consisting in monitoring the effects of inhibitors on the biosynthesis of gaseous isoprene seems to offer an alternative and effective approach, as only two enzymes are needed to convert IPP into isoprene from DMAPP (Zeidler et al., 1997). Oxoclomazone for instance clearly caused an inhibition of isoprene emission at 1 mM in leaf pieces from several tree species including *Quercus robur*, *Populus nigra* and *Platanus x acerifolia* (Zeidler et al., 2000).

Raschke *et al.* (2004) presented a method to separate MEP pathway intermediates using chromoplasts isolated from *Capsicum annuum* and *Narcissus pseudonarcissus*. As McCaskill and Croteau (1993) did more than a decade earlier for the analysis of MVA pathway intermediates, their approach was based on reverse phase HPLC, which additionally allowed to separate the corresponding phosphates and alcohols of the MEP pathway intermediates. According to Raschke et *al.* (2004), this concecpt could easily be adapted to other plant species and serve as an additional analytical tool in the screening for novel MEP pathway inhibitors.

In addition, at least for the bacterial counterparts of the MEP pathway enzymes, structure-based drug design approaches have been reported. For exemple, fluorescent inhibitors of *E.coli* IspF (= MCS or MECPS) have been specifically designed, synthesized and co-crystallized with their enzymatic target

(Crane et al., 2006). Another approach was only recently published by Ramsden *et al*.(2008), who combined available biochemical and crystallographic data about IspF (MDS) to virtually screen (*in silico*) a database of over 1 million commercially compounds by a hierarchical filtering methodology. The data available on these compounds was filtered according to certain criteria, including molecular complexity, topology and functionality to preselect more than 4000 compounds that could virtually dock into the *Ec*IspF active site, before choosing 10 compounds for experimental validation (Ramsden et al., 2008).

A more applied screening assay with purified IspC (DXR) protein from *E.coli* has been performed by Kaiser et al. (2007) to screen the extracts of about 200 Mediterranean plant species for novel inhibitors. This was accomplished by spectro-photometrically monitoring the dehydrogenation/oxidation of NADPH, which is a by-product of the conversion of DXP into MEP (Figure 4) and led to the identification of several plant extracts (12 out of ~200) that showed a strong inhibition of IspC activity (Kaiser et al., 2007). The principle of this assay relies on a decrease of the optical density at A_{340nm} due to the oxidation of NADPH and has already been used to measure DXR activity from various sources, including peppermint (Lange and Croteau, 1999) and *Arabidopsis thaliana* (Schwender et al., 1999).

In summary, several approaches for the characterization and study of all MEP pathway enzymes have been developped, mostly focusing on bacterial enzymes so far (for review see: Eoh et al., 2009).

Most of these assays, however, were performed *in vitro* and needed the recombinant, purified enzyme, rather complicated purification methods, as well as a certain expertise, and do not tell wether the screened compound is bioactive (means is reaching its molecular target *in vivo*). Nevertheless, they provide a promising starting point for intelligent drug design and HTS assay development, once a suitable candidate is found.

Therefore a fast, visual assay to screen for potential inhibitors of the MEP pathway that is able to pre-select these suitable candidates **before** they are used in enzyme specific tests would be highly desirable.

1.4 Goal of this work

In our group, Esther Gerber (Ph.D. thesis, 2005) developed an *in vivo* visualization system based on a stably transformed tobacco BY-2 (TBY-2) cell line for monitoring the prenylation status of a GFP fusion protein, after treatment with various isoprenoid biosynthetic inhibitors. Isoprenylation of proteins, which occurs in all eucaryotic cells, involves the covalent attachment of a C15 (farnesyl) or C20 (geranylgeranyl) group to a C-terminal CaaX motif, followed by a series of post-prenylation reactions. This lipidic post-translational modification plays an important role in the correct membrane targeting of certain proteins and in their interactions with other proteins.

Esther Gerber designed a dexamethasone-inducible cell line that expressed a GFP fused to the carboxy-terminal basic domain of the rice calmodulin (CaM61), which naturally bears a CaaL geranylgeranylation motif (GFP-BD-CVIL). After induction, the prenylated fusion protein predominantly associated with the plasma membrane. By using pathway-specific inhibitors, Esther demonstrated that inhibition of the MEP pathway with oxoclomazone and fosmidomycin, as well as inhibition of the prenyltransferase geranylgeranyltransferase type 1 (PGGT-1), triggered a shift in the localization of the GFP-BD-CVIL protein from the plasma membrane to the nucleus. In contrast, inhibition of the MVA pathway with mevinolin did not affect the localization. Complementation assays with pathway-specific intermediates were also performed. Taken together, these data clearly indicated that the precursors for the cytosolic isoprenylation of the fusion protein were predominantly provided by the MEP pathway.

However, several questions remained unsolved, including the exact nature of the prenyl moiety of the GFP fusion protein. To address this issue, in a first time, I generated a stably transformed TBY-2 cell line with a His-tagged version of the GFP-DB-CVIL protein, which was used in our group to purify and to conduct mass spectral analysis on the prenylated GFP fusion protein isolated from TBY-2 cells. I developed a protocol for a rapid selection of homogenous clonal cell lines, deriving from secondary callus tissue cultures.

Following, I used these clonal cell lines to extend previous studies focusing on the effect of various inhibitors - of both isoprenoid biosynthetic pathways - on the subcellular localisation of the fusion protein. The challenge was to determine the biosynthetic origin (cytoplasmic or plastidial) of the prenyldiphosphate precursors used by the cells to provide the GGPP needed for the prenylation of the fusion protein.
As FPP and GGPP are the substrates of many enzymes (see figure 3), I also studied the impact of sterol biosynthesis inhibitors as well as inhibitors of CaaX processing enzymes (prenylation and post-

prenylation reactions) on the prenylation reaction of the H6-GFP-DB-CVIL fusion protein and on its subcellular localisation. This experimental test system was particularly useful to check new prodrugs that could target the MEP pathway.

Finally, in order to optimize this visualization system from a more qualitative assay to a statistically trustable screening system, I transformed the existing GFP-BD-CVIL cell line with an estradiol-inducible vector, driving the expression of a RFP protein, C-terminally fused to a NLS (nuclear localization signal) sequence. With this new strategy, I intended to quantify the total number of viable cells versus the number of inhibited cells after various treatments. Furthermore, I investigated the potential of the fluorescent reporter system for miniaturization and automatization to fit the requirements of modern drug screening applications. This approach also included a semi-automatic counting system, based on the freely available image processing software Image J.

2 Results and Discussion

2.1 Development of a reporter system to screen for inhibitors that interfere with protein geranylgeranylation

2.1.1 The prenylation of proteins in plants

In eucaryotic cells, certain proteins (e.g. members of the Ras superfamily of GTPases in vertebrates) are modified by a series of post-translational modifications, leading to the creation of a lipidated, hydrophobic domain at the carboxyl terminus of the protein. This post-translational processing, also referred to as protein prenylation, mediates protein-protein interactions, increases the affinity of the prenylated proteins to cellular membranes and is therefore important for the targeting and function of the prenylated proteins. Prenylation depends on the presence of a carboxy-terminal signal in form of a short tetrapeptide, the CAAX motif (C refers to as a cysteine, A denotes an aliphatic amino acid and X represents a specific amino acid) (Clarke, 1992; Schafer and Rine, 1992; Zhang and Casey, 1996; Crowell, 2000)

This C-terminal CaaX motif is recognized by cytosolic CAAX protein prenyl transferases, which either attach a 15-carbon farnesyl (FPP), a reaction catalyzed by a protein farnesyl transferase or PFT) or a 20-carbon geranylgeranyl (GGPP, a reaction catalyzed by protein geranylgeranyl transferase or PGGT1) to the cysteine of the CAAX–motif via a thioether bond. The specificity of the reaction is mainly defined by the C-terminal "X". As a general rule, proteins are geranylgeranyated when the "X" is a leucine residue whereas any other amino acid - most probably a methionine, serine, alanine, glutamine or cysteine - will lead to the covalent attachment of a farnesyl residue (Roskoski, 2003). A third prenylation mechanism is known for the members of the Rab family of small GTPases, which are prenylated at two different C-terminal cysteine residues by Rab geranylgeranyltransferase (also referred to as PGGT2) (Yalovsky et al., 1999; Maurer-Stroh et al., 2003a; Maurer-Stroh et al., 2003b).

Both protein prenyltransferases, PFT and PGGT1, are heterodimeric enzymes that share a common α-subunit, whereas their respective β-subunit is encoded by different genes (Zhang and Casey, 1996; Yalovsky et al., 1999; Crowell, 2000; Galichet and Gruissem, 2003).

Following prenylation in the cytosol, the newly lipidated protein is targeted to the endoplasmic reticulum (ER), where it usually undergoes two subsequent processing reactions (Figure 7): first of all, the removal of the C-terminal amino acid by a specific endoprotease, known as RCE1 (RAS converting enzyme 1); secondly, the carboxyl group of the now exposed, lipidated cysteine residue is carboxyl-methylated by the enzyme isoprenylcysteine carboxyl methyltransferase (ICMT). In contrast to the prenylation reaction and the proteolytic removal of the -AAX tripeptide, this last step in the

maturation of prenylated proteins can be reversed by certain methylesterase enzymes (ICME), which have been identified in animals and plants (Tan and Rando, 1992; Van Dessel et al., 2001; Lamango, 2005; Deem et al., 2006; Huizinga et al., 2008). The proteolytic cleavage of the last three amino acids and the carboxyl-methylation are commonly referred to as "CaaX processing" or post-prenylation reactions (Young et al., 2000).

In addition to these post-translational modifications, certain proteins, such as NRAS, HRAS and KRAS4A in vertebrates or members of the Rop (Rho) family in plants can be palmitoylated as well or S-acylated before their transfer to their cellular destination - most likely the plasma membrane (Hancock et al., 1989; Hancock et al., 1990; Hancock et al., 1991; Sorek et al., 2007). Other proteins, such as KRAS4B do not require a second lipidic modification, but possess a polybasic, lysine-rich sequence in proximity to the C-terminal CAAX motif instead (Hancock et al., 1990).

Prenylated proteins have been particularly well studied in yeast and vertebrates because of their implication in oncogenesis, as mutational constitutive activation of RAS GTPases is responsible for up to 20% of human cancers (Bos, 1989; Downward, 2003) (Malumbres and Barbacid, 2003).

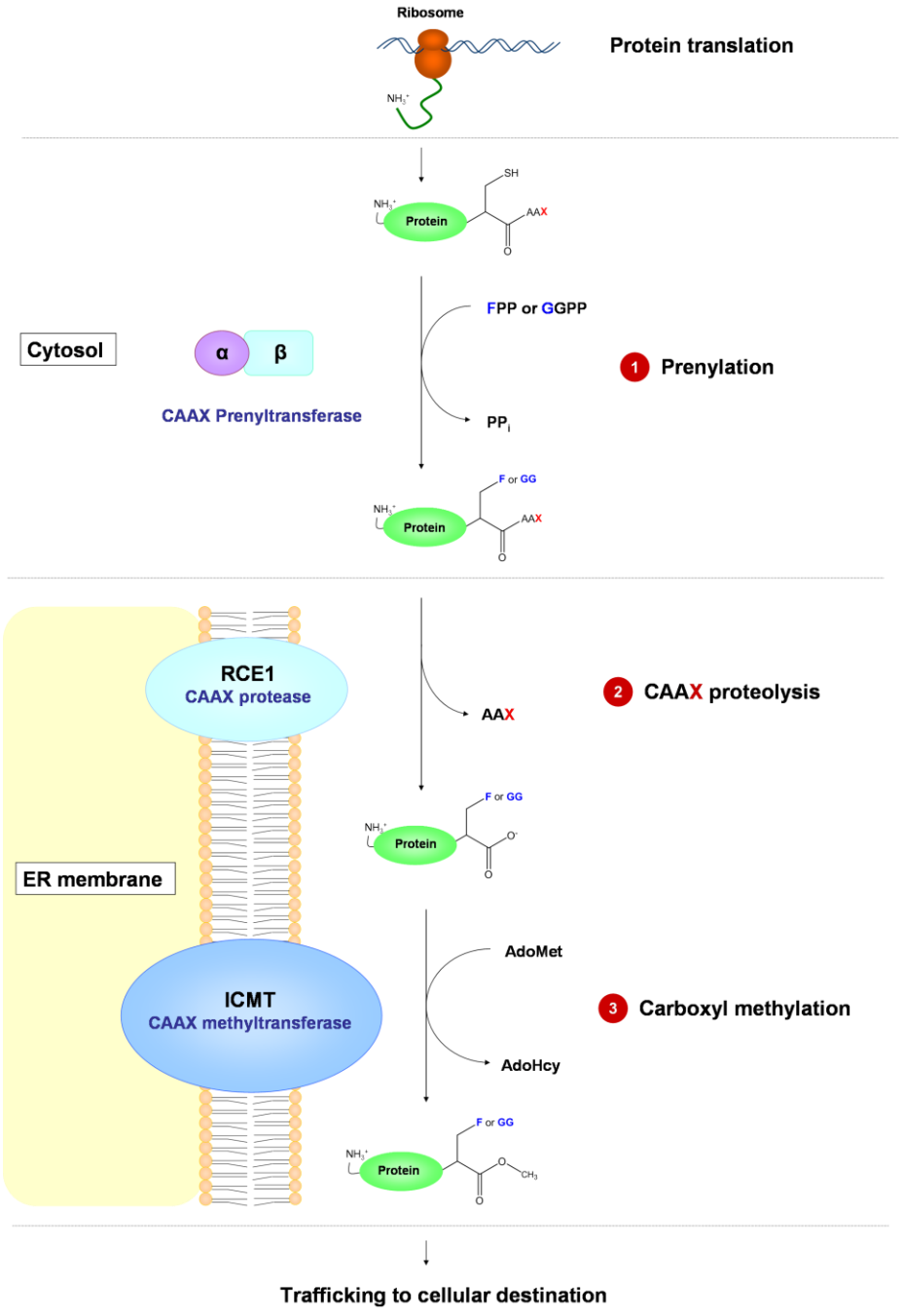

Figure 7. Prenylation and postprenylation reactions: CaaX-protein processing (modified from Winter-Vann and Casey, 2005).

Many proteins in eucaryotic cells contain a carboxy-terminal CAAX motif. Depending on the nature of this motif, these proteins are either farnesylated (F) (X = M, A, S, Q) or geranylgeranylated (GG) (X = L) at the cysteine residue by the cytosolic CAAX protein farnesyltransferase (Ftase) or geranylgeranyltransferase (GGtase I). After the attachment of the isoprenoid group, the AAX tripeptide is proteolytically removed by RCE1 (RAS converting enzyme 1), before a methyl-group is transferred to the C-terminal cysteine residue by isoprenylcysteine carboxymethyltransferase (ICMT). Both reactions take place at the endoplasmic reticulum (ER). The processed Caax-protein can undergo additional modifications (e.g. palmitoylation: NRAS or KRAS4A), before being transported to the final cellular destination or binding to partners that keep them in the soluble state, as it is the case for many RHO GTPases (that bind to RHO guanine nucleotide dissociation inhibitors (GDIs) in vertebrates). **Abbreviations:** FPP, farnesyl diphosphate; GGPP, geranylgeranyldiphosphate; AdoHcy, S-adenoyslhomocysteine; AdoMet, S-adenosylmethionine.

In comparison, relatively little is known about prenylated proteins in plants, even though many studies suggest that these proteins play important roles in cellular processes similar to their yeast and mammalian counterparts, such as growth regulation, signal transduction, cell cycle regulation and membrane trafficking. (Yalovsky et al., 1999; Crowell, 2000; Galichet and Gruissem, 2003; Galichet et al., 2008; Crowell and Huizinga, 2009).

For instance, the three prenyltransferase enzymes (PFT, PGGT I and PGGT II) have been found in plants, including *Pisum sativum* (Yang et al., 1993; Qian et al., 1996), *Solanum lycopersicum* (Loraine et al., 1996; Yalovsky et al., 1996) , *Catharanthus roseus* (Courdavault et al., 2009) and *Arabidposis thaliana* (Cutler et al., 1996; Pei et al., 1998; Caldelari et al., 2001; Running et al., 2004; Johnson et al., 2005). In addition, it has been shown that tomato FTase was able to complement a yeast mutant with a deleted Ftase β-subunit, suggesting that at least the substrate recognition and catalytic mechanism were highly conserved among eucaryotes (Yalovsky et al., 1997).

In *Arabidopsis thaliana*, mutants lacking the common α-subunit of PFT and PGGT I (*PLURIPETALA* or *PLP*) or the respective β-subunits of PFT (*ENHANCED RESPONSE TO ABA* or *ERA1*) and PGGT1 (*GERANYGERANYLTRANSFERASE BETA* or *GGB*) show an enhanced response to ABA and/or auxin and are affected in their development (Cutler et al., 1996; Pei et al., 1998; Running et al., 1998; Bonetta et al., 2000; Yalovsky et al., 2000; Running et al., 2004). Therefore it has been suggested that some prenylated proteins, such as the geranylgeranylated small GTPases Rop2 and Rop6 (Lemichez et al., 2001; Li et al., 2001) or AUX 2-11 (Wyatt et al., 1993; Caldelari et al., 2001) or yet to be identified plant farnesylated proteins may function as negative regulators of ABA (ROP2/ROP6) and auxin signaling (ROP2/AUX 2-11) (Johnson et al., 2005; Crowell and Huizinga, 2009).

In addition to their roles in hormone signalling, prenylated proteins in plants have found to be involved in other cellular processes, including the coordination of calcium signal transduction (Rodríguez-Concepción et al., 1999; Xiao et al., 1999), the response to environmental stresses, such as heat and heavy metals (Zhu et al., 1993; Dykema et al., 1999; Suzuki et al., 2002; Barth et al., 2009), the biosynthesis of isopentenyl-like cytokinins (Galichet et al., 2008) and the regulation of the cell cycle/cellular division (Qian et al., 1996; Hemmerlin and Bach, 1998; Hemmerlin et al., 2000; Galichet and Gruissem, 2006).

Like the prenylation reaction itsself, CaaX processing (proteolysis and carboxymethylation) seems also to be a conserved process (Yalovsky et al., 1999), as attested by the fact that yeast mutants lacking CaaX protease activity could be complemented with the *Arabidopsis thaliana* Caax proteases AtSTE24 and AtRCE1. Like their mammalian and yeast homologs, both enzymes were localized in the ER and found to be expressed in the majority of tissues (Bracha et al., 2002).

Furthermore, recent studies showed that the two ICMT homologs identified in *Arabidopsis thaliana* (AtICMTA and AtICMTB), catalyzing the methylation of the newly formed C-terminus, (Rodríguez-

Concepción et al., 2000; Crowell and Kennedy, 2001; Chary et al., 2002) are colocalized with the CaaX proteases in the endoplasmic reticulum (Bracha-Drori et al., 2008).

Interestingly, treatment of plants with the methyltransferase inhibitor acetyl farnesyl cysteine (AFC) induced ABA hypersensitivity with similar phenotypes to those of *era1* and *plp* mutants (Chary et al., 2002). A similar phenotype consisting in an altered organization of the shoot apical meristem could also be observed in gene-silenced plants ($AtIMCT^{sil}$). However, none of the ICMT silenced *Arabidopsis* plants did show any hypersensitivity to ABA (Bracha-Drori et al., 2008).

These findings suggest that after cytosolic prenylation, proteins in plants undergo the same CaaX processing at the ER as proteins in yeast and vertebrates. These post-prenylation reactions which, among other effects (protection from degradation, protein-protein interactions), are assumed to increase the affinity of proteins to membranes (Hancock et al., 1991; Parish et al., 1995), may be required for their correct subcellular targeting and function. Consistent with that is the observation that the prenylated calmodulin CaM53 (Rodriguuez-Concepcion et al., 1999) accumulated in the endomembranes after treatment with the ICMT inhibitor AFC instead of being transported to the PM (Rodríguez-Concepción et al., 2000).

The above mentioned CaM53 is a functional calmodulin from petunia with a polybasic C-terminal domain and a CaaX-isoprenylation motif. Upon prenylation by PGGT I, the protein was transported to the PM of plant cells, where its physiological activity was regulated, as suggested by the fact that the subcellular localization of this protein was affected *in vivo* by different effectors (light, sucrose, mutagenesis or interference with isoprenoid biosynthesis). If the isoprenylation of the protein was impaired by a mutation of the cysteine of the CaaX-box motif, treatment with mevinolin or incubation of leaves in the dark, a mislocalization of the GFP-fusion protein to the nucleus was observed (Rodríguez-Concepción et al., 1999).

Interestingly, a few other plant proteins have recently been identified that exhibit a different subcellular localization depending on their prenylation status. For exemple, a similar spatial pattern for the functional rice calmodulin isoform OsCaM61 (Xiao et al., 1999), expressed in transgenic tobacco BY-2 cells, has been reported by Dong *et al.* (2002). Masking of the C-terminal prenylation site by a GFP fusion resulted in a partial shift of the localization of the fusion protein from the PM and endomembranes to the cytosol and nucleus. Although both calmodulin proteins have a nuclear localization signal within their amino acid sequence, the reason for which those two proteins are transported inside the nucleus in absence of prenylation still remains unclear until today. They could possibly interact with specific nuclear proteins, most likely transcription factors. In the case of other prenylated proteins, such as the farnesylated and nucleus-localised HIPP26 in *Arabidposis thaliana*, a strong interaction with a zinc finger homeodomain transcription factor has indeed been recently reported (Barth et al., 2009).

2.1.2 The thesis of Esther Gerber (2005) – Development of a bioassay based on a visual marker

The observation that the subcellular localization of some prenylable proteins was dependent on their isoprenylation status and could be modulated *in vivo* by different ways, including chemical inhibition of isoprenoid biosynthetic pathways or various external stimuli, as for the studies with the fluorescent GFP-OsCaM61 fusion protein in tobacco BY-2 cells (Dong et al., 2002), was very interesting and openened the door for different applications. BY-2 cells have already been used in our group for other studies and proven to be an excellent model for the investigation of isoprenoid metabolism-related topics because of their short duplication time and efficient uptake of metabolites. Due to the lack of photosynthetic pigments, they are also particularly suitable for approaches involving fluorescent reporters (Hemmerlin et al., 2003; Hemmerlin et al., 2004). For these reasons, a former Ph.D. student in our group, Esther Gerber, started to develop tools and knowledge for the study of prenylated proteins in BY-2 cells.

The results described in her doctoral thesis (Gerber, 2005) led to the development of an experimental system allowing to visualize the impact of geranylgeranylation on the intracellular localization of a prenylable GFP fusion protein in living plant suspension cells. This *in vivo* visualization system is based on a stably transformed tobacco BY-2 cell line expressing the reporter protein GFP fused to the carboxy-terminal basic domain (DB) of the rice (*Oryza sativa*) calmodulin OsCaM61 (Xiao et al., 1999; Dong et al., 2002). This short polybasic domain bears a CaaL geranylgeranylation motif (CVIL), which is (according to PrePS -Prenylation Prediction Suite (Maurer-Stroh and Eisenhaber, 2005)) predicted to be a substrate of the protein geranylgeranyl transferase PGGT 1.

The expression of the resulting chimeric fusion protein (GFP-DB-CVIL) could be tightly regulated via a dexamethasone-inducible gene expression vector (pTA7001) used for the generation of the stably transformed cell line (Figure 8).

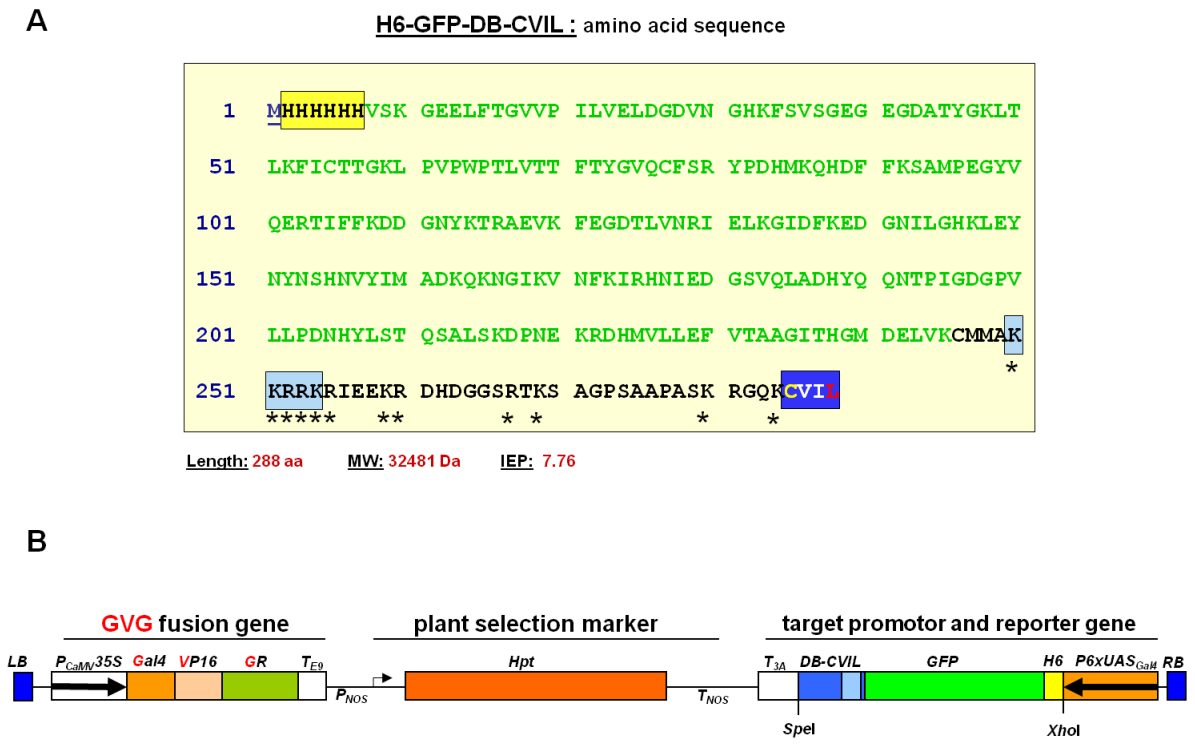

Figure 8. Amino acid sequence of the H6-GFP-DB-CVIL fusion protein and schematic diagram of the pTA7001 vector region relevant for the transformation.

A- H6-GFP-DB-CVIL amino acid sequence The starting methionine is indicated by a blue letter; a N-terminal His-Tag was added in frame with the GFP sequence; green letters, mRFP sequence. The position of the His-Tag (HHHHHH) is indicated by the yellow box. Experiments carried out by Esther Gerber (2005) used the same polypeptide **without** the N-terminal His-Tag. The sequence of the C-terminal basic domain of OsCaM61 (accession number U37936) is displayed in black letters. Asterisks designate the position of basic amino acids. The light blue box indicates the position of a hypothetical NLS sequence found with the NLS prediction software NLSPredict and LocTree (**Table 13**). The dark blue box contains the CaaL-geranylgeranylation motif CVIL. Designations: MW, molecular weight; IEP, isoelectric point. **B-** pTA7001 expression vector, used for the stable transformation of BY-2 cells. For better understanding, only the region between the right (RB) and left borders (LB) of the pTA7001 vector (Aoyama and Chua, 1997) is shown (not to scale). P_{CaMV} is a strong constitutive promotor driving the expression of the chimeric transcription factor consisting of the DNA-binding region of the yeast transcription factor GAL4, the transcription activation domain of VP16 and and the hormone-binding domain (HBD) of the rat glucocorticoid receptor (GR). T_{E9} is a polyadenylation sequence. The plant selection marker is the gene of hygromycine phosphotransferase (Hpt) driven by the nopaline synthase promotor (P_{NOS}); T_{NOS}, nopaline synthase poly (A) addition sequence. The second transcription unit, containing the coding sequence of the chimeric H6-GFP-DB-CVIL protein contains a binding site for the chimeric transcription factors (GVG), consisting of six copies of the Gal4 UAS operator sequence fused to the minimal region of the CaMV 35S promotor. T3A – polyadenylation sequence.

2.1.2.1 Main results obtained by Esther Gerber (2005):

Esther Gerber used this resulting transgenic cell line to perform a series of experiments to study various aspects of protein isoprenylation and the origin of prenyldiphosphate substrates involved in the model system of tobacco BY-2 cells. The major results that are relevant to understand the experimental test system will be briefly summarized:

1. **The prenylable fusion protein is mainly associated with the plasma membrane of intact tobacco BY-2 cells:**

The results Esther Gerber obtained by microscopic analysis indicated that the fusion protein was predominantly targeted to the plasma membrane of transformed tobacco BY-2 cells, several hours (> 6 h) after induction with dexamethasone. As the fusion protein has a natural prenylation motif, it was supposed that the protein association to membrane was due to the posttranslational modification of the C-terminal tetrapeptide –CVIL by prenylation/geranylgeranylation and subsequent CaaX processing. This hypothesis was supported by the fact that the non-prenylable control protein GFP-DB-C/S (GFP-DB-SVIL), in which the cysteinyl residue of the CVIL-motif has been replaced by a seryl residue, thus removing the –SH group necessary for the covalent attachement of the prenyl moiety, nearly completely translocated to the nucleus and in particular to the nucleoli of the cells. Furthermore, these two distribution patterns of the GFP-fusion proteins were clearly different from that of transiently expressed GFP, which could mainly be found in the cytosol and the nucleoplasm of the transformed cells (Figure 9).

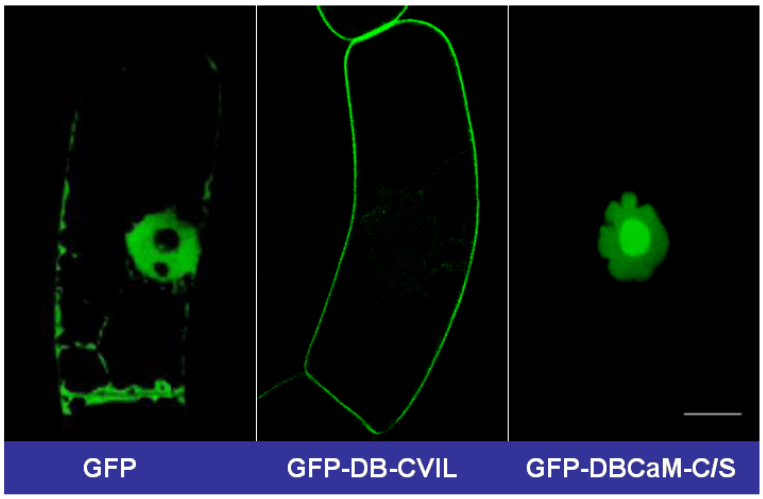

Figure 9: Confocal microscopy images of transformed tobacco BY-2 cells (TBY-2).
GFP- Transiently expressed GFP was mainly found in the cytosol and the nucleus, without staining the nucleolus. **GFP-DB-CVIL-** stably transformed fusion protein with a functional prenylation motif (-CVIL) is

predominantly localized at the PM after induction with dexamethasone. **GFP-DBCaM-C/S-** without a functional prenylation signal (-SVIL), the GFP fusion protein is located in the nuclear compartment with the strongest signal detected in the nucleolus. Images were acquired by confocal microscopy with a LSM510 confocal laser-scanning microscope as described in chapter 4.5.20. The images for the GFP and the GFP-DBCaM expression were taken from the thesis of Esther Gerber (2005). White bar represents 10 µm.

The hypothesis that the peripheral localization of the GFP-DB-CVIL fusion protein observed under standard conditions (induction with 10 µM dexamethasone for 15 h) was mainly caused by its integration into the PM, was verified by two different approaches. First of all, the GFP fluorescence was shown to colocalize with the red fluorescent dye FM4-64, which is known to specifically stain the plasma membrane (Bolte et al., 2004). Secondly, the colocalization of the GFP fusion protein with the FM4-64 stained membrane was maintained after plasmolysis, which was induced by adding the osmoticum D-Mannitol (0,4 M).

2. Inhibition of the isoprenylation reaction triggers a change in the intracellular localisation of GFP-DB-CVIL:

The experiments using the non-prenylable GFP-DB-SVIL fusion protein already demonstrated that a mutation of the acceptor cysteine in the CAAX box led to a completely altered phenotype, consisting in an accumulation of most of the fluorescence in the nucleoplasm and the nucleoli (Figure 9). These results confirmed the assumption that the C-terminal domain of the rice CaM61, which contains a second "signal" in form of a polybasic domain in addition to the prenylation motif, could be sufficient to target the GFP fusion protein to the PM, as it was observed for the full length calmodulin OsCaM61 fused to GFP (Dong et al., 2002) or the petunia CaM53 (Rodríguez-Concepción et al., 1999).
A further proof for the importance of the isoprenylation status for the association of GFP-DB-CVIL to the PM came from a series of experiments using specific chemical inhibitors of both isoprenoid biosynthetic pathways.
These experiments were conducted under standardized conditions that were found to be optimal for the expression of the GFP fusion protein in TBY-2 cells (Figure 10): One-week old BY-2 cultures were diluted 1 to 4 fold in fresh TBY-2 medium before being dispatched into the wells of a commercial 6-well standard plate. Following a 3-hour pre-treatment of the freshly diluted cells with a specific inhibitor, the expression of the GFP-DB-CVIL fusion protein was induced by addition of 10 µM dexamethasone. During this whole period, the cultures were shaken in the dark at 150 rpm and 26°C. After 15 hours, the cells were examined by confocal fluorescence microscopy.

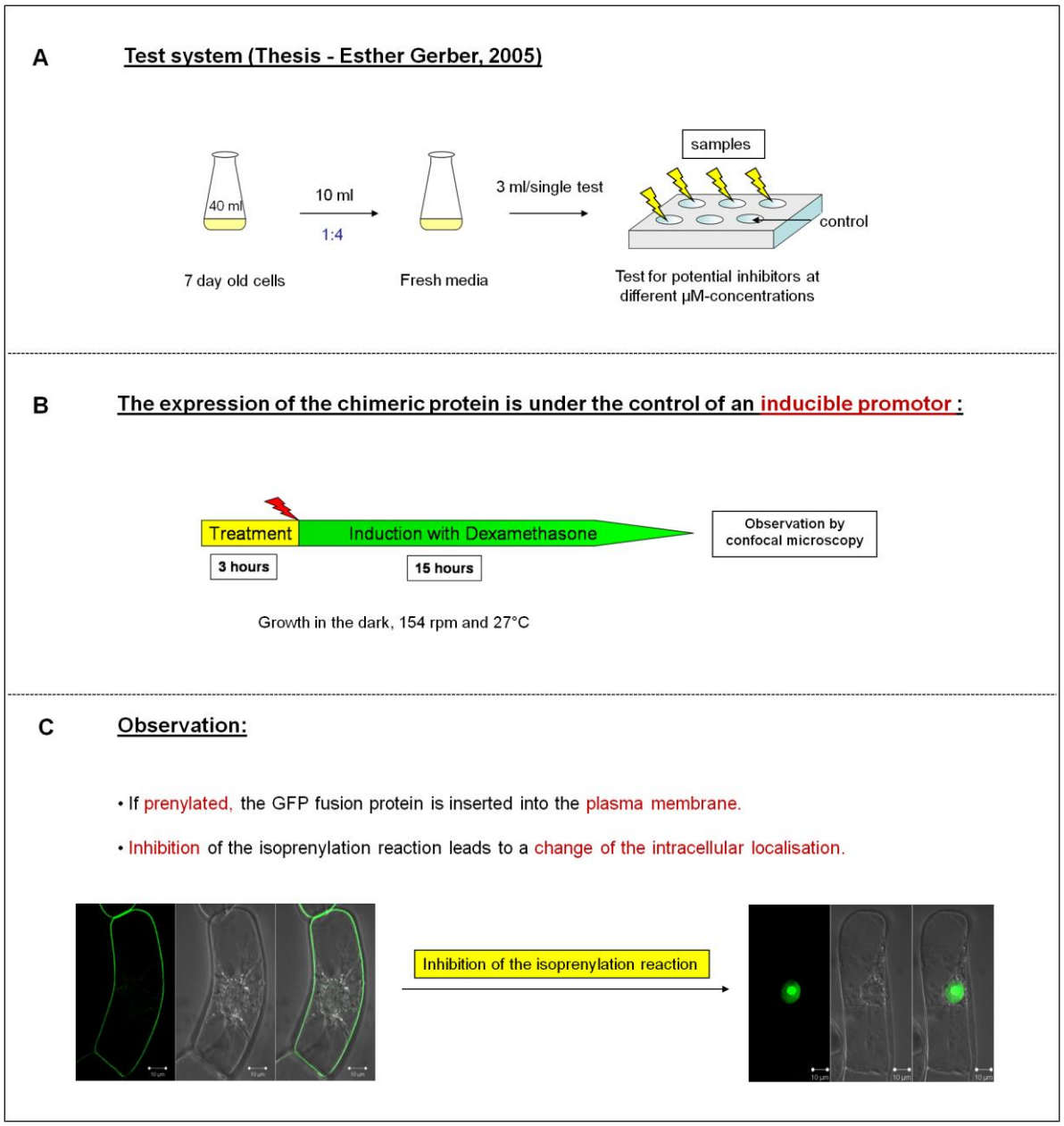

Figure 10. General principle of the test system suggested by Esther Gerber (2005).

A- Experimental setup; **B-** time scale for treatments and induction; **C-** general observations made by Esther Gerber. This bioassay could be used to study the biosynthetic pools of prenyldiphosphate precursors in tobacco BY-2 cells and to screen for potential inhibitors of the plastidial MEP pathway.

Treatments with Fosmidomycin and oxoclomazone, two known inhibitors of the MEP pathway, led to a dramatic mis-localization of the GFP-DB-CVIL fusion protein to the nucleus (Figure 11). Interestingly, the highest intensity of fluorescence was again observed in the nucleoli, in agreement with the results obtained with the non-prenylable GFP-DB-SVIL fusion protein (Figure 9).

On the other hand, treatment with mevinolin, an inhibitor of the MVA pathway enzyme HMG-CoA-reductase (HMGR), did not have any significant effect on the localization of the GFP-DB-CVIL

fusion protein. These results suggested that the MEP pathway played the predominant role in providing the precursors for the prenylation of GFP-DB-CVIL in transgenic tobacco BY-2 cells. Interestingly, the application of mevinolin together with Fosmidomycin or oxoclomazone practically completely prevented the association of the fusion protein to the PM, suggesting some contribution of the MVA pathway to the pool of prenyldiphopshate precursors used for the prenylation of GFP-DB-CVIL (not shown).

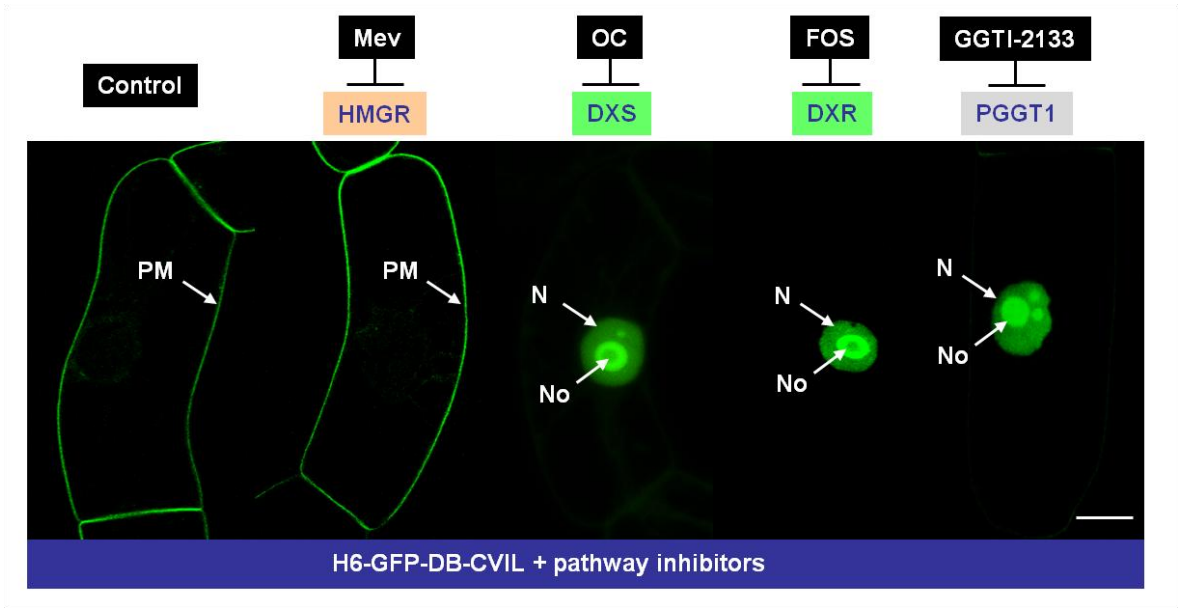

Figure 11. Localization of GFP-DB-CVIL fusion protein in transgenic TBY-2 cells after treatment with inhibitors of key enzymes of the MVA and MEP pathways.

Control cells were induced 15 hours before observation by confocal microscopy as described before. Treatment with inhibitors occurred 3 hours prior to dexamethasone induction. Mevinolin (5 µM) did not cause any detectable effect on the localization of GFP-DB-CVIL fusion protein when compared to the untreated control. GFP fluorescence was predominantly located at the periphery of the cells. By contrast, fosmidomycin as well as oxoclomazone (here, both at 30 µM) caused a mislocalization of the fusion protein to the nucleus and in particular to the nucleolus. The same phenotype could also be observed after application of 40 µM GGTI, a peptidomimetic inhibitor of protein geranylgeranyl transferase 1 (PGGT1). White bar = 10 µm.

In addition, Esther Gerber could show that the GFP-DB-CVIL fusion protein accumulated in the nuclear compartment, after treatment of the cell culture with a specific inhibitor of PGGT1 geranylgeranyl transferase, the peptidomimetic GGTI-2133 (Vasudevan et al., 1999). Treatment of the cell line with known inhibitors of animal farnesyl transferases, the peptidomimetic B581 (Garcia et al., 1993; Cox et al., 1994) and the FPP-substrat analog PFTI-I (Patel et al., 1995) did however not significantly change the localization of the GFP-DB-CVIL fusion protein, further supporting the hypothesis that the GFP-DB-CVIL is mainly geranylgeranylated *in vivo* (Gerber, 2005).

3. The prenyl moiety used for the prenylation of GFP-DB-CVIL is predominantly provided by the plastidial MEP pathway:

Among other experiments, chemical complementation assays were performed to determine if the inhibitory effects of Fosmidomycin and oxoclomazone (40 µM) could be overcome by external feeding with pathway intermediates (MVA: 3mM) and isoprenols (Gol, Fol and GGol: 20 µM each). Whereas geraniol (Gol) did not significantly counteract the accumulation of GFP-DB-CVIL in the nucleus, farnesol (Fol) was able to partially overcome (>60%) the inhibitor effects. External feeding of MVA and GGol did more or less completely trigger recovery of the GFP fluorescence at the PM under defined experimental conditions (3 h pre-treatment, then induction with dexamethasone and addition of intermediates and isoprenols 15 h before observation) (Figure 12)(Gerber, 2005).

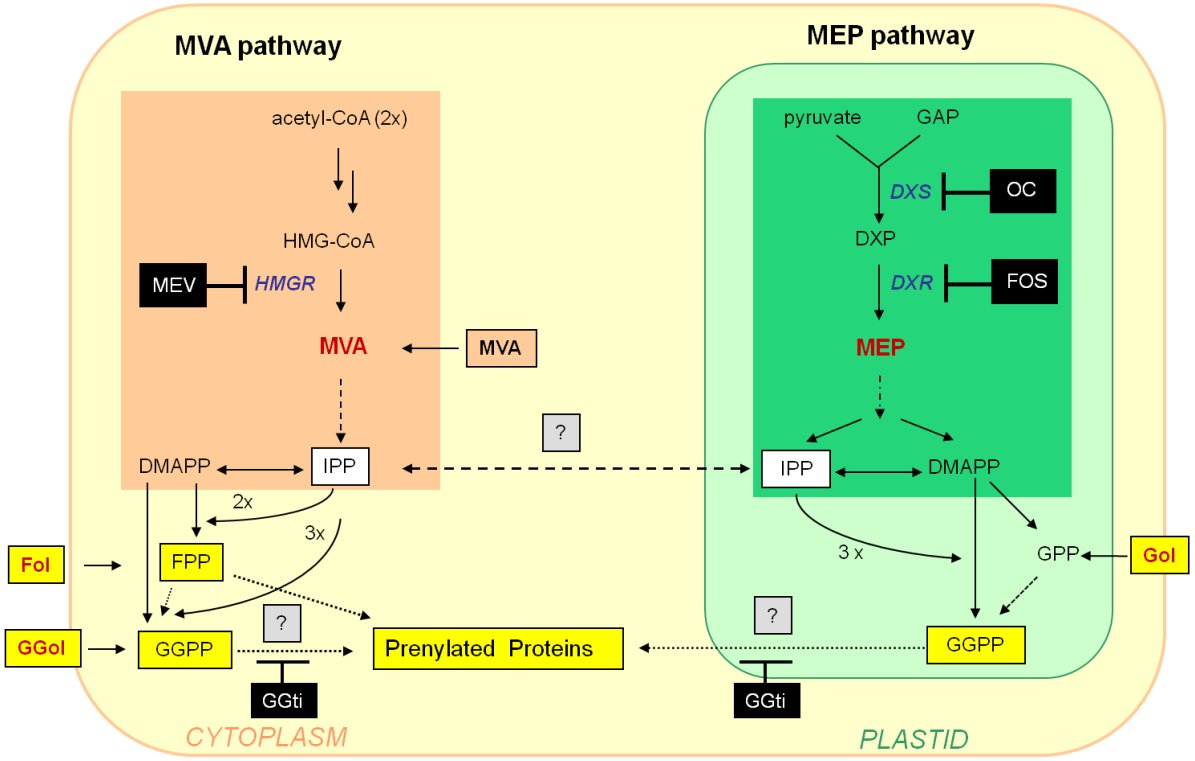

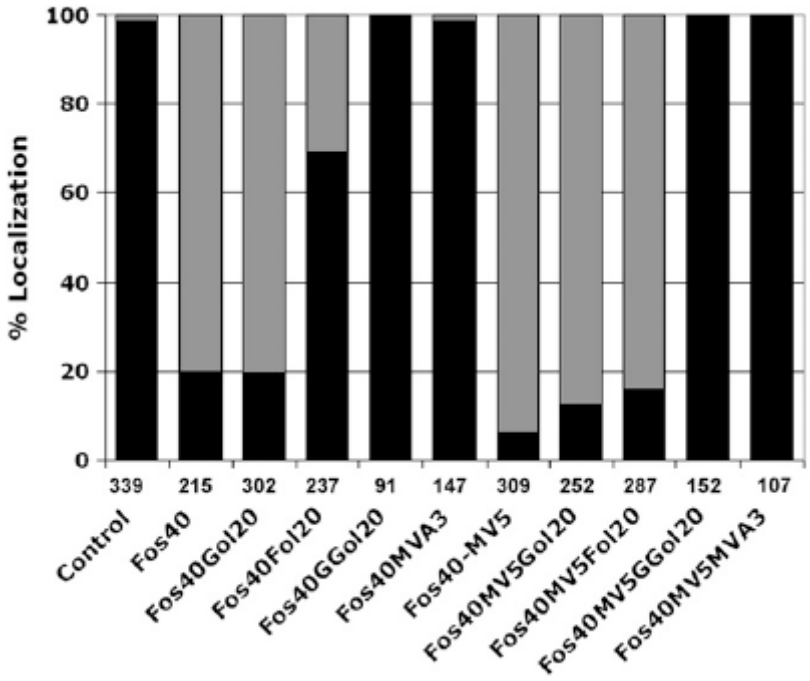

Figure 12. *In vivo* inhibition of GFP-DB-CVIL prenylation and chemical complementation with pathway intermediates and isoprenols.

The generation of the prenyldiphosphate precursors FPP and GGPP is an essential prerequisite for the isoprenylation of proteins. The experiments by Esther Gerber were performed with the GFP-DB-CVIL fusion protein, which contains targeting sequences of the rice calmodulin fused to the C-terminus of GFP. As only the C-terminal basic domain of the calmodulin was used, the fusion protein was supposed to be biologically inert, leaving the membrane trafficking and the lipidation reactions fully functional (Gerber et al., 2009). Experiments carried out with both cell lines (GFP-DB-CVIL and H6-GFP-DB-CVIL) indicated that the MEP pathway seemed to be the primary source of GGPP used for protein geranylgeranylation in our model system tobacco BY-2 cells. This conclusion was based on the observation that the inhibition of the MEP pathway or more specifically of the key enzymes DXS and DXR by addition of 40 µM oxoclomazone (OC) or Fosmidomycin (Fos), respectively, shifted the fusion protein from its predominant localization on the periphery of the cell to the nucleus. By contrast, inhibition of the MVA pathway enzyme HMGR by addition of 5µM Mevinolin (MV) had no detectable effect on the localization. The same partial translocation from the PM to the nucleus/nucleolus was obtained by addition of the specific geranylgeranyl transferase inhibitor GGTI-2133 at 30 µM. Chemical complementation experiments with isoprenols and pathway intermediates, applied at various concentrations (MVA at 3 mM and Gol, Fol and GGol at 5, 10 and 20 µm), showed that only MVA and GGol could completely restore the plasma membrane localization of the GFP-DB-CVIL fusion protein, whereas Gol barely had an effect and Fol only partially complemented the inhibitory effect (50-60%).

These results led to different conclusions:

A major determinant for protein isoprenylation is the generation of the prenyldiphosphate precursors, farnesyl diphosphate (FPP) and geranygeranyl diphosphate (GGPP), used as substrates by the respective protein prenyltransferases. In plants, as already discussed extensively before, two more or less compartimentalized isoprenoid biosynthetic pathways operate, the cytosolic MVA pathway as

well as the plastidial MEP pathway. However their respective contribution to the pool of precursors, needed for the isoprenylation of proteins, is largely unclear. Until a decade ago, it was assumed that the cytosolic MVA pathway was the main source for FPP and GGPP used for the prenylation of proteins in plant cells (Crowell, 2000), which was to some extent supported by incorporation studies with radiolabeled MVA conducted in tobacco BY-2 cells and spinach seedlings (Randall et al., 1993; Shipton et al., 1995) As the prenylation and subsequent CaaX processing reactions take place in the cytosol/ER this assunption was not really called into question, even after the elucidation of the plastidial MEP pathway in plant cells (Rohmer, 1999).

However, different studies casted a shadow of doubt on this theory, including the work from our lab (Hemmerlin et al., 2003), showing that radiolabelled DX, which could serve as precursor for DXP in the plastid, was incorporated in proteins in TBY-2 cells. This study is particularly interesting for two reasons: first of all, it was conducted with the same model system used by Esther Gerber and secondly, it was a further proof for an exchange of prenyldiphosphate precursors ("crosstalk") between the two isoprenoid pathways, demonstrating that MEP derived isoprenoids could be used by cytosolic protein isoprenyltransferases to modify cellular proteins.

The fact that the inhibition of the MEP pathway by specific inhibitors led to an accumulation of the GFP fluorescence in the nucleus, whereas inhibition of the MVA pathway did not have any effect, definitely demonstrated that the prenyldiphosphates used for the isoprenylation of GFP-DB-CVIL were derived from the MEP pathway in TBY-2 cells.

As only the inhibition of the protein-geranylgeranyl transferase triggered the same response, it was also quite probable that the prenyldiphosphate in question was most likely GGPP.

Interestingly, MVA and GGol as well as Fol were able to partially overcome the inhibitory effects induced by the treatments with Fos and OC. This proved two things: First of all, these compounds were successfully imported into the TBY-2 cells, and then metabolized into the prenyldiphosphate precursor(s) used for prenylation (most likely GGPP). As the MEP pathway was found to be the major source for this substrate, it however remained unclear, where the biological activation of the isoprenols, the conversion to their respective prenyldiphosphates took place and how both pathways interacted at this point.

2.1.3 The beginning of my work

As indicated above, at the end of Esther Gerber's thesis, several questions remained unsolved. The most important one was the definite chemical proof that GFP-DB-CVIL was geranylgeranylated *in vivo*.

Further radiolabelling experiments with [^{3}H]-GGPP and [^{3}H]-FPP demonstrated that GFP-DB-CVIL expressed in *E.coli* cells was specifically geranylgeranylated when used in *in vitro* assays with BY-2 cell free extracts (later published in Gerber et al., 2009). Consequently, the next logical step was the purification of the prenylated fusion protein for chemical analyses.

Therefore one of the first tasks upon my arrival in the group of Professor Bach was the generation of a TBY-2 cell line with a His-tagged version of GFP-DB-CVIL (referred to as H6-GFP-DB-CVIL) in order to possibly facilitate the purification of the protein from TBY-2 cells (Figure 8).

2.1.3.1 Generation of a stably transformed, clonal H6-GFP-DB-CVIL cell line

At this point, it is important to mention that Esther Gerber used a simplified version of the *Agrobacterium*-mediated protocol for the stable transformation of TBY-2 cells in order to obtain fluorescent cultures more quickly. This protocol skipped the selection of individual calli on antibiotic-supplemented solid MS-BY2 plates by selecting positive transformants directly in liquid medium. This method has the advantage to yield "working cultures" in a much shorter time scale as it could be achieved with the "classical protocol" that relies on the time-consuming microscopical selection of individual calli (chapter 2.3).

On the other hand, the major disadvantage of using this approach was that all those experiments were carried out with stably transformed cultures, consisting of a collection of agroinfected cells instead of individual clones (Gerber, 2005).

As such cultures tend to display a high heterogenity in the expression of recombinant proteins for various reasons such as the locus of insertion, the number of individual copies, etc. (Pröls and Meyer, 1992; Iglesias et al., 1997; van Leeuwen et al., 2001), it was therefore essential to generate a clonal selection of the H6-GFP-DB-CVIL to confirm the initial results obtained by Esther Gerber (besides the reason that the original GFP-DB-CVIL line did not exist anymore).

Thus, my first experiments focused on adjusting the *Agrobacterium tumefaciens* - mediated transformation protocol (An, 1985) for the generation of stably transformed BY-2 cultures (chapter 4.5.5). These attempts were successful after a few months and first calli were obtained. As soon as these calli reached a critical size (~4 weeks after the transformation), they were transferred onto new plates supplemented with the respective antibiotic (pTA7001: 30 µg/ml Hygromycin) for at least two weeks. Liquid suspensions were then prepared by gently resuspending a portion of the calli in 10 ml of

liquid media containing the required antibiotic. These suspensions were subcultured in fresh tobacco BY-2 medium as soon as they reached the stationary growth phase and after one additional week, the resulting culture was tested for GFP expression according to the protocol described in Figure 10 A.

With this protocol, 48 suspension cultures were tested for inducible GFP expression using fluorescence microscopy. Out of those 48 cultures, 23 (~48 %) contained fluorescent cells. However, only four of those cultures had cells with high intensities of fluorescence under our induction conditions (10 µM dexamethasone, 15 h induction).

These suspension cultures were sufficient to perfom the first tests. As only a certain ratio of those cells was strongly fluorescent, the two best performing suspension cultures were used to generate secondary calli, using a very early version of the protocol described in chapter 4.5.5.3. After repeating the above-described steps, the secondary suspensions were tested until two highly fluorescent cell suspension lines with more than 90% of cells with induced GFP expression were found. The best performing cell line (L1-16) was then used for further experiments (Figure 13). The generation of those homogenously expressing transgenic lines was particularly important for the purification of the H6-GFP-DB-CVIL fusion protein (Gerber et al., 2009).

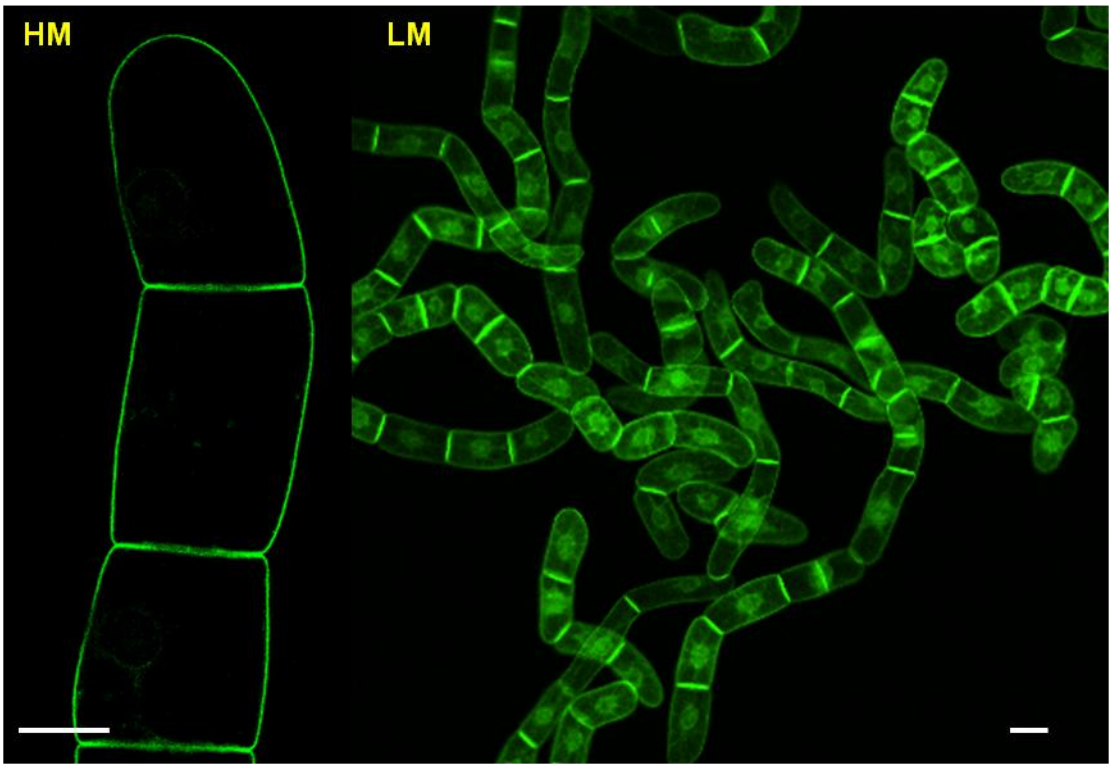

Figure 13. Clonal transgenic tobacco BY-2 cell line expressing the H6-GFP-DB-CVIL fusion protein.

GFP expression was induced according to the previously dsecribed standard protocol. Both images were taken with a confocal laser scanning microscope (Zeiss LSM510 equipped with an inverted Axiovert 100M). **HM-** High magnification image taken with a 63 x water immersion objective (C-Apochromat 63x/1.2W M27), that is specifically designed for the examination of an aqueous specimen and delivers high resolution in optical thin sections, with satisfying levels of fluorescence brightness. **LM-** Low magnification image taken with a 10 x "Enhanced Contrast Plan-Neofluar" universal objective (EC Plan-Neofluar 10x/0,3 M27), adapted for general

observations in fluorescence microscopy. If not otherwise stated, the label HM and LM designates the use of these both types of objectives for the image acquisition with the confocal laser scanning microscope. White bars = 20 µM. Please note the different saturation of the images and the significantly higher saturation in the LM image that was used to highlight the homogenous levels of bright fluorescence of the re-selected clonal cell line.

The purification and analysis of the H6-GFP-DB-CVIL protein from treated and untreated tobacco BY-2 cultures, conducted in our group, finally revealed that the plasma membrane-associated form was geranylgeranylated and carboxyl-methylated *in vivo* (Gerber et al., 2009), which corroborated the results obtained during the studies of Esther Gerber (2005).

Verification of the results obtained by Esther with the newly transformed cell line:

In order to determine whether Esther's results were reproducible with the new transgenic cell line expressing H6-GFP-DB-CVIL, instead of the non-His-tagged version of the protein, all major inhibitor treatments and chemical complementations performed during the thesis of Esther Gerber (2005) were repeated. However, to avoid too much redundancy at this point, only the missing complementation experiments relevant for the paper from our group in 2009 (Gerber et al., Plant Cell 2009) will be shown.

2.1.3.2 DX completely restores the PM localization of H6-GFP-DB-CVIL in cells treated with oxoclomazone (OC)

During the experiments of Esther Gerber, Fosmidomycin as well as oxoclomazone (5-ketoclomazone) were used to inhibit the biosynthesis of prenyldiphosphate precursors through the MEP pathway. Whereas the molecular target of Fosmidomycin, DXR, has been identified shortly after the elucidation of the MEP pathway (Kuzuyama et al., 1998), the situation for oxoclomazone was far less clear. Oxoclomazone is known to be one of the metabolites that can be found in plants after application of the herbicide clomazone (also referred to as dimethazone) (ElNaggar et al., 1992; Liu et al., 1996) (TenBrook and Tjeerdema, 2006). As mentionned before, clomazone is a soil-applied pre-emergence herbicide that has been developped for the use against annually emerging broad-leafed and grassy weeds, menacing a number of crops, including soybeans, sugar cane, corn, cotton, tobacco and rice (Warfield et al., 1985; Chang et al., 1987; FMC corporation, 2001).

Application of clomazone leads to a bleaching phenotype in susceptible plants, which is mainly caused by a dramatic decrease in chlorophyll and carotenoid contents (Duke and Kenyon, 1986; Weimer et al., 1992) This loss of photosynthetic pigments was attributed to an inhibition of the biosynthesis of chloroplast-bound isoprenoids in general (Sandman and Boger, 1986) which correlated with the

impaired chloroplast development, commonly observed in clomazone-treated plants (Sandman and Boger, 1986) (Duke et al., 1985; Duke and Kenyon, 1986; Duke and Paul, 1986; Argenta and Lopes, 1991).

For several years, the site of action of clomazone remained a mystery, although different studies narrowed down the possible target sites and showed that the inhibition had to occur before the synthesis of IPP (Sandman and Boger, 1987; Lutzov et al., 1990; Zeidler et al., 2000). It took several years until it was shown that clomazone itself did not induce the toxicity observed in green plants but that it was rather one of the breakdown products, such as oxoclomazone, which inhibited the formation of IPP in the plastidial MEP pathway. The final proof was provided by Müller et al. (2000), who were able to demonstrate that oxoclomazone inhibited DXS, the enzyme catalyzing the first step of the MEP pathway that had just been elucidated shortly before. The fact that oxoclomazone was the bioactive metabolite of clomazone and acted on DXS was later confirmed by Ferhatoglu et *al.* (2006) by *in vitro* assays using intact spinach chloroplasts. Interestingly, oxoclomazone was already shown to be an active herbicide nearly 20 years before (Chang et al., 1987) and assumed to be one of the metabolites that strongly contributed to the herbicidal potency of clomazone (ElNaggar et al., 1992; Zeidler et al., 2000).

Recent studies also gave evidence for a P450-mediated bioactivation of clomazone in susceptible plants (Ferhatoglu et al., 2005; Yasuor et al., 2008; Yasuor et al., 2010), explaining earlier observations made with oxoclomazone-susceptible and -tolerant plant species (Norman et al., 1990a, , 1990c).

Experiments in barley leaves demonstrated that the effects induced by addition of oxoclomazone could partially be reversed by DXP, the product of DXS (Zeidler et al., 2000). The same year, Estevez et *al.* (2000) were able to show that DX could successfully overcome the bleaching phenotype of the *Arabidopsis* knock-out mutant *cla1*. Incorporation of DX in bacteria and plants has been successfully shown in severeal cases (Lois et al., 2000; Wolfertz et al., 2004). Recent studies in our group provided evidence for a cytosolic D-xylulose kinase identified from *Arabidopsis thaliana* protein extracts that was able to catalyze the phosphorylation of DX to DXP in *in vitro* assays, suggesting a sequence of events leading to the final import of DXP into the plastidial compartment. Furthermore, complementation experiments with knock-out-mutants of DXS treated with oxoclomazone and DX showed that this cytosolic D-xylulose kinase was responsible for the phosphorylation of DX *in planta* (Hemmerlin et al., 2006).

In initial screenings, both *Arabidopsis* and TBY-2 protein extracts were able to phosphorylate DX, but later *Arabidopis thaliana* was chosen for the cloning because of obvious advantages, such as genomic ressources and availibility of T-DNA insertion mutants. These data strongly suggested that TBY-2 cells should also be able to overcome the inhibition of DXS caused by oxoclomazone treatment.

In our visual bioassay, based on the prenylable H6-GFP-DB-CVIl, this inhibition is indicated by a clear phenotype, the accumulation of GFP fluorescence in the nucleus. To test the hypothesis that DX can also be incorporated in the plastidial MEP pathway in TBY-2 cell, oxoclomazone and fosmidomycine–treated cell cultures were incubated with DX (Figure 14). As a positive control, both inhibitor-treated cell cultures were complemented by addition of the isoprenol GGOH that was able to completely overcome the inhibition of both compounds in previous experiments at very low concentrations (Gerber, 2005).

Results:

As suggested by earlier studies (Estévez et al., 2000; Wolfertz et al., 2004; Hemmerlin et al., 2006), DX was able to overcome the inhibitory effects induced by treatments of the transgenic TBY-2 cell line with oxoclomazone (OC). The complete recovery of fluorescence in the PM of all the cells after DX addition was surprising and suggested a very efficient integration of DX into the plastidial MEP pathway. This result is in line with the observations made by Hemmerlin et *al.* (2006) and demonstrates that TBY-2 cells are able to import DX from the extracellular medium, to phosphorylate and to transport it into the plastid (in whatever sequence of events), where it is used as precursor for the biosynthesis of IPP/DMAPP and /or GGPP. The latter, whether of plastidial or cytosolic origin, was then incorporated into the prenylated H6-GFP-DB-CVIL fusion protein.

As a proof of the concept that DX is specifically bypassing the DXS catalyzed reaction, cells were treated in parallel with Fosmidomycin, which inhibits DXR, the enzyme that catalyzes the conversion from DXP to MEP. As expected, DX was not able to overcome the inhibition, whereas addition of GGol completely reversed the effects of both inhibitors in all observed cells.

Treatment (Abbreviation)	MW [g/Mol]	Solvant	Stock solution	Final concentration
Oxoclomazone (OC)	253,69	MeOH	100 mM	40 µM
Fosmidomycin (FOS)	183,1	H2O	100 mM	40 µMM
1-deoxy-D-xylulose (DX)	134,13	H2O	150 mM	0,5 mM
Geranylgeraniol (GGOH)	290,5	EtOH	20 mM	5, 10 and 20 µM

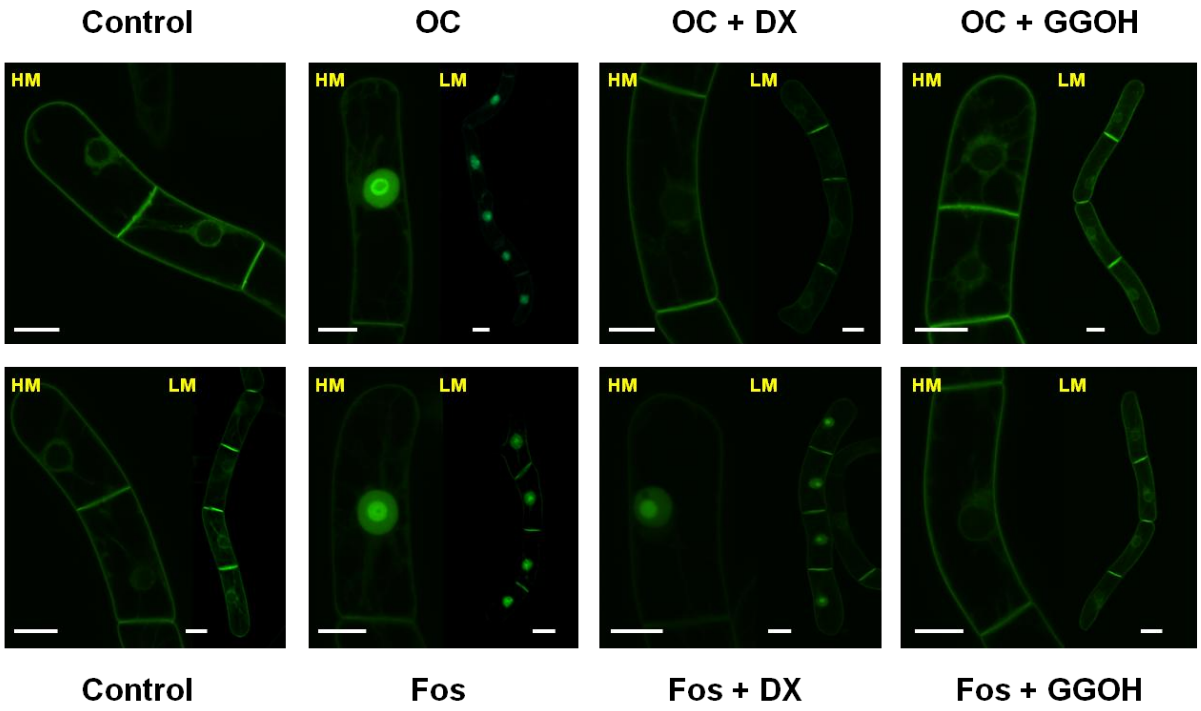

Figure 14. Localization of the H6-GFP-DB-CVIL fusion protein after treatment of TBY-2 cells with oxoclomazone (OC) and Fosmidomycin (Fos) and complementation assays with the MEP pathway intermediate DX and the isoprenol GGOH.

Control- Control cells were treated with the respective solvants (compare table above). Both oxoclomazone and Fosmidomycin induced a very important mislocalization of the fusion protein (more than 95 % of OC treated cells and more than 85 % of Fos-treated cells). DX successfully complemented OC treatments (at 100 %, no single cell with a partial mislocalization was observed in over 300 counted cells), whereas it did not visibly change the ratio of cells showing a mislocalization in Fos-treated cultures. GGOH was used as a second control and entirely complemented all observed cells after treatments with both inhibitors. HM = high magnification; LM = low magnification. White bars represent 20 µm.

The results obtained by this particular complementation experiment were very interesting, as they not only confirmed the observations by Hemmerlin et al., (2006), made with BY-2 cell extracts, but showed that the inhibition of the two key enzymes of the MEP pathway can be distinguished by chemical complementation (Figure 16 A).

This validated the bioassay as a tool to study the metabolic flux of isoprenols and prenlydiphosphates through both pathways and as a test system for potential inhibitors of the (plastidial) MEP pathway or PGGT-1 (Figure 15 and Figure 16).

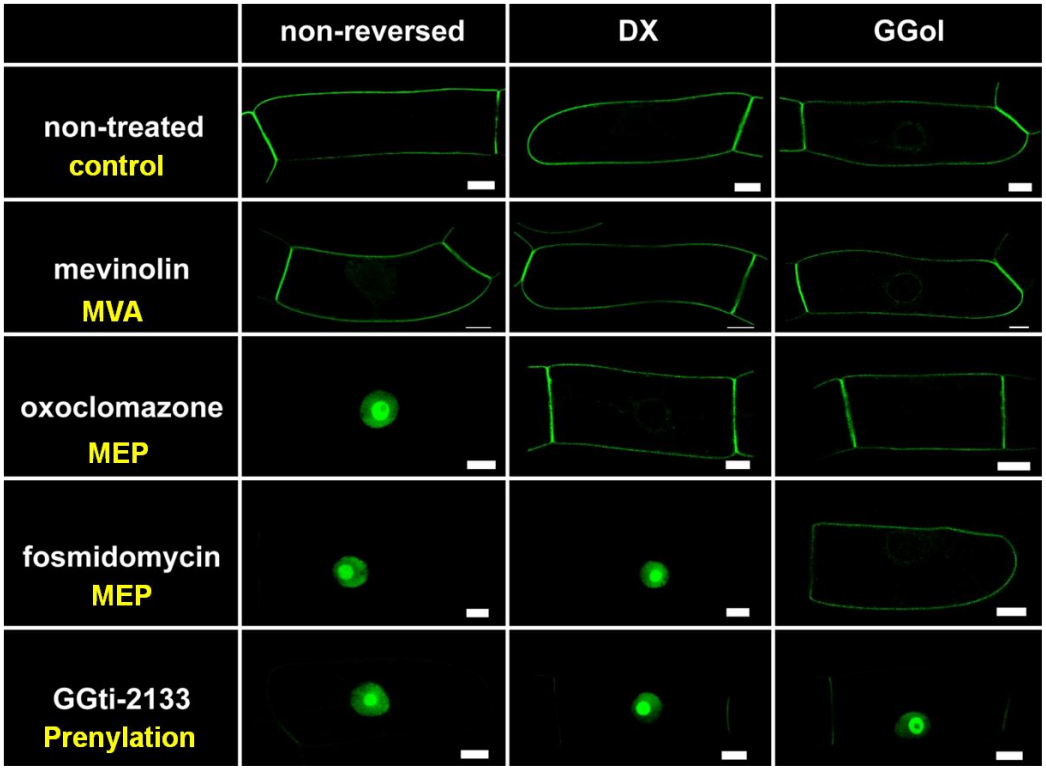

Figure 15. Chemical complementation assays and the phenotypes that were induced by various treatments.

Treatments and image acquisitions were carried out according to standard protocols, with mevinolin (5 µM), oxoclomazone and Fosmidomycin (40 µM), DX (0,5 mM), GGol (5 µM) and GGti-2133 (30 µM). White bars = 10 µm.

However, as indicated earlier, BY-2 cells represent a very particular model system, especially because they do not have differentiated plastids and synthesize significantly less MEP-derived isoprenoids than photosynthetically active plants. This lack of chloroplasts, as well as the presence of high concentrations of sucrose in the culture medium very likely causes a completely different metabolic situation in BY-2 cells. Therefore, results should always be evaluated and interpreted very carefully.

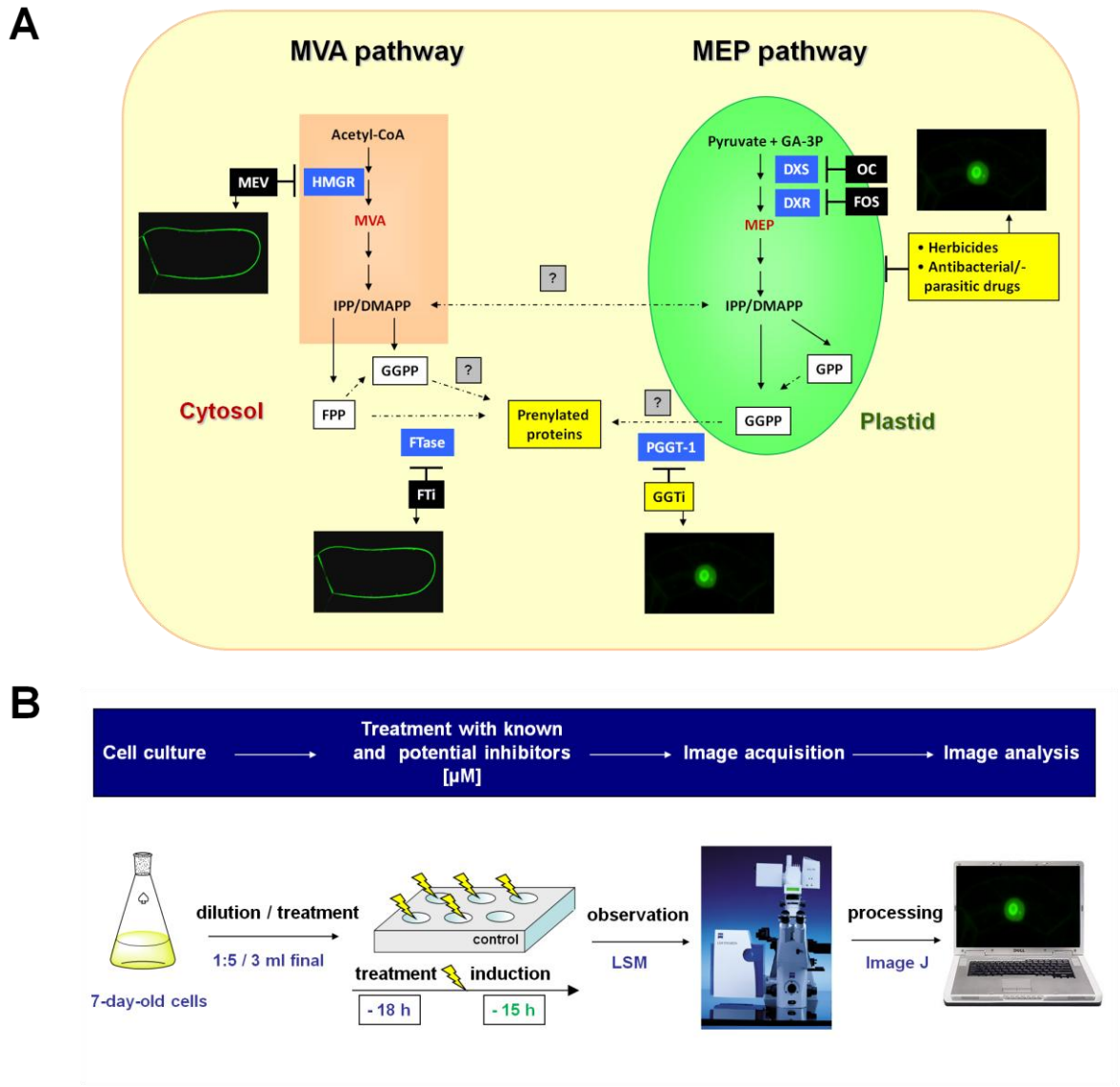

Figure 16. Pathways for isoprenoid biosynthesis in plant cells and visualization of the phenotypes observed after various treatments.

A- Phenotypes observed after treatments of the transgenic H6-GFP-DB-CVIL cell line with inhibitors of both isoprenoid biosynthetic pathways. B- Setup of the bioassay developped during the studies of Esther Gerber (2005) and used for my experiments with the generated (clonal) H6-GFP-DB-CVIL cell line.

Many new results, but more new questions!

The results obtained with the prenylable fusion protein H6-GFP-DB-CVIL so far showed that the MEP pathway was the predominant source of the GGPP used for the geranylgeranylation of the transgenic reporter protein and perhaps for all proteins in TBY-2 cells.

This very remarkable result raises the question whether GGPP is synthesized by a plastidial GGPP synthase and then exported by a still unknown transport mechanism, or whether MEP-derived IPP/DMAPP and/or GPP are exported instead and processed by cytosolic prenyl diphosphate synthases, thereby providing the GGPP used for the prenylation reaction.

As mentioned before, there is strong evidence for a crosstalk between the two isoprenoid biosynthetic pathways and export of plastid-derived prenyldiphosphates to the cytosol has been shown on several occasions, in different plant species. For instance, it has been reported in chamomile (*Matricaria recutita*) and snapdragon (*Antirrhinum majus*) that sesquiterpenoids, which are considered to be exclusively synthesized in the cytosol via the MVA-pathway (Tholl, 2006), may in some cases contain IPP and DMAPP units of plastid origin (Adam et al., 1999; Dudareva et al., 2005). According to Dudareva et al. (2005), IPP and DMAPP would be exported to the cytosol and converted to FPP by a cytosolic FPP synthase (FPS). This was supported by earlier reports on the transport of isoprenyl diphosphates, in particular, IPP and DMAPP, from the plastid to the cytosol (Bick and Lange, 2003).

The fact that radiolabeled DX was incorporated in low molecular weight proteins in TBY-2 cells clearly demonstrates that any scenario involving the export of IPP, GPP or GGPP from the plastid is possible (Hemmerlin et al., 2003).

In addition, *Arabidopsis thaliana*, for instance, possesses several GGPP synthases, with different expression patterns and subcellular localizations. Out of the 12 putative GGPP synthase genes in *Arabidopsis* (Lange and Ghassemian, 2003), five have been further studied by Zhu et al. (1997) and Okada et al. (2000). According to these authors, two GGPP synthases were found in the ER, two in the plastids and one in the mitochondria. Alternatively, a cytosolic FPS could catalyze the conversion of the exported GPP to FPP, which could further be metabolized into GGPP by a cytosolic GGPP synthase. A less likely but nevertheless possible scenario could be a FPP synthase catalyzing the conversion of FPP to GGPP, a reaction occurring *in vitro* under certain conditions (Eberhardt and Rilling, 1975).

In contrast to *Arabidopsis thaliana*, the situation in tobacco BY-2 cells is however to date largely unknown, and for this reason the chemical complementation experiments conducted with the inhibitor-treated cell lines were very useful (Gerber et al., 2009) (Figure 12, page 48):

The chemical complementation experiments were for example performed with Fosmidomycin-treated cells (40 µM), to which the isoprenols, geraniol (Gol), farnesol (Fol) and geranylgeraniol (GGol) were added (20 µM each) simultaneously with the dexamethasone induction.

Whereas externally fed Gol was not able to significantly overcome the Fos-induced delocalization of the GFP fusion protein, Fol was able to partially counteract the effect induced by Fosmidomycin (~ 65 %). The best complementation, however, was observed with GGol at the same concentration, which complemented the inhibitory effect in 100% of cells, thereby even eliminating the 1-5 % of cells that statistically show a partial mislocalization in normal control treatments. Furthermore, the same effect was even observed at concentrations of 5 µM GGol.

This effect can most likely be explained by an efficient uptake of GGol and its conversion to its corresponding diphosphate derivative. Phosphorylation of Fol and GGol in plants has been described previously (Thai et al., 1999) and the observation that exogenously fed, radiolabeled Fol could be incorporated into ubiquinone in TBY-2 cells, strongly supports the existence of a phosphorylation mechanism for isoprenols. Interestingly, the prediction that Gol would not be accepted as a substrate for the described sequentially working phosphorylation system (Thai et al., 1999) correlates with the observation that Gol could not overcome the inhibition of both pathways as Fol and GGol did.

However, Fol only partially complemented the effects observed after Fos treatment and parallel inhibition of the MVA pathway by mevinolin further reduced the complementation.

These observations can be interpreted in different ways:

On one hand, the IPP used for the formation of GGPP, after addition of exogenously applied Fol, would be derived from the MVA pathway. On the other hand, Fol would stimulate the MVA pathway by up-regulating cellular HMGR activity (Hemmerlin and Bach, 2000), the IPP in excess would be imported into the plastids, converted to GPP or GGPP, before being re-exported to the cytosol and used for the prenylation of the GFP-DB-CVIL protein. However, this up-regulation of HMGR activity was observed at Fol concentrations that were considered as highly cytotoxic and only affected a stress-induced HMGR isoform (Hemmerlin et al., 2004). A similar sequence of events could also explain the ability of very high concentrations of MVA (3 mM) to completely overcome the inhibition induced by Fosmidomycin (import of excess MVA-derived IPP into plastids, biosynthesis of GPP or GGPP and re-export to the cytosol). The fact that exogenously applied MVL was able to partially rescue both the developmental arrest of the *dxs*-mutant *cla1-1* (Nagata et al., 2002), and the fosmidomycin-induced growth inhibition of TBY-2 cells (Hemmerlin et al., 2003) supports this interpretation.

A third interpretation in relation to the substrate specificities of the prenyltransferase enzymes (PFT) and GGTase I could be proposed. Whereas the results of *in vivo* prenylation experiments (control and Fos-treated cells) clearly showed that the H6-GFP-DB-CVIL was specifically geranylgeranylated under our experimental conditions, with no detectable farnesylation, the *in vitro* isoprenylation assays suggested that, in the presence of substrates in excess, the substrate specificities might not be absolute. Thus, one could imagine that excess FPP (formed after addition of 3 mM MVA) could be used by FTase to prenylate the fusion protein, in agreement with the observation that application of the geranylgeranyltransferase inhibitor GGTi-2133 together with mevinolin induced a more complete

delocalization than application of only GGTi-2133 (data not shown). A substrate-cross-specificity for FTase isolated from *Arabidopsis thaliana* under in-vitro conditions has only recently been reported by Andrews et *al.* (2010).

Interestingly, although Fol was able to overcome mevinolin-induced cell cycle inhibition in TBY-2 cells, it proved nevertheless to be toxic for cells, at concentrations exceeding 12,5 µM, in long term-treatments (7-days) and 25 µM, in short-term treatments (48 h) (Hemmerlin and Bach, 2000).

Previous studies demonstrated that radiolabeled Fol was incorporated into phytosterols, proteins and mitochondrial ubiquinone, after a two-step conversion to FPP (Thai et al., 1999; Hartmann et al., 2000; Hemmerlin and Bach, 2000). FPP is considered to be synthesized exclusively by the MVA pathway in plants. In *Arabidopsis* for example, FPP synthases are represented by two genes (Cunillera et al., 1996; Cunillera et al., 1997), *FPS1* and *FPS2*, that encode three isozymes with different subcellular localizations (FPS1L, in mitochondria; FPS1S and FPS2, in the cytosol) and only recently, it has been reported that the double knockout of both *Arabidopsis* genes results in a lethal embryonic phenotype, whereas the respective single knockout mutants did not display any major developmental and metabolic defects (Busquets et al.).

In plants, FPP can follow different routes (Figure 17). Firstly, FPP can be converted to squalene by squalene synthase, which is the route leading to phytosterols and brassinosteroids (Benveniste, 2004). Secondly, FPP can be used to synthesize geranylgeranyl diphosphate (GGPP) or dolichols, which are long-chain, poly-unsaturated isoprenoids found in cellular membranes with largely unknown functions (Swiezewskaa and Danikiewiczb, 2005; Zhang et al., 2008). Finally, FPP can be used to prenylate different substrates, including the transfer of the farnesyl moiety to the C-terminus of proteins. This reaction is catalyzed by protein farnesyltransferase (FTase).

Interestingly, FPP might also be dephosporylated *in vivo* to its alcohol farnesol (Nah et al., 2001), as it was shown in animal systems ((Bansal and Vaidya, 1994; Meigs and Simoni, 1997). In addition, there is strong evidence for a recycling mechanism of FPP from isoprenylated proteins, catalyzed by a prenylcysteine lyase (Zhang et al., 1997).

In animals and yeast, it was shown that the three main enzymes using FPP have different affinities for their substrate as attested by a Km value for FPP of about 2 µM, for the squalene synthase (Soltis et al., 1995), of about 1 µM, for the GGPPsynthase (Sagami et al., 1994), and around 5 nM, for the protein farnesyltransferase (Furfine et al., 1995).

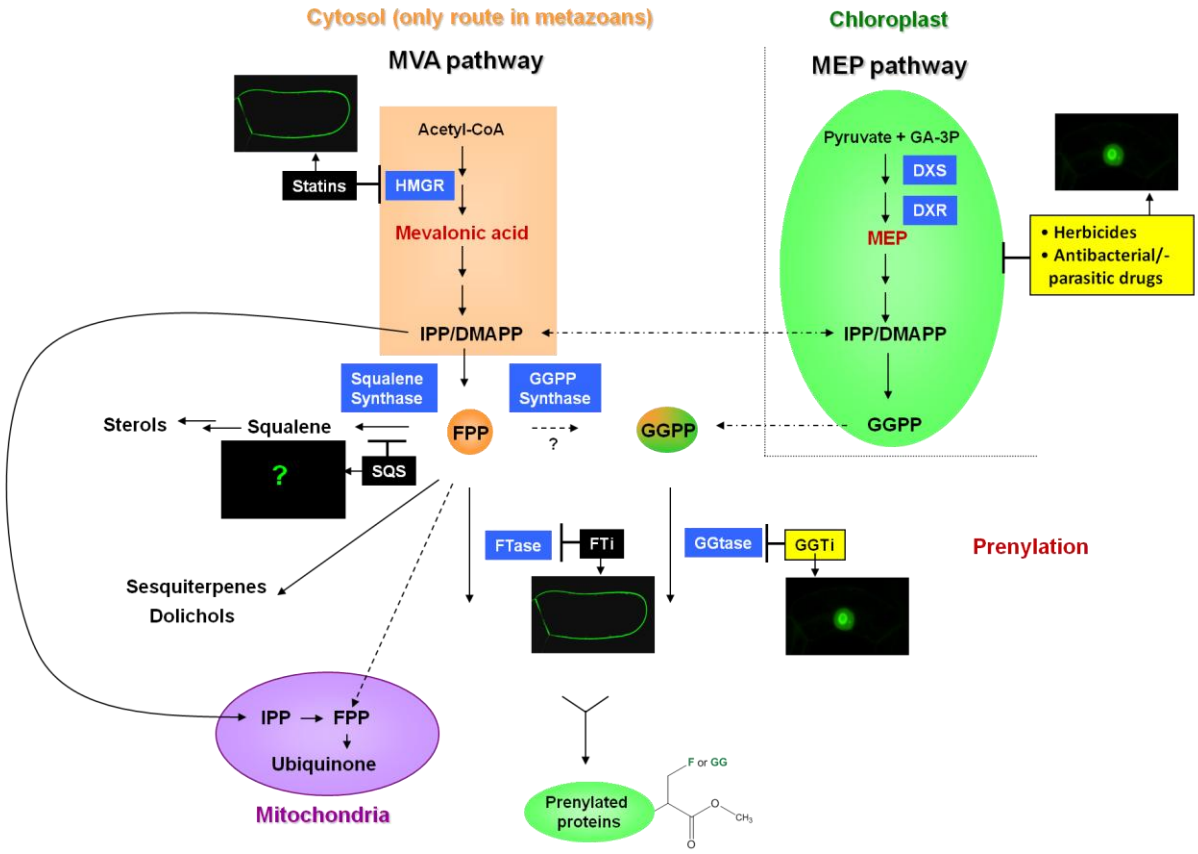

Figure 17. Different metabolic fates of FPP in the plant cell.
FPP can follow different routes in the plant cell. The main route leads to phytosterols, but FPP can also participate to the formation of sesquiterpenes and dolichols as well as ubiquinone synthesis or protein prenylation as a substrate for protein farnesyltransferase or for GGPP synthase.

One can therefore conclude that an inhibition of isoprenoid biosynthesis by statins will have the greatest impact on sterol biosynthesis, closely followed by a decrease in GGPP production, then, in protein farnesylation. This is supported by previous observations showing that the inhibition of the MVA pathway by mevinolin had a strong impact on the biosynthesis of sterols in plants (Bach and Lichtenthaler, 1987; Bach et al., 1990).

Compared to animals and yeast, the situation in plants might be even more complex as different factors strongly influence the pool of FPP and its cellular fates. One of the best-known examples is the down-regulation of sterol biosynthesis and up-regulation of the synthesis of the sesquiterpenoid capsidiol in response to fungal elicitation (Vögeli and Chappell, 1988).

Keeping in mind that the inhibition of the MVA pathway by mevinolin had a significant impact on the capability of Fol to overcome the inhibition of the MEP pathway by Fosmidomycin, we decided to have a closer look on the effects induced by an inhibition of the sterol biosynthetic pathway with specific inhibitors.

In this context, two general considerations have been taken into account:

A block of the sterol biosynthesis should lead to a larger pool of FPP available for other reactions. Thus, 1) will some of this FPP be redirected to the biosynthesis of GGPP and if this is the case, 2) will this GGPP be sufficient to induce a chemical complementation similar to the one observed by addition of Fol or GGol ?

2.1.4 Impact of the inhibition of the sterol biosynthetic pathway on the localization of the H6-GFP-DB-CVIL fusion protein in BY-2 cells

a) Sterols in plants – general facts

Sterols are described as isoprenoid-derived, lipophilic membrane components with essential functions in eukaryotic cells. While only one major sterol is produced in fungal and vertebrate cells, ergosterol and cholesterol, respectively, plant cells contain a complex mixture of so-called "phytosterols" including sitosterol, campesterol (24-methylsterol) and stigmasterol as major constituents (Benveniste, 2004). Although sitosterol appears to be the most abundant plant sterol, as many as 61 sterols and pentacyclic triterpenes have been identified in maize seedlings (Guo et al., 1995). Chemically, phytosterols differ from cholesterol by an extra alkyl (methyl or ethyl) group, located at C-24 in the side chain. The introduction of these alkyl groups is catalyzed by several sterol-C24-methyltransferases. This modification was found to be of central importance for plant growth and development (Schaeffer et al., 2001; Schaller, 2003, , 2004).

Free sterols, such as cholesterol in mammalian cells, are known to intercalate with phospholipids in the membrane bilayer and thereby to directly influence the mechanical properties of the PM by regulating its permeability and fluidity (Schuler et al., 1991; Hartmann, 1998; Mouritsen and Zuckermann, 2004; Roche et al., 2008). In addition, they contribute to the formation of so-called "lipid rafts", which are considered as highly dynamic membrane micro-domains (10-200 nm), with a functional role in the compartmentalization of membranes and cellular processes. In mammalian cells, these micro-domains are enriched with specific proteins that play key functions in various cellular processes, including signal transduction, cell growth and polarization as well as cytoskeleton reorganization and infectious diseases (Simons and Ikonen, 1997; Simons and Toomre, 2000; Freeman and Solomon, 2004; Hancock, 2006) (Guy, 2000; Karpen et al., 2001).

As these rafts are generally characterized by their insolubility in cold non-ionic detergents (*e.g.* Triton X-100), they are also referred to as "detergent-resistant membranes" (DRMs) (Christian et al., 1999; Rothblat et al., 1999).

In plants, however, the situation is less clear and only a few investigations gave evidence for PM micro-domains similar to those described from mammals, *e.g.* in the PM of tobacco (Peskan and Oelmuller, 2000; Mongrand et al., 2004). Analysis of these DRMs from tobacco revealed an increased amount of sphingolipids, phytosterols and steryl-glycosides in these structures as compared to the rest of the PM. Keeping in mind their mammalian counterparts, the characterization of proteins identified in these plant DRMs suggested a crucial role of these structures in cellular signaling events and in the response to biotic and abiotic stresses (Borner et al., 2005; Morel et al., 2006; Lefebvre et al., 2007).

The importance of phytosterols for the formation of plant DRMs was demonstrated only recently in isolated BY-2 PM fractions, after treatment with MßCD, a cyclodextrin that is known to affect the sterol content in mammalian cells, yeast and *Arabidopsis thaliana* (Baumann et al., 2005; Zidovetzki and Levitan, 2007; Kierszniowska et al., 2009). Treatment with MβCD resulted in a 50% decrease in the PM sterol content, thus preventing the isolation of DRMs (Roche et al., 2008). Studies with artificial raft-like structures from plants also showed that the presence of stigmasterol and sitosterol significantly extended the scale of sensitivity to temperatures compared to model membranes containing cholesterol (Beck et al., 2007), supporting the hypothesis that the sterol composition of the plant PM might play a crucial role in the adaptation and response of plants to temperature (Dufourc, 2008; Minami et al., 2009).

Besides their primary role as structural membrane constituents, phytosterols are involved in the embryogenic development, cell division and elongation as well as in cellulose accumulation during cell wall formation (Benveniste, 2004; Suzuki and Muranaka, 2007; Boutte and Grebe, 2009). Finally, phytosterols (campesterol) serve as precursors for brassinosteroids, a class of steroid hormones in plants (Li et al., 1996).

b) Biosynthesis of sterols

The biosynthesis of sterols in higher plants share the same steps as in yeast and mammals until the formation of squalene oxide. (Benveniste, 2004). In the cytosolic MVA pathway, acetyl-CoA serves as the precursor for the formation of IPP, which is converted to DMAPP by Isopentenyl Isomerase1. IPP and DMAPP are then used for the biosynthesis of FPP, catalyzed by the farnesyl diphosphate synthase (FPS). After conversion of FPP to squalene by the squalene synthase (SQS) and the subsequent epoxidation to 2,3-oxido-squalene, catalyzed by the squalene epoxidase (SQE), different routes lead to sterol end products in plants, yeasts and mammals.

In yeast and mammals, 2,3-oxidosqualene is cyclized into lanosterol by lanosterol synthase (LAS); it serves as a precursor for ergosterol and cholesterol, respectively (Baker et al., 1995; Corey et al., 1996). In contrast, phytosterols are almost exclusively synthesized via cycloartenol, the cyclization product of 2,3-oxidosqualene formed by the cycloartenol synthase (CAS) (Corey et al., 1993).

However, recent studies focusing on the lanosterol synthase1 gene (LAS1) from *Arabidopsis thaliana* demonstrated that the lanosterol pathway in this plant was functional and might contribute to about 1,5 % of the sitosterol production (Ohyama et al., 2009). The biological role of this route in plants is still under investigation and the gene expression profile of *Arabidopsis LAS1* suggests that the lanosterol pathway may contribute to the production of plant-defense related secondary metabolites (Zimmermann et al., 2004; Ohyama et al., 2009).

In plants, sterols are synthesized at the endoplasmic reticulum (ER) (Hartmann and Benveniste, 1987; Moreau et al., 1998; Busquets et al., 2008) and supposedly transported to the PM via the trans-Golgi-network (TGN) (Moreau et al., 1998; Grebe et al., 2003).

Phytosterols have recently gained special attention from food and medical industries due to their potential as cholesterol-lowering agents and their anti-cancer effects (AbuMweis and Jones, 2008; Sanclemente et al., 2009; Woyengo et al., 2009).

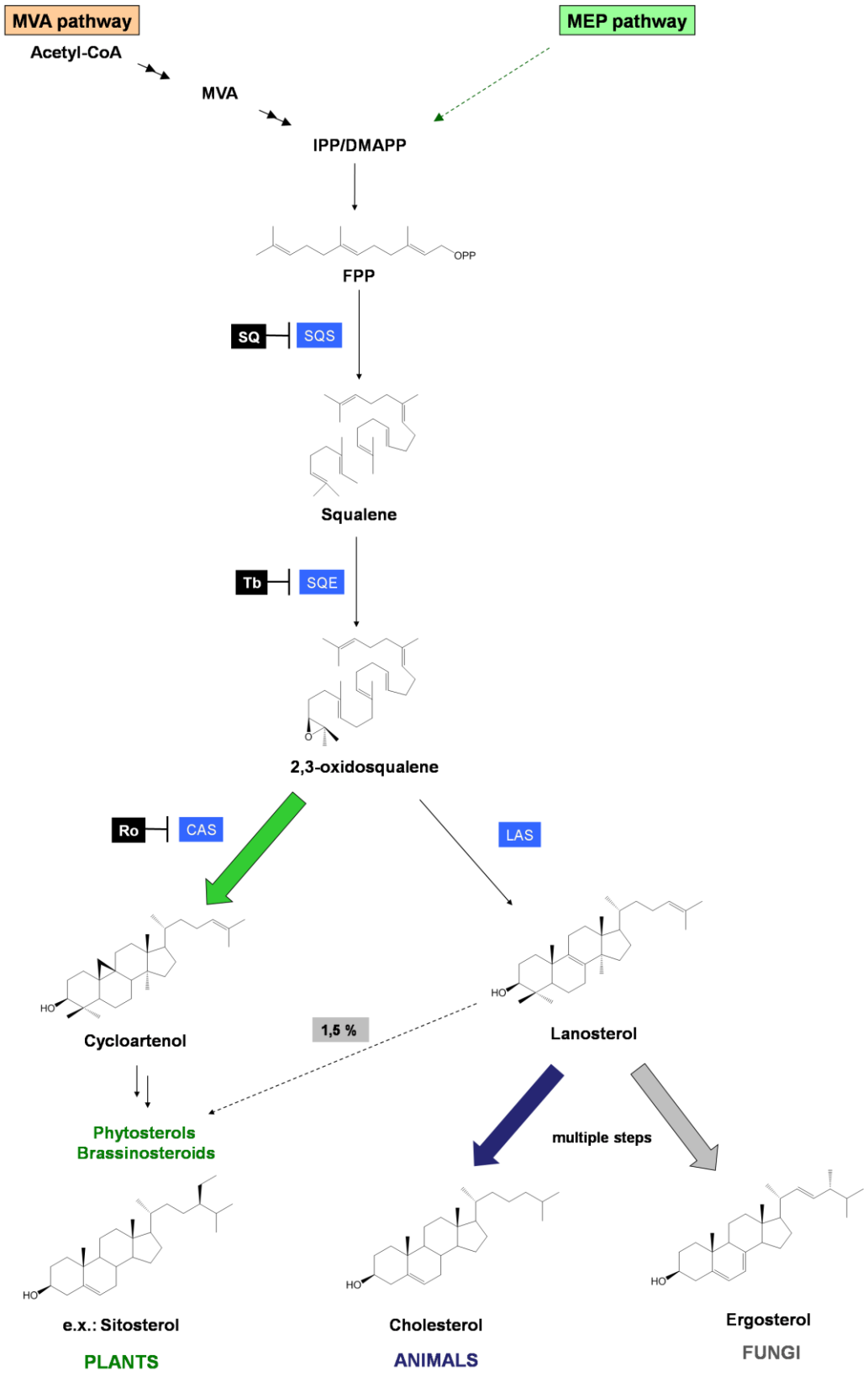

Figure 18. Sterol biosynthesis in yeast, mammals and higher plants.

The rate-limiting step for the biosynthesis of sterols is the formation of mevalonate (MVA) in the cytosolic MVA pathway. In plants, IPP and DMAPP are both produced by the MVA and MEP pathway, whereas the contribution of the MEP pathway to the formation of FPP and sterols remains largely unclear and is still under investigation. The conversion of FPP to squalene and the formation of 2,3-oxidosqualene are catalyzed by the

squalene synthase (SQS) and the squalene epoxydase (SQE), respectively. The pathway of sterol biosynthesis is thought to be identical in all organisms until the cyclization step of 2,3-oxidosqualene. Sterols in plants are synthesized via cycloartenol synthase (CAS), whereas animals and fungi use lanosterol, catalyzed by the lanosterol synthase (LAS) for the production of their respective end sterols, cholesterol and ergosterol. In 2009, however, Ohyama and colleagues observed a minor contribution of lanosterol to the biosynthesis of sitosterol in *Arabidopsis thaliana* seedlings, suggesting that plants might also produce sterols via lanosterol under certain conditions. Squalestatin (Sq), Terbinafine (Tb) as well as Ro48-8071 (Ro) inhibit SQS, SQE and CAS, respectively.

c) Experimental part: Treatment of TBY-2 cells with inhibitors of the sterol biosynthetic pathway

In order to study the effects of inhibiting the sterol pathway on the localization of the H6-GFP-DB-CVIL fusion protein, treatments with three different inhibitors were performed (Table 3):

First of all, **squalestatin-1 (SQ)**, also referred to as zaragozic acid (Baxter et al., 1992), was used to specifically inhibit SQS, which catalyzes the conversion of FPP to squalene. Squalestatin is a competitive inhibitor of SQS (Figure 18. Sterol biosynthesis in yeast, mammals and higher plants.) and structurally mimics the reaction intermediate presqualene diphosphate (Baxter et al., 1992; Bergstrom et al., 1993; Procopiou et al., 1994; Thelin et al., 1994).

Seven day-old TBY-2 cells were diluted at a ratio of 1 to 6 in fresh TBY-2 medium and treated with 1 µM SQ for 18-24 h (in different independent experiments). 15 hours before observation of the cells by fluorescence microscopy, expression of the prenylable fusion protein H6-GFP-DB-CVIL was induced by addition of 10 µM dexamethasone (150 rpm, 26°C, growth in the dark).

The results of this treatment are shown in Figure 20. Two general observations can be made. First of all, treatment with SQ resulted in a partial mislocalization of the prenylated fusion protein from the PM to the nuclear compartment, with the strongest signal being emitted by the nucleolus. In addition, the overall morphology of the treated cells was changed. Cells treated with 0.5 or 1 µM SQ showed stunted growth with clearly reduced length to diameter ratios as compared to control cells.

Secondly, TBY-2 cells were treated as before with **terbinafine (Tb)**, a specific, non-competitive inhibitor of the fungal SQE. In mammals, however, it acts as a competitive inhibitor (Ryder, 1992). Its inhibitory power in plant cells has been demonstrated with celery (*Apium graveolens*) cell suspension cultures (Yates et al., 1991), wheat (*Triticum aestivum*) seedlings (Simmen and Gisi, 1995), cat's claw (*Uncaria tomentosa*) cell suspension cultures (Flores-Sánchez et al., 2002) and with our model system, TBY-2 cell suspension cultures (Wentzinger et al., 2002).

Treatments with Tb were performed at 30 µM up to 24 hours (as well as 18 h). The cells treated with Tb showed a very slightly stunted growth as compared to the control cells and displayed fainted GFP signals in the cytosol, close to the PM. However, no mislocalization of the prenylable fusion protein to the nuclear compartment could be observed under the chosen experimental conditions (Figure 20).

Finally, **Ro48-8071 (Ro)** was used to inhibit one of the key steps of sterol biosynthesis, the conversion of the linear triterpene oxido-squalene into cycloartenol, the first cyclic precursor of phytosterols (Figure 18). This reaction is catalyzed by cycloartenol-synthase (CAS) in plants (Abe et al., 1993). Ro48-8071 is a potent inhibitor of oxidosqualene cyclases (OSC) in general, including lanosterol synthase (LAS) in mammals and fungi (Morand et al., 1997). The structure of Ro48-8071, which is an orally active inhibitor of human hepatic OSC, has been determined in complex with the squalene-hopene cyclase (SHC), the prokaryotic counterpart of OSCs, responsible for the conversion of squalene into cyclic compounds in bacteria, and suggested that Ro48-8071 binds to the expected binding site of squalene (Lenhart et al., 2002).

Ro48-8071 treatments were performed at 2 µg/ml under the same experimental conditions as described previously for SQ and Tb applications. Cells treated with Ro for 18/24 h looked morphologically like the control cells. The GFP fusion protein was mainly localized at the level of the plasma membrane, although there were also fainted signals (small speckles) of fluorescence near the PM like those observed for the previous Tb treatments. However, no mislocalization of the GFP fluorescence to the nucleus/nucleolus was observed.

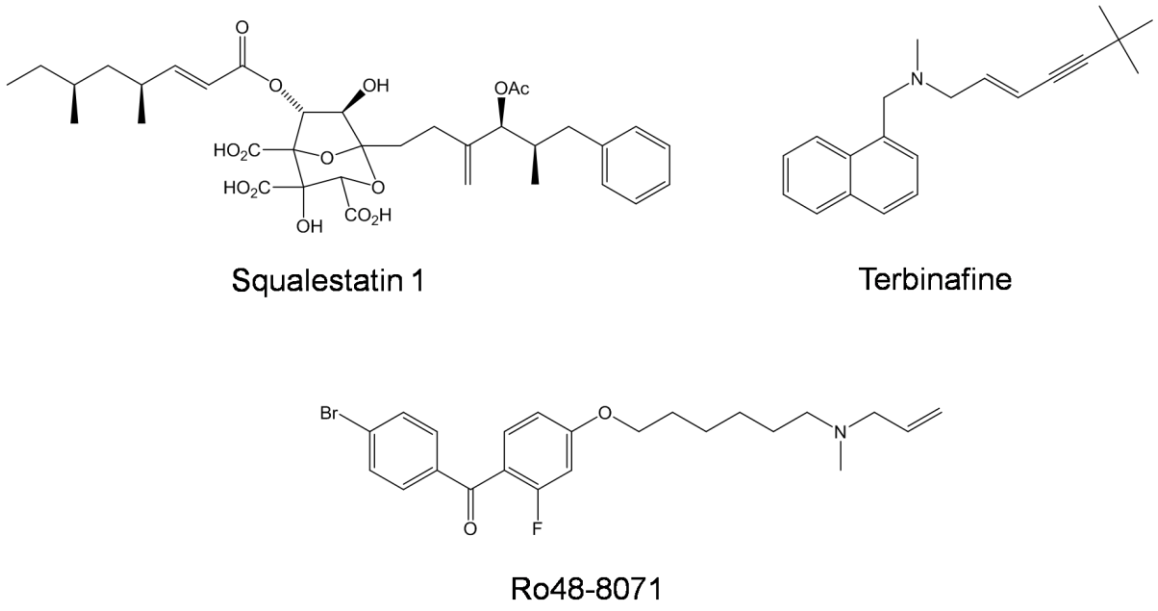

Figure 19. Inhibitors of sterol biosynthesis used in this work

Inhibitor (Abbr.)	MW [g/Mol]	Solvant	Stock solution	Final concentration(s)
Squalestatin (SQ)	804,93	KH_2PO_4 (50 mM)	1 mM	1 µM (0,5 µM)
Terbinafine (Tb)	291,43	DMSO	27,5 mM or 8 mg/ml	30 µM
Ro48-8071 (Ro)	448,4	methyl acetate	2 mg/L	2 µg/ml

Table 3. Inhibitors of sterol biosynthesis used during this work.

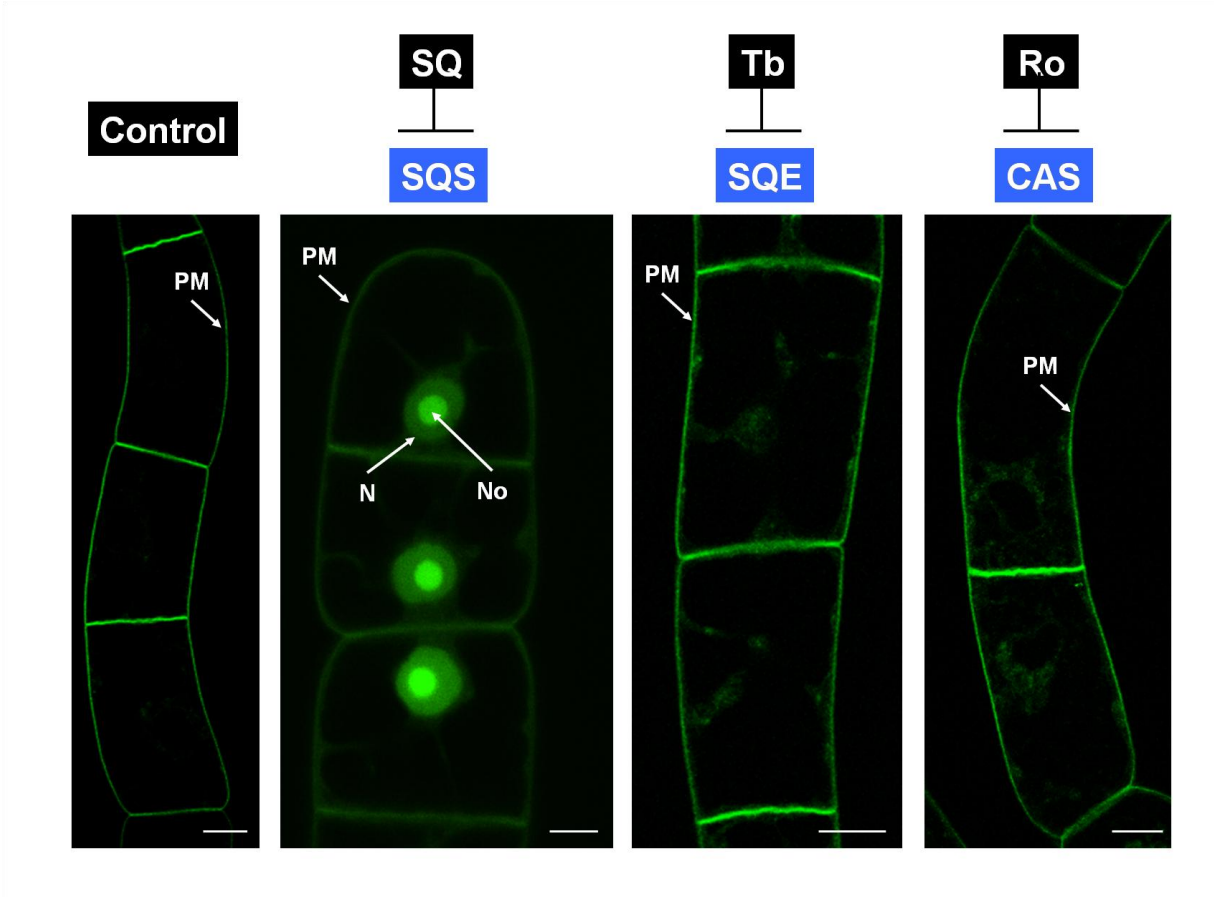

Figure 20. Localization of H6-GFP-DB-CVIL in transgenic TBY-2 cells after treatment with inhibitors of sterol biosynthesis.

Control: GFP fluorescence is almost exclusively associated with the plasma membrane (PM). **SQ:** Cells treated with squalestatin-1 (SQ), a specific inhibitor of squalene synthase (SQS) show partial translocation of GFP fluorescence to the nucleus (N) and the nucleolus (No). **Tb:** Cells treated with terbinafine (Tb), inhibitor of squalene epoxidase (SQE), showing GFP fluorescence associated with the plasma membrane (very faint fluorescence is also seen in the cytoplasm). **Ro:** Localization of H6-GFP-DB-CVIL in cells treated with Ro48-8071, a general inhibitor of oxidosqualene cyclases (OSC), such as cycloartenol synthase (CAS) in plants, showing GFP fluorescence associated with the plasma membrane. White bars = 10 µm.

Discussion - Treatment of TBY-2 cells with inhibitors of the sterol biosynthetic pathway

As mentioned above, inhibition of the sterol biosynthetic pathway was used as a tool to check whether a possible re-direction of the metabolic flux in TBY-2 cells, in particular, FPP molecules non-incorporated into sterols, could lead to a change in the GFP fluorescence pattern or even contribute to overcome the Fos-induced mislocalization of the H6-GFP-DB-CVIL, reported earlier. The fact that MVA, at high concentrations, was able to rescue the fluorescence at the PM, whereas Fol only partially complemented the inhibition by Fos suggested, among other possibilities, the existence of a bottleneck for the synthesis of GGPP from FPP in the cytosol (no GGPP synthase expression, under our conditions), or the incapacity of FPP to be imported into the plastid, where the formation of GGPP could take place.

This bottleneck is maybe HMGR, which is generally considered as the rate-limiting step in sterol synthesis, for both animals (Goldstein and Brown, 1990) and plants, which is supported by the fact that tobacco plants over-expressing HMGR were shown to produce higher amounts of sterol intermediates and end products (Chappell et al., 1995; Schaller et al., 1995) whereas the over-expression of a FPP synthase in *Arabidopsis* did not result in an increased production of sterols (Masferrer et al., 2002).

Since previous experiments with sterol biosynthesis inhibitors have been performed in our laboratory, we had some knowledge about the effective concentrations of SQ and Tb in TBY-2 cells (Wentzinger et al., 2002).

SQ, for instance, was shown to be a very efficient inhibitor of SQS (IC_{50} = 5.5 nM), almost completely inhibiting SQS activity after treatment for 24 h at 50 nM. In addition, the same concentration of SQ led to a 97% decrease of total radioactivity incorporated into sterols, when radiolabeled [^{14}C] sodium acetate was added for 2 h before cell harvesting. At 0.5 µM, the cells showed a significant decrease in cell mass (50%), which correlates very well with the stunted growth observed during this study. Interestingly, another study conducted in our laboratory could show that the presence of SQ led to a growth arrest of TBY-2 cells in the G1/G0 phase, but did not cause any cytotoxic effect or apoptosis (Hemmerlin et al., 2000).

Inhibition of SQS by SQ was also shown to trigger a stimulation of HMGR expression and activity (Wentzinger et al., 2002).

Inhibition by Tb was shown to cause a significant decrease in the cell sterol content as well as a massive accumulation of squalene, which accumulated in cytosolic lipid bodies, However, the cell growth was not impaired as indicated by the analyses of the cell mass after treatment with 30 µM Tb for 24 hours. Interestingly, Tb treatment did also stimulate HMGR activity, but not the corresponding transcript levels (Wentzinger et al., 2002).

Keeping the above data in mind, how to interpret our results, especially the particular phenotype observed with SQ-treated cells *i.e.* the partial mislocalization of the GFP fusion protein?

In fact, in a first set of experiments, we added 20 µM exogenous Fol to TBY-2 cells treated with both Fos and SQ. Surprisingly, in cells treated only with SQ (control experiment), a partial mislocalization of the fluorescence was observed in the majority of treated cells (> 85 %), whereas neither Tb nor Ro-treated cells displayed a similar effect. In cells treated with both SQ and Fos and complemented with Fol, the same pattern of partial mislocalization of the fluorescence was observed. In this context, it is important to point out that this mislocalization was clearly visible, but less pronounced at the level of a single cell, as compared to Fos- or OC- treatments. Pixel-by-pixel analysis of several cells could deliver a definite value, but was not performed yet, as the Fos and OC treatments have absolutely to be performed the same day, with the same cell cultures and under the same conditions.

As several repetitions could exclude an error occurring during the experimental procedures, a plausible explanation had to be searched for and in fact several interpretations of the results could be possible.

First of all, because of the SQS inhibition, the redirection of the metabolic flux could provide much more FPP to other FPP-metabolizing enzymes, such as GGPP synthase or Protein farnesyltransferase. FPP in excess could also be transported to mitochondria or other organelles or converted to Fol, in order to prevent a toxic accumulation of high amounts of FPP in the cytosol (Hartmann and Bach, 2001). Feeding experiments with radiolabeled farnesol showed that all these scenarios could occur (Hemmerlin and Bach, 2000; Hartmann and Bach, 2001). However, the inhibition with SQ did not lead to an additional incorporation of FPP into the ubiquinone side-chain (Hartmann and Bach, 2001).

Thus, a protein farnesyltransferase might use the excess of FPP to nonspecifically farnesylate the H6-GFP-DB-CVIlL fusion protein, despite its geranylgeranylation motif. The cross-reactivity of PFTase from *Arabidopsis* (Andrews et al., 2010) has already been mentioned before. In addition, experiments conducted by Esther Gerber with a GFP fusion protein, in which the CVIL motif was mutated to CVIM, thus transforming it into a potential substrate for PFTase, resulted in a fluorescence pattern with the majority of fluorescence still associated to the PM of the cell, but also significantly present in the nucleus and nucleolus (Gerber, 2005). As the basic domain of the chimeric protein not only serves as a second signal for protein prenylation (besides the CaaX motif), but also contains a putative NLS sequence, it is possible to imagine that the farnesyl moiety is not sufficient either to guarantee an efficient integration in the PM (because of a shorter hydrophobic domain) or to mediate the transport to the PM (which by the way is an open question for H6-GFP-DB-CVIL). In addition, the occurrence of several farnesylated, nuclear proteins have been recently reported (Barth et al., 2009).

This scenario however was challenged by studies with SQ in mammalian systems, which revealed that besides being a specific inhibitor of SQS, SQ was able to successfully inhibit mammalian prenyl-transferases, in particular protein farnesyl transferase (PFTase) (Dufresne et al., 1993; Gibbs et al., 1993).

PFTase and PGGtaseI, purified from bovine brain, were inhibited by SQ *in vitro* with an IC_{50} of 216 and 620 nM, respectively. As I used rather high concentrations of SQ (500 nM to 1 µM), the possibility that the treatment with SQ might also have affected the PGGT-1 enzyme, responsible for the prenylation of the H6-GFP-DB-CVIL, cannot be ruled out. In addition, taking into account that PFTase would be inhibited at lower concentrations than PGGT-1, the first scenario is less probable.

A final and definite answer to this question could be obtained by measuring the catalytic activities of both prenyltransferases in presence of different concentrations of SQ. As one of our former collaborators, Prof. Dring Crowell, just recently used purified *Arabidopsis* protein prenyl transferases expressed in *E. coli* for similar studies (Andrews et al., 2010), this test could even be an option to solve this question.

In addition, by using lower concentrations of SQ (50 nM already blocked most of SQS activity), the protein prenyltransferase should theoretically not be inhibited, allowing more or less to rule out the cross-reactivity and the farnesylation scenario.

d) Experimental part: Chemical complementation with pathway intermediates

Different complementation experiments were performed with SQ-treated cells (Table 4). Wheras, DX (0,5 mM) and GGol (20 µM) were able to re-establish the membrane localizatzion in 100% of the cells ("better than the control"), neither Gol (20 µM) nor MVL (5mM) and its opened form MVA (3mM) could complement the mislocalization indcuded by complementation under the chosen experimental conditions. Finally, squalene was added at 2-4 mM, but did not overcome the SQ-induced effect either (Figure 21).

Treatment (Abbreviation)	MW [g/Mol]	Solvant	Stock solution	Final concentration
1-deoxy-D-xylulose (DX)	134,13	H2O	150 mM	0,5 mM
Mevalonolactone (MVL)	130,14	H2O	1,15 M	5 mM
Mevalonic acid (MVA)	130,14	see protocol	3M	3mM
Geraniol (GOH)	154,3	EtOH	10 mM	5 and 20 µM
Farnesol (FOH)	222,4	EtOH	20 mM	5 and 20 µM
Geranylgeraniol (GGOH)	290,5	EtOH	20 mM	5, 10 and 20 µM
Squalene (SQN)	410,7	stock solution	~2 M at 25°C	~ 2 and 4 mM

Table 4: Overview about chemical complementations and experimental conditions.

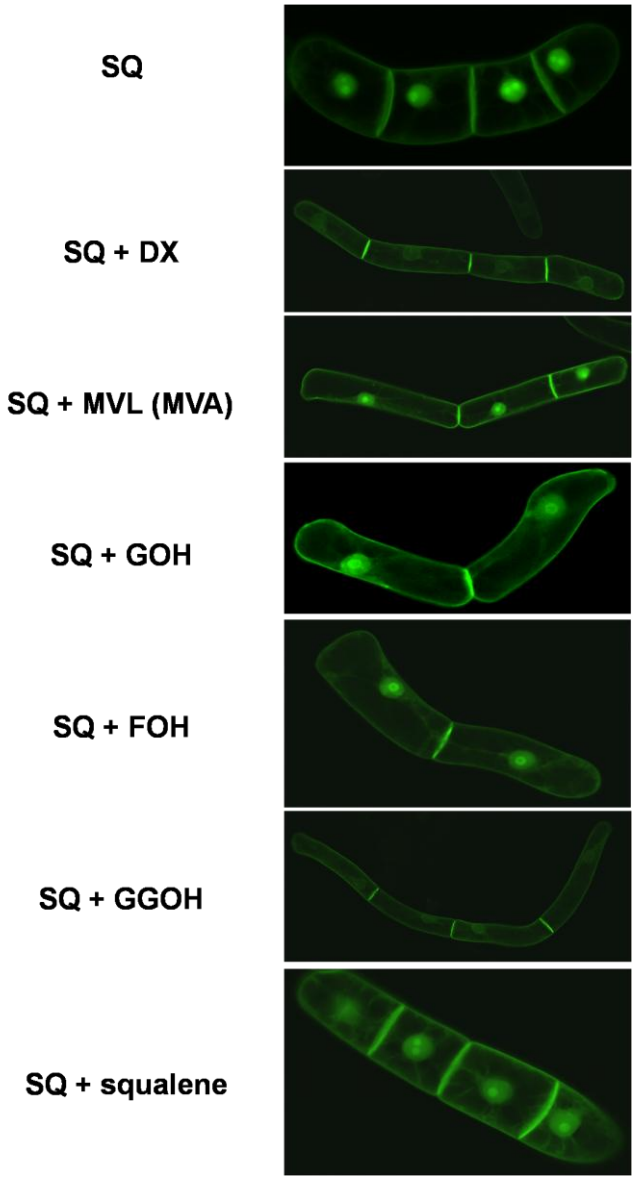

Figure 21: Chemical complementation of squalestatin-induced H6-GFP-DB-CVIL partial delocalization (from the PM to the nucleus/nucleolus) with pathway intermediates, prenols and squalene.

Discussion - Chemical complementation with pathway intermediates

In order to investigate the capability of isoprenols (Gol, Fol and GGol) and intermediates of both isoprenoid biosynthetic pathways (MVA-pathway: MVL and MVA; MEP-pathway: DX) to overcome the (partial) mislocalization induced by SQ, different chemical complementation experiment were performed (Figure 21).

Interestingly, both DX and GGol completely complemented the SQ-induced effect, which was also observed in experiments with Fos-treated cells. As discussed extensively before, the most likely explanation is an efficient uptake and metabolization of both compounds: DX entering the plastid and being incorporated in IPP, GPP and GGPP, which is then exported toward the cytosol, where its serves as substrate for prenylation of the H6-GFP-DB-CVIL. For GGol, again, two scenarios are thinkable: either import into the plastid, phosphorylation and export to the cytosol or direct phosphorylation in the cytosol. The existence of a system for phosphorylation of prenyldiphosphates was mentioned before (Thai et al., 1999).

SQ is known to be an irreversible, competitive inhibitor of squalene synthase (SQS). Therefore, the DX-induced recovery of the PM fluorescence itself cannot result from an effect on SQS. As SQ structurally resembles FPP, it would be more likely that, by increasing the pool of bio-available GGPP, we succeeded to replace SQ by GGPP at the substrate-binding site of PGGT-1 (or even both prenyltransferases) and thereby to restore the correct geranylgeranylation of H6-GFP-DB-CVIL.

The fact that Gol does not complement the effects of SQ is in agreement with our previous results and suggests that Gol is not accepted as substrate for the phosphorylation system, assumed to exist in plants. Intriguingly, exogenously applied Fol was previously able to restore the PM localization of H6-GFP-DB-CVIL to over 60% in Fos-treated cells (Gerber, 2005). However, no significant effect (<10%) was observed in independent experiments with SQ-treated cells. Furthermore, neither MVL nor MVA could restore the PM-localization of fluorescence in SQ-treated cells. This was surprising, as at least MVA (3mM) was able to completely overcome the inhibition induced by Fos.

In the case of Fol, the following scenario could be possible: after import in the cytosol, Fol would be phosphorylated to FPP. In SQ-treated cells, however, FPP should not be limiting and, therefore, be available in sufficient amounts to serve as a substrate for a putative cytosolic GGPP synthase, catalyzing its conversion into GGPP. Thus, the incomplete prenylation of H6-GFP-DB-CVIL might be due to a lack or insufficient GGPP synthase activity in the cytosol (lack of expression or downregulation). In addition, the excess of FPP could also be used by the protein farnesyl transferase to farnesylate H6-GFP-DB-CVIL, as described before, which could lead to the same phenotype as observed with GFP-DB-CVIM-transformed cells (Gerber, 2005). However, again, the possible inhibition of the protein farnesyltransferase by SQ challenges this scenario.

Finally, a possible explanation for this observation could come from results obtained with the yeast model system. Very recently, a bio-engineered yeast (*S .cerevisiae*) strain down-regulated at the level of SQS was used in an approach to re-direct the isoprenoid biosynthetic flux towards the production of the diterpene casbene (Kirby et al., 2010). This strain contained several casbene synthase genes from *Euphorbia* and was specifically engineered for an enhanced flux through the MVA pathway. This was accomplished by combining knowledge of previous studies (Ro et al., 2006; Paradise et al., 2008), such as over-expression of GGPP synthase, to yield more efficiently the casbene precursor, GGPP. In addition, the *ERG9* SQS promotor was replaced by the *MET3* promoter, allowing repression of SQS expression by addition of methionine to the culture medium. However, the down-regulation of SQS in these cells did not lead to the expected redirection of FPP to GGPP and further on to casbene. Instead, several possible rate-limiting steps, including the conversion of FPP to GGPP, were found. At the same time, elevated levels of the FPP-derived alcohols, nerodiol and farnesol, were observed, suggesting a transformation process to avoid toxic concentrations of FPP in the cell. Indeed, in the past, several prenyldiphosphates have been reported as cytotoxic in bacteria (Martin et al., 2003; Withers et al., 2007) and mechanisms to avoid their accumulation to toxic levels have been reported from different organisms (Gardner et al., 2001; Grabinska and Palamarczyk, 2002; Paradise et al., 2008), including plants (Nah et al., 2001).
Interestingly, it has been shown previously that mevalonate kinase is down-regulated at the post-transcriptional level by high levels of FPP and GGPP (Hinson et al., 1997). Therefore, if the tobacco BY-2 mevalonate-kinase is also sensitive to the feedback-regulation by FPP and GGPP, this could very conveniently explain why externally fed MVA could not complement the SQ-induced phenotype due to a large pool of FPP. Moreover, the resulting decrease in cytosolic IPP due to the block in the MVA pathway could also prevent a sufficient supply of IPP for the synthesis of FPP to GGPP, as it was observed in Fol-complemented cells treated with Fos and mevinolin, simultaneously.

However, in order to completely understand the complex regulatory network that modulates the pools of precursors, especially in extreme scenarios such as the treatment with SQ, different approaches will be necessary, including gene expression profiles and activity measurements of the key enzymes involved in the conversion reactions (under the condition they are already identified in tobacco). In addition, determining metabolic profiles to monitor the concentrations of intermediates of both isoprenoid biosynthetic pathways in response to SQ treatment would be desirable. Last, but not least, the question of the ability of SQ to inhibit the activity of plant protein prenyl transferases should be solved.

2.1.5 Post-prenylation inhibitors and transport of GFP-DB-CVIL to the plasma membrane

As mentioned earlier, the purification and analysis of the His-tagged GFP-DB-CVIL fusion protein revealed that it was geranylgeranylated and carboxyl-methylated in TBY-2 cells (Gerber et al., 2009).
The physiological importance of the two post-prenylation steps has been demonstrated in several studies and discussed before (2.1.1 The prenylation of proteins in plants). The study of post-prenylation inhibition has become a very attractive topic in the past, as both reactions are essential for the localization of many prenylated proteins by mediating their attachment to membranes and protein-protein interactions. In particular, many recent research approaches are focusing on the posttranslational modifications of the Ras superfamily of GTPases, as the inhibition of Rce1 and ICMT function had shown anti-transformation and anti-cancer-efficacy *in vivo* (Bergo et al., 2002; Winter-Vann et al., 2005; Konstantinopoulos et al., 2007). In addition, it has been reported that K-ras and N-Ras, which are both important oncogenes, are able to bypass the inhibition of protein farnesyl transferases by being cross-prenylated by geranylgeranyl transferases (Whyte et al., 1997).
The RAS GTPases are ubiquitously found in mammals and are encoded by three genes that are translated into four RAS proteins: HRAS, NRAS, KRAS4A and KRAS4B (the two last being splice variants). These small GTPases are signaling proteins that cycle between a GDP-bound inactive and a GTP bound active state (molecular switches) and play key roles in regulating numerous cellular processes, including proliferation, differentiation and apoptosis (Hancock, 2003). Interestingly, all three isoforms contain lipid-based PM targeting motifs and their proper targeting and anchoring to membranes is essential for their biological activity. Ras proteins have become a widely used model for the study of prenylated proteins, in particular due to their implication in cancer development. It is estimated that mutational permanent activation of members of the RAS superfamily is thought to account for up to 30 % of all known human cancers (Bos, 1989; Malumbres and Barbacid, 2003).
One of the topics Esther Gerber was particularly interested in during her Ph.D. studies was the intracellular transport of the prenylated GFP-fusion protein from the ER to the PM. Experiments focusing on the membrane trafficking of the GFP-DB-CVIL protein showed that the transport of this protein was not significantly affected by any treatments targeting either components of the cytoskeleton (microtubuli: taxol and oryzalin; actin-filaments: cytochalasin D) or the trans-Golgi-network (TGN: brefeldin A) (Gerber, 2005). These results strongly suggested that GFP-DB-CVIL was not transported to the PM via the classical secretory pathway. This result was surprising, as this vesicular transport route is used by the majority of identified prenylated proteins (Choy et al., 1999), such as HRAS, NRAS, KRAS4A in mammals.
The correct targeting of Ras proteins is successfully accomplished only when the proteins contain a second “signal” in addition to their prenylation. In the case of HRAS, NRAS and KRAS4A this

second signal consists of one or more S-acylation sites (“palmitoylation”) (Hancock et al., 1989; Goodwin et al., 2005), whereas KRAS4B contains a lysine-rich polybasic (hypervariable) domain, located nearby the prenylation side (Hancock et al., 1990; Hancock et al., 1991; Meder and Simons, 2005). The same combination, a polybasic domain with a cluster of basic amino acids, in addition to the CAAX motif is also found in the H6-GFP-DB-CVIL fusion protein.

Besides this structural resemblance, KRAS4B is also insensitive to inhibitors of vesicular transport and transits to the PM by a largely unknown, non-vesicular (Golgi-independent) pathway (Choy et al., 1999; Apolloni et al., 2000; Silvius et al., 2006) that requires, at least in yeast, mitochondrial function and vps proteins (Wang and Deschenes, 2006).

Thus the study of molecules that interfere with the localization or transport of the H6-GFP-DB-CVIL fusion protein might be a promising tool to observe the effects of post-prenylation inhibition in plants in general, and possibly, this knowledge might even be transferred to other models.

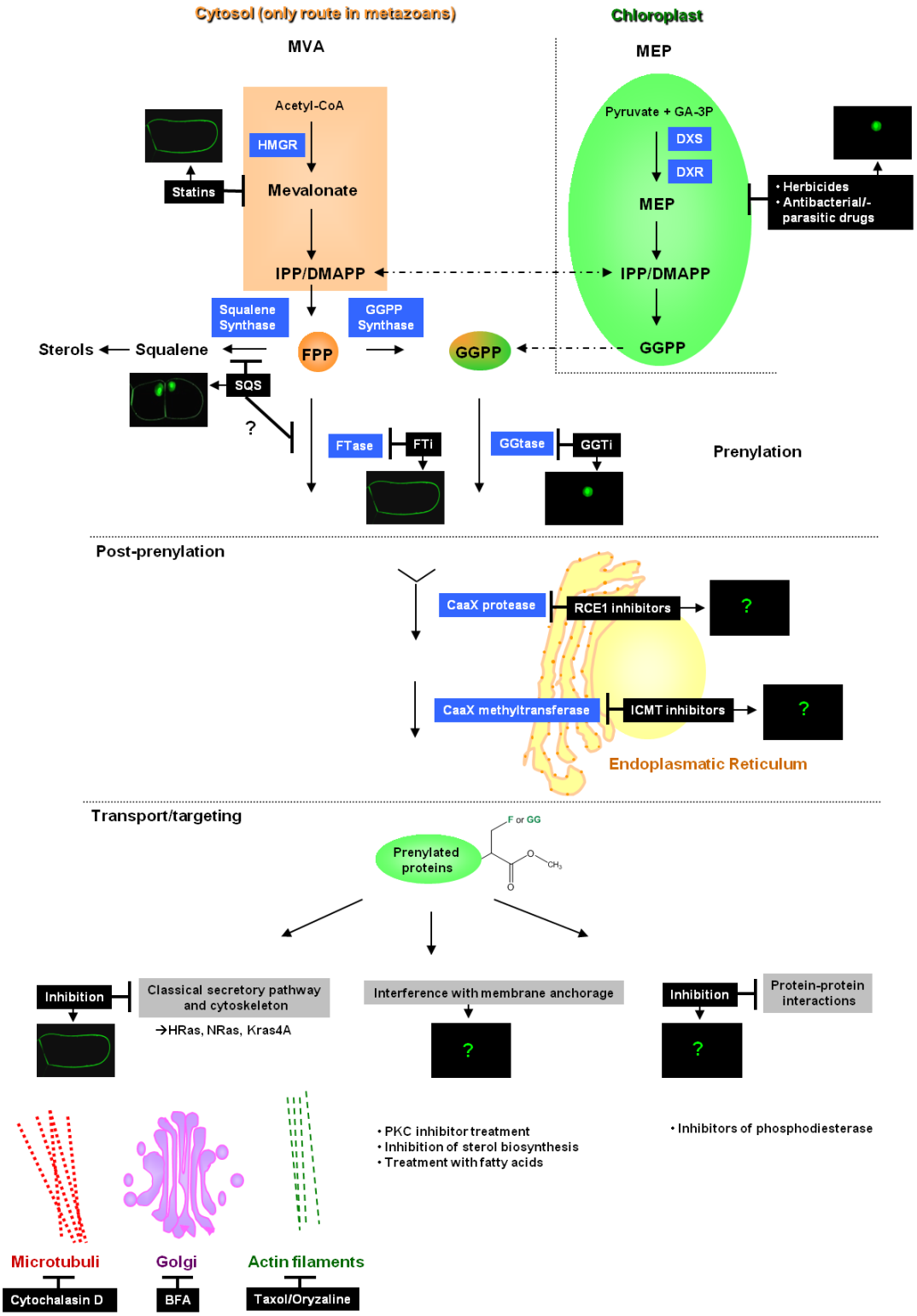

Figure 22. Impact of different treatments on the localization of the geranylgeranylated fusion protein H6-GFP-DB-CVIL.

Experimental part:

Until now, different known inhibitors of Rce1 and ICMT, have been purchased and tested in preliminary experiments (Figure 23), but most of them induced cell death, when used in commonly cited concentrations and time-scales in our model system. This is most likely due to the efficient uptake and high metabolic activity of BY-2 cells mentioned before and requires adjusting of the experimental conditions. Therefore only preliminary results will be shown at this point and hopefully more detailed results will be available in the near future.

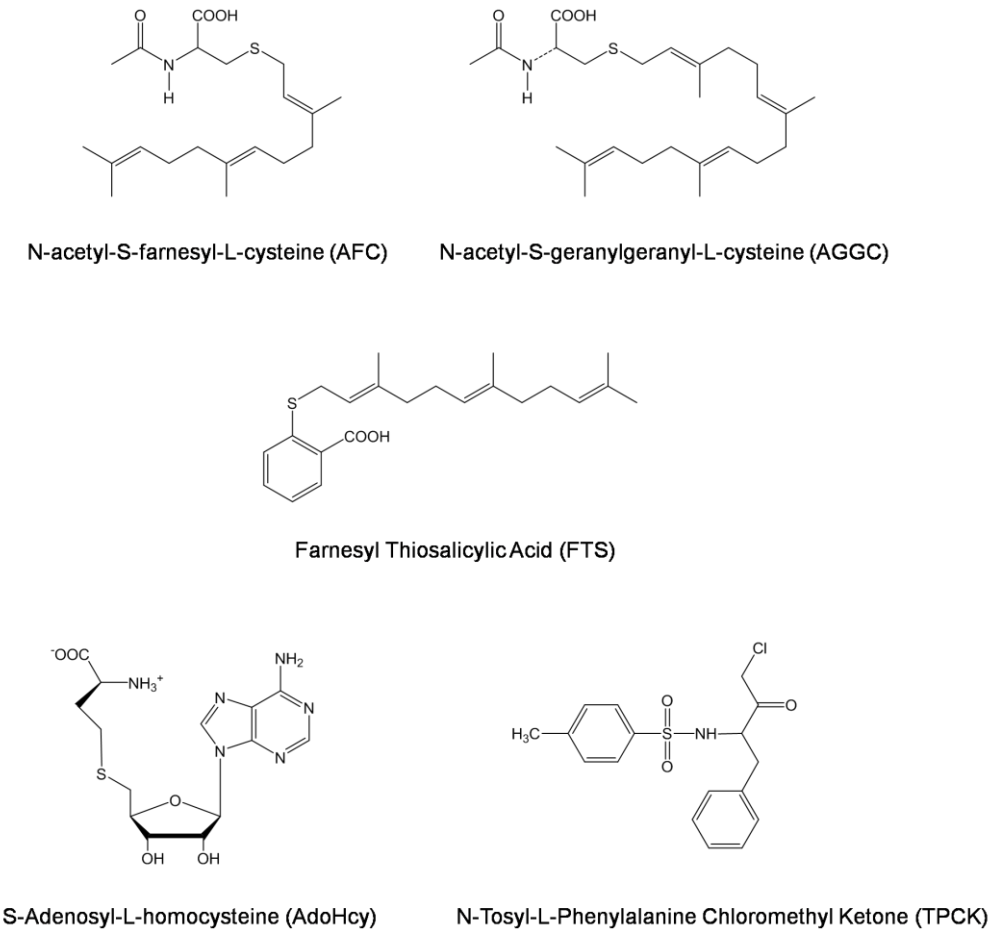

Figure 23: Inhibitors of CaaX-processing used in this experimental approach.
Inhibitors of Rce1 (-AAX-proteolysis): TPCK (protease inhibitor); Inhibitors of ICMT (carboxylmethylation): a) analogs of prenylcysteine: AFC, AGGC. b) other substrate analogs: FTS, AdoHcy.

First results obtained after various treatments indicated that both inhibition of Rce1 and ICMT affected the localization of H6-GFP-DB-CVIL. For instance, short-term treatment (15 h induction, then treatment for 3 h with 200 µM AFC) with the prenylcysteine analog AFC strongly changed the distribution pattern of the H6-GFP-DB-CVIL and besides the PM, both the cytosol as well as the nucleolus displayed strong GFP signals. Interestingly, a similar effect on the localization of the prenylated GFP-CaM53 fusion protein of petunia (Rodríguez-Concepción et al., 1999) was observed by Rodríguez-Concepcíon et *al.*, (2000), in response to AFC treatment (200 µM), in bombarded petunia leaves. Long-term treatments (>10 h), however, led to loss of GFP fluorescence and cell death. Inhibition of the –AAX-proteolysis by TPCK (Chen, 1999) led to a partial mislocalization of the fusion protein to the nuclear compartment. However, optimal conditions to observe the induced effects have still to be found (Figure 24).

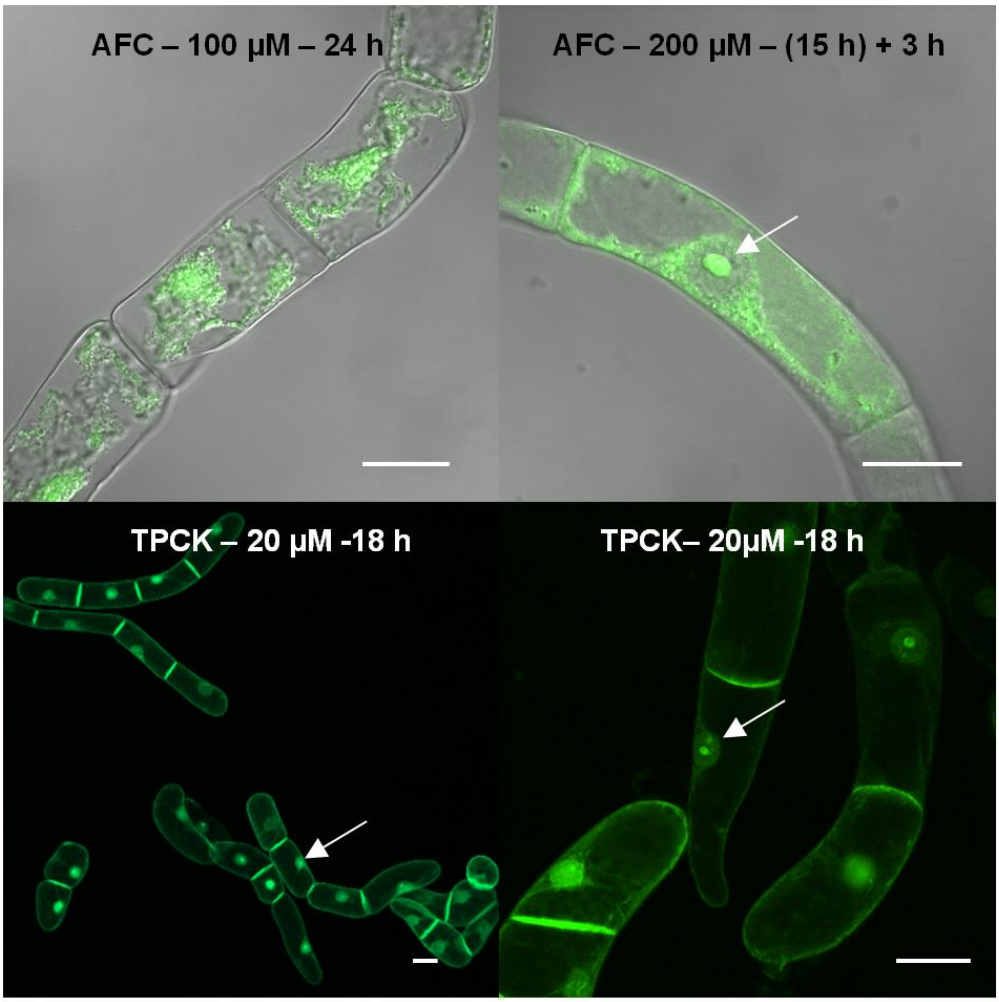

Figure 24: Impact of different treatments on the localization of the geranylgeranylated fusion protein H6-GFP-DB-CVIL. White bars = 20 µm.

2.1.6 Testing and evaluating novel inhibitors of the MEP pathway: from qualitative to quantitative analysis

Soon after its discovery it was assumed that the MEP pathway, which is not present in humans but occurs in higher plants as well as in several human pathogens, would be a promising target for the development and evaluation of drugs (see chapter 1.2). As expected, this hypothesis could quickly be confirmed, when different studies identified the first two enzymes of the MEP pathway, DXS and DXR, as the molecular targets of the bleaching herbicide clomazone (more precisely, its active metabolite oxoclomazone) and the antibioticum Fosmidomycin, respectively. Interestingly, both compounds were known for their antibacterial effects years before the elucidation of the MEP pathway, although it was unclear at which point of the cell metabolism they were interfering. For instance, although Fosmidomycin was isolated from its natural source *Streptomyces lavendulae* (Kuroda et al., 1980) and recognized for its antibacterial activity against gram-positive and gram-negative bacteria (Mine et al., 1980; Kuemmerle et al., 1987) in the early 1980s, it took several years to reveal more detailled information about its antibiotic activity (Shigi, 1989) and to identify its specific molecular target, DXR (Kuzuyama et al., 1998).

2.1.6.1 DXS as a molecular target for Oxoclomazone and derived compounds

DXS – General informations

DXS (1-deoxy-D-xylulose 5-phosphate synthase) catalyzes the first step of the alternative MEP pathway, the condensation of glyceraldehyde 3-phosphate (GAP) and pyruvate, yielding 1-deoxy-D-xylulose 5-phosphate (DXP) (see Introduction).

The *DXS* gene is essential in *E.coli* and its disruption in *Arabidopsis thaliana* (*cla1*) results in a lethal albino phenotype, mainly caused by a lack of photosynthetic pigments (chlorophylls and carotenoids).

DXS genes are highly conserved in bacteria and plants and analyses of their sequences revealed a weak homology with other thiamine-dependent enzymes, transketolases, and the pyruvate dehydrogenase E1 subunit (Sprenger et al., 1997; Lange et al., 1998; Lois et al., 1998; Walter et al., 2002; Xiang et al., 2007). These enzymes all catalyze similar biochemical reactions, thereby using thiamine diphosphate as a cofactor and pyruvate as a substrate. In addition to thiamine diphosphate, DXS also requires a divalent cation (Mg^{2+} or Mn^{2+}) for optimal enzymatic activity (Kuzuyama et al., 2000a; Hahn et al., 2001).

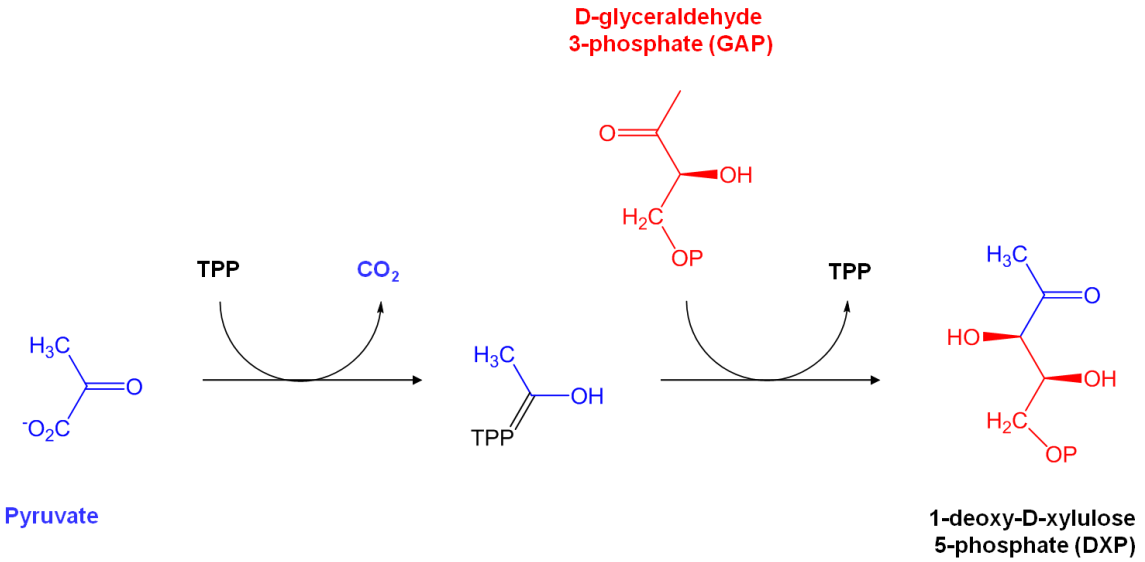

Figure 25. (Very) Simplified scheme of the reaction catalyzed by DXS (modified from Xiang et al., 2006).

Only recently, efforts were successful to partially crystallize DXS from *E.coli* and *Deinococcus radiodurans* (in complex with TPP), after *in situ* proteolysis of the purified enzyme by a fungal protease (Xiang et al., 2007).

Although incomplete, these data suggest a tightly associated homodimer, consisting of 3 domains per monomer and the active site being located between the domains I and II of the same monomer. Interestingly, the residues forming the active site appear to be highly conserved across species and can even be found in other transketolases and pyruvate dehydrogenase complexes. Several residues have already been shown to be essential for the catalytic activity of DXS by site-directed mutagenesis (Querol et al., 2001; Xiang et al., 2007) and remarkably, a mutation in the active site of PDH (E636Q) was able to rescue a *dxs*-null mutant phenotype in *E.coli* (Sauret-Güeto et al., 2006).

This finding further confirms the importance of structural information for understanding the catalytic mechanism of DXS and in particular, for the future design of novel active inhibitors of DXS as to date, only two inhibitors of this enzyme are known: oxoclomazone, for the plant DXS (Müller et al., 2000) and fluoropyruvate, for the DXS of *E.coli* (Eubanks and Poulter, 2003).

For this reason, Jeanne Toulouse, a Ph.D. student in the laboratory of Professor Michel Rohmer synthesized different classes of pyruvate analogs that were inspired by known inhibitors of pyruvate decarboxylases and pyruvate dehydrogenases. These compounds were then tested with our bioassay for possible effects on the localization of the GFP-DB-CVIL, thus indicating an inhibitory effect on the biosynthesis of GGPP by the MEP pathway.

1. Pyruvate analogs, according to Menon-Rudolph et *al.*, (1992):

Three surrogates, based on a conjugated substrate analog with a *p*–chloro-substituent, were synthesized:

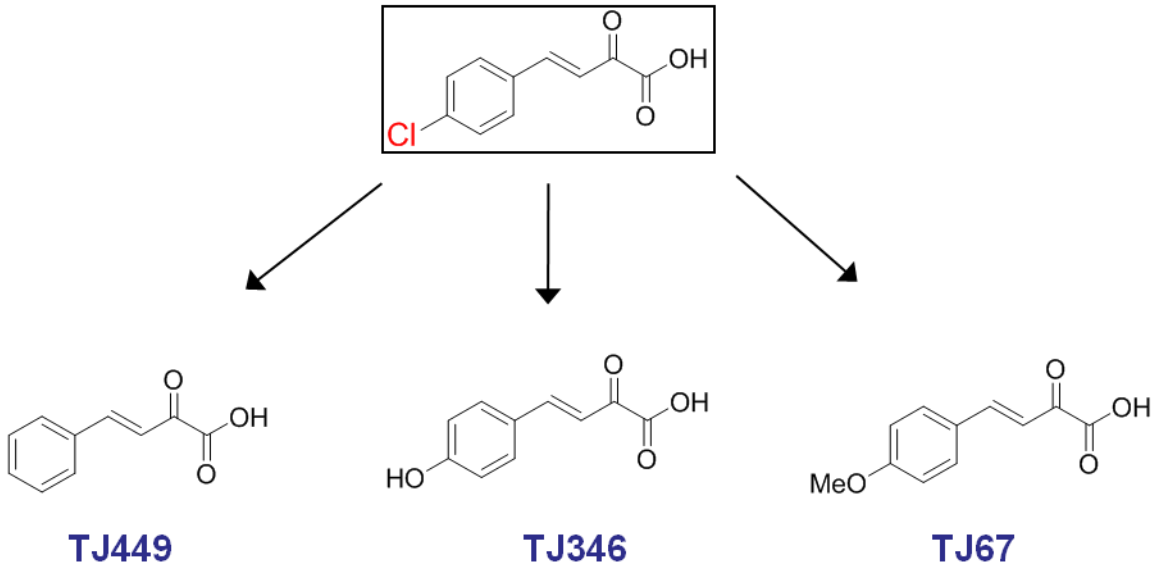

Figure 26. Conjugated α-keto acids according to Menon-Rudolph et *al.*, (1992) – potential inhibitors of pyruvate decarboxylase.

2. Pyruvate analogs, based on 2-oxo-3-alkynoic acids, as potential inhibitors/inactivators of pyruvate dehydrogenase (Brown et al., 1997):

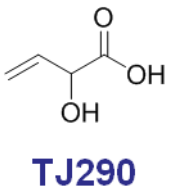

Figure 27. 2-oxo-3-butenoic acid, an analogue of 2-oxo-3-butynoic acid, a known inhibitor of *E.coli* pyruvate dehydrogenase (Brown et al., 1997).

2-oxo-3-butynoic acid has been shown to be rather unstable and to irreversibly inactivate the PDHc (pyruvate dehydrogenase multienzyme complex) from *E. coli.*

Inactivation of the purified enzyme already occurred at 100 µM, under saturating substrate concentrations. However, due to the instability of the compound, the tested concentrations might have been too low.

3. Di- and tri-halogenated analogs of pyruvate based on β-fluoropyruvate, a known inhibitor of DXP synthase.

Fluoropyruvate is a known inhibitor of the pyruvate dehydrogenase complex of *E. coli* (Flournoy and Frey, 1989). In addition, it is also an efficient dead-end inhibitor of *Rhodobacter capsulatus* DXP synthase (Eubanks and Poulter, 2003). For this reason, Jeanne Toulouse synthesized a di- and a tri-halogenated derivative, as some of these compounds have been confirmed as efficient inhibitors of pyruvate dehydrogenase from *E. coli* (Lowe and Perham, 1984).

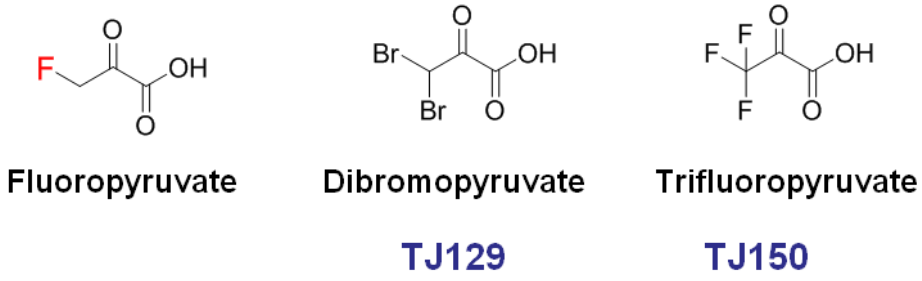

Figure 28. Halogenated pyruvate analogs

Analog	MW [g/Mol]	Solvant	Stock solution	Final concentration
TJ449	214,26	H_2O	100 mM	100 µM
TJ129	142,03	H_2O	100 mM	100 µM
TJ346	192,17	CH_3CN	100 mM	100 µM
TJ67	206,19	CH_3CN	100 mM	100 µM
TJ150	245,85	H_2O	100 mM	100 µM
TJ290	102,09	H_2O	100 mM	100 µM

Table 5. Analogs of pyruvate tested with our bioassay.

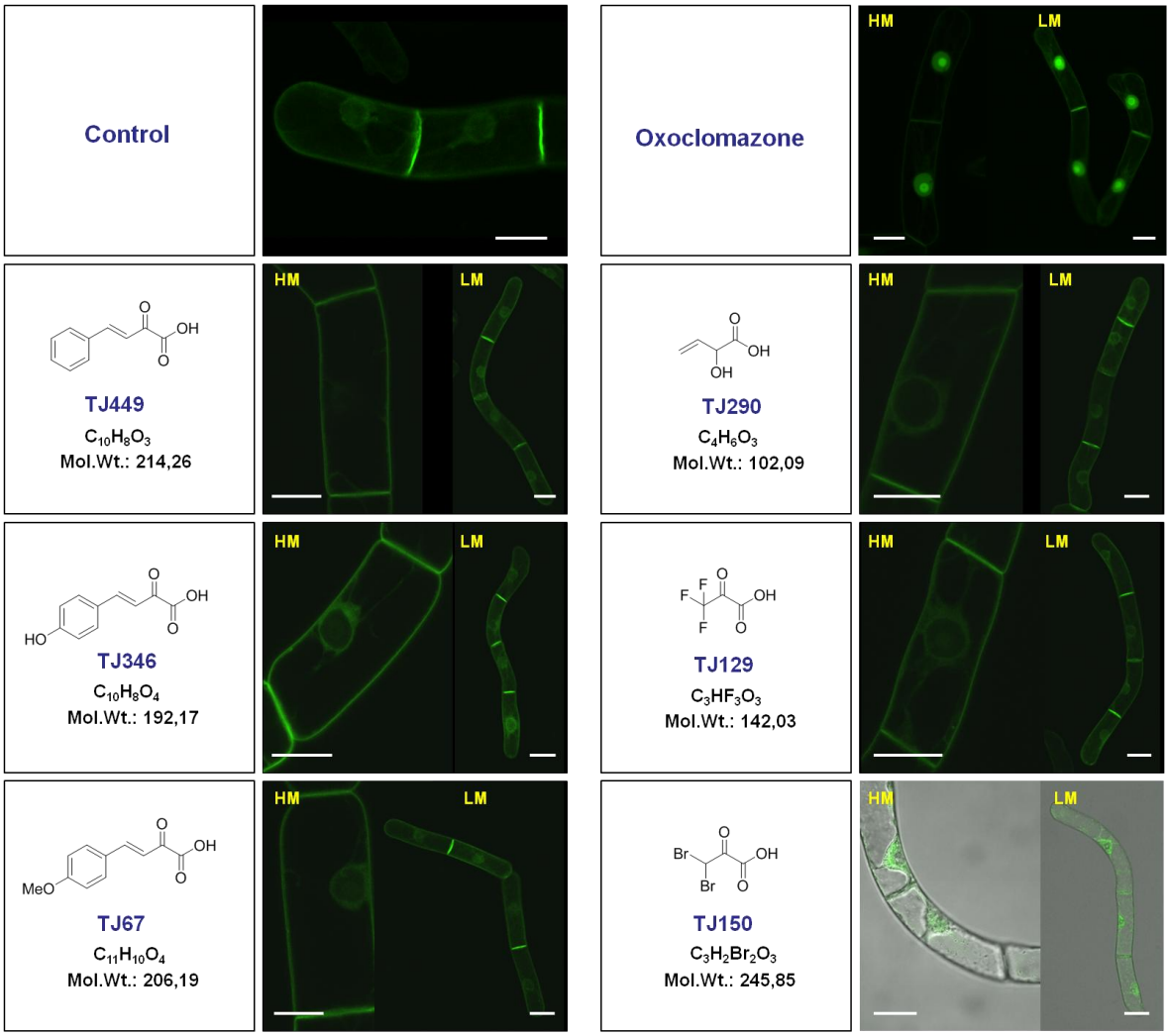

Figure 29. Confocal microscopy images showing the subcellular localization of the H6-GFP-DB-CVIL fusion protein, after treatment with different analogs of pyruvate based on known inhibitors of pyruvate decarboxylase and pyruvate dehydrogenase.

The molecules were synthesized by Jeanne Toulouse, a Ph.D. student in the laboratory of Prof. Michel Rohmer (Institut de Chimie de Strasbourg). The molecules were dissolved according to Table 5 and tested under standard conditions (3 hours treatment, followed by induction with 10 µM dexamethasone and examination by fluorescence microscopy 15 h later) at a final concentration of 100 µM. Cells were also treated by 50 µM oxoclomazone as described previously (positive control). None of the six tested compounds showed a mislocalization of the GFP fluorescence to the nucleus. The compound TJ150, however, appeared to be cytotoxic at the given concentration as cells showed typical signs of cell death (over 90% of treated cells did not show any fluorescence).

Results:

All compounds have been dissolved directly before the experiment and were completely soluble in their respective solvent. The only exception was TJ346, which did not dissolve but gave a homogenous, yellow suspension.

The cells were treated for 18 h, in presence of 100 µM of pyruvate analogs, and examined by confocal fluorescence microscopy, the next day (Figure 29). None of the tested compound did lead to a mislocalization of the fluorescence, as it was observed for the positive control, treated with 50 µM oxoclomazone. However, the dibromopyruvate-treated cell culture showed significant cytotoxic effects as over 90% of treated cells did not display any GFP-related fluorescence. The fluorescence in the remaining cells appeared in cytoplasmic strands and in the cytoplasm surrounding the nucleus.

Discussion:

In parallel to the tests conducted with the H6-GFP-DB-CVIL cell line, DXS activity was determined in presence of some of the tested molecules (TJ449, TJ346, TJ67, TJ129). These experiments have been performed in the laboratory of Prof. Michel Rohmer and used an end-point assay, in which the remaining pyruvate substrate was converted to lactate by lactate dehydrogenase. The consumption of NADPH (and the formation of NAD^+) can be measured by spectrometry at 340 nm (for details: *e.g.* Xiang et al., 2007). None of the tested enzymes exhibited an inhibitory effect, in agreement with the results obtained with our bioassay.

2.1.6.2 DXR as molecular target for Fosmidomycin and derived compounds

DXR (1-deoxy-D-xylulose 5-phosphate reductoisomerase) is the second enzyme of the MEP pathway and catalyzes the conversion of DXP (1-deoxy-D-xylulose 5-phosphate) to MEP (2-*C*-methyl-D-erythritol 4-phosphate). Part of this transformation is an intramolecular rearrangement, yielding 2-*C*-methyl-D-erythrose 4-phosphate, which is then reduced to MEP in an NADPH dependent reaction step (Figure 30) (Takahashi et al., 1998; Kuzuyama et al., 2000b; Hoeffler et al., 2002; Koppisch et al., 2002).

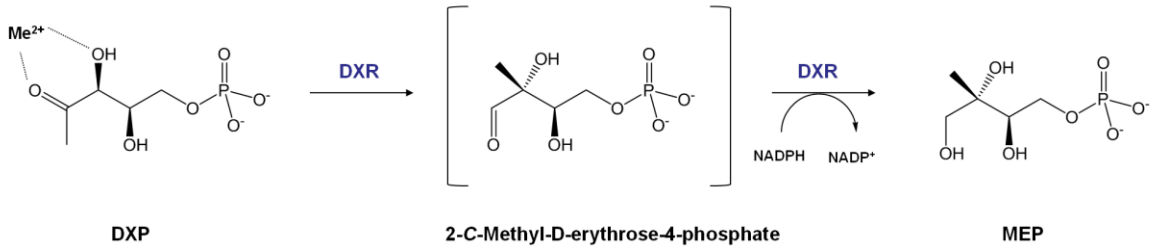

Figure 30. Simplified scheme of the conversion of DXP to MEP catalyzed by DXR.

After the elucidation of DXR as target for Fosmidomycin in *E.coli* (Kuzuyama et al., 1998), major interest was revived in this longtime neglected antibiotic, when Jomaa *et al.* (1999) demonstrated its high activity against various *Plasmodium ssp.*, including the human malaria pathogen *Plasmodium falciparum* (Fosmidomycin was able to inhibit the growth in a dose-dependant manner, with an IC50 of 28 nM *in vitro)*. These results led to the cloning and characterisation of DXR from a variety of other organisms, including *E.coli* (Takahashi et al., 1998) the cyanobacteria *Synechosystis* (Yin and Proteau, 2003), the universal model plant *Arabidopsis thaliana* (Schwender et al., 1999) , the malaria parasite *Plasmodium falciparum* and *Mycobacterium tuberculosis* (Argyrou and Blanchard, 2004).

In the last decade, several studies have revealed detailed informations about the structure and biochemical properties of the DXR enzyme from *E.coli* (Hoeffler et al., 2002; Reuter et al., 2002). Those results - including the three-dimensional crystal structures of DXR in a ternary complex with DXP/Fosmidomycin and the co-factor NADPH – suggest a physiologically active homodimer, with each subunit consisting of three distinct domains (Steinbacher et al., 2003; Mac Sweeney et al., 2005). In addition to NADPH, DXR requires a divalent metal cation, such as Mn^{2+}, Mg^{2+} or Co^{2+}, which is bound by three highly conserved amino acid residues (Steinbacher et al., 2003; Takenoya et al.). This metal cation is chelated by DXP before the first step of the conversion to MEP - the intramolecular rearrangement - takes place (Figure 30).

Fosmidomycin

Fosmidomycin (FR-31564) and its methylated analog, FR-900098 are phoshonohydroxamic acids. In both compounds a hydroxamate function is linked to a phosphonic acid function by a propyl chain (Figure 31).

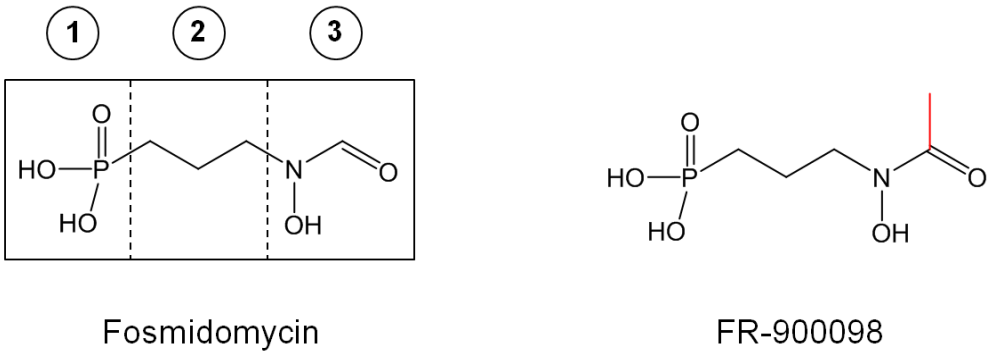

Figure 31. Structures of Fosmidomycin and its methylated analogon FR-900098. 1 Phosphonate moiety; 2 propyl linker; 3 hydroxamic acid moiety.

According to three-dimensional data, binding of DXR to its substrate (or Fosmidomycin) involves a major conformational rearrangement of the enzyme. Fosmidomycin acts as a competitive inhibitor, chelating a bivalent cation with its hydroxamate group and binding slowly but very tightly to the catalytic site of DXR (Steinbacher et al., 2003).

The substrate binding site of the DXR enzyme can be divided into three distinct regions: first of all, a positively charged pocket which interacts with the phosphonate function of fosmidomycin ("phosphate-recognition site"), a hydrophobic region covering the backbone of the molecule, as well as an amphipathic region which binds the hydroxamic acid function of the molecule. This results in a conformation with a flexible loop covering the central catalytic site, thus forming a barrier with the surrounding solvent (Mac Sweeney et al., 2005).

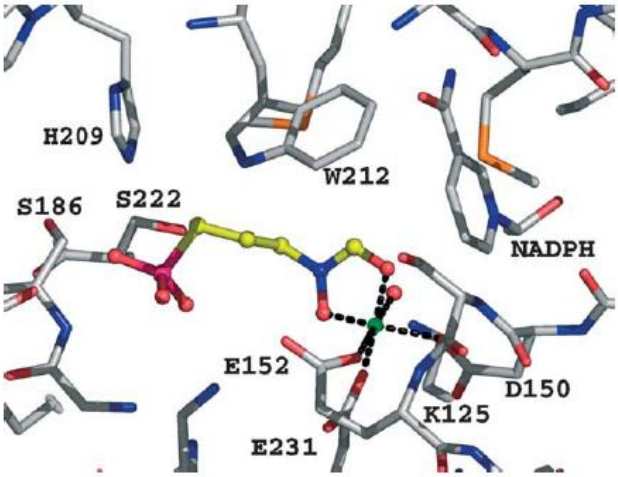

Figure 32. A model of Fosmidomycin in the tight binding conformation together with the co-factor NADPH and the chelated metal cation (green). Image taken from MacSweeney et al., 2005.

As mentioned before, Fosmidomycin and FR-900098 were both able to inhibit the recombinant DXR enzyme from *Plasmodium falciparum in vitro* (Jomaa et al., 1999). Furthermore, Fosmidomycin successfully cured mice, infected with *Plasmodium vinckei* (Jomaa et al., 1999) and has been used in clinical trials to cure uncomplicated "malaria tropica" in humans (Lell et al., 2003; Wiesner et al., 2003).

Interestingly, Fr-900098 is about twice as efficient as Fosmidomycin in *in vitro* assays with parasites and in animal models. ((Wiesner et al., 2003), This higher efficiency may be attributed to a putative hydrophobic interaction of the methyl group with a conserved amino acid (Trp212) in the loop structure, covering the catalytic site (Figure 32).

In the past, several attempts were performed to enhance the antimicrobial activity of Fosmidomycin and FR-900098 by introducing structural modifications at different positions of the molecule (Figure 33 A). However, the majority of these approaches led to compounds with clearly reduced anti-microbial activities (Hemmi et al., 1982; Kurz et al., 2003; Silber et al., 2005) and corroborated the importance of the phosphonic acid and hydroxamic acid moieties of the molecule for the anti-malarial activity (Haemers et al., 2006; Kurz et al., 2006).

Modifications of Fosmidomycin

The group of our collaborator Prof. Michel Rohmer from the "Institut de Chimie de Strasbourg" only recently synthesized analogs of Fosmidomycin and FR-900098 with a rearrangement of the hydroxamate group (Figure 33 B). Enzymatic assays showed that both compounds (here referred to as LK1 and LK2 - Lionel Kuntz) successfully inhibited *E.coli* DXR in *in vitro*-assays. The IC_{50} values measured were 170 nM and 48 nM for LK1 and LK2, respectively. The IC_{50} value of LK2 was even

comparable to that of Fosmidomycin (Fos: 32 nM). In addition, both molecules inhibited the growth of *E.coli*, but with a significantly less efficiency than Fosmidomycin (Kuntz et al., 2005).

Interestingly, the N-methylated compound (LK2 – derived from FR-900098) also successfully inhibited the growth of an *E.coli* strain that was cross-resistant to Fosmidomycin and fosfomycin. Among other reasons, this could be due to a difference in the uptake or detoxification of these two antibiotics, which are known to share a common import mechanism via the L-α-glycerolphosphate and the glucose-6-phosphate pathway in *E.coli* (Sakamoto et al., 2003). As the N-methylated compound nearly equaled Fosmidomycin in terms of *in vitro* inhibition of the DXR enzyme, changing the bioavailibility of this compound was a promising strategy to further enhance the performance of the hydroxamic drugs and provide new active compounds against resistant pathogen strains.

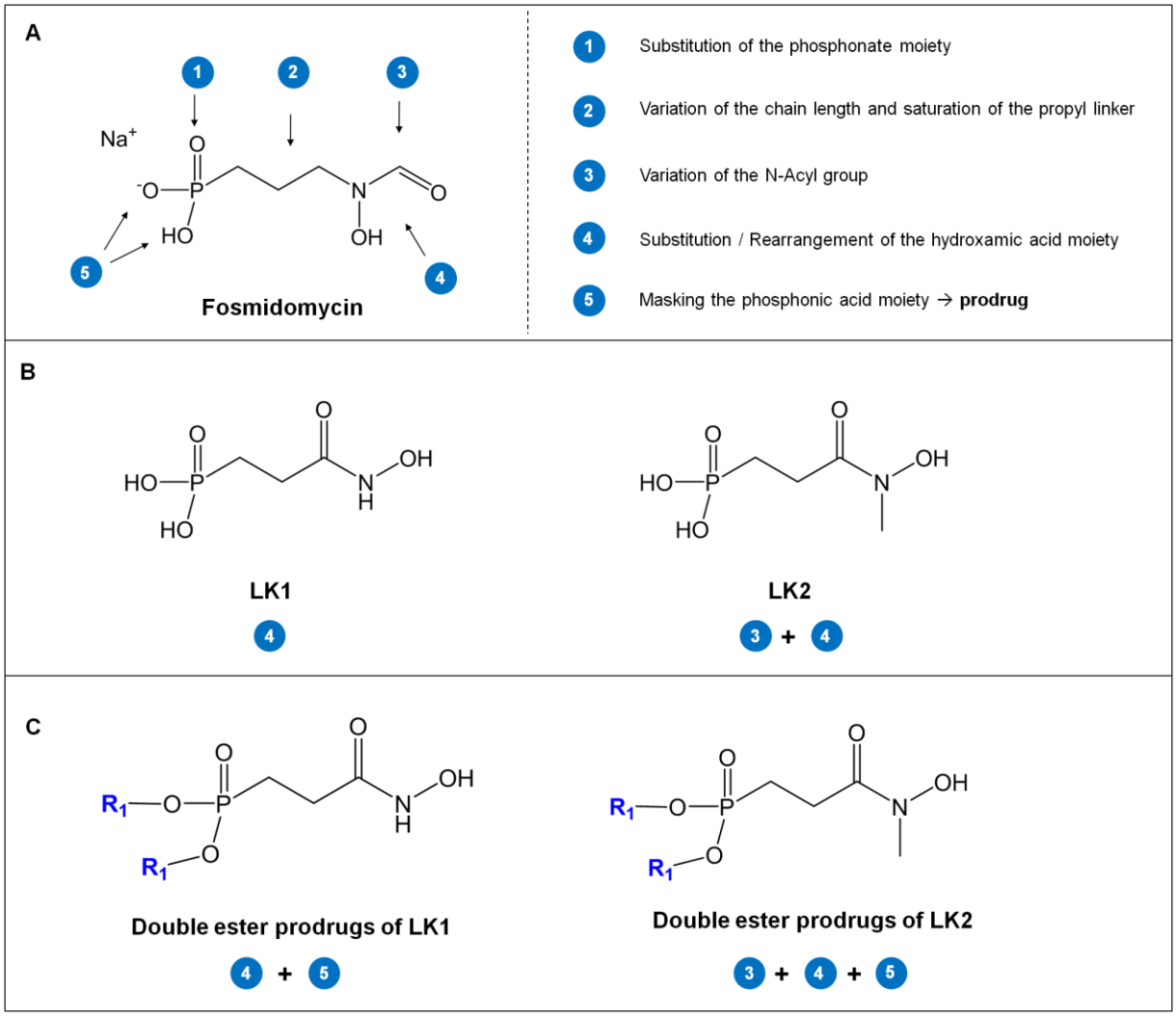

Figure 33. Simplified overview of possible modifications of fosmidomycin (modified from Schlüter, Thesis 2006).

A- Known modifications of the parent molecule; **B**- LK1 and LK2 were previously synthesized by Lionel Kuntz and are both characterised by a rearrangement of the original hydroxamic acid moiety (reverse phoshonohydroxamic acids). The N-methylated derivative LK2 has proven to be much more effective as its non-methylated analog LK1 in enzymatic assays (Kuntz et al., 2005), which is in accordance with the observations

made with Fosmidomycin and its methylated analogue FR-900098 (gute referenzen raussuchen: macsweeney , lange 2005; jomaa, wiesner 1998 ?). **C**- Ester prodrugs based on LK1 and LK2 were only recently synthesized by Sarah Ponaire. The goal of this approach was to enhance the bioavailability of both parent compounds by overcoming barriers, such as poor uptake of the drug by target organisms.

One of the known disadvantages of phosphonate drugs is the fact that the phosphonate group is highly deprotonated at physiological pH. Because of the resulting high polarity (and/or low lipophilicity), the transport across biological membranes and the general bioavailibility are strongly restricted. A common strategy to overcome this problem is masking the phosphonic acid moiety by a derivatisation. For instance, double ester drugs of FR-900098 have shown a 2-3 fold higher biological activity compared to their unmodified models in experiments with malaria-infected mice (Ortmann et al., 2005).
For this reason, Sarah Ponaire, a PhD student in Michel Rohmer's laboratory, synthesized double ester prodrugs based on the original structures of LK1 and LK2 (Figure 33 C).

The prodrug concept

The term prodrug was first used by Albert in 1958 in his book "Selective toxicity" (Albert, 1958). A prodrug can be defined as a bioreversible derivative of a known drug molecule that has to undergo a transformation in order to release the active drug ("bioactivation") (Figure 34). Alternatively and depending on the purpose, it can more generally also be described as "an inactive drug carrier form that requires metabolic activation, before it exhibits its pharmacological effects..."(Chung et al., 2008). The overall goal is to overcome different kinds of barriers depending on the organism or host/pathogen system that is targeted. This barrier may be the poor aqueous solubility of a very polar compound, the chemical instability of a molecule, an insufficient oral absorption, a rapid pre-systemic metabolism, undesired toxic effects etc. (Han and Amidon, 2000; Stella, 2007; Rautio et al., 2008).

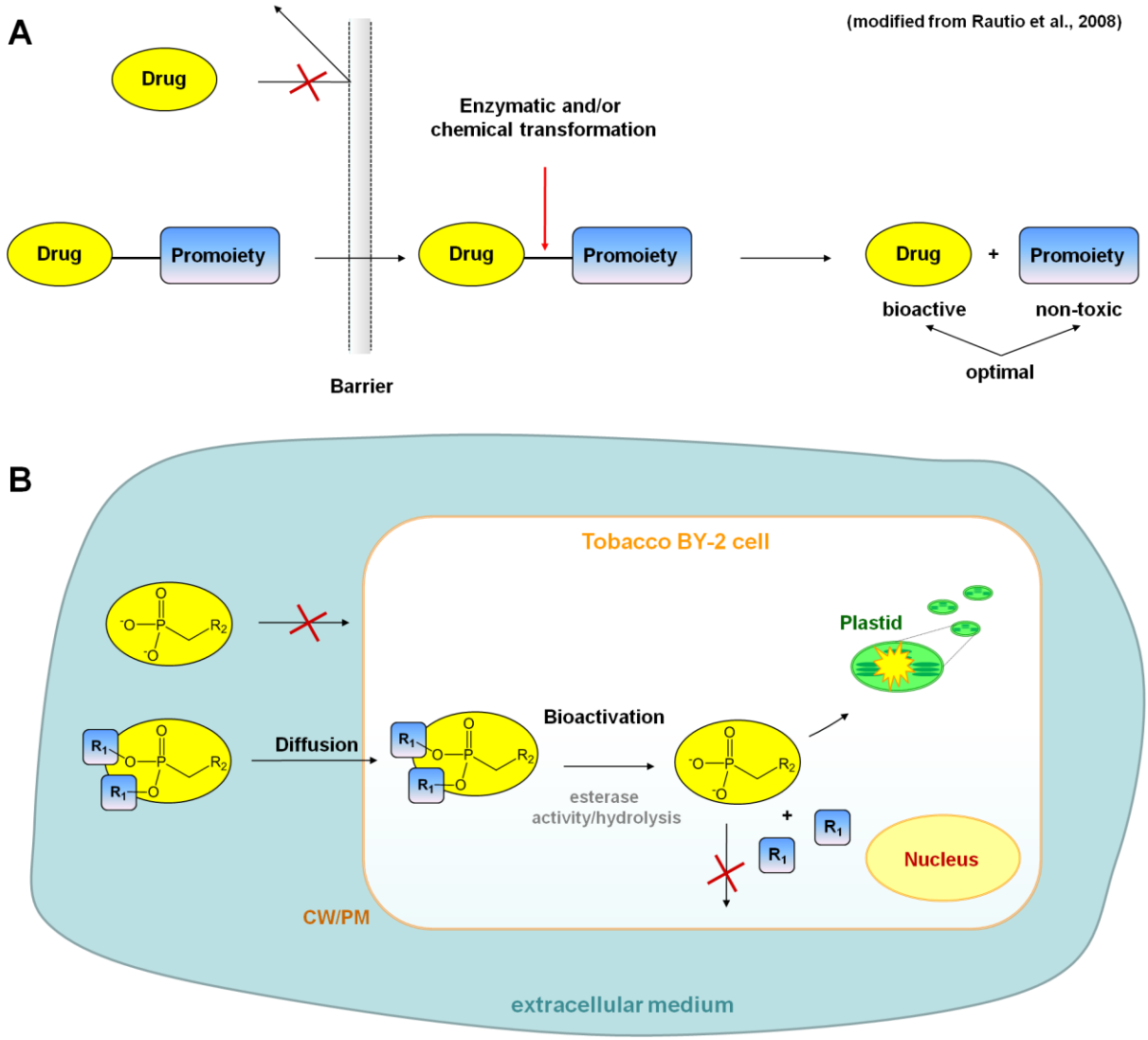

Figure 34. Simplified illustration of the prodrug concept (modified from Rautio et al., 2008).

The prodrug is a chemically modified version of the pharmacological active compound. The addition of a covalently linked "promoiety" masks the parent drug and improves for example its physicochemical or pharmacokinetic properties. **A**- If the parent drug has difficulties to overcome a barrier, such as a biological membrane or is poorly soluble, the addition of a promoiety can be seen as a strategy to overcome this barrier. In an optimal scenario, the prodrug releases the active drug after removal of the promoiety by enzymatic or chemical transformation ("bioactivation"). The drug should ideally be recovered at high rates and the promoiety should be non-toxic. **B**- In case of the inhibitors synthesized by Sarah Ponaire and the model system BY-2, the prodrugs are ester derivatives of phosphonohydroxamic drugs. After entering the cell by diffusion through the cell wall and transport through the PM, the drug is released by esterases and chemical hydrolysis. In addition, the drug has to overcome a second barrier within the cell, the double membrane of the plastid, to reach its target within the plant cell.

The simplest version of a prodrug consists of the drug and a promoiety that are covalently linked to each other, such as esters of carboxyl, hydroxyl and thiol functions. Esters are by far the most common forms of prodrugs, as they usually enhance the lipophilicity of water-soluble drugs by masking the

charged groups and thus facilitate the passive membrane permeability of the prodrug (Ettmayer et al., 2004).

Once inside the cell, the prodrug will most likely be activated by ubiquitous esterases of the target organism (Liederer and Borchardt, 2006). In an optimal case, the unmasked drug will then stay inside the cell and exhibit its pharmacological effect, whereas the released promoiety is biologically inert (non-toxic) (Rautio et al., 2008).

Prodrugs synthesized by Sarah Ponaire

Sarah synthesized six different prodrugs in total. Three prodrugs based on LK1 (derived from Fosmidomycin) and three prodrugs based on LK2 (derived from FR-900098). Three different acyloxyalkylester groups were chosen for the synthesis of the prodrugs (Figure 35). The details concerning the synthesis of the prodrugs are described in the PhD thesis of Sarah Ponaire (2010) and will not be discussed here.

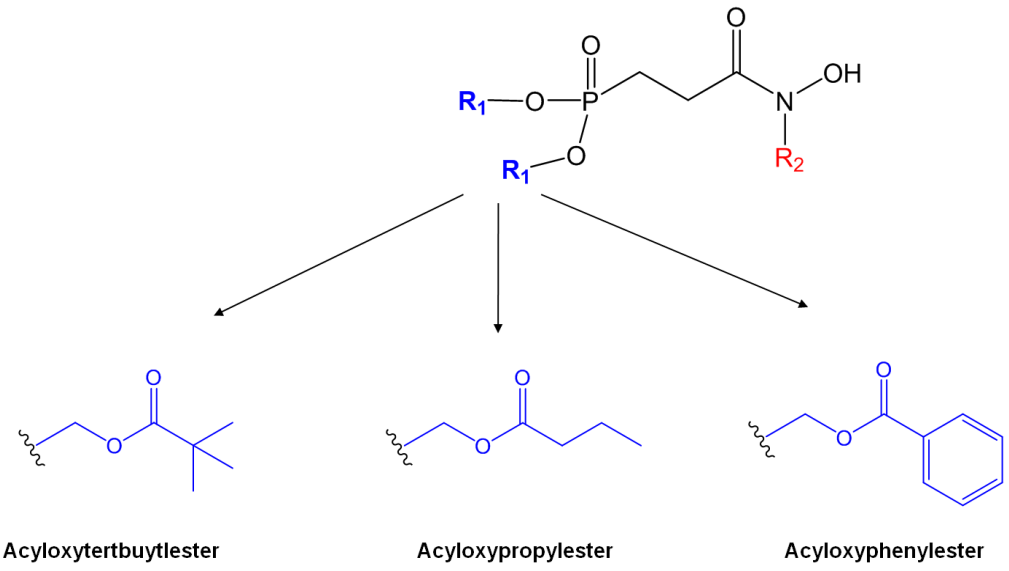

Figure 35. Different acyloxyalkylester groups chosen for the synthesis of the prodrugs by Sarah Ponaire.

Testing the compounds for possible herbicidal activity in the bioassay

Fosmidomycin is known to inhibit the DXR enzyme from higher plants (Zeidler et al., 1998; Fellermeier et al., 1999) and experiments with various plant species have demonstrated its potential as herbicide, as approved by the chlorotic and bleaching phenotypes that have been observed after its application (Kamuro et al., 1991).

In addition, Fosmidomycin successfully inhibited the isoprenylation of the GFP-DB-CVIL fusion protein in our fluorescent bioassay at concentrations in the micromolar range (Gerber et al., 2009).

Therefore it was a logical step for the evaluation of the newly synthesized compounds to test their potential to inhibit the formation of GGPP in our bioassay and thereby also to validate the test system.

Results

Fosmidomycin, FR-90098 as well as the two hydroxamate derivatives LK1 and LK2 have been tested on the transgenic BY-2 cell line expressing the GFP-DB-CVIL marker protein using the standard conditions described in Figure 10.

At 100 µM, the majority of fluorescence emitted by the GFP marker protein of the cells treated with Fosmidomycin, FR900098 or LK2 accumulated in the nucleus, indicating an efficient inhibition of the MEP pathway (Figure 36). At this concentration, the mislocalization affected about 95 % of the observed cells. The only exception was LK1, which needed considerably higher concentrations to cause a similar effect.

Inhibitor (Abbr.)	MW [g/Mol]	Solvant	Stock solution	Final concentration
Fosmidomycin (FOS)	183,1	DMSO	100 mM	100 µM
FR-900098	197,13	DMSO	100 mM	100 µM
LK1	183,1	H_2O	100 mM	100 µM
LK2	197,13	H_2O	100 mM	100 µM

Table 6. Inhibitors of DXR used in this experiment.

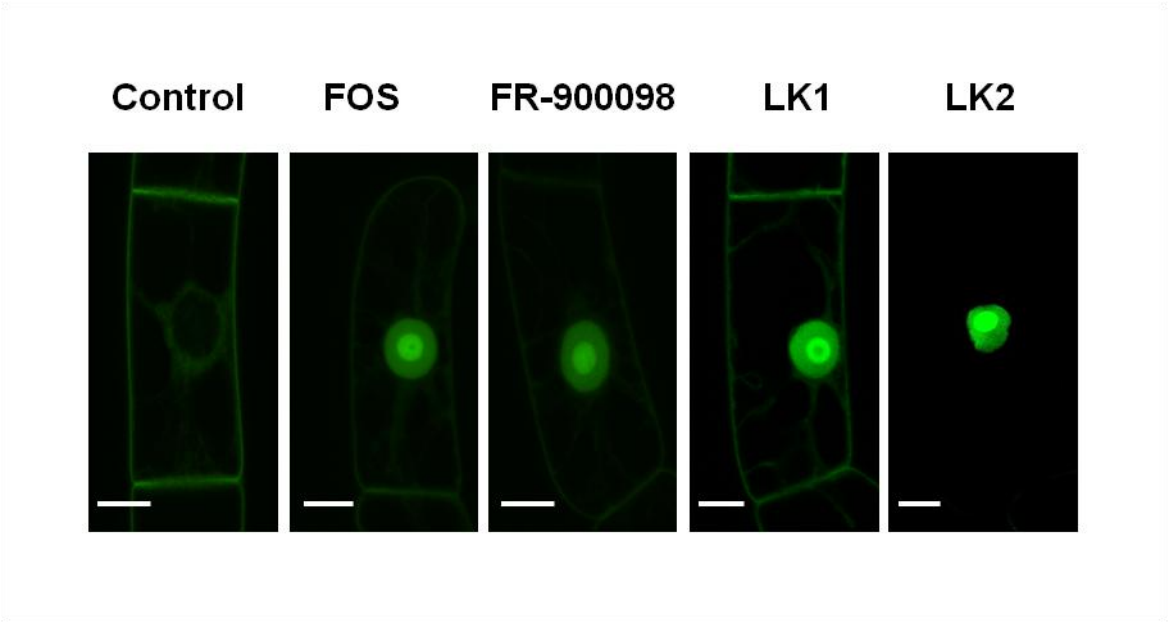

Figure 36. Localization of his-tagged GFP-DB-CVIL in transformed BY-2 cells after treatment with different inhibitors of DXR.

Confocal images were taken after treatment with different inhibitors of DXR, under standard conditions (3 hours pretreatment, followed by 15 h induction with 10 µM dexamethasone). **Control**- Cells were treated with the same volume of solvant (DMSO). **Inhibitors**- All inhibitors were tested at 100 µM and caused a significant translocation of the GFP fusion protein to the nucleus/nucleolus. White bars = 10 µM.

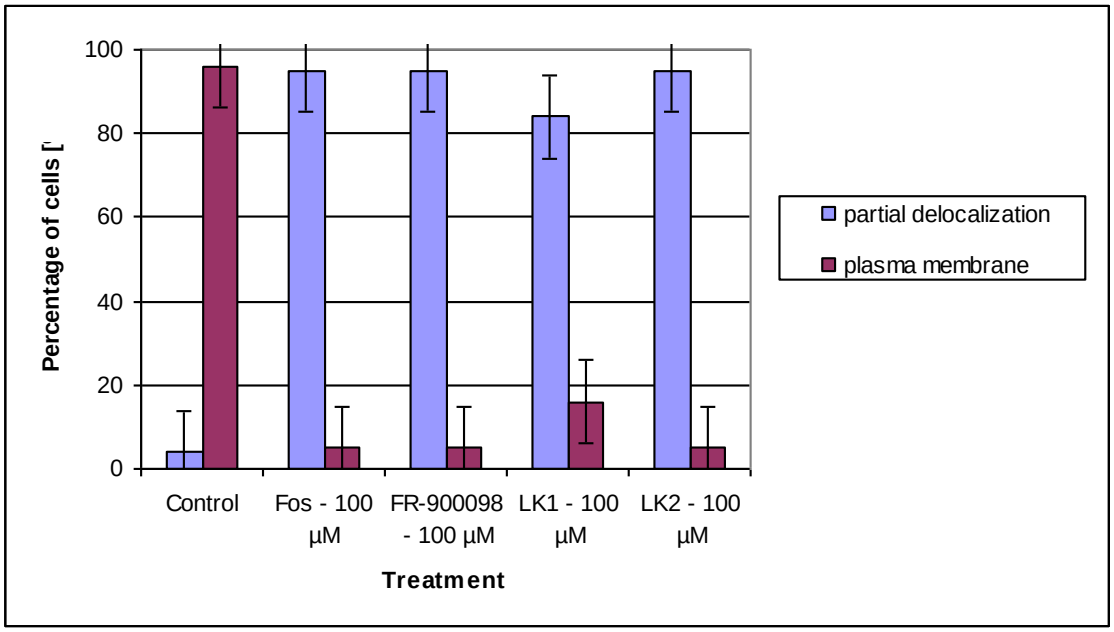

Table 7. Quantitative analysis of H6-GFP-DB-CVIL localization in BY-2 cells treated with inhibitors of DXR.

Percentage of cells showing a partial localization of the fluorescence to the nucleus and nucleolus (without taking care of the total intensity of this translocation) and the plasma membrane. For each treatment more than 100 individual cells were counted.

Test of the prodrugs provided by Sarah Ponaire

In as second set of experiments, we tested the capacity of the six prodrugs synthesized by Sarah Ponaire to inhibit the *in vivo* isoprenylation (more precisely: geranylgeranylation) of H6-GFP-DB-CVIL. This test was performed for two major reasons. First of all as a proof of concept to validate the bioassay with yet untested inhibitors. This part of the experiment should lead to a qualitative result: The prodrug inhibits the isoprenylation of the fusion protein and thus leads or not to a shift of the fluorescence from the membrane to the nuclear compartment.

In addition, it was desirable to see how the prodrugs will act in comparison to Fosmidomycin or the direct drug "role models", LK1 and LK2. This aspect was also important to check whether the bioassay may prove to be valuable for a statistical approach, as one of the primary goals of creating a prodrug is to enhance the bioavailability of a compound and gain a higher effect/activity at the target site.

As all inhibitors with the exception of LK1 were very well eficient at 100 µM, we started testing the six prodrugs at 50 µM to detect a first "all-or-nothing-effect" (Figure 37).

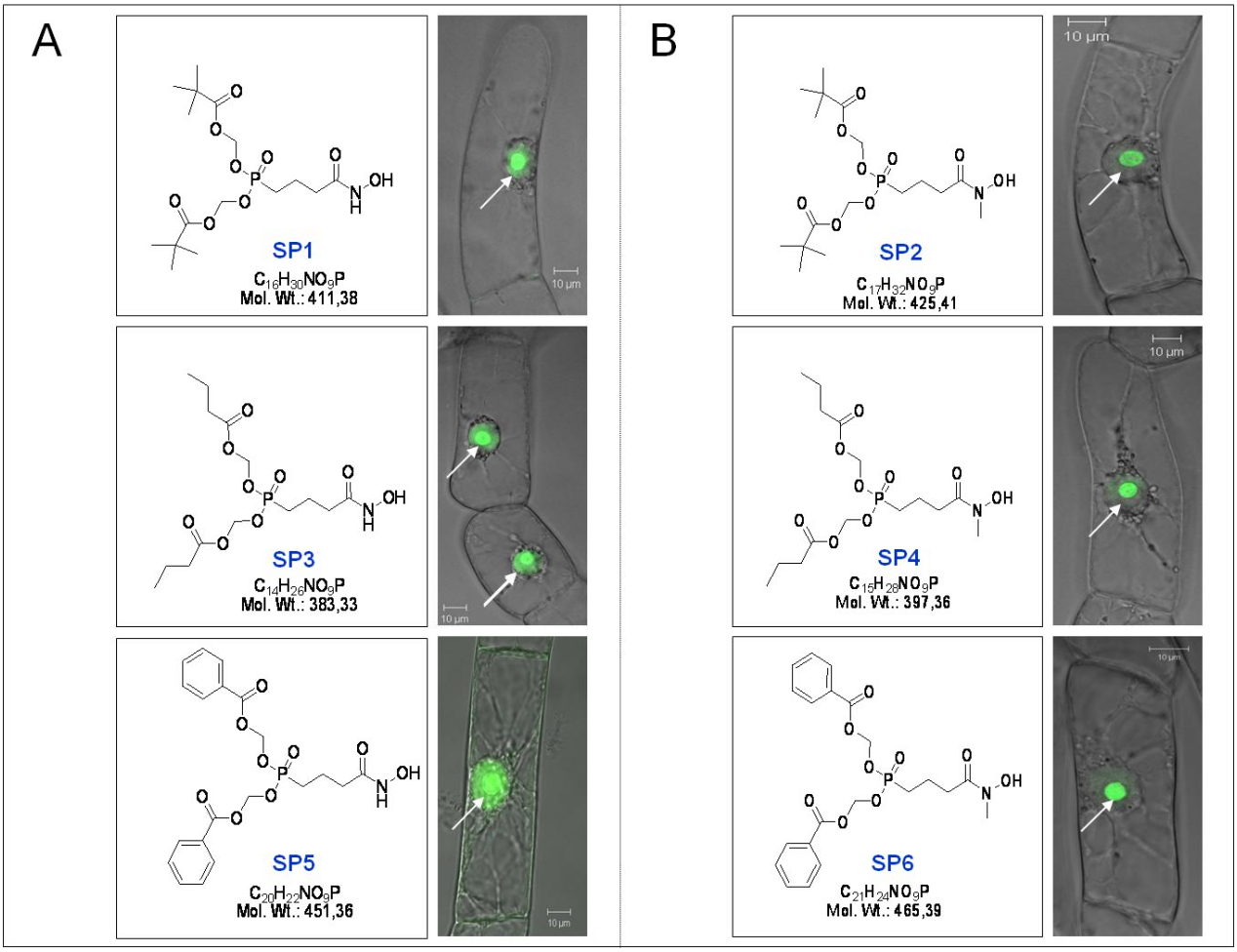

Figure 37. Confocal microscopy images showing the subcellular localisation of H6-GFP-DB-CVIL fusion protein after treatment with a series of prodrug molecules (SP1 – SP6) derived from Fosmidomycin, an effective inhibitor of DXR.

The tested molecules can be divided in two groups. **A-** Non-methylester prodrugs (derived from LK1). **B-** Molecules with a methyl group bound to the N-atom. Cells were pre-treated for 3 h with 50µM of each inhibitor (solvant: methanol) before expression of H6-GFP-DB-CVIL was induced by addition of dexamethasone (10 µM final concentration). At the chosen concentration, the majority of all treated cells showed partial or very dominant delocalization of the fluorescence from the plasma membrane to the nucleus/nucleolus. The images are overlays from pictures in transmission light and fluorescence mode and were acquired as described in chapter 4.5.20. Bars = 10 µM.

At 50 µM final concentration, all the six prodrugs were able to induce a mislocalization of the H6-GFP-DB-CVIL fusion protein in at least 50 % of treated cells. The cells were counted by the operator of the fluorescence microscope at low magnification (using a 10x apochromatic objective) and divided in three major groups - according to their respective phenotype - to facilitate a statistical evaluation (Table 8):

1. cells in which the fluorescence emitted from the nucleus was clearly dominant
2. cells with significant amounts of fluorescence still emitted from the PM (nucleus and membrane were more or less equal in fluorescence intensity)

3. cells in which the fluorescence was mainly associated with the PM and looked like the untreated control (important: no fluorescence at all visible in the nucleolus).

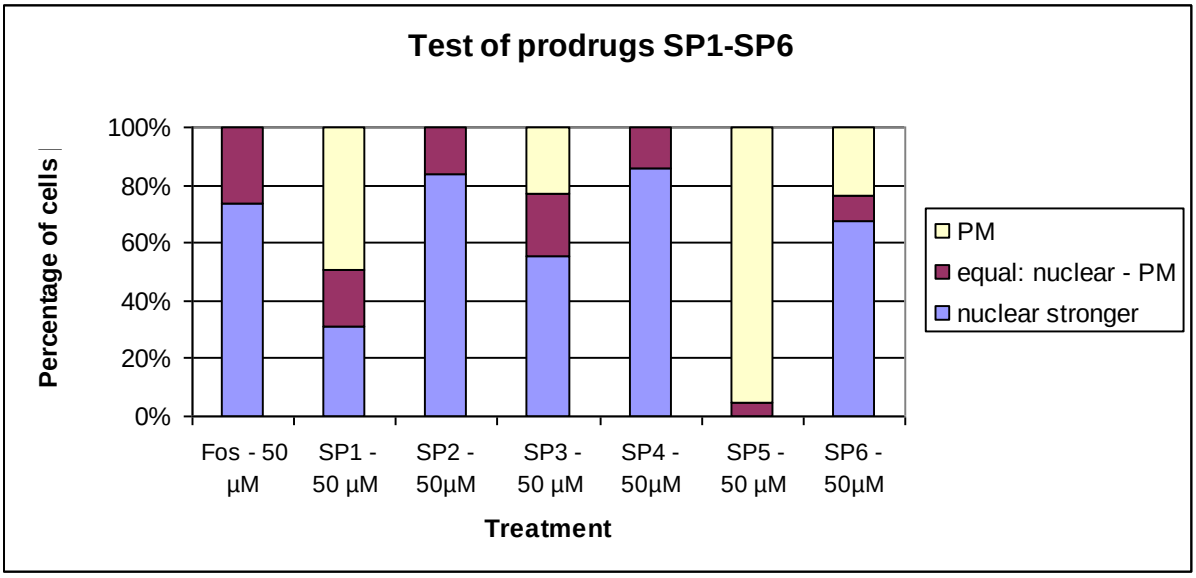

Table 8. Statistical approach to compare the impact of six different pro-drugs on the in-vivo localization of the prenylable fusion protein H6-GFP-DB-CVIL.

The results obtained at a final concentration of 50 µM indicated, that especially SP2 and SP4 caused a fluorescence shift comparable to that observed after treatment with 50 µM Fosmidomycin. Surprisingly, in the case of the Fosmidomycin treatment at 50 µM, we observed a very high ratio of cells with a mislocalized GFP fusion protein (more or less all cells), a result slightly different from previous data obtained after treatment at 40 µM, which indicated at least 30 % of total cells with a fluorescence in the PM (Gerber et al., 2009).

Among the six prodrugs, SP2 and SP4 appeared to be very active. In both cases, more than 80 % of counted cells showed a dominant fluorescent signal from the nuclear region of the cell, indicating a significant inhibition of GGPP biosynthesis through the MEP pathway. The other compounds did not act as well as Fosmidomycin. In summary, a general tendancy could be observed, clearly indicating that the methylated analogs of the respective prodrugs were far more efficient than their non-methylated counterparts. This corroborates the results obtained with LK1 and LK2 (Kuntz et al., 2005) as well as those obtained with Fosmidomycin and FR-900098 (Ortmann et al., 2005).

At 50 µM however, it was not possible to determine whether the prodrugs SP2 and SP6 were better inhibitors than Fosmidomycin. To adress this issue, we therefore conducted a second set of experiments, using the inhibitors at a final concentration of 5 µM.

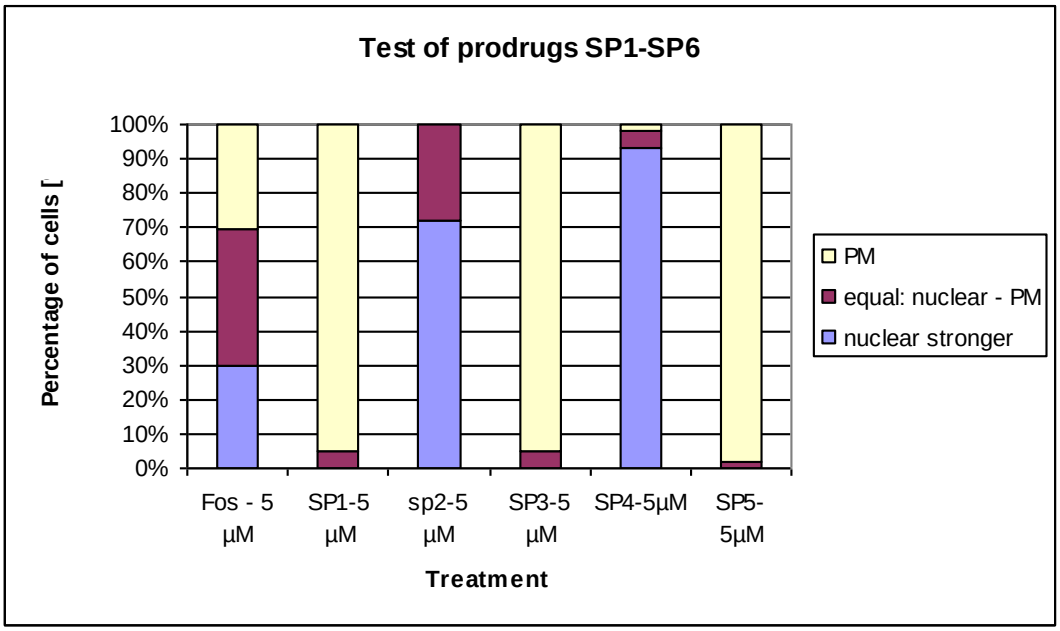

Table 9. **Statistical approach to compare the impact of six different pro-drugs on the *in vivo* localization of the prenylable fusion protein H6-GFP-DB-CVIL.**

The cells were treated with 5 µM of the respective inhibitor like described above. Cells were counted by view and sorted in three main categories. Unfortunately, there is no data available for the SP6 treatment.

At 5 µM, two major results are noteworthy (Table 9). First of all, the efficiency of Fosmidomycin to induce a mislocalization of the fusion protein drops dramatically. More than 30 % of the cells treated with 5 µM Fosmidomycin did not show any fluorescence translocation to the nucleus and gave a phenotype similar to that of the untreated control cells. In addition, the percentage of cells with a dominant fluorescence signal emitted by the nucleus (among the remaining cells with a partial mislocalization) decreased by more than 50 %. By contrast, SP2 as well as SP4 did only show a slightly reduced efficiency to induce a dominant mislocalization of the GFP fusion protein from the PM to the nucleus. In the case of SP2, 74 % of the cells were still significantly inhibited by the treatment at 5 µM. For SP4, the value higher than 90 % indicated that there was almost no detectable loss of efficiency after a 10-fold dilution from 50 µ to 5 µM.

As both inhibitors successfully induced a mislocalization of the geranylgeranylated GFP fusion protein at 5 µM, we decided to further test SP2 and SP4 at a final concentration of 0,5 µM. Unfortunately, the overall physiological state of the cell line worsened dramatically, which was indicated by a more or less spontaneous loss or important reduction of the fluorescence intensity. This phenomenon occurred gradually over a couple of weeks and concerned most of the cells within a population and forced us to stop the statistical approach at this point, to avoid a bias caused by the bad physiological state of the

cell line. This was one of the major reasons to establish a protocol for the reselection of a homogenous cell line with satisfying fluorescence levels (for more details see chapter 2.3).
Nevertheless, we could observe that at least 50 % of the remaining fluorescent cells still showed a partial mislocalization (of the fluorescence to the nuclear compartment of the cells) after treatments with SP2 and SP4 , indicating that both inhibitors are still partially efficient at a concentration of 0,5 µM.
By contrast, neither a treatment with Fosmidomycin nor a treatment of the cell line with LK1 of did cause any statistically relevant mislocalization at 0,5 µM. The data obtained with LK2 at this concentration was not statistically exploitable due to the bad condition of the cell line, even though more than 90 % of the remaining, fluorescent cells looked like untreated control cells at 0,5 µM (data not shown).

Discussion of the results:

During her thesis, Esther Gerber (2005) had already used statistical approaches based on this visual bioassay, in order to determine the contribution of various externally fed pathway intermediates/isoprenols to the prenylation and the localization of the GFP-DB-CVIL fusion protein, in the presence or not of inhibitors of both isoprenoid biosynthetic pathways (chapter 2.1.2.1).
The experiments described in this chapter were conducted under similar conditions; cells tested under pre-defined standard conditions were counted by view after different treatments.
However, the test of the prodrugs synthesized by Sarah Ponaire includes a whole new aspect: For the first time, novel drugs specifically designed on the basis of known pathway inhibitors were tested under standardized conditions and the generated data were exploited in both a qualitative and a quantitative/statistical way. This means that, besides answering the question, if an inhibitor candidate efficiently blocks the MEP pathway, the exploitation of the same set of data will allow a direct comparison of the efficiency of this compound with established MEP pathway inhibitors.
By testing the inhibitors at different concentrations, we were able to first define a starting point for the experiments, which consisted in a concentration that inhibited the majority of cells (> 95 % of cells showing a dominant mislocalization).
The results obtained at 100 µM clearly proved that Fosmidomycin and FR-900098 as well as LK2 were applied at saturating concentrations. We therefore decided to start our direct comparison at 50 µM. At this concentration, Fosmidomycin, SP2 and SP4 were very active, causing a partial mislocalization in nearly 100 % of the cells. The other tested prodrugs did not act as well at this concentration, even though they were able to induce a partial mislocalization in at least 50% of treated

cells. At 5 µM, only SP2 and SP4 proved to be more efficient than Fosmidomycin, wheras the other inhibitors only induced a barely detectable effect.

Obtaining only two out of the six compounds with a higher efficiency than the respective model drugs might appear deceiving at first view. However, it is a fine exemple confirming the prodrug concept. The efficiency of a prodrug in an *in vivo* assay depends indeed on several parameters, such as the transfer through biological membranes and the stability of the prodrug against hydrolysis or esterases.

All the six prodrugs tested in these experiments were able to induce to some extent a localization shift of the prenylable GFP fusion protein, which indicates that the active drug entered at least partially the plant cell, where it could inhibit the DXR enzyme (located in the plastidial compartment). This point is important to mention, as it indicates that: i) the prodrugs were soluble in the BY-2 medium; ii) they successfully crossed the plant cell wall; iii) they were imported inside the plant cell across the PM. How this transport took place and which transporters were involved remains unclear, even though data from bacteria suggest that a cAMP dependent glycerol-3-phosphate transporter could be a likely candidate. Until today, a similar transporter has only been identified in the mitochondrial membrane of plant cells (Shen et al., 2006).

By relating the results to the structural features of the tested molecules, another important observation can be made. The data obtained for all inhibitors showed that the methylated prodrugs displayed a far better activity than their non-methylated counterparts. This result correlates with observations obtained with Fosmidomycin, FR-90098, LK1 and LK2 in bacterial systems. Interestingly, the best performing methylated prodrug SP4 also shared the same promoieties with the best performing non-methylated prodrug SP3.

Although the better performance of the methylated drugs, such FR-900098 or LK2, is thought to be attributed to the hydrophobic interaction of the methyl-group at the catalytic site of the DXR enzyme, the methyl group may also have an influence on the lipophilicity of the prodrug and be responsible for an overall better import rate of the prodrug in tobacco BY-2 cells. Other factors could be the different preferences of endogenous esterases for the three types of substituents used to synthesize the prodrugs or the rate of spontaneous hydrolysis (that may occur either in the extracellular medium or the cytosol).

Only recently, Amanda Brown and Tanya Parish (2008) were able to demonstrate that the resistance of *Mycobacterium tuberculosis* and *Mycobacterium smegmatis* to Fosmidomycin is mainly due to a lack of uptake of the molecule by the cell. Interestingly, the recombinant DXR of *Mycobacterium tuberculosis* was however sensitive to Fosmidomycin in earlier studies (Dhiman et al., 2005). This lack of uptake may occur for two reasons. First of all, Mycobacteria are known to be particular antibiotica resistant, mainly because of the nature of their cell wall which is nearly impermeable to commonly used antibiotics. Secondly, no genomic evidence has been found in these mycobacteria for a transporter system, similar to the one used by *E.coli* or other susceptible bacteria. Furthermore, the

porins, which could also participate to the antibiotic import, are neither abundant nor particularly active in mycobacteria (Trias et al., 1992).

Therefore, it is very promising that all of the methylated prodrugs (SP2, SP4 and SP6) were shown able to inhibit the growth of *Mycobacterium smegmatis* on solid medium, when applied on paper discs (results communicated by Sarah Ponaire). Interestingly, the zones of inhibition were growing in size in the following order: SP4>SP2>SP6. This trend was also observed when testing the N-methylated inhibitors in our bioassay and indicates that in both cases, the prodrug with the acyloxybutylester groups protecting the phosphonate moiety (SP4) was the most efficient (Figure 38).

Although both model systems used for testing the efficiency of the prodrugs cannot be completely compared due to physiological differences in cell wall architecture and uptake mechanisms, this result is nevertheless very encouraging. Wether the passive import of the prodrug is improved or is recognized with a higher affinity by esterases remains to be determined, but an explanation is not obvious. However, our results clearly show that the observations made with this visual bioassay are of biological relevance and that knowledge gained from experiments with tobacco BY-2 cells may be applied to other model systems, such as *Mycobacterium smegmatis*.

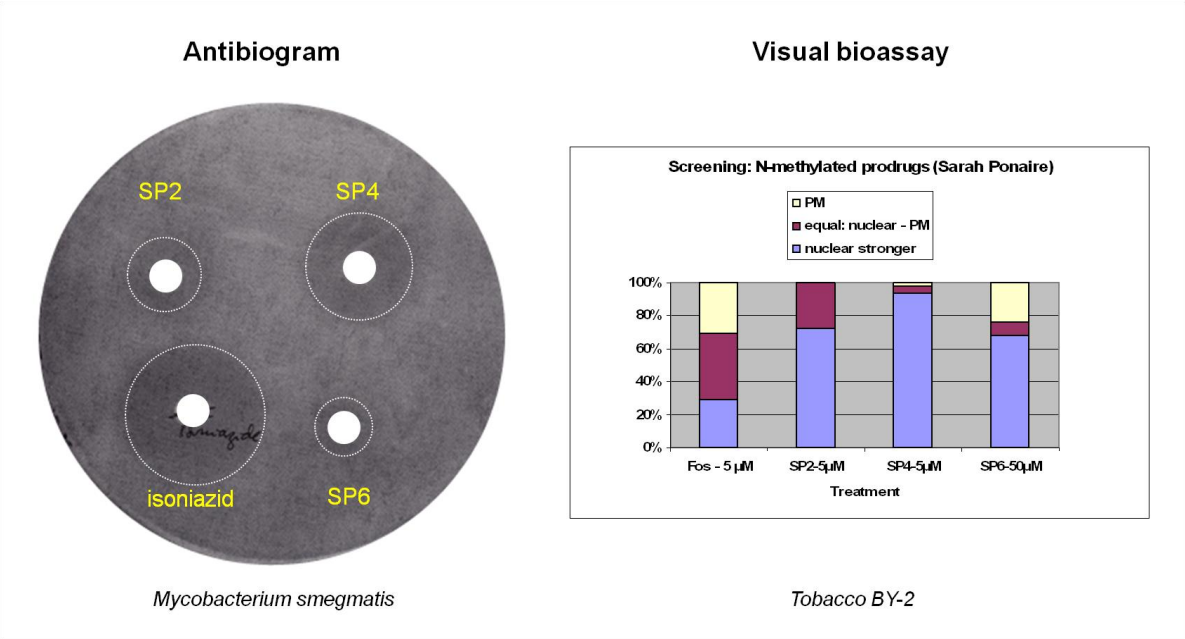

Figure 38. Comparison of the results obtained with the N-methylated prodrugs by two different approaches.

Of course, as a further proof of concept, the inhibitors have to be tested for their potential to act as bleaching herbicides. Such experiments are underway with tobacco seedlings and hopefully I will be able to present recent data during my defence.

2.2 Development of an image-based chemical screening system for inhibitors of the plastidial MEP pathway

By successfully testing novel drug candidates *in vivo*, we illustrated the possibility to establish the existing bioassay as qualitative **and** quantitative approach for the identification and evaluation of MEP pathway inhibitors.

However, all analyses performed so far with the bioassay were relying on the performance of a single microscope user, observing biological processes and counting individual cells through the eyepiece of the microscope. Although all parameters of the bioassay had been optimized and provided us with a sufficiently robust and repeatable protocol, further developments were required, in particular to reduce the unvolontary bias of results by the user and to increase the speed and reproducibility of the application.

Therefore a major emphasis of my thesis was to further improve the initial test system and to evaluate its potential for miniaturization, automatization and, if possible, high-throughput applications.

2.2.1 Introduction: State of the art of modern drug screening

Over the last decade, technological advances have dramatically changed the importance of image-based assays for modern cell biology. In the past, classical, non-microscopic approaches have been systematically used to investigate protein functions and interactions or to screen small-compound libraries in high-throughput. Thanks to the knowledge and tools developed during the evolution of various technologies in the last few years, including proteomics and genetics approaches (Uetz and Hughes, 2000; Rual et al., 2005; Foster et al., 2006; Gavin et al., 2006), protein and DNA microarrays (Hughes et al., 2000; Smith et al., 2005; Starkuviene et al., 2007) or RNA interference experiments (Carpenter and Sabatini, 2004) (Baum and Craig, 2004; Moffat and Sabatini, 2006), fluorescence microscopy has become a powerful method to study protein functions and interactions in the living cell (Starkuviene and Pepperkok, 2007; Terjung et al.). This was in particular accomplished due to the availability of a great variety of fluorescent proteins and fluorophores (Zhang et al., 2002; Verkhusha and Lukyanov, 2004; Miyawaki et al., 2005), which can be used to tag a protein of interest and to reveal information about its localization, its interaction with other cellular components and proteins or even to visualize biochemical reactions, *e.g.* the effect of a given treatment at a cellular level. This may give conclusions on the physiological relevance of the protein, in contrast to classical, biochemical assays, where an isolated protein is tested in an artificial environment. In this way, data

acquired by fluorescence microscopy can help to complement the above mentioned genetic and proteomic approaches.

Because of the availability of automated microscopes and more powerful image analysis softwares, multiple features of a cell can be measured, analyzed and compared, even over a certain period of time.

Previously, researchers were often forced to inspect their acquired microscopic images by eye, which is a time-consuming and subjective task, even for an experienced user (Eggert et al., 2004; Lang et al., 2006; Lamprecht et al., 2007). Nowadays, modern, automated image acquisition platforms provide highly quantitative data and allow image-based screens of several thousand compounds a day depending on the experimental set-up. In addition, fluorescence microscopy also allows following reactions at different scales. For instance, changes at the subcellular level can be observed using high resolution (Wouters et al., 2001; Watson et al., 2005), whereas a population of cells can be monitored using low resolution (Burnett et al., 2003; Wu et al., 2004), providing the examinator with lots of data for every single image. This combination of high throughput-screening (HTS) methods and automated image acquisition and analysis has therefore been dubbed “high-content-screening” (Giuliano et al., 1997; Giuliano et al., 2003; Carpenter, 2007b, , 2007a; Starkuviene and Pepperkok, 2007).

Nevertheless, image-based chemical screening still remains a field in development, the majority of users belonging to the pharmaceutical industry (Hoffman and Garippa, 2007). This means, that even though the technologies are pushed by those companies, only few results of large screens have been generally published and made available for a great number of users (Gururaja et al., 2006; Richards et al., 2006; Wilson et al., 2006). In addition, not every academic research unit, that has developed a biological assay with the potential for high-throughput/content screening will be able to use modern image platforms, as all the hardware and software components of a complete screening pipeline (not counting the time for development and validation) represent a significant financial investment , although commercial solutions are provided by different companies (Smith and Eisenstein, 2005).

Another trend in high-content screening microscopy goes to multidimensional image read-out. This approach is also known as multiplexing (Levenson et al., 2005; Mansfield et al., 2005). Technically, it consists in using multi-color fluorescence microscopy and several distinct fluorescent markers in the same cell system. Of course, the spectral properties of the used fluorescent dyes and fluorophores as well as the detection gain and the computing ability of the microscopy platform are limiting factors, although this can be partially resolved by linear unmixing of fluorescent signals, "a method allowing the reliable separation of even strongly overlapping fluorescence signals..." (Zimmermann et al., 2003; Zimmermann, 2005). Multiplexing is particularly interesting, if more than one phenotype needs to be analyzed. As a side effect, changes in the morphology of the cells can also be monitored, which can reveal a potential toxicity event during the screening experiment. For example, multiple fluorophores, staining nucleus, cytoplasm, microtubules, golgi or endoplasmatic reticulum could be detected in

parallel, revealing additional information about cellular changes, as part of a small compound screen (Perlman et al., 2004; Tanaka et al., 2005). As a result, a pre-selection of drug-candidates can be performed at an early stage in the whole screening pipeline. This aspect can be quite important, considering that up to 30% of potential drug candidates are rejected because of toxicity issues (Kola and Landis, 2004). Likewise, efficiency can be increased and the costs, significantly reduced (Kola and Landis, 2004; Starkuviene and Pepperkok, 2007).

However, one of the most critical steps still remains analysis of images, especially in purely cell-based assays. Although there are several commercial softwares for numerous purposes, many applications - especially those with complex cellular phenotypes - require custom-made solutions. This chapter will focus on the key steps that are necessary for the development of a screening pipeline (Carpenter, 2007b) to demonstrate the feasibility of establishing a high-throughput compound screen on the basis of our protein prenylation assay (Figure 39).

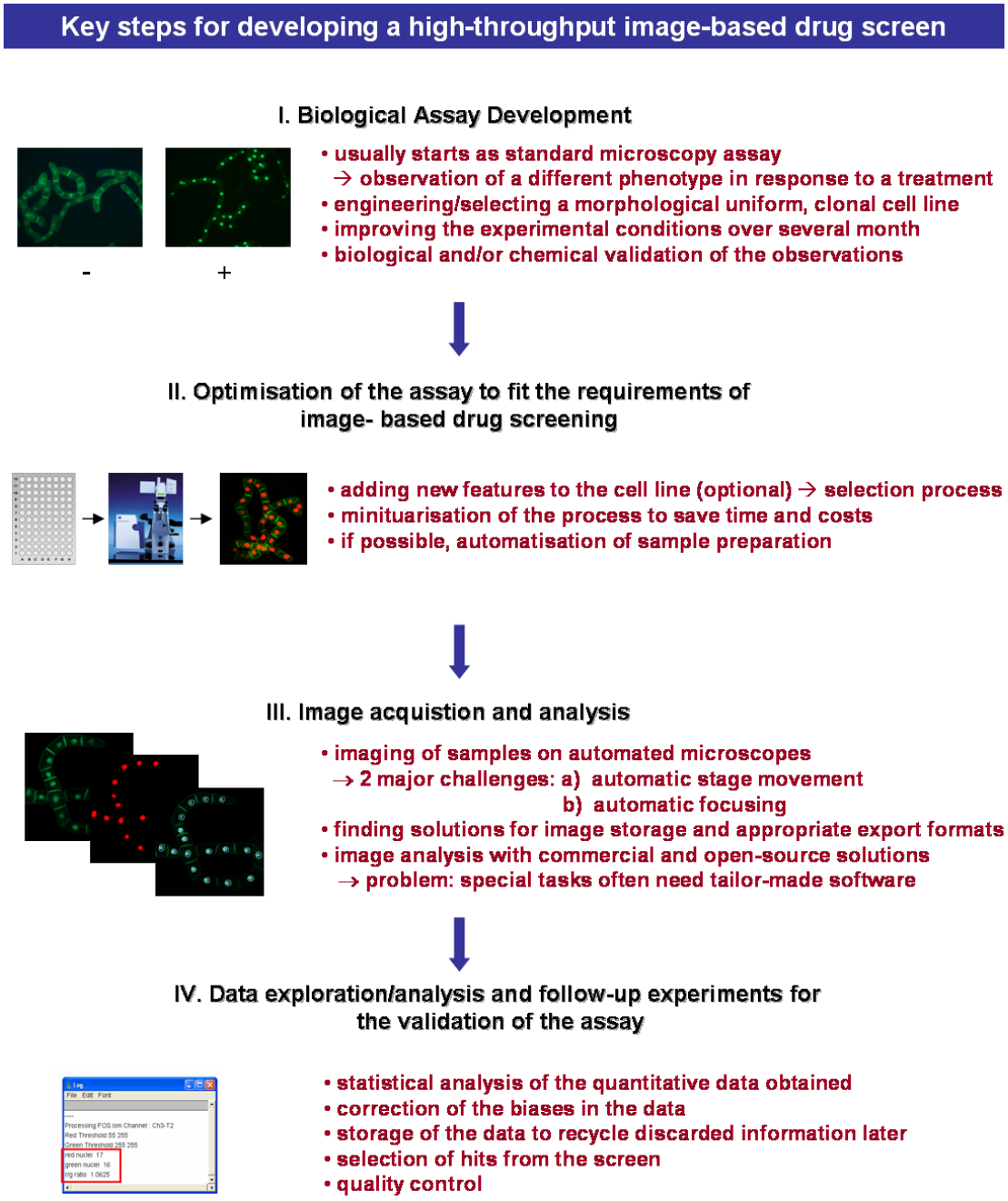

Figure 39. Principal steps involved in the development of an image-based drug screening assay.

2.2.2 Biological assay development

2.2.2.1 Reproducibility of inhibitor effects on a population of BY-2 cells

The results described in the previous chapters provided critical evidence for an essential role of the MEP pathway in the biosynthesis of the prenyldiphosphate GGPP and in the prenylation of the H6-GFP-DB-CVIL fusion protein in BY-2 cells (Gerber et al., 2009). As the inhibition of both processes leads to a characteristic phenotype - the mislocalization of the fluorescent fusion protein from the PM to the nucleus - the microscope assay developed during the thesis of Esther Gerber can be used as a qualitative test system to identify potential inhibitors of the MEP pathway or the prenyltransferase PGGT1. The importance of the MEP pathway as a target for the development of novel inhibitory agents (antibiotics, antimalarial drugs, bleaching herbicides) has been described in detail before.

However, the acquisition of images at high magnification (HM) only allows observing the effects on a few cells within the treated population and its non-quantitative side can cause user-generated bias. Counting cells by eye as it has been done for the statistical analysis of the localization of the GFP-BD-CVIL protein after treatment with pathway-specific inhibitors (Figure 12) takes hours, is highly subjective and barely manageable. In addition, this kind of experiment does not provide an image that could be reanalyzed with a closer look for other features of the cells such as specific phenotypes that might not be evident at first sight and remain unseen during the examination of the whole population (Levsky and Singer, 2003; Carpenter, 2007b). Especially, the results obtained after treatment of the H6-GFP-DB-CVIL lines with squalestatin demonstrated that the effects on the morphology and localization of the fusion protein could be more complex than initially expected (partial delocalization, roundish cell shape *versus* "all-or-nothing" – phenotype). Some important aspects can escape to the human eye during a visual observation and sometimes, it is difficult to make conclusions of biological significance by analysis of single cells. Therefore, it was important to check the reproducibility of the results with a random collection of cells. Furthermore, the quality of the acquired digital images had to be high enough for an automatic identification and measurement of biological features, such as the nuclear fluorescence observed in inhibitor-treated TBY-2 cells.

The use of TBY-2 cells as a suitable model to investigate effects of various treatments on the whole cell level has various advantages, including the efficient uptake of exogenous compounds and the short reproduction time. However, as discussed in detail in chapter 3.3 (Generation of transgenic tobacco BY-2 cell lines) an important problem was the heterogeneity of fluorescence of liquid suspensions derived from the first generation calli. This problem has been solved successfully and was an important prerequisite for the further development of a statistically significant screening system.

Results:

In order to demonstrate the feasibility and reproducibility of such an image-based approach, TBY-2 cells expressing the His_6-tagged GFP-DB-CVIL fusion protein were treated with the MEP- or MVA pathway inhibitors, OC (30 µM) or MV as well as with a combination of both inhibitors according to standard protocols. Images were acquired at low magnification using a Nikon E800 microscope. Low magnification fluorescence microscopy uses a resolution of 500 µm to 1mm and is used to monitor phenotypic effects on entire cell populations. Medium-magnification fluorescence microscopy by definition is applied for subpopulation analysis at a resolution between 10-50 µM, whereas high-magnification fluorescence microscopy focuses on intracellular events and uses resolution of 1 µm or lower (Lang et al., 2006). The phenotypes of the untreated control and the MV-treated cells were more or less identical, with the majority of fluorescence at the cell periphery, especially at the boundary between cells in the files. In addition, GFP fluorescence was also clearly visible at the peri-nuclear membrane, whereas the GFP fluorescence in OC-treated cells was mostly localized in the nucleus. The combination of both inhibitors gave the same results as cells treated with OC alone (Figure 40).

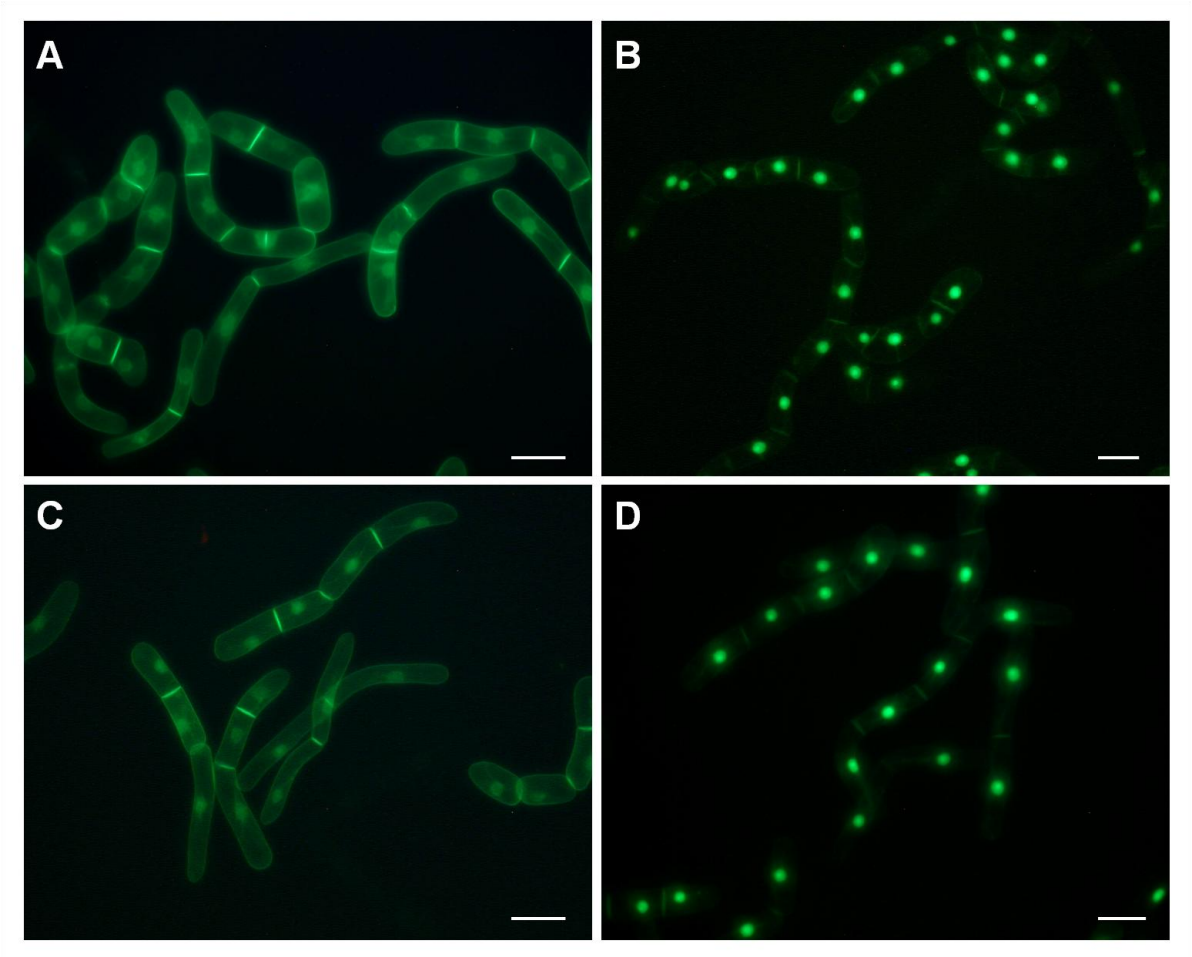

Figure 40. Reproducibilty of results on a random population of treated BY-2 cells.

Low magnification fluorescence images of large numbers of cloned BY-2 cells expressing His_6-GFP-DB-CVIL. Images were taken with a Nikon E800 micrsocope equipped with a DXM11200 CCD color camera (Specifications: 20 x 0,45 objective; filters: Ex460-500, DM505, EM510-560). **A** Untreated cells **B-D** cells treated with 30 µM OC (**B),** 5 µM MV(**C**) and 30 OC plus 5 µM MV (**D**)**.** The white bar represents 50 µm.

2.2.3 Image acquisition and analysis

Cellular imaging is a process that involves multiple steps and usually starts with the acquisition of an image by a specialized detection device. In our case, this device was a confocal fluorescence microscope, that visualizes and collects signals from the sample and generates a digital image, which may be defined as "a two-dimensional pixel array of information extracted from a particular biological event (..)" (Lang et al., 2006). In a second step, this information has to be processed by an image analysis software to convert it into exploitable parameters. Depending on the nature of the experiment and the kind of information that is needed, multiple parameters may be extracted and analyzed at the level of either the entire cell population or only one cell, sometimes (like in our case) at both levels. The process of analysis of information from microscopy images normally can be divided into several distinct steps:

- identification of single cells
- measurement and calculation of various values for each cell
- analysis of the data

In general, microscope based cytometry methods take advantage of fluorescence to identify cells. Various algorithms for edge detection, thresholding and watershed seperation are able to provide the user with good initial separation between the fluorescent features within the cells and the non-fluorescent background (Gordon et al., 2007). How these features (e.g. the GFP fluorescence emitted by the nucleus in inhibitor-treated BY-2 cells) can be used for the detection and counting of cells, will be shown in detail in the following chapter.

2.2.3.1 Automatic image processing as tool to determine the impact of drugs and inhibitors on the H6-GFP-DB-CVIL-line

Automatic image analysis was performed to study and quantify the effects of different treatments on the H6-GFP-DB-CVIL cell line with a time-saving and reproducible method that reduces as much as possible the influence of the user and leaves a visual "trace" of the analysis.
Therefore, overview images, taken under well-defined conditions, were analyzed with professional image processing software.

Image analysis with ImageJ

For image analysis, we first used ImageJ (http://rsb.info.nih.gov/ij/index.html), version 1.41 – 1.43, the core program of which was developed by Wayne Rasband, a researcher at the National Institutes of Health (NIH).
ImageJ is a Java-based image-processing program, publicly available, inspired by NIH Image for the Macintosh (Abramoff et al., 2004). The use of the Java programming language makes ImageJ independent from any individual operating system. It can be installed on every platform able to run a system-specific Java runtime environment (JRE). The code of the program is open-source and because of a constantly increasing user community, over 400 individual plug-ins are available, significantly increasing its functionality. ImageJ supports a large number of different file formats. Many proprietary out-put formats are directly related to microscopy.
The MBF ImageJ bundle used in this study provides an excellent selection of the most important plug-ins for microscopy users and is available with a richly illustrated on-line manual. It is developed, released and maintained by Tony J. Collins, who is currently working at the McMaster Biophotonics Facility (MBF: www.macbiophotonics.ca).

Important pre-requisites when starting with the image analysis

One of the major aspects when working in fluorescence microscopy is the level of saturation of the images. For instance, within an optimal scenario, all images taken in the green channel – displaying the localization of the geranylgeranylable protein- should be acquired with a minimum of saturation to reduce signals corresponding to unspecific background noise or non-specific fluorescence associated with cellular structures. For the subsequent image analysis, it is quite important to be able to differentiate any object from its surrounding background. This process is referred to as "segmentation". Most of the programs operating in the microscopes and used for image acquisition, such as the LSM image browser or the AxioVison software (Table 12: List of all software packages and programs relevant to this study), offer the option to control the saturation levels of the images during or after the acquisition process.

The general principle of the particle analysis with ImageJ (http://www.macbiophotonics.ca/imagej/particle_analysis.htm) will be explained in the following sections, using an image of OC-treated cells (40 µM final concentration OC; acquired with the E800 epifluorescence microscope from Nikon), where the delocalization of the GFP-DB-CVIL protein is clearly visible.

The overall process can be divided into the following parts:

- "thresholding"
- "watershed separation"
- "particle analysis"

The process was adjusted to fit our purposes (later sections).

a) Thresholding

One of the first steps in automatic particle analysis is the "thresholding". The image needs to be converted into a "binary" image, for instance into a black and white image. This can be achieved by using the menu command "Image/Type/8-bit". Depending on the image parameters, such as luminosity and brightness, the contrast may be enhanced, with "Process/Enhance Contrast" (Figure 41).

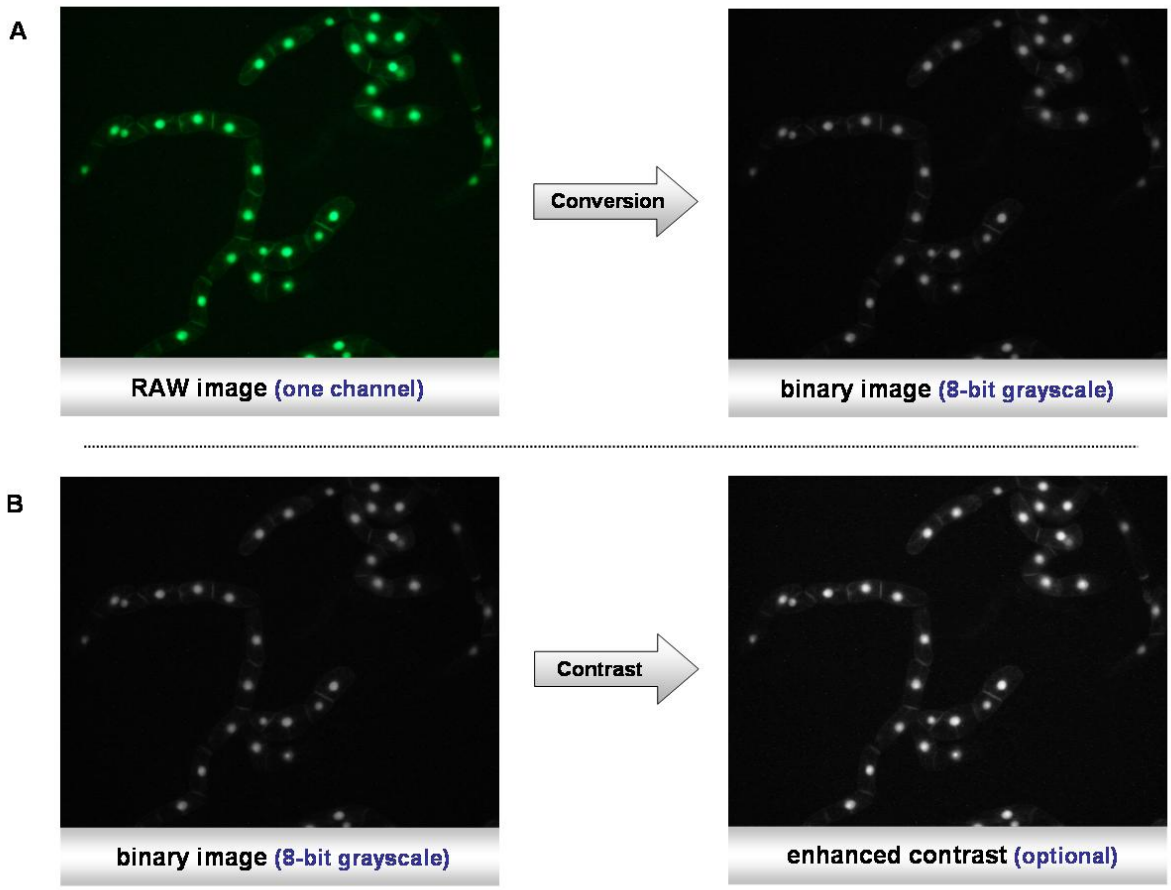

Figure 41. First steps of the Segmentation process. A- Conversion of the RAW image to a binary image file. **B-** Enhancement of the contrast

The thresholding is necessary as the software has to discriminate between the background and the borders of the object to be analyzed. The principle is quite simple: A threshold range is set, either manually or automatically, and all the pixels within this range are converted to black and those with values outside this range, converted to white (colors can be inverted).

During this process, the pixels within the range are displayed in red, whereas the background remains black. By moving the scroll bars in either direction, pixels at the periphery of objects are added or deleted from the image, as it is demonstrated in Figure 42.

Automatic thresholding (GFP-DB-CVIL BY-2 cell line treated with 40 µM KC) results in removing most of the pixels related to membranes. Only the strongest signals coming from the fluorescent nuclei remain visible.

This step is particularly important as it bears the danger of user-generated bias. To guarantee as much as possible reproducibility, the MBF ImageJ bundle comes with a whole collection of plug-ins, using different algorithms for image thresholding (Overview: “Plugins/Segmentation”).

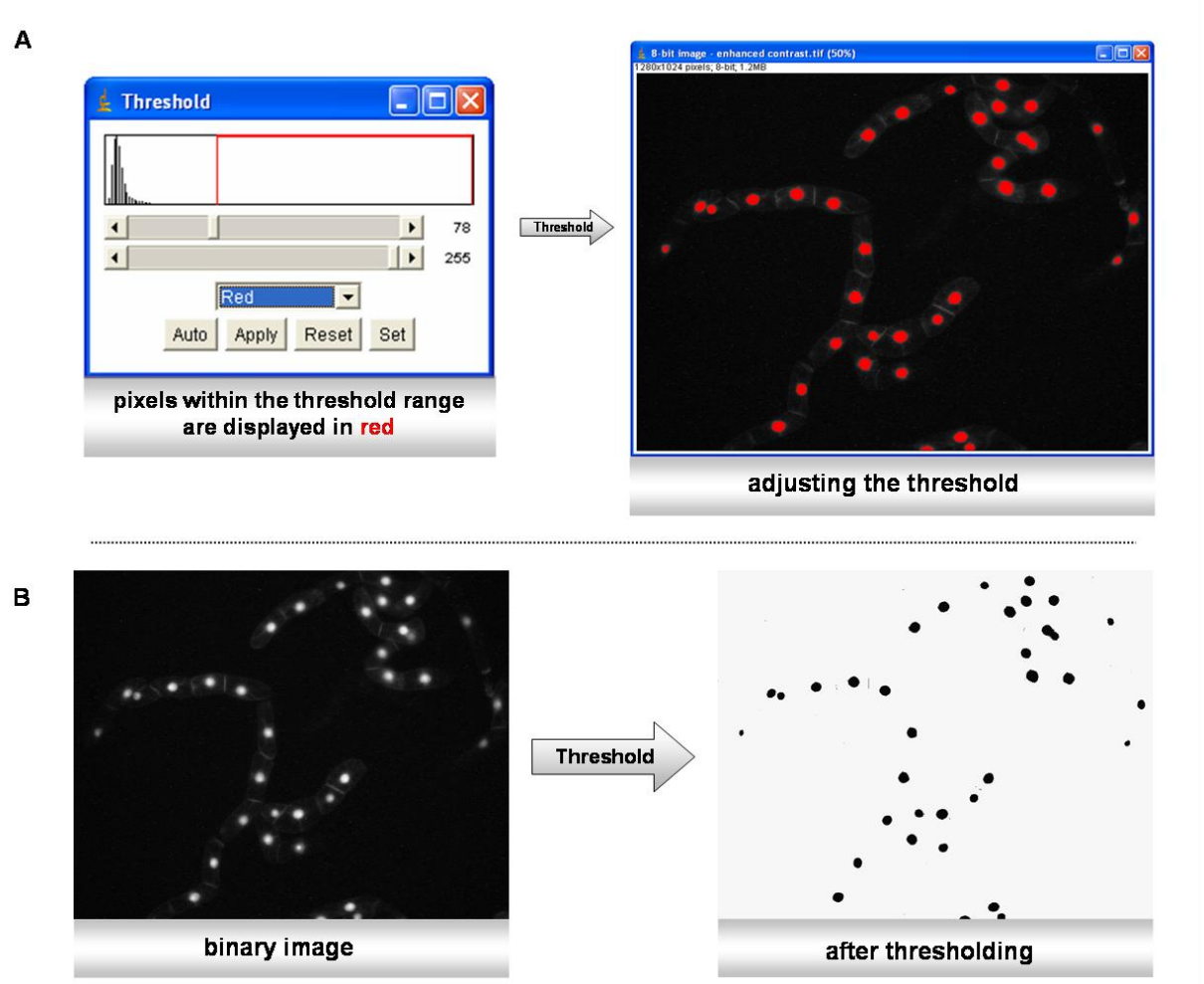

Figure 42. Automatic thresholding

A- The threshold range can be adjusted automatically. Red pixels show objects that are within the threshold range; **B-** after pushing the "apply" button, the image is converted to black and white.

b) Segmentation process: Watershed separation

When using cell suspensions in microscopy, it is almost unavoidable to obtain images without overlapping cells or cells clumped and clustered into small groups, even if the dilution of the cells has been optimized before.

To minimize counting errors due to features, such as - in our case - nuclei, that are slightly in contact each other, watershed separation was used ("Process/Binary/Watershed"). The principle of watershed seperation is quite simple (Roerdink and Meijster, 2001). This technique is based on the so-called "Euclidian Distance Map" (EDM). Any black pixel in the image is replaced with a grey pixel, whose intensity is proportional to its distance from the next white pixel. The intensity increases the closer it gets to the the center of the object. In summary, the algorithm is eroding objects from a binary image

until they disappear. Then, it dilates them back, until they touch another black pixel. At the point of contact, a watershed line is drawn (Figure 43).

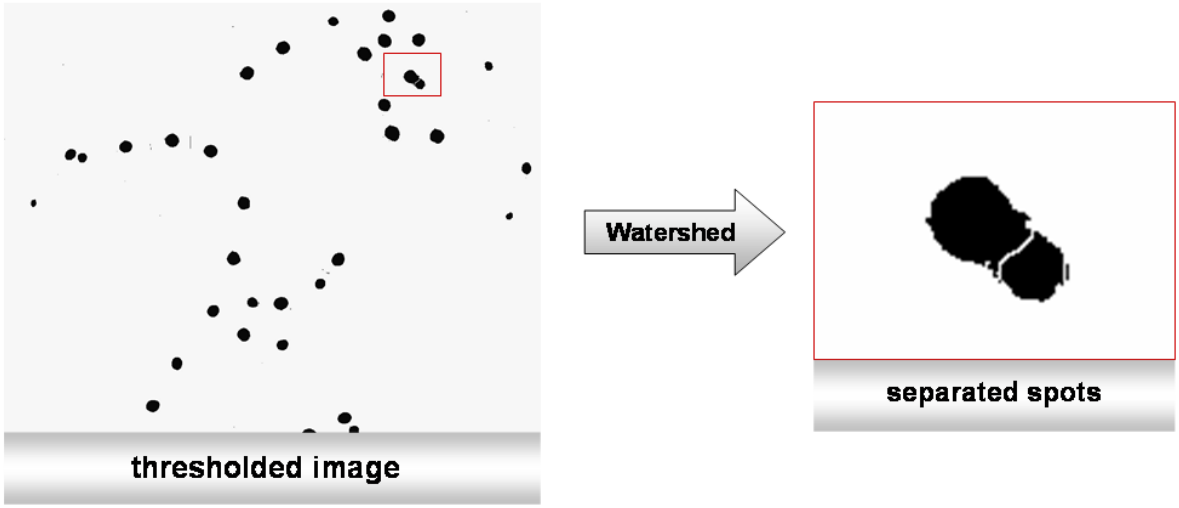

Figure 43. Overlapping objects can be separated using the watershed method

c) Particle analysis

There are several different options for counting particles with ImageJ. The menu command "Plug-ins/Particle analysis" shows a variety of plug-ins coming with the MBF ImageJ bundle. Among those are the "cell counter" and the "nucleus counter" plug-ins.

In the context of our screening system, the default particle-counting menu "Analyze/Analyze particles" proved to be sufficient.

The desired parameters for particle-counting can easily be adapted for this purpose. By setting the minimum size of the object and the degree of circularity to a certain level, all objects not corresponding to the selected requirements will be excluded.

Other menu points concern the visual output of the results in graphical or tabular form. The submenu point "Show: Outlines" for example allows to display the outlines of the detected objects with a reference number (Figure 44).

The "nucleus counter" plug-in mentioned before summarizes and automatizes many of the steps discussed before.

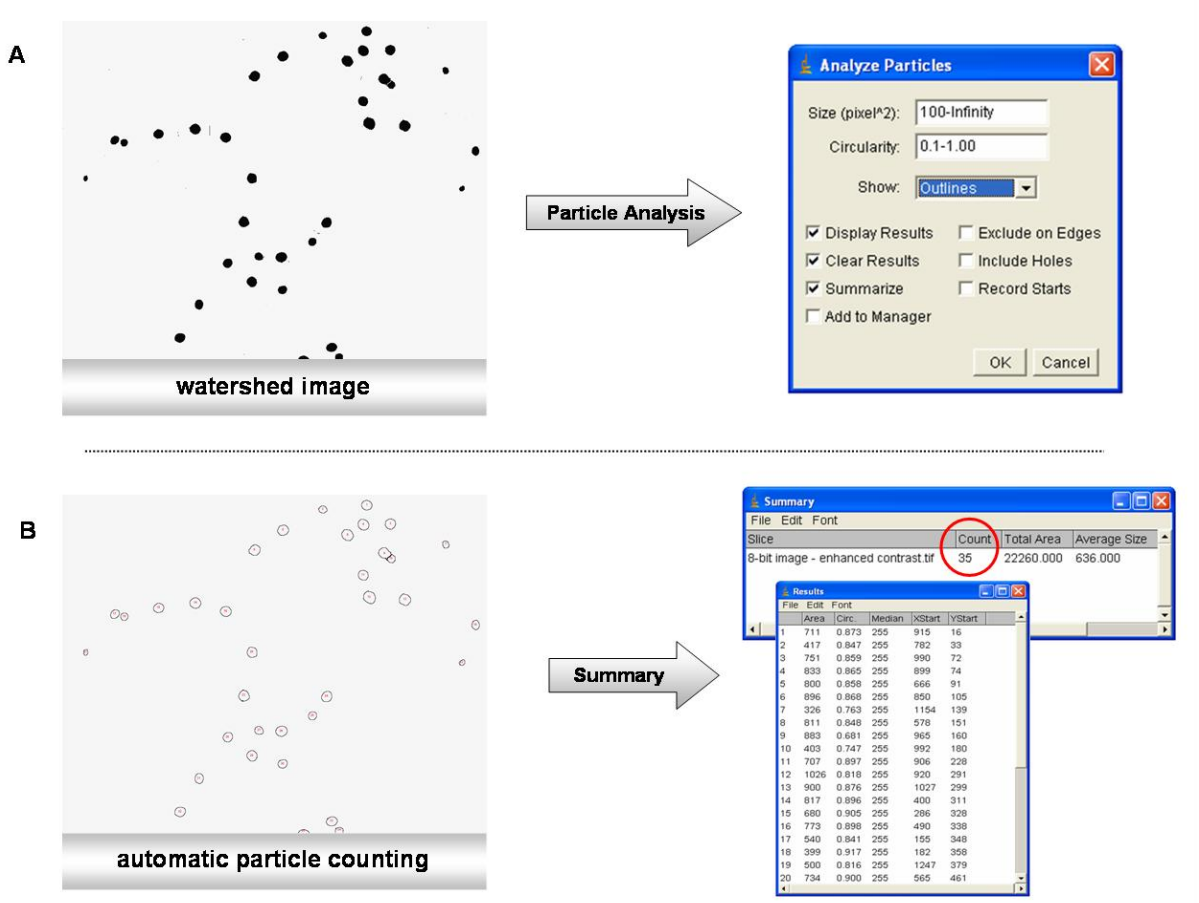

Figure 44. Automatic Nucleus-Counting with ImageJ. A- Particle Analysis; **B-** Automatic particle-counting

Optionally, a summary of the results can be displayed and exported to other applications such as Microsoft Excel.

In addition, ImageJ offers the possibility to create macros with the integrated macro editor ("Plugins/ Macros/Record or Edit"). This feature allows organize the entire segmentation and particle analysis process by creating a customised step-by-step analysis pipeline.

2.2.3.2 Limitations of the test system

As shown in the previous chapter, detecting and counting of cells, which exhibit a shift of the GFP localization to the nucleus, for instance, after a specific inhibitor treatment, is achievable with modern image analysis software like ImageJ.

Nevertheless, these results also suggested that in order to get a clearer picture of the effects of an inhibitor treatment in statistical terms, it was necessary to develop a quick and inexpensive method to also detect the cells unaffected by the treatments. But, in contrast to other model systems like yeast or bacterial cells, tobacco BY-2 cells display a great variety of phenotypes in a given population of cells, such as significantly different sizes and shapes. In addition, they grow in files (optimally in tetrades, four cells in a row) or clusters. On a regular microscope slide these tend to overlap depending on the dilution of the cell suspension, which makes automatic detection/recognition of individual cells nearly impossible with the software solutions at our hand. Of course, there are several possible solutions, including the development of a custom-made algorithm, but this is usually very time-consuming and involves the work of software experts, as well as a whole cascade of follow-up validation experiments. We also discussed the possibilty of fixing the cells before examination by standard protocols, which is however inconvenient for monitoring a treatment over a certain period of time.

A direction that has not been explored so far either for eliminating at least the problem of heterogenous cell shapes, would be the generation of protoplasts and their analysis by flux cytometry. Different protocols for the formation of protoplasts have been described previously (Kajita et al., 1980; Tamaru et al., 2002). However, this approach was not considered during this work for several reasons: First, we did not have such a device at our hand and secondly, because of the fact that the digestion reaction might trigger a massive stress response in cells, which could have a direct effect on the localization of the H6-GFP-DB-CVIL. For instance, we could observe that cells that were exposed to different stress factors (high temperatures, no agitation over-night) were less sensitive to inhibitor treatments. Preliminary tests showed that addition of MeJa to cells treated with 40 µM oxoclomazone could partially complement the inhibitor effects, suggesting that different hormones might influence the pool of prenyldiphosphates in response to biotic or abiotic stress.

Therefore, we decided to choose a less rude approach for counting untreated cells. Finally, I decided to stain the nucleus with another fluorophore, as this technique already proved valuable for the detection of inhibitor-treated cells before. This approach should theoretically allow to easily determine the ratio of affected (GFP fluorescence in the nucleus) to non-affected cells (GFP fluorescence mainly localized at the PM).

Results:

In a first attempt, we tested different commercial nuclear stains. These nuclear stains were pre-selected upon certain criteria, including, “availability in our laboratory”, “easy application” and “low cost”.
Different fluorescent DNA stains were tested that are commonly used to visualize nuclei (in dead and living cells): DAPI (4'-6-diamidino-2-phenylindole) and two different Hoechst stain variants, Hoechst 33258 and Hoechst 33342. The latter is supposed to be more lipophilic due to an additional ethyl group. The goal was to to establish conditions to stain living cells by addition of the DNA stains directly to the growing cells and thereby avoid cell fixation and subsequent washing steps, that are normally used prior to examination by fluorescence microscopy (e.g. (Banu et al., 2009)). All three stains were tested under multiple conditions (1- 5 µg/ ml final concentration; incubation between 10 min and 2h; in presence of small concentrations of different detergents). However none of these conditions led to satisfying results.
We had also a closer look at the results obtained with other nuclear stains in BY-2 cells, such as the Syto stains (Invitrogen) (Rose and Meier, 2001; Dhonukshe et al., 2005; Jeong et al., 2005). The main flaw of these DNA stains is however that they serve as marker for DNA and RNA, and tend to stain relatively unspecifically all DNA/RNA containing cell compartments (nucleus, mitochondria and chloroplasts). As for Hoechst 33342, unspecific interactions with cellular membranes due to the lipophilic character of the molecule have been reported and also observed during my experiments (Figure 45).
In conclusion, none of the used stains appeared suitable under our conditions, even though they are commonly used to determine cell viability and nuclear morphology in combination with other stains, such as propidium iodide (Ormerod et al., 1993; Yuan et al., 2002). In addition, the intenisty of the nuclear staining did not look very convincing, especially given the fact that most probably the best images have been used for the publications.

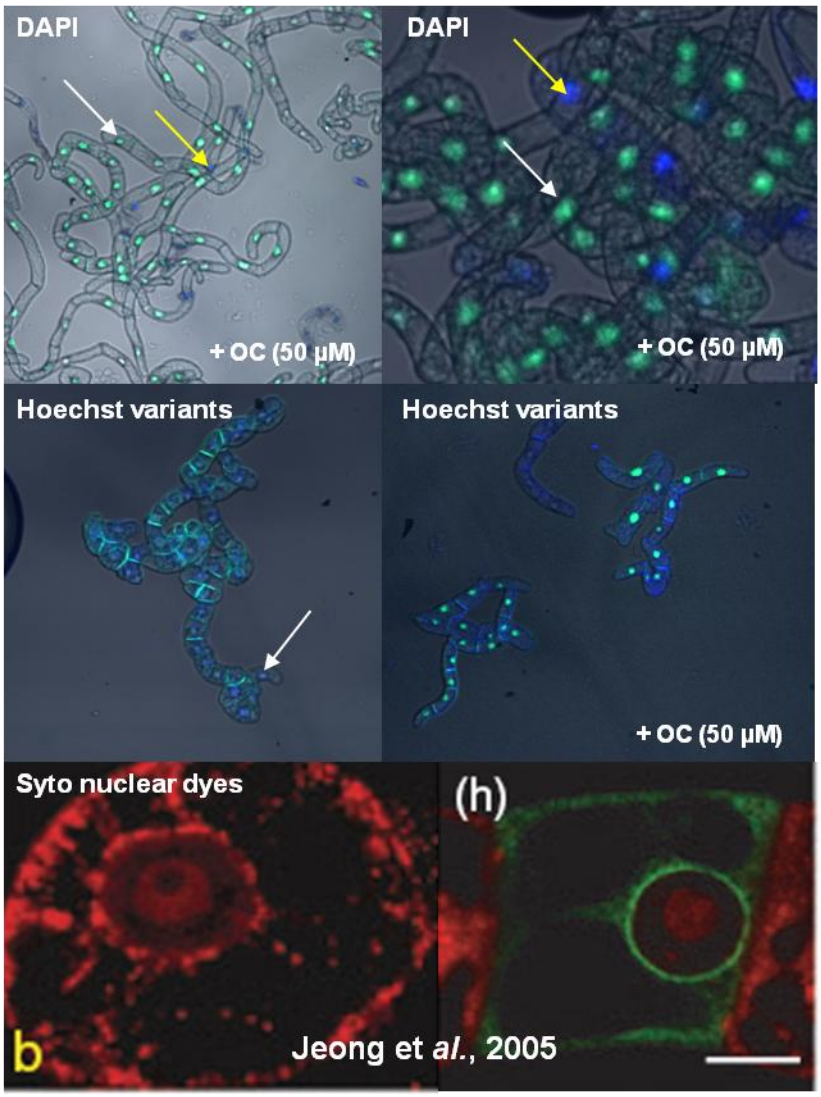

Figure 45. Various nuclear stains and their phenotypes in tobacco BY-2 cells.

2.2.4 Optimization of the assay

2.2.4.1 New features: Inducible nuclear staining of the cell line (NLS-mRFP)

Due to the difficulties to efficiently stain living tobacco BY-2 cells a new strategy was chosen, consisting of transforming the existing GFP-BD-CVIL cell line with an estradiol-inducible vector (Zuo *et al.*, 2000), driving the expression of a RFP protein, C-terminally fused to a NLS (nuclear localization signal).

a) Nuclear import in eucaryotic cells

In eukaryotic cells, ions, small neutral proteins and macromolecules (< 40 kDa) are thought to enter the nucleus by diffusion (Görlich and Kutay, 1999), whereas larger proteins only gain access to the nucleus by selective targeting through the nuclear pore complex (NPC) (Feldherr et al., 1984; Rout et al., 2000; Fahrenkrog and Aebi, 2003; Vollmar et al., 2009), a large multi-protein complex embedded in the nuclear envelope (NE), consisting of about 30 different proteins, called nucleoporins (Dingwall and Laskey, 1992; Raikhel, 1992; Sorokin et al., 2007).

The NPC functions as a gateway between the cytoplasm and the nucleoplasm. Import and export of most proteins are complex and energy-dependent processes, which are mediated by specific soluble carrier proteins, often referred to as "caryopherins" (Radu et al., 1995), which can be divided into two groups: the importins (Görlich et al., 1994) and the exportins (Stade et al., 1997).

Protein import into the nucleus is achieved in two steps, the docking and the translocation. Docking involves the action of caryopherins, which bind their protein cargo after recognition of nuclear localization signals (NLS) for import (Jans et al., 2000; Lange et al., 2007; Kosugi et al., 2009). In the classical nuclear import cycle of eukaryotes, importin alpha recognizes and binds the NLS and links it to importin beta to form a trimeric complex (Görlich et al., 1995). This step takes place at the cytoplasmic site of the NPC and is energy-independent. Importin beta mediates the interaction with the NPC. Then, the NPC, usually 8-10 nm wide and about 45 nm long, increases its diameter up to 40 nm, allowing the trimeric complex to be translocated into the nuclear compartment (Keminer and Peters, 1999). The interactions of the caryopherins with their cargo proteins are regulated by the small Ras family GTPase (Ran), which provides the energy for the translocation process. As soon as the complex enters the nucleus, RanGTP binds to importin beta, resulting in a conformational change and the dissociation of the importin alpha – cargo complex (Lee et al., 2005). Finally the cargo is released into the nucleus, and importins alpha and beta are exported back to the cytoplasm (Kutay et al., 1997; Hood and Silver, 1998; Matsuura and Stewart, 2005) to prepare a new round of nuclear import (Figure 46).

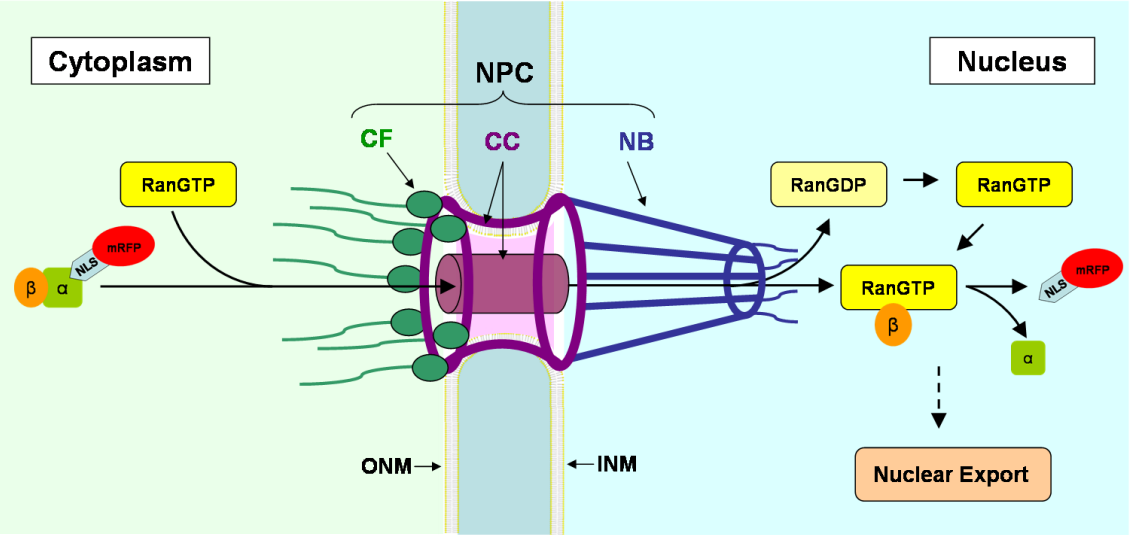

Figure 46. Simplified model of the classical Ran-dependent nucleocytoplasmic import cycle of proteins (modified from Sorokin et al., 2007).

In the cytoplasm, the adaptor protein importin α recognizes its cargo via the NLS motif and establishes the interaction with importin β, leading to the formation of a trimeric complex. Importin β mediates the contact with the NPC, which afterwards increases the diameter of its central core/channel and translocates the cargo complex inside the nucleus, where it is dissociated by the action of RanGTP. After the release of the cargo, importins α/β are transported back to the cytoplasm to prepare a new nuclear import cycle. Designations: NPC, nuclear pore complex; CF, cytoplasmic filament; CC, central core; NB, nuclear basket; ONM, outer nuclear membrane; INM, inner nuclear membrane, α/β; caryopherin/importin α/β; NLS, nuclear localisation signal; mRFP, monomeric RFP.

b) Nuclear localization signals

By definition, a nuclear localization signal (NLS) is a "short stretch of amino acids that mediates the transport of proteins into the nucleus" (Cokol et al., 2000). This polypeptide may be localized at various positions within the protein sequence. In general, before active protein transport to the nucleus can occur, importins have to discriminate between their cargo and other cytosolic proteins. This step is of central importance and occurs when the importin alpha recognizes specific amino acid sequences within the protein, the above mentioned NLSs.

NLS are distributed into three broad classes. The first two classes contain either one (= monopartite) or two (= bipartite) stretches of basic amino-acids and can be considered as the best characterized targeting sequences (Boulikas, 1993). They are also sometimes referred to as classical NLS (cNLS) for nuclear protein import (Kalderon et al., 1984a).

The most prominent as well as a very frequent example for a monopartite NLS is the SV40 large tumor antigen NLS (Kalderon et al., 1984b; Lassner et al., 1991), which is in fact a highly conservative repeat of positively charged residues (**PKKKRRV**). The bipartite NLSs are examplified

by the nucleoplasmin NLS (Dingwall and Laskey, 1991; Robbins et al., 1991; Stewart et al., 2001), which contains two stretches of basic amino acids, usually separated by a spacer of 10-12 residues (**KR**-10-12aa- **KKKL/K**).

The third class of NLS includes those resembling to the NLS of the yeast Mat 2 protein, in which charged, polar residues are interspersed with non-polar ones (**VRILESWFAKNIEPYLDT**) (Hall et al., 1990).

In an experimental context, two aspects about NLS are particularly interesting: First of all, a deletion of a known NLS usually disrupts nuclear import. Moreover, after fusion to a NLS, non-nuclear proteins will be imported into the nucleus. Both experimental approaches, disruption and introduction of promising peptide sequences, are routinely used to confirm NLS motifs (Tinland et al., 1992; Moede et al., 1999). However, for a small fraction of nuclear proteins (less than 10 %), NLS have been experimentally determined (Cokol et al., 2000; Nair et al., 2003).

In silico approaches lately focused on improving the prediction of NLS sequences and led to the development of publicly available databases and tools to analyze and predict NLS motifs like **NLSdb**, **PredictNLS** and **LocTree** (Cokol et al., 2000; Nair et al., 2003; Nair and Rost, 2005, , 2008).

Interestingly, in proteins containing both NLS motifs and DNA-binding regions, up to 90% of the predicted NLS motifs co-localized with putative DNA-binding regions (LaCasse and Lefebvre, 1995; Nair et al., 2003).

c) Construction of the vector

The goal of this experiment was to stably transform the existing TBY-2 cell line (GFP-DB-CVIL) with a second, inducible gene construct, which specifically stains the nuclear region of BY-2 cells. Therefore, the NLS sequence of the large SV40 T-antigene was fused N-terminally to the coding sequence of a mRFP (monomeric red fluorescent protein) and put under the control of an estradiol-inducible promotor. The resulting vector was then used to stably transform the GFP-DB-CVIL cell line. The following section describes the components of the NLS-mRFP-vector (Figure 47 and Figure 48):

1. NLS:

The NLS chosen for this experiment was the NLS of the large SV40 (simian virus 40) T-antigen (**PPKKKRKV**), which is known to be sufficient to target several proteins to the nucleus of mammalian and plant cells (Kalderon et al., 1984b; Raikhel, 1992; Hicks et al., 1995; Xiao and Jans, 1998; Launholt et al., 2006), In *Arabidopsis thaliana*, this NLS proved to be specific enough to mediate nuclear targeting after fusion to a RFP (Lee et al., 2001). Subcellular localization studies also revealed that this classical, monopartite NLS targets T7 RNA polymerase not only to the nucleus of mammalian cells (Dunn et al., 1988; Lieber et al., 1989) but also to the nucleus of tobacco TBY-2 cells (Lassner et al., 1991). In addition, Lee et al. (2001) showed that transformation of tobacco protoplasts with a *SV40:RFP* construct resulted in an efficient targeting of the fusion protein to the nucleus, making this protein as a promising candidate.

2. Fluorochrome:

For the colocalization studies and the experimental test system, we chose an enhanced RFP (**r**ed **f**luorescent **p**rotein) described by Campbell et *al.* (2002). The **m**RFP (**monomeric** RFP) is a substantially modified version of the RFP from *Discosoma* coral (DsRed or drFP583) (Matz et al., 1999), which was improved in major characteristics, especially in the context of dual color imaging with GFP, one of the most important aspects relevant to a visual test system. For instance, the enhanced fluorophore is stable and bright, has a significantly shorter maturation time and its emission peak occurs at approximately 605 nm, thus facilitating the optical separation from the emission of the sGFP (synthetic GFP) (Chiu et al., 1996), which is a codon-optimized version of the green fluorescent protein (GFP) from *Aequorea victoria* (Shimomura et al., 1962; Prendergast and Mann, 1978; Tsien, 1998) (Prasher et al., 1992), with an emission peak at 488 nm.

In silico analysis of the amino-acid sequence by different methods also strongly emphasized the high probability of a nuclear targeting of the *NLS:mRFP* fusion protein.

NLS-SV40-mRFP: amino acid sequence

```
  1   MPPKKKRKVA SSEDVIKEFM RFKVRMEGSV NGHEFEIEGE GEGRPYEGTQ
 51   TAKLKVTKGG PLPFAWDILS PQFQYGSKAY VKHPADIPDY LKLSFPEGFK
101   WERVMNFEDG GVVTVTQDSS LQDGEFIYKV KLRGTNFPSD GPVMQKKTMG
151   WEASTERMYP EDGALKGEIK MRLKLKDGGH YDAEVKTTYM AKKPVQLPGA
201   YKTDIKLDIT SHNEDYTIVE QYERAEGRHS TGA
```

Length: 233 aa MW: 26386 Da IEP: 6.99

Figure 47. Amino acid sequence of the NLS-SV40-mRFP fusion protein

The starting methionine is indicated by a blue letter; black letters, N-terminal fusion peptide added by PCR to the mRFP sequence; red letters, mRFP sequence. The position of the SV40 peptide (PKKKRKV) is indicated by the blue box. Designations: MW, molecular weight; IEP, isoelectric point.

3.Vector:

For the transformation of the transgenic H6-GFP-DB-CVIL TBY-2 line, a chemical induction system based on the regulatory mechanisms of vertebrate steroid hormone receptors (Zuo et al., 2000) was chosen. The multiple advantages of inducible promoters over common promoters have been the subject of several reviews (Gatz, 1997; Zuo and Chua, 2000). One of the most important aspects is the high flexibility of the inducible system in terms of controlling the expression of a transgene in a time and dose-dependent manner and of minimizing undesired toxic effects linked to constitutive expression.

The general principle of action of this **XVE system** (NLS-mRFP vector) is the same as for the **GVG system** used to create the H6-GFP-DB-CVIL cell line (Gerber, 2005).

Both expression systems use a combination of a trans-acting factor, consisting of a chimeric transcription activator (XVE for per10 and GVG for pTA7001/2) and a cis-acting transcription unit under the control of a target promoter.

The central element of the chimeric transcription factor is the hormone-binding domain (HBD) of vertebrate steroid hormone receptors. *In vivo*, these receptors usually act as receptor molecules and transcription factors at the same time (Beato, 1989) and their hormone-binding domains are known to have repressive effects on covalently linked, neighbouring domains in the absence of their ligands, a regulatory transcription mechanism referred to as de-repression (Gatz et al., 1992; Picard, 1993).

In the per8/10 vector, the hormone-binding of the human estrogen receptor (hER) domain is fused C-terminally to a chimeric, constitutively active transcriptional activator, consisting of the DNA-binding domain (DBD) of the bacterial repressor LexA and the trans-activating domain of VP16. The resulting transcription factor XVE (Le**x**A-**V**P16-**E**R) is set under the control of the strong constitutive promoter $G_{10\text{-}90}$ (Zuo et al., 2000).

The chimeric transcription factor of the pTA7001 vector, GVG (**G**AL4-**V**P16-**G**R), combines the DNA-binding domain of the yeast transcription factor GAL4 with the trans-activating domain of VP16 and the HBD of the rat glucocorticoid receptor under the control of the CaMV 35S promoter (Aoyama and Chua, 1997).

The second transcription unit of each vector contains a binding site for these chimeric transcription factors (XVE or GVG). Therefore, eight (GVG: six) copies of the LexA operator sequence (GVG: Gal4 UAS) were fused to the minimal region of the CaMV 35S promoter.

The XVE system used for the transformation is known to be highly inducible by estrogen (up to 8-fold higher induction than the 35S promoter within 24 h), to bind estrogen with a very high affinity (0,05 nM) (Mueller-Fahrnow and Egner, 1999) and to be activated by relatively low inducer concentrations (8 nM to 5µM). This is also due to the fact that VP16 interacts very well with a wide range of general transcription factors. In addition, there is no detectable background expression as the DBD (DNA-binding domain) of LexA does not resemble structurally to the DBD of most known eukaryotic factors.

Lately, several studies used the XVE system to successfully transform tobacco BY-2 cells (Zuo et al., 2000; Magyar et al., 2005; Dohi et al., 2006). For these reasons, the chimeric sequence, consisting of the SV40 NLS and the mRFP gene (Figure 47) was inserted into the target expression cassette of pER10 (**Oligos:** **BO4-MH-NLS-mRFP-F1** 5'- CCG **CTC GAG** ATG CCT CCT AAG AAG AAG CGC AAG GTC GCC TCC TCC GAG GAC GTC – 3'**;** **BO4-MH-NLS-mRFP-R1** 5' – CTAG **ACT AGT CTA TTA** ggc gcc ggt gga gtg gcg – 3').

This vector is based on the pER8 vector described by Zuo et al. (2000), in which the plant selection marker for hygromycine resistance has been replaced by the gene for neomycine phosphotransferase II (Hyg^R → Kan^R).

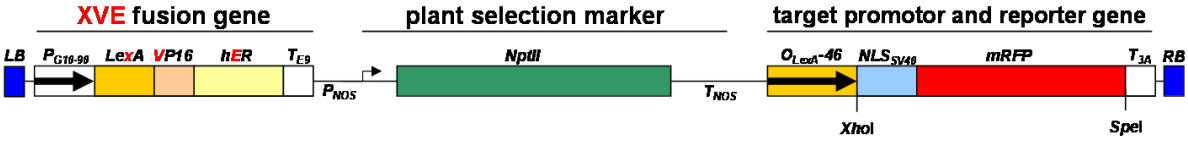

Figure 48. Schematic diagram of the NLS-mRFP vector (modified after Zuo et al., 2000)

For better understanding only the region between the right (RB) and left borders (LB) is shown (not to scale). $P_{G10\text{-}90}$ is a strong constitutive promoter driving the expression of the chimeric transcription factor consisting of

the DNA-binding region of LexA, the transcription activation domain of VP16 and the regulatory region of the human estrogen receptor (hER); T_{E9}, polyadenylation sequence. The plant selection marker is the gene of neomycine phosphotransferase II (NPTII) driven by the nopaline synthase promoter (P_{NOS}); T_{NOS}, nopaline synthase poly (A) addition sequence. O_{LexA}; eight copies of the LexA operator sequence; - 46, 35S minimal promoter. NLS_{SV40}; nuclear localisation sequence from SV40 fused in frame to the mRFP gene. T_{3A} poly(A) addition sequence. The direction of transcription is indicated by arrows.

d) The N-terminal fusion of the SV40-NLS peptide efficiently targets mRFP to the nucleus of the double transformed tobacco BY-2 cell line

To investigate if the NLS fusion protein localize to the nucleus and can be properly co-expressed with the GFP fusion protein of the H6-GFP-DB-CVIL line, three days-old BY-2 cells (L2.9) were transformed with the pER10-NLS-mRFP vector by agroinfection (chapter 4.5.5). Calli were selected on TBY-2 solid medium supplemented with 30 µg/ml hygromycin and 50µg/ml kanamycin. First calli appeared after 3-4 weeks of growth in the dark and at 26°C and were subcultured twice on solid medium until liquid pre-cultures (10 ml with antibiotics) were started. These pre-cultures were grown for 7-10 days under permanent shaking, until they reached an optimal density. After parallel induction with estradiol and dexamethasone for 15 h, the pre-cultures were screened visually by fluorescence microscopy. Pictures were acquired using the microscope settings described in Table 23 (Properties of the fluorochromes and fluorescent proteins used in this work). Twelve cultures out of 36 (33,3 %) showed cells expressing both fluorescent proteins.

The most promising cell line (N-20) showed bright fluorescence in both channels and had a significant ratio of positive cells (>50 % of total cells), making it a good candidate for first tests and further re-selection efforts to obtain a performing cell line suitable for statistical approaches.

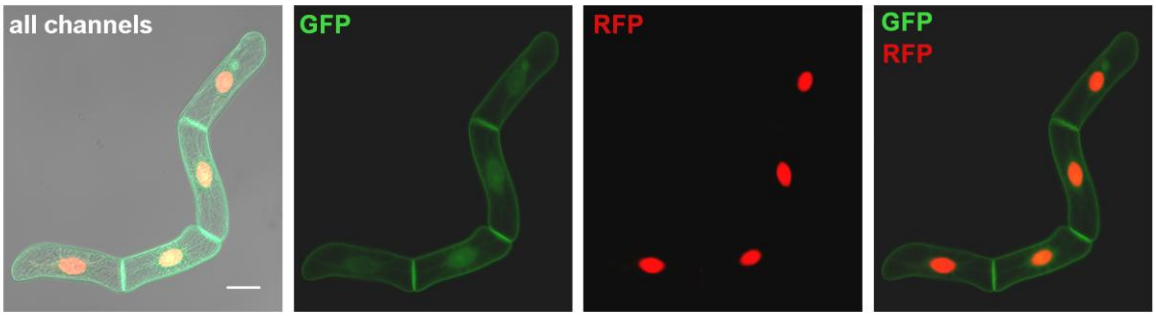

Figure 49. Double-transformed TBY-2 cell line (N-20) showing different intracellular localization of fluorescent fusion proteins (after induction)

All channels: Four TBY-2 cells growing in a tetrade with red and green fluorescence induced at the same time (+ DIC). **GFP-** the GFP-DB-CVIL fusion protein is visualized after induction with 10 µM dexamethasone and is mainly localized to the PM and cytosol. **RFP-** The monomeric RFP fused to the C-terminus of the SV40 NLS is visualized after induction with 5 µM estradiol and is predominantly found in the nuclear compartment.

GFP/RFP- Overlay of the GFP and RFP channels. Induction time with both elicitors was 15 h. Images were acquired using a LSM510 confocal laser scanning microscope equipped with an inverted Zeiss axiovert 100 M microscope. Dual color imaging was performed using dual excitation/emission scanning in the multitracking mode (Zeiss LSM). White bars represent 20 µm.

e) The newly created double fluorescent cell line NLS-mRFP/H6-GFP-DB-CVIL shows no visible cross-induction of fluorescence after treatment with estradiol or dexamethasone

In order to establish a reliable visual test system, it was necessary to verify that the two co-existing induction systems in the NLS-mRFP (estradiol) and H6-GFP-DB-CVIL (dexamethasone) lines only respond to their specific inducers. As both chemical-inducible systems are based on a similar principle of induction (see chapter c)) - the action of chimeric trans-activators whose transcriptional activities are regulated by specific hormones and/or structurally related compounds (Zuo et al., 2000) - the cell line was separately treated with both inducers under standard conditions. In addition, fluorescent cell dyes were used in parallel as negative controls (Figure 50).

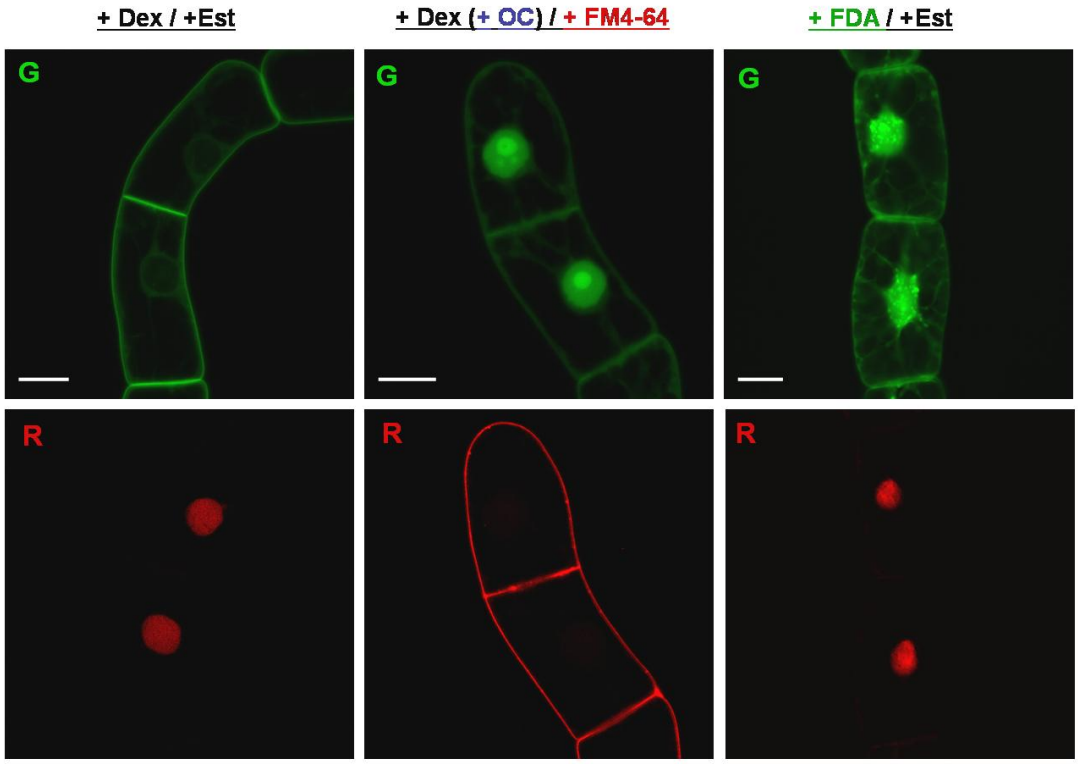

Figure 50. Expression of fusion proteins is tightly regulated by their specific inducers.
No cross-induction of fusion gene expression was visible. Induction time for dex (10 µM final) and est (6 µM final) was 15 h in all experiments. **+ Dex / + Est:** control experiments with both inducers with the GFP fusion protein targeted to the PM (G) and the mFRP fusion protein located in the nucleus (R). **+Dex (+OC) / + FM4-64:** Dexamethasone alone is only inducing the expression of the GFP fusion protein (G). The negative control

with FM4-64 (5 µg/ml; membrane stain) shows no signals from the nucleus (R). For better understanding, cells were treated with 50 µM Oxoclomazone (OC) 3 h before induction, to indicate the position of the nucleus. **+FDA / + Est:** Estradiol only is not able to induce GFP fusion protein expression (G). FDA (7,5 µM final) is used as negative control, also indicating that the cells were alive during the imaging process. **G** and **R** indicate the green and the red channel, respectively. Bars = 20 µm.

Simultaneous treatment of the cell line with both inducers (24 h induction, 10 µM Dex, 6 µM Est) resulted in a phenotype with green fluorescence predominantly located at the peripheral membrane region and red fluorescence mainly located in the nuclear compartment.

After treatment with dexamethasone only (24h, 10 µM Dex), the observed cells did not show any detectable signal in the red channel (RFP). As negative control, the cells were treated with the plasma membrane stain FM4-64 (5µg/ml, 5 min treatment). This amphiphile molecule is known to be a potent membrane stain and a marker of membrane traffic and the endocytotic pathway in animal cells, fungi and plant cells (Belanger and Quatrano, 2000; Bolte et al., 2004; van Gisbergen et al., 2008). It was also used in previous studies from our lab, for instance, to show that the H6-GFP-DB-CVIL fusion protein is located in the plasma membrane of TBY-2 cells (Gerber et al., 2009). FM4-64 fluorescence is clearly visible in the red channel, whereas no detectable signal appear in the nuclear region (for a better understanding, the cells have been treated with 50 µM OC to indicate the position of the nucleus).

Cells treated with estradiol only (24h, 6µM Est) showed an accumulation of red fluorescence in the nuclear region and no detectable green fluorescence. As a negative control, the viability cell stain FDA (Fluorescein diacetate) (Widholm, 1972; Kovarik and Fojtova, 1999) was used (7,5 µM final, 2 min). Green fluorescence could be observed in the whole cell, which also indicated that the cells were living when the image was taken.

f) 24 hours are sufficient to obtain homgenous red fluorescence

Another important aspect was the optimal duration of the induction times for both fusion proteins, in order to find out at which time point the intensities of the emitted signals were sufficiently strong and homogenous for detection and image acquisition. To address this issue, the cellular localization of the *NLS:mRFP* reporter protein was examined at various times after induction with estradiol by fluorescence microscopy. Seven day-old cells were diluted 6-fold in MS-BY-2 medium and 3 ml were dispatched into the wells of a 6-well plate. These cells were then cultured at 26°C in obscurity and under permanent shaking. Induction with 6 µM estradiol (solubilized in benzene/ethanol 1:1) took place at 48, 36, 24, 18, 15, 12, 6 and 3 hours before observation. The settings for image acquisition in the red channel did not change during the whole experiment.

To determine the level of saturation, images were converted to a rainbow scale with the Zeiss LSM image browser. Red signals indicate saturation. As seen in Figure 51-A, nuclear localization of the NLS:mRFP protein could already be observed 3 hours after the induction. Nevertheless, it took at least 24 h until most of the signal arising from the nuclei was saturated (red dots).

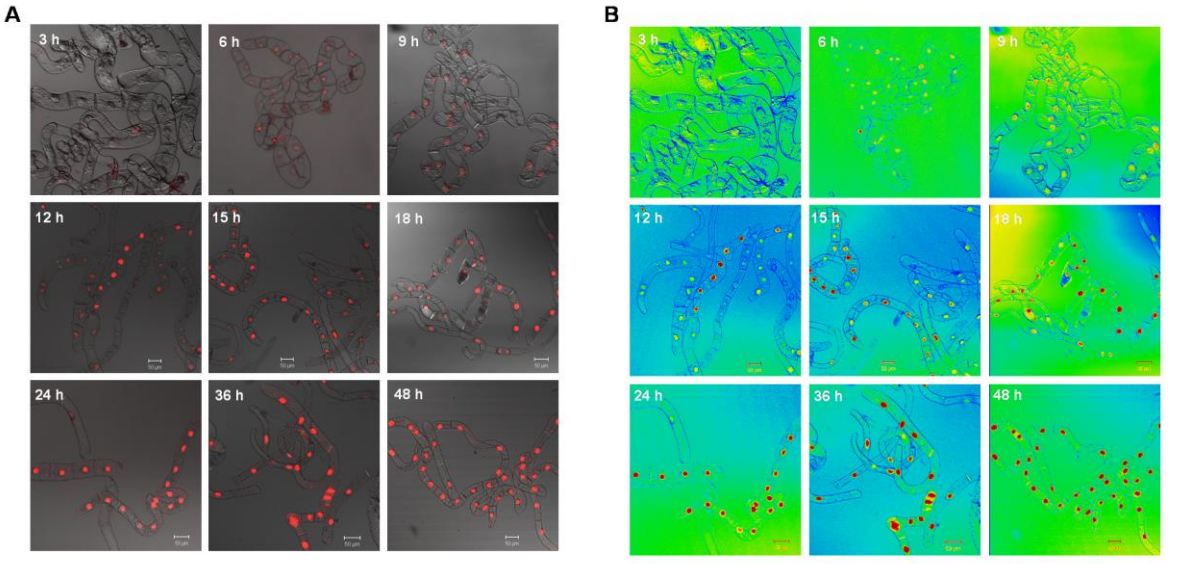

Figure 51. Time course of induction for the NLS-mRFP.

In vivo targeting of the NLS-mRFP fusion protein after induction with estradiol [6 µM] (and in the presence of 10 µM dex – not shown). The red fluorescent signals were examined at different time points after induction. **A-** Overlay of transmission microscopy images with the RFP channel. **B-** Same images as in A shown in LSM image browser rainbow mode (red indicates saturated areas). Saturation is already reached after 24 h of induction with both elicitors. All images were acquired with the same microscope settings (red channel, LSM510 microscope; EC-Plan-Neofluar, 10x/0,3 M27)

g) Cloning of transgenic BY-2 cells: generation of a cell line with strongly reduced heterogeneity

To generate a performing double-transformed cell line was a process of constant selection and engineering of the initial GFP-DB-CVIL TBY-2 cell line in order to obtain a clonal selection of cells responding appropriately to different stimuli. To achieve this goal, the most promising double-fluorescent cell line (N-20) was chosen for a rigorous re-selection process as described in chapter 4.5.5.3.

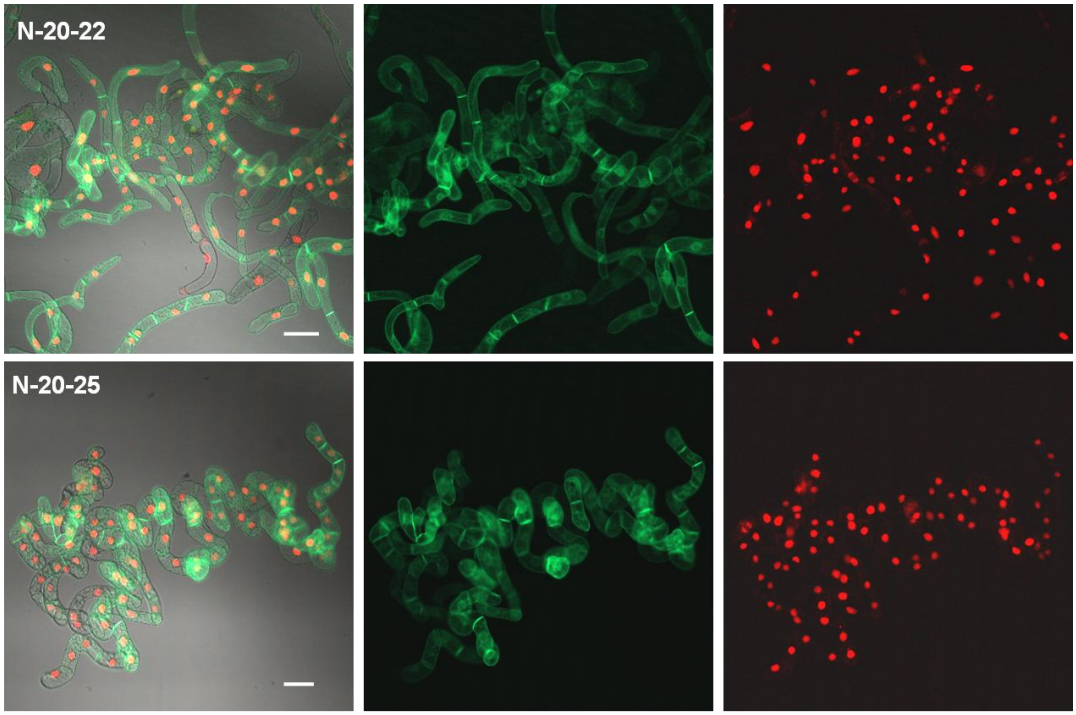

Figure 52. Two different clonal selections of the double-transformed cell line N-20.
The most promising cell line N-20 was re-selected in order to obtain a performing cell line. The resulting cell lines (N20-22 and N20-25) are characterized by a high ratio of bright fluorescent cells (> 95%). Images were taken as described in previous chapters. Cells were induced for 24 h with 10 µM dexamethasone and 6 µM estradiol (final concentrations). White Bars represent 50 µM.

Two liquid cultures started from these secondary calli showed bright fluorescence in both channels as well as a high ratio of fluorescent cells (> 95 %) and were maintained for further experiments (Figure 52).

h) Response of the double-transformed cell line to various treatments

As the major emphasis of this project was the development of a tool to screen for inhibitors of the MEP pathway and the prenylation reaction itself (Figure 53), it was necessary to verify that the newly generated cell line showed the same phenotype in response to various treatments as the initial cell line H6-GFP-DB-CVIL despite the presence of a second, inducible fusion protein.

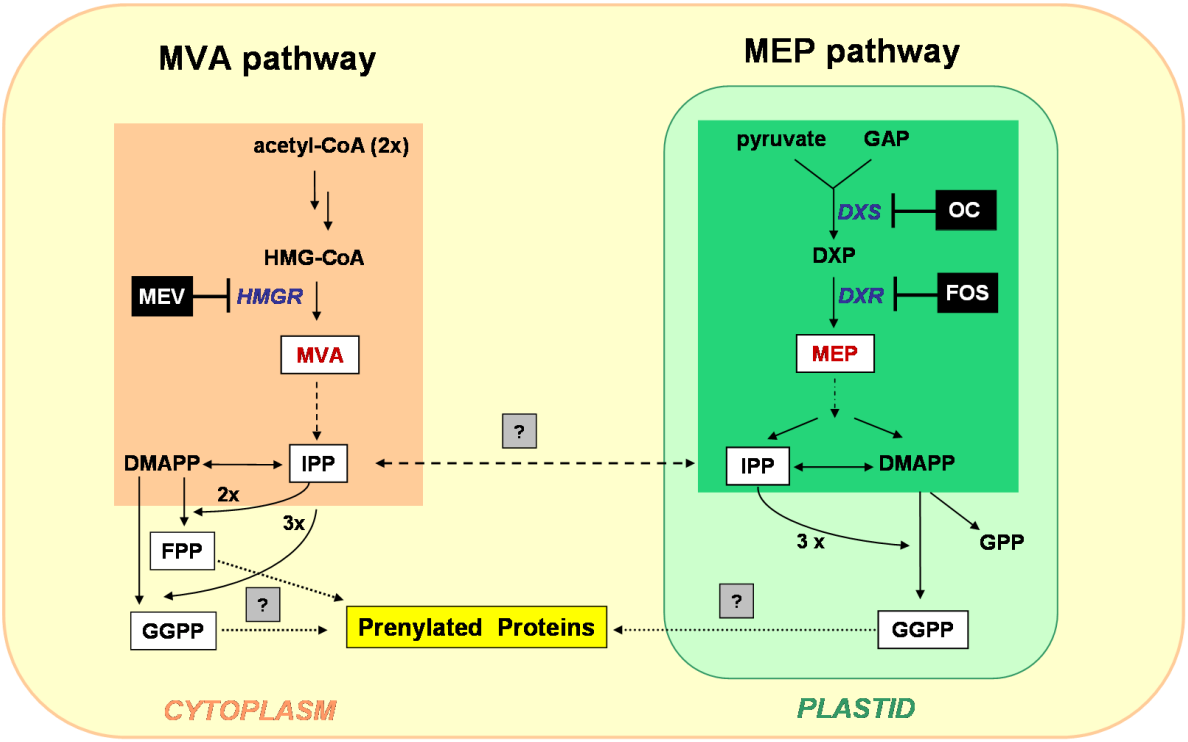

Figure 53. Simplified scheme showing the pathways for isoprenoid biosynthesis in plant cells.
Dashed arrows represent multiple enzymatic steps. The MEP and the MVA pathways are boxed. The enzymatic steps specifically inhibited by mevinolin (MEV), oxoclomazone (OC), and fosmidomycin (FOS) are indicated. HMG-CoA, hydroxymethyl glutaryl-CoA; MVA, mevalonic acid; IPP, isopentenyl diphosphate; DMAPP, dimethylallyl diphosphate; FPP; farnesyl diphosphate; GGPP, geranylgeranyl diphosphate; GAP, glyceraldehyde 3-phosphate; DXP, deoxyxylulose 5-phosphate; MEP, methylerythritol 4-phosphate; GPP, geranyl diphosphate. Enzymes are indicated in italics: HMGR, HMG-CoA reductase; DXS, DXP synthase; DXR, DXP reductoisomerase.

The double-transformed TBY-2 cell line was treated for 18 h with different inhibitors affecting key enzymes of the MEP and MVA pathways. Induction with 10 µM dexamethasone and 6 µM estradiol took place 24 h before observation (Figure 54).

As expected, inhibition of the cytosolic MVA pathway by mevinolin did not show any effect on the predominant localization of the green fluorescent fusion protein at the periphery of the treated cells, which is very similar to the fluorescence pattern of untreated cells. In contrast, inhibition of DXS and DXR activity by oxoclomazone and fosmidomycin at 40 µM final concentrations resulted in the

previously described, nearly complete translocation of GFP-DB-CVIL to the nucleus, which is consistent with the results obtained in our previous study (Gerber et al., 2009).

In all cases, the NLS-mRFP protein could be induced and co-expressed without affecting the expression or localization of the GFP-DB-CVIL protein.

As a further proof of the concept, Dr. Elisabet Gas-Pascual – postdoctoral researcher in the Bach group - generated different cell lines targeting HMGR and DXR genes with an artificial micro-RNA (amiRNA) strategy (Schwab et al., 2006) in order to confirm the effects of the inhibitors on their target proteins on a biological level (Figure 54). DXR-silenced cells exhibited a phenotype similiar to FOS and OC treatment, whereas the silencing of HMGR did not have any effect on the localization of GFP-DB-CVIL.

These first results further confirmed the hypothesis that plastidial isoprenoid synthesis is the major contributor to the geranylgeranylation of GFP-DB-CVIL and once again proved the use of transformed BY-2 cells valuable for the study of isoprenoid precursors.

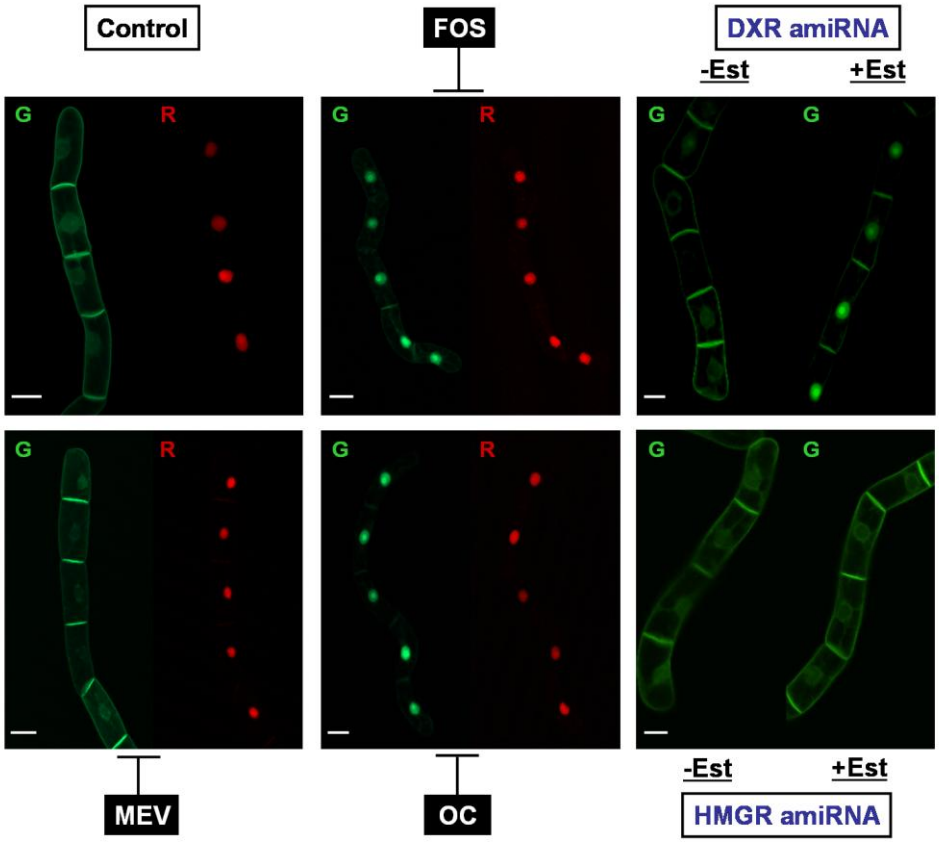

Figure 54. Two Channel imaging of the N-20 cell line after various treatments.

The cell line was treated with different inhibitors affecting the **MVA pathway** (mevinolin) and the **MEP pathway** (Fosmidomycin, oxoclomazone). Induction of the cell line with estradiol and dexamethasone was carried out 24 h before observation. The cell line was treated with specific inhibitors 18 h before observation. Fosmidomycin (**FOS**) and oxoclomazone (**OC**) clearly shift the localization of the GFP fusion protein to the

nucleus, whereas mevinolin (**MEV**) treatment has no visible effect on the cells. In addition, we used two new cell lines with **RNA-silencing constructs** as "biological controls". For instance, DXR silenced cells show the same phenotype as those inhibited *in vivo* by fosmidomycin. HMGR silencing however does not have any visible effect on the localization of the GFP fusion protein. These results underline the specificity of the test system for the MEP pathway. White bars represent 20 µm.

i) The mRFP fluorescence can be used for the identification/counting of cells

The proposed approach to count the total number of fluorescent tobacco BY-2 cells in an image consisted of staining the nucleus, as this technique was succesfully applied to identify cells that showed a mislocalization of the GFP fluorescence to the nucleus in response to the treatment with the MEP pathway inhibitor oxoclomazone (Figure 44). Figure 55 shows and explains three different scenarios for the detection of cells, ranging from selected cells to whole-population images.

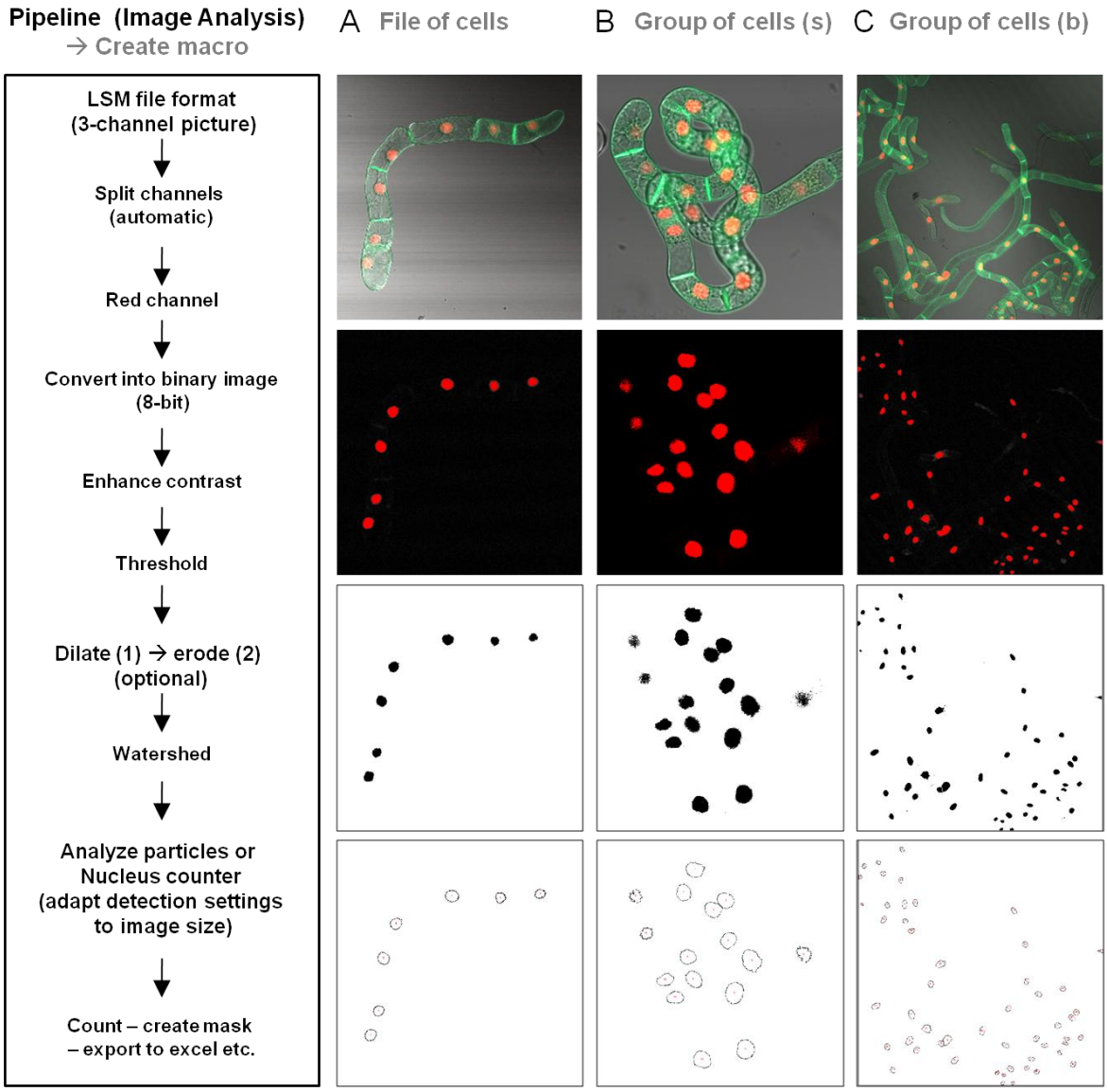

Figure 55. Use of the mRFP fluorescence (red channel) to detect and count BY-2 cells.

A 7-day-old BY-2 cell line was diluted tenfold in fresh medium and treated with both inducers, according to the self-developed protocol. Estradiol (5 µM) and dexamethasone (10 µM) were added 24 h and 15 h, respectively, before examination of the cells by fluorescence microscopy. All images shown in the figure were obtained by multi-channel scanning using a 10 x "Enhanced Contrast Plan-Neofluar" universal objective (EC Plan-Neofluar 10x/0,3 M27), adapted for general observations in fluorescence microscopy. Images were split into green, red and white channels, before being analyzed. For the detection of cells only the red channel was relevant. The image analysis "pipeline" is shown on the left. The single steps mentioned are part of standard image analysis softwares used during this work, such as ImageJ and CellProfiler and can be combined in form of a "macro" or a "pipeline". The analysis shown in this figure was done with ImageJ. Three different scenarios are shown. **A** – a "file" of tobacco BY-2 cells (here consisting of 7 cells). This is the easiest scenario, all cells are in one single plane and individual cells could also easily be counted by an experienced observer. **B** – a group of cells (s = small; b= big) with individual cells being superimposed. Due to the overlap of individual cells, it is challenging to identify the exact borders of single cells (a task that is by the way nearly impossible to accomplish for any default image analysis software). The red fluorescence of the nuclei allows the identification of single cells without difficulties. Out-of-focus nuclei might also be eliminated by adjusting the threshold. **C –** a large group of cells that represents a medium-sized (512x512 pixel) field of view. This is a realistic scenario that is usually observed. Cells of different sizes and forms are randomly positioned in the z-plane and overlaps occur frequently. However, it is possible to identify and count individual (fluorescent) cells. After the nucleus detection, a mask can be created that might be useful for the subsequent analysis of the green-channel. No size bars are shown, as this would lead to a misidentification by the software.

To obtain statistical data, we combined the analyzed images of the red and green channels. The detected nuclei in the red channel are used as a mask that serves as landmark for the zone we intend to investigate in the green channel, the nucleus (Figure 56). This proved to be a promising approach for the analysis of rather simple scenarios and its applicability for more complicated scenarios has to be further investigated. Critical points are the homogeneity and intensity of the fluorescence. This protocol can however be saved and be re-used for the quick analysis of multiple images or sets of images, given that the image acquistion settings are identical. Therefore, the more constant the conditions of treatments, the less follow-up adjustments for the image analysis have to be done.

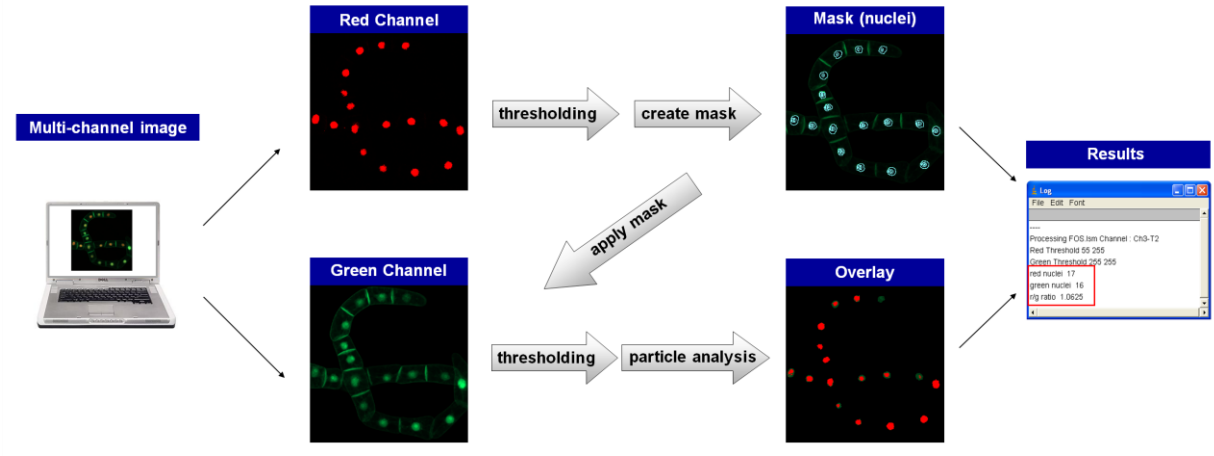

Figure 56. Flow diagram showing the principal steps of image processing and analysis.

Image analysis is performed with freely available software, such as ImageJ (Abramoff et al., 2004). At first, a multi-channel image is split into the red and the green channel. After adjusting the threshold of the red channel, the signals of the nuclei are converted to a layer mask, which is applied to the image of the green channel. After adjusting the threshold of the green channel, automatic particle counting is performed. The ratio of red to green

signals indicates the amount of total fluorescent cells *versus* those showing a delocalization of the GFP fusion proteins to the nucleus. This is most likely caused by an inhibition of the MEP pathway or of the prenylation of the GFP fusion protein. This statistical approach allows us to estimate the efficiency of a potential inhibitor at a given concentration *in vivo*.

j) The mRFP fluorescence emitted at the nucleus can be used to find the optimal focal plane for the acquisition of images in double fluorescence mode

Modern image-based screening approaches typically use multi-well plates to be able to efficiently screen chemical libraries at a medium to high throughput (Lang et al., 2006; Carpenter, 2007b; Starkuviene and Pepperkok, 2007). This requires the acquisition of several images from every well, a task that is commonly accomplished by automated microscope platforms. One of the major challenges of these systems until these days remains the focusing technology (Liron et al., 2006). Depending on the application, individual routines often have to be developed in order to acquire images of satisfying quality for later image analysis. Fluorescence-based focusing has several disadvantages, including photobleaching and possible phototoxicity (Santos et al., 1997; Gordon et al., 2007) however observations made during manual focusing with the double-fluorescent cell line indicated that the maximal intensity in the red channel (nuclear-localized mRFP) correlated with the focal plane, found by a human observer. These early results suggested that the fluorescence emitted by the mRFP could be used for later autofocusing purposes, especially keeping in mind, that one of the main features we are interested in, is the change of subcellular localization of the prenylable GFP fusion protein from the periphery of the cell to the nucleus after inhibition.

To confirm these early observations, a series of multichannel images of BY-2 cells (expressing both fluorescent proteins) spanning a total distance of 50 µm in the Z-plane was acquired at different focal planes. Afterwards, each optical slice of this Z-stack was analyzed using ImageJ software (Figure 57). The images of the green channel were analyzed by the edge finding algorithm of ImageJ, whereas the integrated density was calculated for the red channel. The results clearly show that - for the green channel - the sharpest image (as perceived by a human observer) of the Z-stack (identified by the edge finding algorithm of ImageJ) is also the image with the highest integrated density in the red channel, which is defined as "the sum of the values of the pixels in an image or selection" (ImageJ online manual: http://rsbweb.nih.gov/ij/docs/menus/analyze.html). This correlates very well with general observations about fluorescence images that indicate a maximum of image contrast at the Z-stage height corresponding to the focal position (Santos et al., 1997; Gordon et al., 2007). Therefore, a fluorescence-based autofocusing approach could use the nucleus-located maximum of red fluorescence to define the plane of focus and acquire additional pictures at an offset from this position (in both directions). This vertical series of images could then be summed up into a single projection or used to choose the best focal plane for each fluorophore. In an optimal scenario, two different images in different focal planes should be taken, when working with different fluorophores/wavelength, due to the chromatic aberration of optical lenses (objectives), which means that different colors/wavelength of light are focused to different points. (Dunn and Wang, 2000).

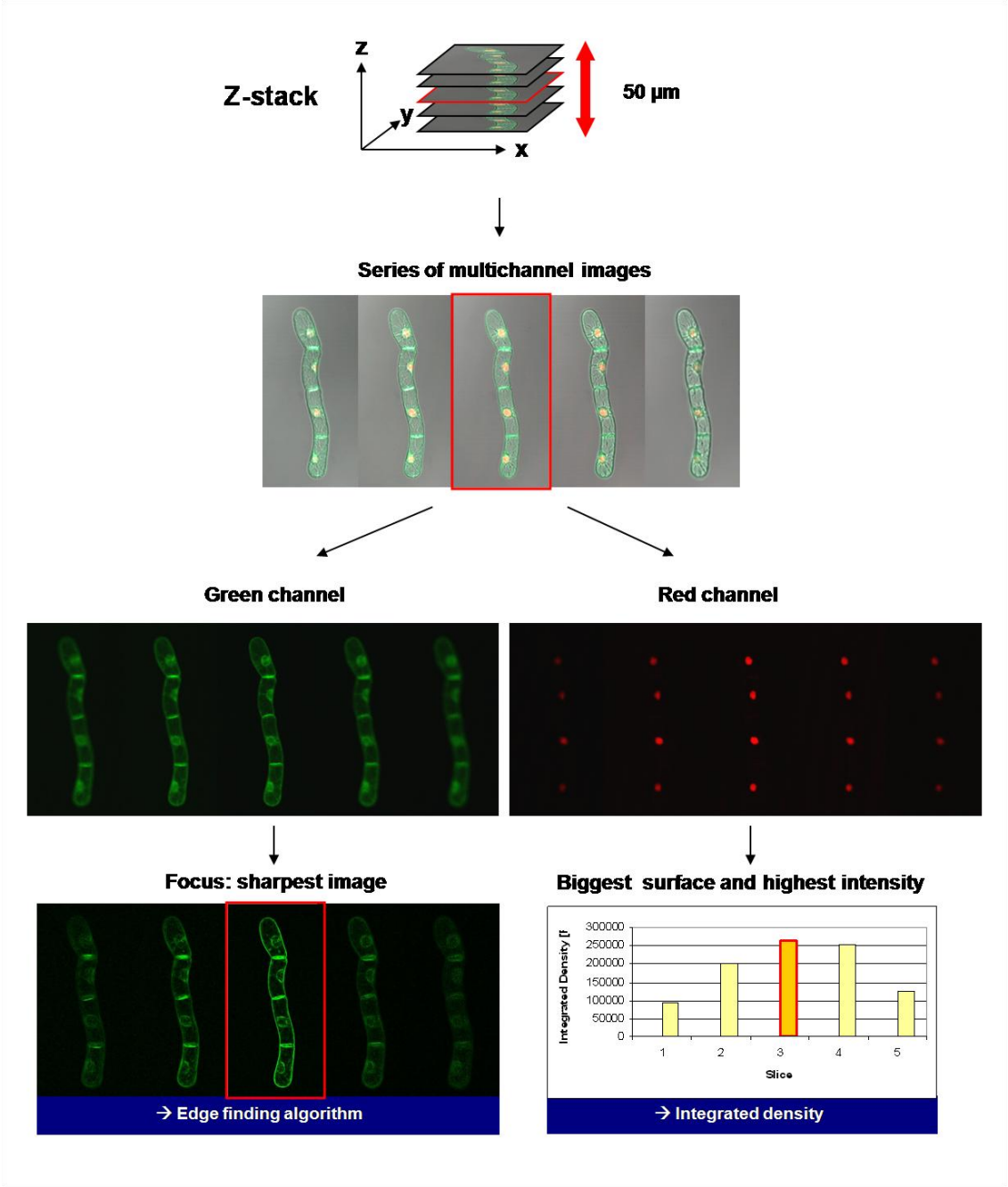

Figure 57. Correlation between the focal plane and the strongest signals in the red channel.

2.2.4.2 Miniaturization of the assay

The trend towards miniaturization and the right choice of the format

In the last decade, rapid technological advances, in particular, the advent of automated microscopes and more powerful software solutions, made it possible to perform compound screens on the basis of visual phenotypes and thereby also pushed the development of higher density formats for these image-based chemical assays.

Modern microscope-based screening approaches typically use multi-well plates, as these allow to significantly increase the number of tested compounds per day and to save reagents and consumables at the same time due to the miniaturisation of the experimental setup (Mayr and Fuerst, 2008).

The most common format for classical medium (up to 10000 compounds/day) to high throughput (between 10000-100000 compounds/day) screening assays are 96- or 384-well plates with average working volumes of 100-200 µl and 50 µl per well, respectively. Nowadays, most of the assays are adapted to this format and make it the favorite choice for screening assays adopted by pharmaceutical and biotechnological companies (Fox, 2006; Lang et al., 2006). Nevertheless, there are also examples of applications for even smaller formats, like the 1536-well plates, with a volume downscaled to 5 µl and a hypothetical throughput rate of up to 200000 compounds per day ("ultra-high-throughput") or ultra-density formats like the 3456-well plates, with assay volumes downscaled to 1-2 µl (Fox, 2006; Klumpp et al., 2006; Zheng, 2006).

Despite the possible efficiency gains connected with these high-density formats, there are severe technical hurdles for their use in routine HTS assays, most importantly, the adaptation of automated liquid handling and dispensing technology, which is better established for the bigger 96 and 384-well formats (Houston et al., 2008; Mayr and Fuerst, 2008).

In this context, it is important to make general considerations about the desired application of the bioassay. Our goal was to significantly decrease the working volume for the assay and to use a format fulfilling the requirements of modern cellular imaging platforms, capable of (automatically) acquiring images at a (reasonable) medium to high throughput rate. However, the image quality should still be sufficiently good to monitor whole cell populations, on the one hand and to measure intracellular events, on the other hand.

Ideally, multiple images at different positions and different magnifications should be acquired from each well. This kind of read-out however would be extremely time-consuming and take several hours in order to process an entire multi-well plate. Therefore, it was necessary to find the right balance between high content and a reasonable throughput or in other words, between time, cost and quality, which Mayr and Fuerst called "the magic triangle of HTS".

Results:

In order to find the format that provided us with the largest flexibility, as far as the quality of the image acquisition, the growth conditions of the TBY-2 cells and the general liquid handling were concerned, it was first necessary to take a closer look at some of the characteristics of the model system used in the bio-assay.

TBY-2 cells usually grow in files and individual cells (in the exponential growth phase), easily reaching 50 to 100 µm in length and more than 30 µm in width, with the nucleus having a diameter between 10 and 20 µm (personal observations, after measuring hundreds of cells). Previous results already indicated that the images taken in a medium to low magnification-mode (10 x objective – resolution in the µm range) could be exploited by image analysis software and provide sufficient information for the analysis of the observed phenotypes (chapter 2.2.3.1 Automatic image processing as tool to determine the impact of drugs and inhibitors on the H6-GFP-DB-CVIL-line). For images acquired with the 10 x objective (EC-Plan Neofluar 10x/0.30 M27), the field of view ranges from about 900 µm x 900 µm to 1272 µm x 1272 µm (stack size: x-plane x y-plane) in the largest possible configurations. A field of this size (approximately 1 mm x 1mm) allows studying up to 100 cells on a conventional microscope cover slide, depending on the dilution factor of the culture. In order to obtain data from a statistically significant number of cells for each treatment, images from multiple fields should be collected from each well. Typically, 96 plates have an internal diameter at the bottom of the well of approximately 5 mm. The diameter of the next larger format, the 384 well plates is already significantly smaller of about 3 mm. Considering the size of the cells and the image field, as well as the need to acquire multiple images, all formats smaller than 96-well did not make any sense for our experimental system.

The diameter of a conventional round-shaped well allows the acquisition of at least 9 independent fields of more than 1 mm x 1 mm, without interfering with the walls of the wells. However, one of the limitations reamains the possible read-out pattern, which cannot exploit the whole surface of the well. In order to maximize the surface for the read-out, commercial square-shaped micro-array plates (with glass-bottoms) could offer an interesting alternative to round 96-well plates (Figure 58).

Figure 58 shows a field of view of 1 mm^2 that was acquired using an inverted fluorescence microscope and a 96-well plate with a glass-bottom that resembles a conventional cover slide in thickness (96-well glass bottom plate No. 1.5, γ – irradiated MatTek Corporation - Ashland, MA – USA). In order to be able to use 96-well plates, a special stage adaptor for multi-well plates was purchased from Zeiss. In contrast to the image acquisition for cells from a normal cover slide, the situation is a little more complex for cells in a well as hardware and software have to cope with cells in a three-dimensional space (a suspension of cells with a height of several mms). This means that not all of the visible cells are in the right focal plane and align perfectly parallel to the z-axes. Nevertheless, this lack of

"substrate flatness" (Liron et al., 2005) should partially be solved by the presence of a reference point for the focusing software, such as the red fluorescence emitted by the nuclear-localized mRFP fusion protein.

Results obtained by manual focusing clearly demonstrated that it is possible to resolve subcellular details at a satisfying resolution (Figure 58) (1024 x 1024 pixels x 8) and deliver enough information to distinguish the phenotypes of interest.

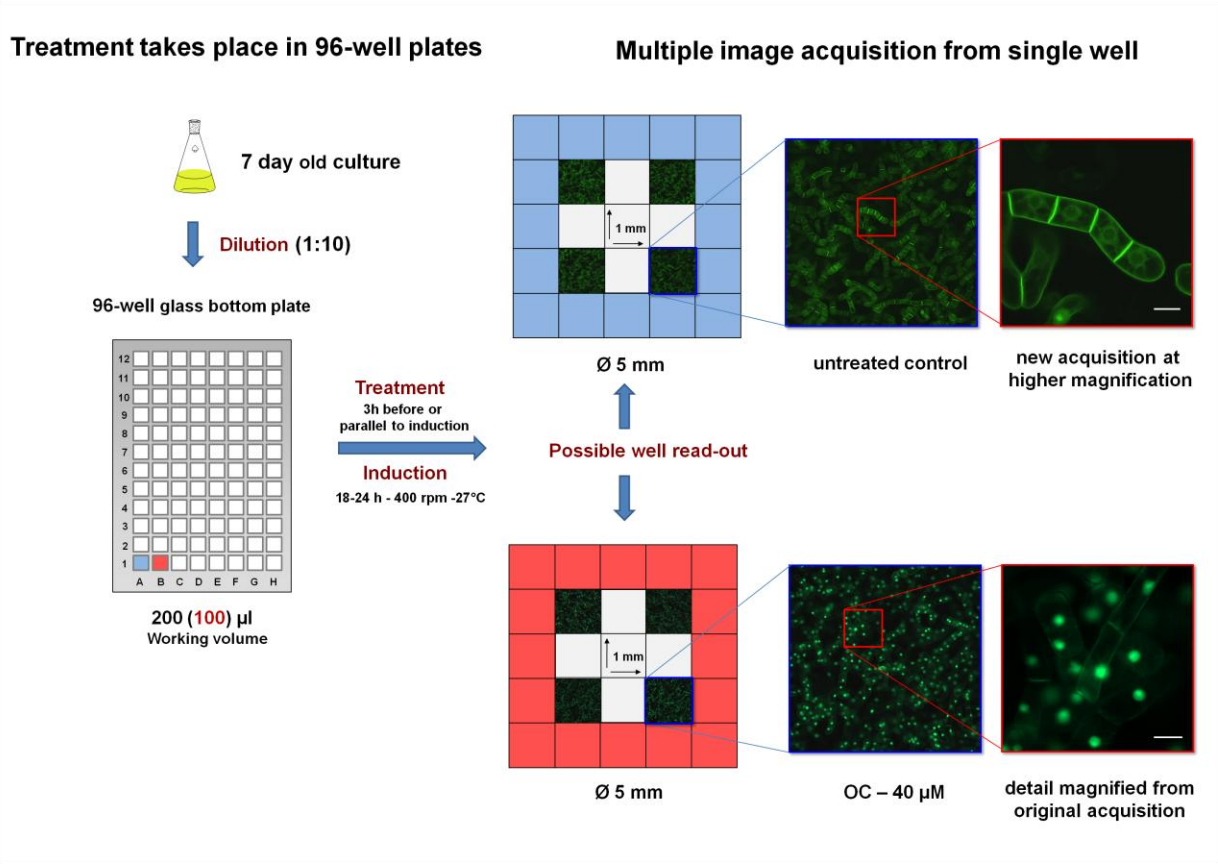

Figure 58. Image acquisition takes place in 96-well glass bottom plates.

Besides the quality of the image acquisition process, another important factor for the miniaturization of the assay was the nature of the biological material, which sets distinct limits for the downscaling process and needs the adaptation of various parameters for the significantly smaller format (adjusting minimal and maximal fill volumes; agitation; minimizing the evaporation; liquid handling technology etc.)

In this context, it is essential to keep in mind, that this bioassay, in contrast to most cell-based imaging approaches, is based on the observation of living cells. The majority of image-based screens at a high-throughput rate are usually performed with fixed cells (Starkuviene and Pepperkok, 2007). TBY-2 cells are grown in liquid medium, which means that the treated and induced cultures require permanent shaking for more than 20 hours to prevent cell sedimentation, as this may lead to sub-

optimal nutrient and oxygen supply and could interfere with the expression of the fluorescent reporter proteins.

The influence of suboptimal agitation in this small-scale system (volume 100 – 200 µl) on the expression of the reporter proteins was observed in several independent experiments, in which different shaking conditions for the BY-2 cultures were tested.

Therefore, 7-day old cells were diluted (1:10) in fresh BY-2 medium and then induced by addition of 10 µM dexamethasone and 5 µM oestradiol. Then 200 µl of this dilution were transferred into the wells of a 96-well plate (conventional round-shaped wells, with conical bottom) and incubated for 20 hours in the dark under permanent shaking (160 rpm or 320 rpm). Cells that were shaken at 150 rpm (which corresponds to the shaking frequency of 6-well plates and culture flasks) showed a normal induction of the GFP fusion protein, whereas the mRFP fusion protein was barely expressed. However, in cells that were cultivated at 320 rpm clearly the expression of the NLS-mRFP protein could clearly be detected by fluorescence microscopy (Figure 59).

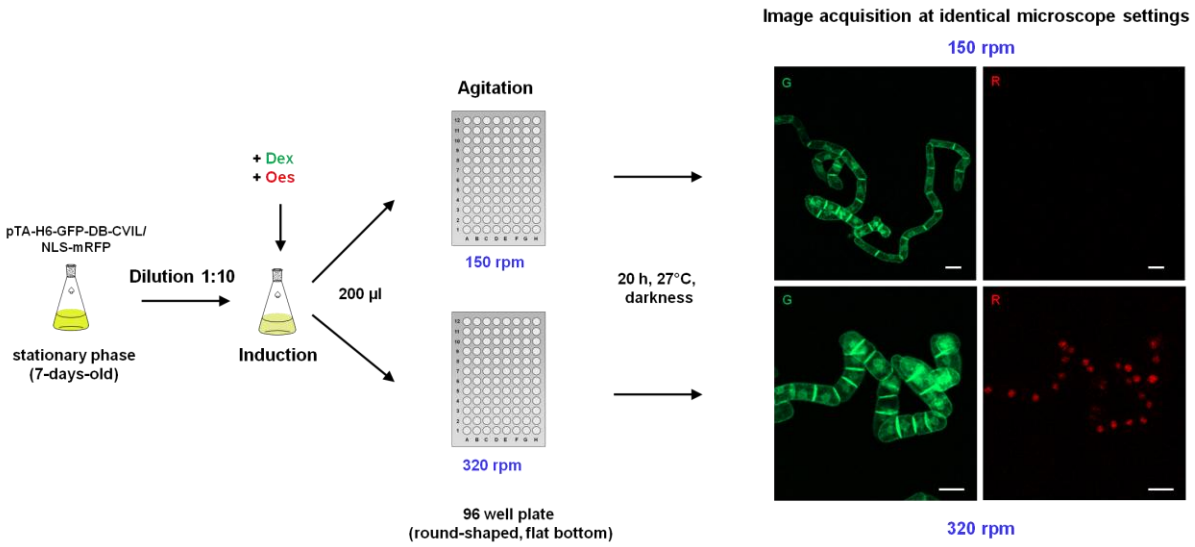

Figure 59. Influence of different shaking conditions on the expression of both fluorescent reporter proteins in transgenic tobacco BY-2 cells incubated over night in the wells of a 96-well microtiter plate.

A 7-day-old culture was diluted tenfold in fresh culture medium before the inducers dexamethasone (10 µM) and estradiol (5 µM) were added. Afterwards 200 µl of the cell suspension were given into the wells of a 96-well glass-bottom microtiter plate and shaken under different conditions (150 rpm and 320 rpm) before being examined by fluorescence microscopy as described previously. White bars = 10 µm.

The gas-liquid mass transfer properties of shaken 96-well plates have been investigated in detail by Hermann et *al.* (2003) and revealed that the oxygen transfer rate (OTR) measured in the wells was strongly influenced by different parameters, such as the surface tension of the medium, the material of the well, the filling volume and the shape of the well (Hermann et al., 2003). In round-shaped wells, for example, due to the high surface tension, no liquid movement occurred until a critical shaking intensity was reached: for 200 µl water shaken at shaking diameter of 25 mm, the rate had to exceed

300 1/min. On the other hand, frequencies above 450 1/min could not be used, the liquid risking to spill out of the well (Hermann et al., 2003). As a general rule, one can say that the OTR increases proportionally with shaking amplitude and frequency due to an increase in the total surface that is available for oxygen (gas) transfer. The same effect was observed by replacing roundish wells by rectangular or square wells, which can be explained by the increase of the turbulence of the system due to the effect of the corners. A higher fill volume on the other hand decreases the oxygen transfer rate if all other parameters stay constant (Duetz et al., 2000; Hermann et al., 2003; Betts and Baganz, 2006).

These results correlate very well with the initial tests made to test the compatibility of the bioassay with different shaking conditions in standard 96-well microtiter plates. No agitation of the fluid (diluted cells in BY-2 medium) was observed for 250 µl until around 300 1/min (using a Heidolph unimax 1010 shaker, 10 mm). Therefore a frequency of 320 rpm and higher was used. However the limitation for further testing was the maximal speed of the available shaker (500 1/rpm). In addition, these results were obtained for wells with a conical bottom. The use of an inverted microscope required 96-wells with a flat-bottom for the imaging process, and the hydrodynamic behaviour of a BY-2 culture in a flat-bottomed well differs from a conventional deep-well and preliminary results indicate that the speed has to exceed 500 rpm to assure an optimal agitation of the cells for a filling volume of 200 µl. This result now prompted us to purchase 96-well glass-bottom plates with a square-shaped cross-section area /ground profile. Besides increasing the OTR at lower shaking frequencies compared to round wells, it should also confer an additional advantage for the read-out process by significantly increasing the total surface of the well.

2.2.4.3 Automatization of the assay

A prerequisite for an image-based screening system is a certain degree of automatization as far as repetitive tasks are concerned. The use of the "AutofocusScreen for LSM" macro provided by Zeiss allows the automatization of different steps of the image acquisition process. First tests performed with the 96-well-glass bottom plates indicated that all features could be used, including the autofocus routine and the automatic well-readout (Figure 60). However, in order to find the right balance between speed and image quality, the protocol still requires refinement and further validation before reproducible and exploitable data sets may be obtained.

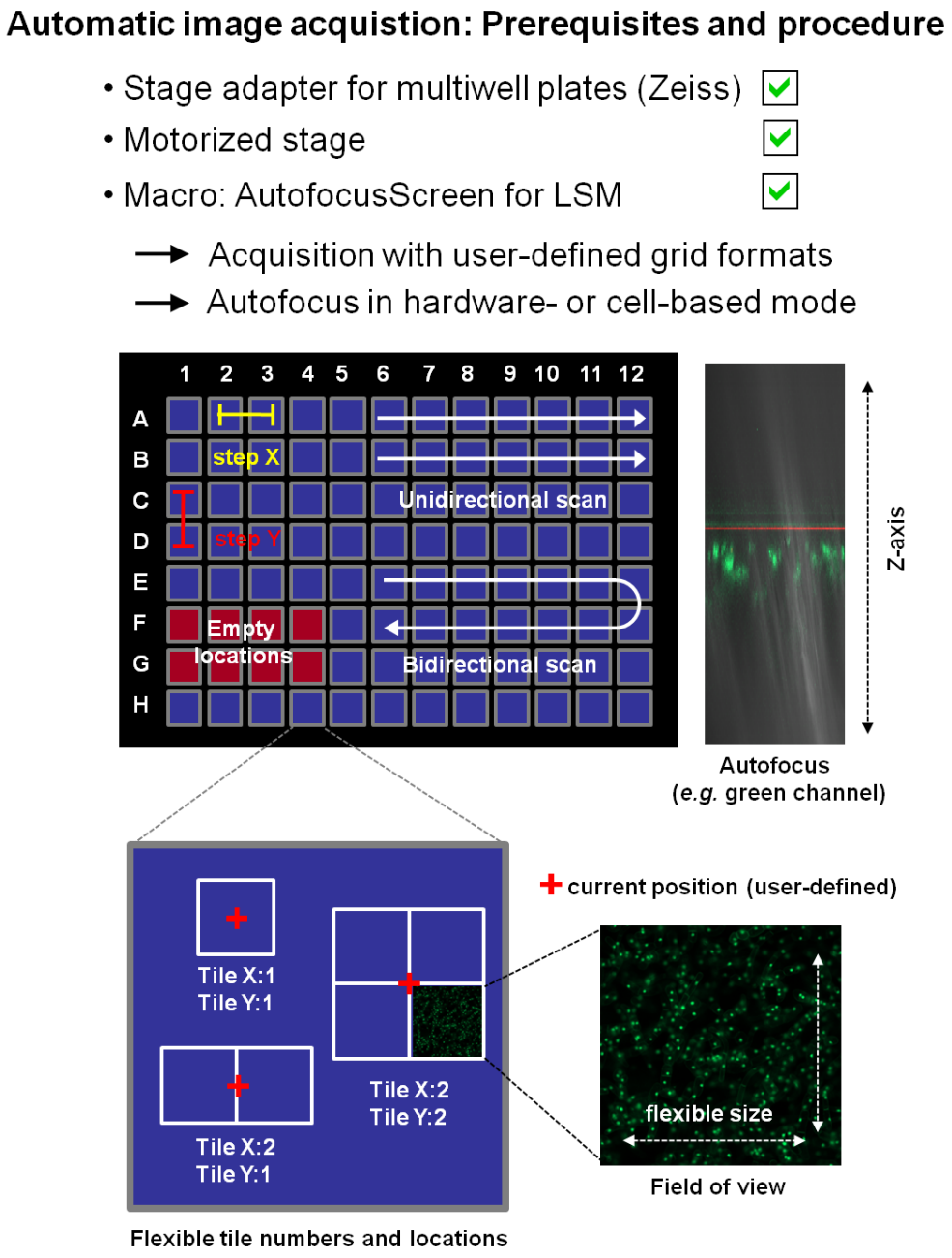

Figure 60. Automatic image acquisition from multiwell plates.

Images from multiple locations can be taken using the "AutofocusScreen for LSM" macro, developped in a collaboration between Carl Zeiss MicroImaging GMBH (Jena, Germany) and the Group of Dr.Jan Ellenberg at the European Molecular Biology Laboratory (EMBL, Heidelberg, Germany). Is is freely downloadable at http://www.zeiss.de/LSM-Macros. Well positions that want to be scanned can be defined by simple mouse clicking. Steps X and Y define the distance between two acquisition locations. The exact position (here marked by a red cross) will be defined by the user at the beginning of the image acquisition procedure. The user has also the option to define multiple tiles (with no or partial overlap to each other) around this position. The size of the scanned image will also be defined by the user and the scanning settings he choses. Autofocus can be hardware- or cell-based, acquiring the emitted laser light or the emitted light of the sample, respectively (the above shown image displays a cell-based scan across the Z-axis, using the green channel). Initial experiments with tobacco-BY-2 cells however showed that at multiple positions in the Z-axis above the glass bottom, a significant amount of cells could be visualized in the respective focal plane. This factor however will have to be adjusted for the scanning of multiple wells, as BY-2 cells will sediment quite fast (within minutes) to the bottom of the well, resulting in a significant change in the conditions and number of cells in the Z-axis.

2.2.4.4 Data exploration and validation of the assay

Follow-up experiments – drug working concentration and toxicity assessment

One important aspect about a cell-based assay is the fact that it gives an idea of the so-called "drug working concentration", which can be compared to known compounds, run as controls. Very often, the working concentration is referred to as "desired pharmacological" activity, to distinguish it from the concentration at which it becomes toxic.

In addition, before being admitted to preclinical trials, a positive hit in a compound screen has to undergo numerous tests, to rule out mutagenic or carcinogenic activities (Pritchard et al., 2003). Once again, fluorescence microscopy plays an important role in toxicity studies, measuring for example chromosome aberration and DNA damage (Tice, 1988; Fenech, 2005), effects on calcium homeostasis, mitochondrial transmembrane potential and the permeability of cellular membranes (Abraham et al., 2004). As suggested earlier, the use of nuclear stains, such as DAPI and PI for testing the cell viability in response to a treatment could be included in standard screening protocols.

2.3 Generation of transgenic tobacco BY-2 cell lines

The generation of transgenic tobacco BY-2 cell lines was an early step in the development and improvement of the screening system (chapter 2.1.3.1) and according to the published "standard protocols", a routine method. Nevertheless, it proved to be a time-consuming challenge, as within cell suspensions of supposedly clonal origin (primary suspensions derived from primary calli), important variations were regularly observed. These variations not only concerned the morphology of the cells, but also more importantly the homogeneity and the fluorescence intensity level. Therefore, attempts were made to re-select homogenous cell lines of transgenic BY-2 cells with high intensity levels of fluorescence (Figure 61), resulting in the protocol described in chapter 4.5.5.3.

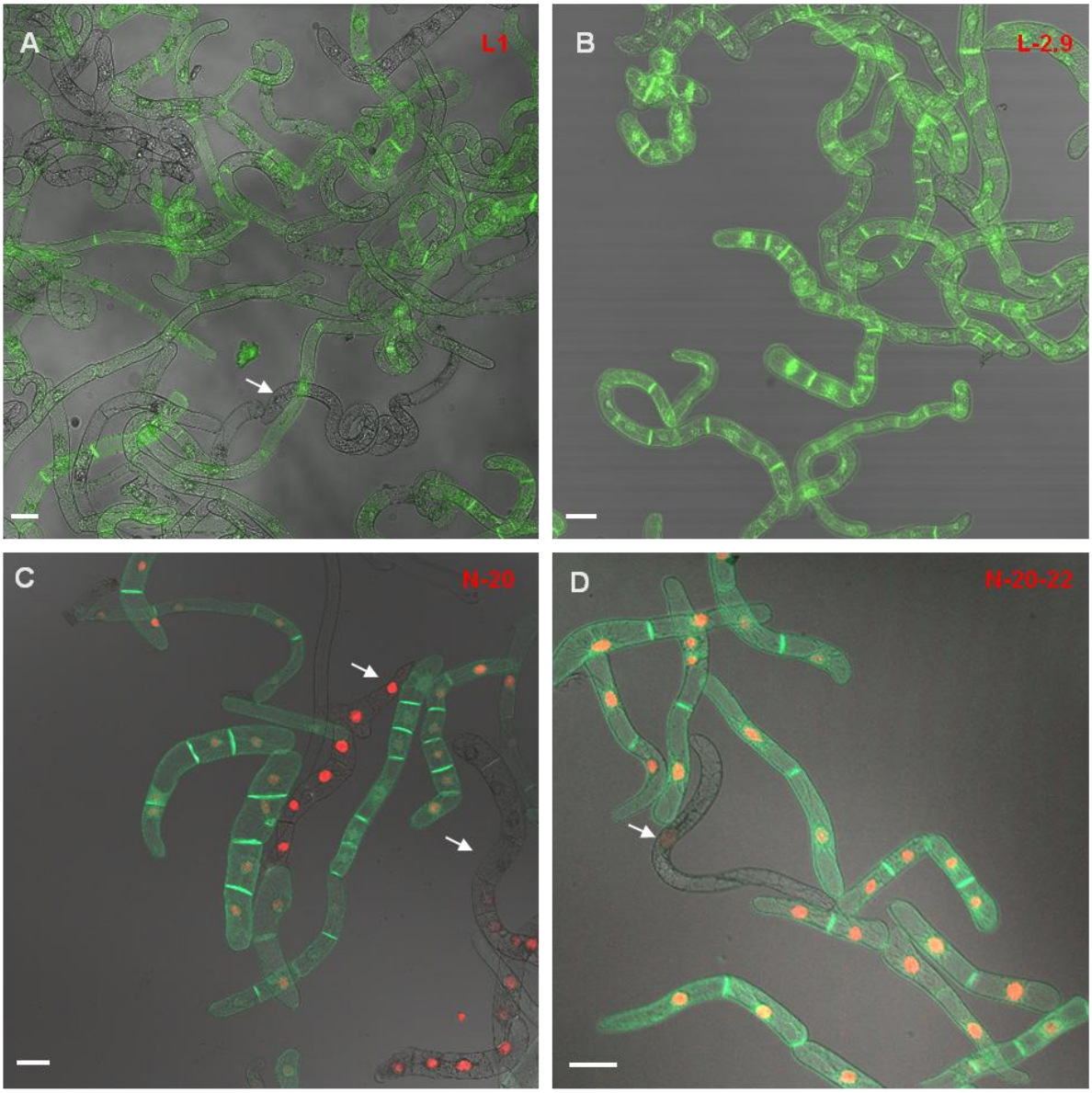

Figure 61. GFP and RFP fluorescence in primary and secondary suspensions.

A- and **C-** Heterogeneity of GFP and RFP fluorescence in a suspension of transgenic BY-2 cells derived from primary calli. Arrows indicate cells with missing fluorescence or significant variations in fluorescence intensities (red and green fluorescence). **B-** and **D-** Cell suspensions derived from re-selected calli (secondary calli). The fluorescence is strong and homogenous in both channels. Nevertheless some cells (less than 5%) show heterogeneity in fluorescence. Possible reasons are discussed in the main text. White bars indicate 20 µm.

What are the reasons for such variations?

According to Anne Carpenter in her 2007 review in *Nature Methods* on "cellular imaging by fluorescence microscopy", variations from cell to cell might occur for various reasons including differences in cell cycle position, stochastic variations in gene expression, pre-existing amounts of proteins and metabolites in each cell and micro-environment differences (due to cell medium or cell-to-cell-contacts).

However, these are only a few examples, and in order to better understand the impact of multiple factors on the growth and expression capacity of transgenic tobacco BY-2 cells, possible causes of variations will be shortly reviewed and discussed in the context of the results and observations made during these studies.

a) Expression noise and cell-to-cell variations

Variations in the expression of proteins in a population of genetically identical cells may occur for various reasons and there are many aspects that may contribute to this behavior (Levsky and Singer, 2003). For instance, several studies in bacterial and yeast model systems have shown that a certain amount of this cell-to-cell variation resulted from so-called "expression noise", that may be defined as stochastic fluctuations in the expression of a gene (Elowitz et al., 2002; Raser and O'Shea, 2004). In 2005, a study by Pedraza and van Oudenaarden focused on the expression noise in gene networks, and showed that these stochastic variations were caused by intrinsic noise at the level of the gene (e.g. number of mRNA copies), transmitted noise from upstream genes and global noise affecting all the genes (Pedraza and van Oudenaarden, 2005).

Other studies however suggested that expression noise was rather a minor source of total cell-to-cell variations (Colman-Lerner et al., 2005) and showed that the differences may be caused by other factors, such as the capacity of individual cells to express proteins from genes (expression capacity). For instance, differences may occur in the levels of cellular components needed for protein expression (e.g variations in the global pool of housekeeping genes, cell cycle position or fluctuations of environmental conditions discussed later). As an example, Gordon et al. (2007) monitored the expression levels and maturation rates of YFP (yellow fluorescent protein) in exponentially growing yeast cells with a pheromone-inducible gene expression system. Interestingly, they observed that the total amount of the reporter protein YFP could vary up to a factor 4 in inducer-treated yeast cells (*Saccharomyces cerevisiae)*, whereas the maturation rates of the protein only showed little variations

(39 min +/- 7 min). Even though these studies used less complex model systems than plant cells, this could explain the variations in fluorescence levels observed during this work..

b) Natural heterogeneity of transgene expression in tobacco BY-2 cells

The visual reporter system used during this work was based on transgenic tobacco (*Nicotiana tabacum* L.) BY-2 cells. Tobacco BY-2 cells are often referred to as the HeLa cells of plant molecular biology and were used in hundreds of studies focusing on various aspects of plant physiology (Geelen and Inze, 2001; Hemmerlin et al., 2004; Nagata et al., 2009). Under standard growth conditions, the cell duplication time is around 14 h (Nagata et al., 1992) and the cell divisions can be synchronized, which allows cell-cycle related studies (Hemmerlin and Bach, 1998; Kumagai-Sano et al., 2006; Kuthanova et al., 2008). In addition, they can easily be transformed, either by particle bombardment (Klein et al., 1988) or *Agrobacterium tumefaciens*-mediated gene transfer (An, 1985).

Although they are not able to form chloroplasts and have to be grown under heterotrophic conditions, they nevertheless contain active proplastids and leucoplasts (Nagata et al., 1992) and have been shown to be an excellent system to study the synthesis of sterols and isoprenoids (Wentzinger et al., 2002; Hemmerlin et al., 2004).

Given the higher complexity of plants, such as tobacco (*Nicotiana tabacum L.*), compared to bacteria or yeast, variations in the expression levels of endogenous and reporter proteins from one cell to another can easily be imagined. This aspect is particularly interesting in connection with the observations made during my thesis, where transgene expression in individual cells of the newly-generated H6-GFP-DB-CVIL TBY-2 cell line proved to be unstable and heterogenous in many cases (Figure 61).

These often dramatic changes in the brightness of fluorescent cells, as well as the unstable ratio of fluorescent to non-fluorescent cells in a supposedly clonal cell line led me very early in my work to hypothesize that the cultured cell suspensions, derived from primary calli (the first calli obtained after *Agrobacterium tumefaciens*-mediated transformation), could contain (epi-)genetically different cells. The heterogeneity of callus cultures is a well-known phenomenon for many plant species and consequently, the selection of highly productive cell lines that show the desired attributes is a common step, especially for commercial efforts to produce secondary metabolites *in vitro* (Verpoorte and Memelink, 2002; Georgiev et al., 2006; Georgiev et al., 2009). Therefore, a simple method to generate more homogenous cell lines, derived from secondary calli, was established and constantly improved over time, leading to the final protocol summarized in Table 10.

This method proved to be highly efficient, as we succeeded to obtain several secondary suspension cultures of the double-transformed mRFP-cell line that exhibited a high percentage of bright fluorescent cells (> 95%) under our experimental conditions. This result was very satisfying, as

homogenous and stable expression of transgenes is highly desirable, especially for the design of a reliable, statistical test system.

Cloning procedure	Nocarova and Fischer, 2009	Thesis (2006-2010)
Transformation method	*Agrobacterium tumefaciens*	*Agrobacterium tumefaciens*
culture preparation from primary calli	1 ml of fresh calli in 30 ml medium (+ AB) by pipeting	small calli (diameter ~ 5 mm) in 10 ml medium (+ AB) with a spatula
subculturing of primary suspensions	after 7 days: 1,5 ml in 30 ml medium	after 7 days: 1-2 ml in 40 ml medium
cloning of secondary calli	7-day-old transgenic cells are diluted 1:3 and mixed with 4ml of similarly prepared WT cells in a ratio 1: 1000	7-day-old WT cells are diluted 1:10 (3 ml + 27 ml of medium) and mixed with 7 day old transgenic cells (60 µl) in a ratio 1:500
dilution factors and ratios	7-day-old wild-type: 1:3 7-day-old transgenic cells: 1:3 transgenic:wild-type: 1:1000	7-day-old wild-type: 1:10 7-day-old transgenic cells: - transgenic:wild-type: 1:500
spread on solid medium (+ AB)	500 µl on Ø 6 cm Petri dish	7 ml on Ø 12 cm Petri dish (sufficient to cover the surface)
calli appearing (after 3-6 weeks)	~ 25	~ 25 - 100

Table 10: Comparison of the cloning procedures of transgenic tobacco BY-2 cells.

Such variations in the expression levels among independent transgenic lines (from the same initial transformation event) might also arise from the inserted sequence itself. Changes can indeed be induced by the methylation degree of chromosomal insertion regions (Pröls and Meyer, 1992), the locus of the insertion (Iglesias et al., 1997), the number of insertion copies or transgene silencing (van Leeuwen et al., 2001; Schubert et al., 2004; Francis and Spiker, 2005). For instance, only recently experiments demonstrated that the integration site of a transgene significantly influences its susceptibility to RNA silencing, rather than affecting its initial expression level (Fischer et al., 2008).
In the past, several studies (Müller et al., 1996; Down et al., 2001) helped to get a clearer picture of the variations of transgene expression in genetically identical clones. However, the most interesting contribution to this poorly understood topic came very recently from Eva Nocarova and Lukas Fischer. In April 2009, they reported a method to clone transgenic tobacco BY-2 cells with the goal to reduce the high natural heterogeneity of transgene expression. The cell lines generated in their laboratory "repeatedly produced only a low frequency of cell lines with well-balanced and stable fluorescence in all cells". These observations corroborated the results obtained during the generation of both cell lines (H6-GFP-DB-CVIL and SV40-mRFP/H6-GFP-DB-CVIL) during my thesis and with the results of my co-worker Dr. Elisabet Gas-Pascual.

In order to identify the sources of such heterogeneity, Nocorava and Fischer transformed tobacco BY-2 cells with a gene encoding a free GFP under the control of the CaMV 35S promotor driving the constitutive expression of the transgene. Then, they monitored the expression levels of GFP in primary calli and the derived suspension cultures (primary suspensions) as well as in secondary calli and suspensions they obtained by a simple cloning procedure (Table 10: Comparison of the cloning procedures of transgenic tobacco BY-2 cells.). Interestingly, only about 40 % of the (primary) calli obtained after *Agrobacterium*-mediated transformation showed homogenous GFP fluorescence. The remaining calli displayed heterogenous GFP expression, either in a mosaic (m) or sectorial (s) distribution pattern within the calli. In addition, up to 90% of the (primary) suspension culture lines derived from all primary calli consisted of cells with heterogenous levels of GFP fluorescence. On the other hand, secondary calli, obtained with their cloning method, showed homogenous fluorescence in approximatley 90% of the cases, whereas only little more than 40 % of secondary suspensions had homogenous GFP fluorescence intensities (Figure 62).

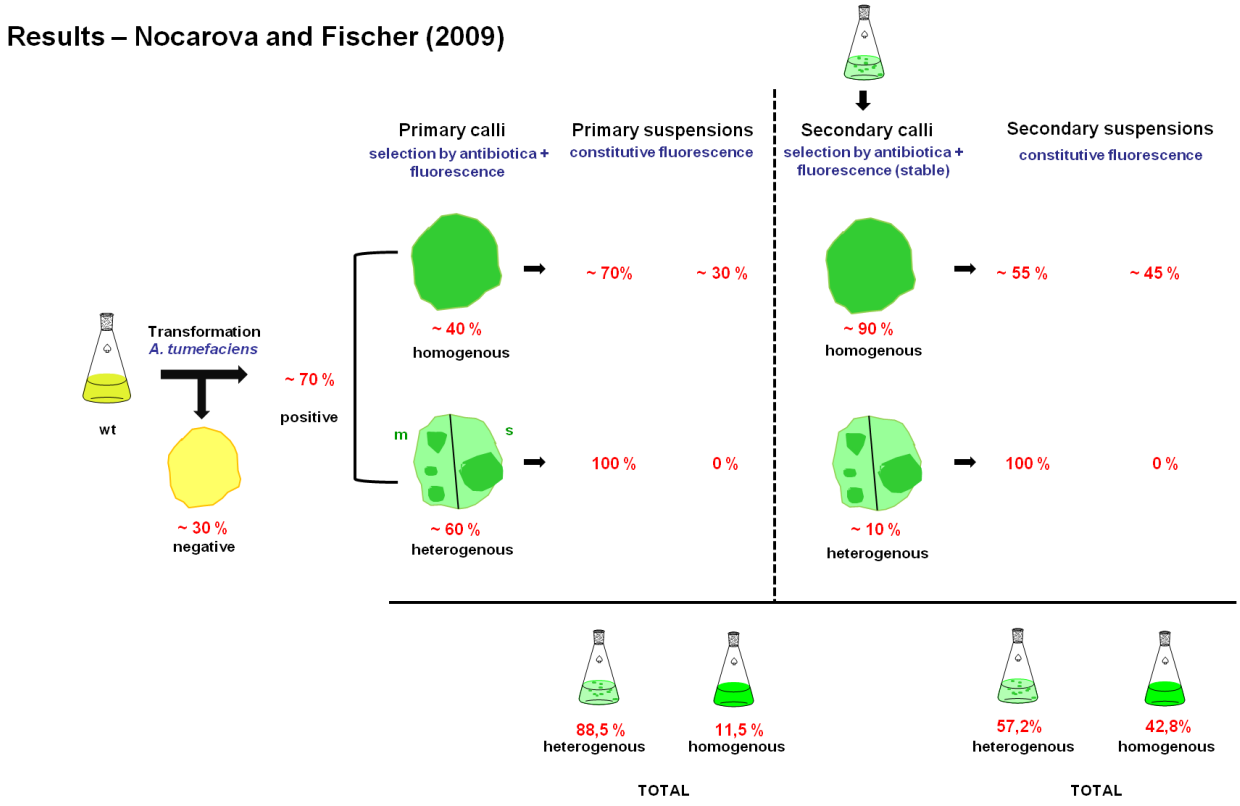

Figure 62. Results obtained by Nocarova and Fischer (2009).

The scheme shows the frequencies of BY-2 calli and derived suspensions with homogenous and heterogenous GFP fluorescence. Please note that the secondary lines were generated by cloning of primary heterogenous suspensions. In addition, calli and derived suspensions were both screened and evaluated by fluorescence. It is important to consider that the terms "homogenous" and "heterogenous" do not describe the intensity of the fluorescence, but only if a culture shows well-balanced and stable fluorescence in the cell population. Values were rounded to nearest, reasonable values considering the error margins indicated by the authors (M = mosaic arrangement of fluorescence; s = sectorial arrangement, with sharp borders).

Molecular analysis of the primary clones by Nocarova and Fischer (2009) by Southern hybridization identified two causes for the observed heterogeneity:

First, genetic heterogeneity due to the presence of cells with different T-DNA insertions, and second epigenetic heterogeneity, caused by transgene silencing at the transcriptional level in connection with DNA-methylation, as treatment with the DNA-demethylation drug 5-azacytidin (Christman, 2002) reactivated GFP expression in some lines. In many cases this heterogeneity could be resolved by subsequent cloning, but nevertheless a certain fraction showed what the authors called a "permanent expression heterogeneity" which could, for example, be due to temporal changes in the accessibility of promotor sequences to transcription factors (van Leeuwen et al., 2001).

In another context, not related to the initial heterogeneity of transformed cell lines, we made an interesting observation: We suddenly lost all the mRFP fluorescence in one of the double-transformed cell lines, whereas the level of GFP fluorescence remained completely untouched. After elimination of all evident sources of error (replacing the inducer, subculturing the two-week old line, replacing the medium), the culture was incubated over a whole 7-day-growth cycle in presence of 10 µM 5-azacytidine, a nucleotide analog that cannot be methylated, and, remarkably, the mRFP fluorescence could be partially restored (Figure 63).

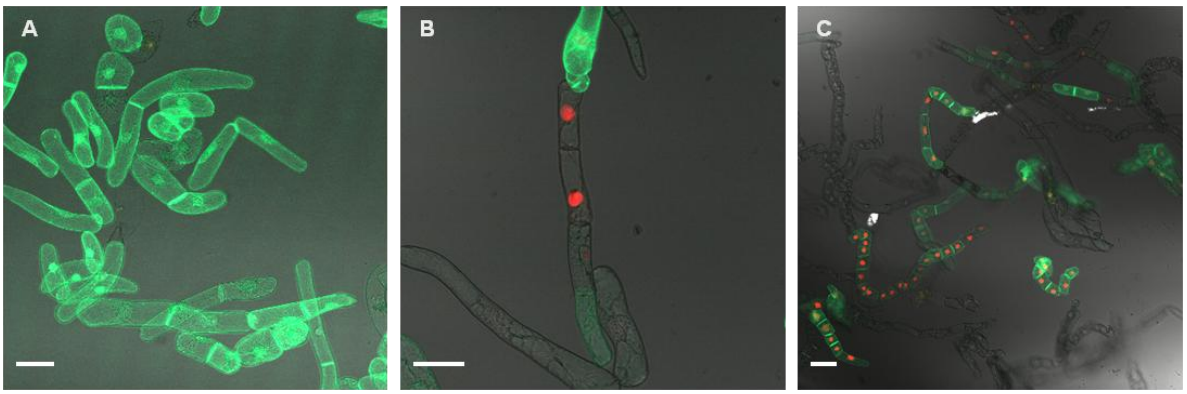

Figure 63. Restoration of RFP fluorescence after treatment with 5-azacytidine.

A Double fluorescent cell line that suddenly lost mRFP expression. **B** and **C**. Cells were treated with 10 µM azacytidine for one week. RFP fluorescence could be recovered, but many dead cells were due to overall toxic effects. Even though the concentration was scaled down 10-20x compared to values that are indicated in the literature for treatments, the concentration still seemed to be to high for the use in tobacco BY-2 cells (good uptake rate and fast metabolism). All images are shown as merged images taken in green and red fluorescence, as well as white light mode. White bars = 50 µm.

As this result clearly suggested a DNA methylation event, we searched the literature for common sources of such sudden drops in gene expression levels of transgenes in plant cultures. As we had already observed the same phenomenon in the original H6-GFP-DB-CVIL cell lines during the inhibitor tests with fosmidomycin-derived prodrugs (chapter 2.1.6.2), this point was quite important,

given all the efforts put into the generation of the cell lines. Schmitt et al. (1997) reported indeed that the antibiotics kanamycin, hygromycin and cefotaxim caused a DNA hypermethylation at CpG sites in the genome of tobacco plants grown *in vitro*, as shown by the *Sss*I methylase accepting assays and genomic sequencing with sodium bisulfite. Interestingly, these methylations occurred in a time and dose-dependent way, and were not reversed when the progeny was not grown anymore in the presence of the antibiotics (Schmitt et al., 1997).

The methylation of plant genomes is a common process, which can affect up to 30 % of the cytosine residues (Adams and Burdon, 1985). It also occurs as part of the "natural" gene regulation in plants (Finnegan et al., 1993; Finnegan et al., 1998). However, increased DNA methylation was observed in several cases associated with PTGS (post-transcriptional gene silencing) and TGS (transcriptional gene silencing) or different forms of stress (De Wilde et al., 2000; Matzke et al., 2004; Halpin, 2005; Meng et al., 2006). For instance, transgene silencing was induced in petunia, after a period of high light intensity and temperature (Meyer et al., 1992), whereas high temperatures alone were shown sufficient to silence different transgenes in tobacco (Vaucheret et al., 1995; Neumann et al., 1997; Köhne et al., 1998). Thus, the frequent major breakdowns of the air-conditioning system of our growth chambers, which occurred during my experiments, might also have contributed to the observed silencing.

However, although recovery of the mRFP expression by azacytidine treatment had confirmed our assumption that the sudden loss of fluorescence, due to a DNA methylation event, could explain the heterogeneity of the cells, we did not maintain and subculture the recovered lines, as azacytidine is a powerful mutagenic agent, which has toxic effects on cells.

In conclusion, these results are interesting in different ways. First, they helped to explain the heterogeneity in the fluorescence levels of the transgenic cell lines generated in this work. This heterogeneity was observed in our lab independently from other sources, and various approaches were discussed how to eliminate or reduce it. Finally, we developped a simple and inexpensive method to generate secondary calli, and the resulting transgenic lines proved to be more homogenous. For the GFP-DB-CVIL line, 23 out of 48 suspension cultures (~ 48%) derived from primary calli showed fluorescent cells. However, the majority of these lines displayed weak ratios of fluorescent cells to non-fluorescent cells. The four lines with the best ratios and highest fluorescence intensities were chosen to reselect calli with our protocol. Two out of 15 secondary lines showed strong, homogenous fluorescence and a very high ratio of fluorescent to non-fluorescent cells.

For the double transformation of the GFP-DB-CVIL line with the SV40-mRFP gene construct, 20 appearing calli were screened and about seven out of them showed strong fluorescence in the first generation of cell suspension cultures (35%). In order to obtain a more homogenous line, calli from suspension cultures were reselected and four promising cell lines were obtained, but only the best performing line was subcultured in liquid medium (Figure 64).

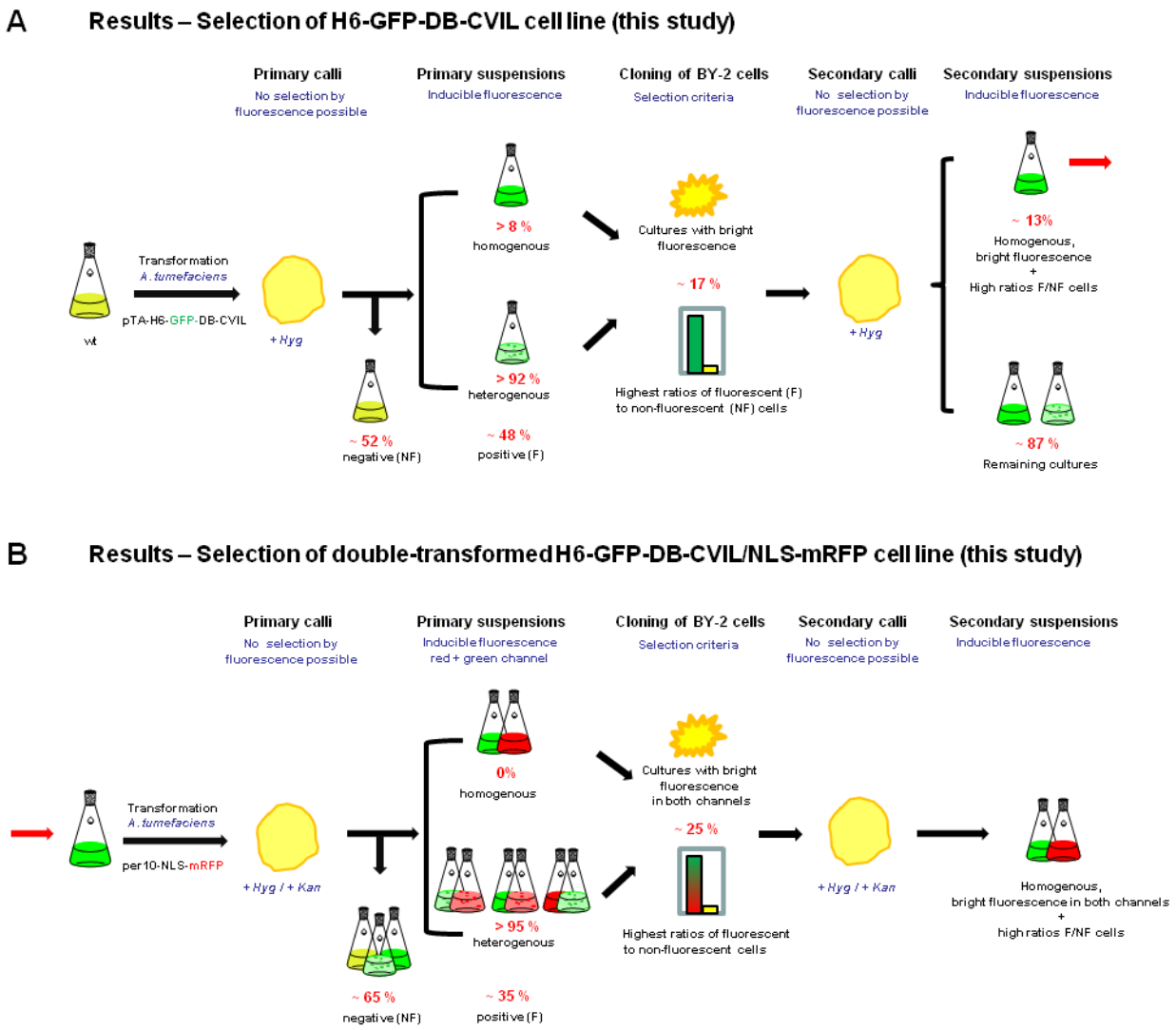

Figure 64. Scheme of the cloning procedure used for the selection of homogenous, transgenic tobacco BY-2 cell lines.

A – Selection of H6-GFP-DB-CVIL cell line. **B** – Selection of the double-transformed H6-GFP-DB-CVIL/NLS-mRFP cell line. The selection of primary and secondary calli was performed on antibiotica-supplemented solid plates. As the expression of both fluorescent reporter proteins was inducible, no pre-selection by fluorescence microscopy could be used to eliminate non-fluorescent calli (it was tried by incubation of the calli in presence of the inducers, but no fluorescence could be detected with this method). The selection criteria for cultures used in the cloning procedure were based on the properties optimal for the bioassay (homogenous, bright fluorescence and high ratios of fluorescent to non-fluorescent cells.). Rounded values for statistical evaluation are indicated if available. F = flourescent; NF = non-fluorescent.

Quite independently, Nocarova and Fischer (2009) developped a very similar strategy to generate secondary calli in order to obtain homogenous cell lines with high ratios and intensities of transgene expression (see Table 10: Comparison of the cloning procedures of transgenic tobacco BY-2 cells.). Although the emphasis of my thesis was not the development of a cloning technique to obtain secondary cell lines, the results ressemble those of Nocarova and Fischer in many ways. Of course, in my case, the purpose of the re-selection process did not include a statistical evaluation of its

efficiency. Even though each plate contained between 25 and 100 calli emerging over a period of 1-2 weeks, only the fastest growing calli were transferred to new plates and were used to start secondary liquid suspension cultures. Liquid cultures were launched by dissociating a small portion of the callus with a sterile spatula in 10 ml of antibiotica-supplemented medium. Afterwards, it took 1-2 weeks before a normal weekly subculturing and screening could begin (see chapter 4.5.5.3). As soon as positive cultures were found, no more calli were screened for obvious reasons, what explains that the statistics obtained during the selection processes in this thesis are not really extensive and therefore not comparable to those obtained by Nocarova and Fischer.

However, in contrast to the reporter system used by Nocarova and Fischer (2009), which is based on a constitutively expressed GFP, the selection of well-performing cultures for both cell lines, the single-transformed H6-GFP-DB-CVIL and the double-transformed SV40-mRFP/GFP-DB-CVIL cell line, was by far more challenging, as the expression of both transgenic fusion proteins was inducible and optimal expression conditions had to be established first.

c) Culture conditions

Other important factors, which play a key role for the successful set-up as well as for the miniaturization of the assay, are changes in growth conditions, such as the inoculum ratio, agitation, aeration and temperature.

Growth conditions for tobacco BY-2 cells, subcultured on a weekly basis in 250 ml erlenmeyer flasks were more or less constant during my thesis: 0,75-2 ml of a 7-day-old, stationary liquid suspension culture were used to inoculate 40 ml of TBY-2 medium supplemented with the required selection markers and the cells were grown in the dark on a rotary shaker at 154 rpm and at 26°C (Hemmerlin et al., 2004; Gerber, 2005; Gerber et al., 2009). Nevertheless, given the various problems with the culture room facilities, conditions were not always as stable as desired. In addition, downscaling the whole test system from commercial 6-well plates to high-tech glass bottom 96 well plates (see chapter 2.2.4.2) made it necessary to re-examine all growth conditions to determine optimal conditions for this smaller format.

For instance, **agitation** of plant culture cells plays an essential role as it provides homogeneity of the culture, in respect to nutrients, enhances mass and heat transfer and reduces at the same time cell clumping and formation of aggregates, a phenomenon often observed in plant cell cultures, due to secretion of extracellular polysaccharides (EPS) for exemple: (Scragg, 1995; Kieran et al., 1997; Abdullah et al., 2005). For example: Insufficient mixing triggers the formation of aggregates and some heterogeneity in oxygen and nutrient supply inside the cell population. Therefore, sub-optimal agitation conditions may also explain the differences in transgene expression levels observed during my thesis (Figure 59).

Aeration of plant suspension cultures is also an important parameter as it leads to desorption of volatile products and removes metabolic heat. Oxygen supply is hence a very critical factor, as excess or lack can both have negative effects. Without going into details, the mass transfer coefficient, $K_L a$ is a function of agitation and aeration at the same time and is part of an equation commonly used to optimize growth conditions in modern bio-reactor systems (Georgiev et al., 2009). Plant cells grow relatively slowly and are known to be particularly sensitive as far as their optimal oxygen supply is concerned. They adapt their metabolism even to minor changes in gas composition. This may result in an alteration of growth characteristics and of production of secondary metabolites (Verpoorte and Memelink, 2002). Under sub-optimal growth conditions, one can easily imagine that an insufficient supply of the prenylation precursor, GGPP and its hydrolyzed product geranylgeraniol (GGol) in some cells could result in the shift to the nucleus of a part of the fluorescent GFP-DB-CVIL protein. This view is supported by the fact that exogenous GGol is able to completely reverse inhibition of the MEP pathway, whereas the control experiments statistically had always a fraction (< 5%) of cells with signals from the nuclei (Figure 12).

Finally, the **temperature** is a major factor for the cultivation of plant cell cultures. Conditions are dependent on the plant species and even for the same species optimal temperatures may vary as far as the synthesis of a distinct metabolite is concerned (Ten Hoopen et al., 2002 ; Georgiev et al., 2004; Georgiev et al., 2009).

Of course, all these parameters have to be adapted to the scale of the system, the cell culture line, the culture conditions and the growth phase. Figure 65 illustrates, for instance, the changes induced in cell growth by the modification of the inoculum size over a small period of time (2 days).

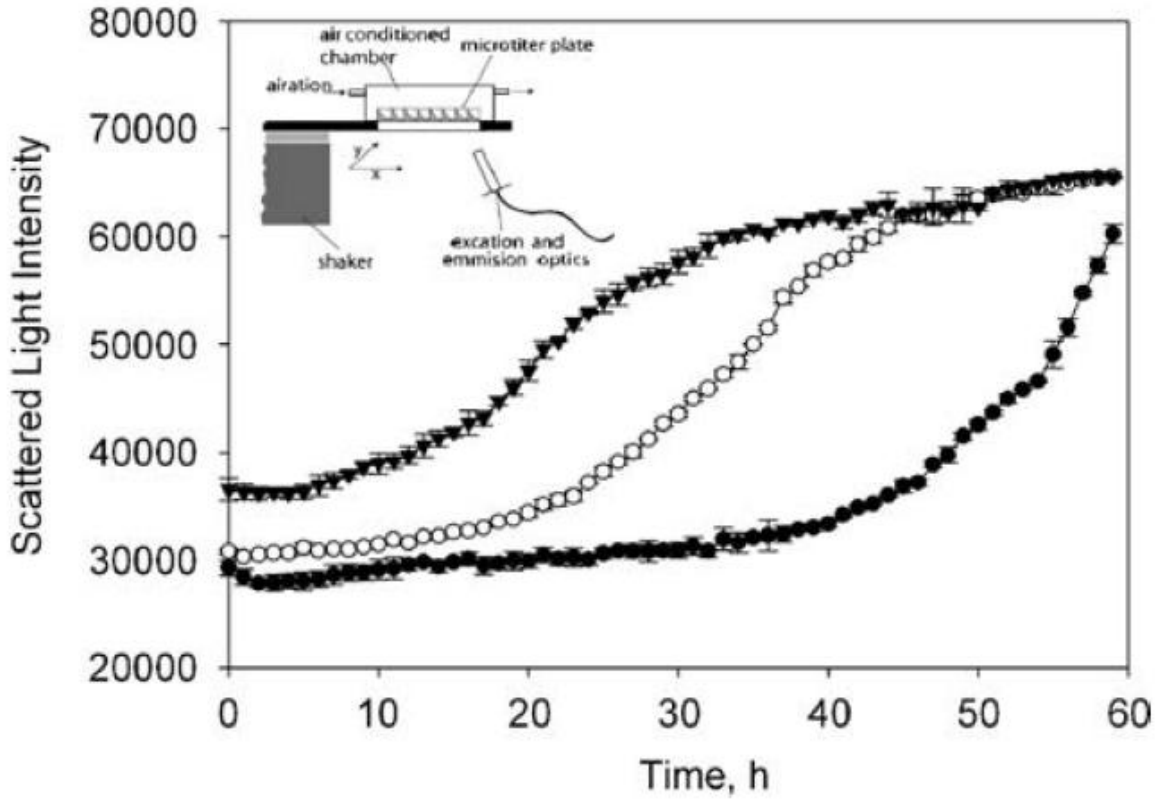

Figure 65. Influence of different fractions of inoculum on the biomass accumulation in multi-well plates (taken from Georgiev et al., 2009)

Cultivation of *Nicotiana tabacum* CV BY2 HAS in the microtiter plate cultivation system BioLector (48 well plate, 26°C, 800 rpm, 3 mm shaking diameter, and 500 µl volume) with different fractions of inoculum: 20% (closed circles), 40% (open circles), and 60% (closed triangles). Please note the differences at the time window used for our test system (18-24 h).

d) Possible improvements:

Shake-flasks have been used in laboratories all over the world to grow small-scale cultures, but, as discussed earlier in this chapter, there are great differences in the expression of reporter proteins/fluorescence due to differences in the culture conditions.

Thus, modern cell culture systems (e.g. bioreactors) are able to monitor multiple parameters during the growth of the cultures and to acquire kinetic data that will help to investigate the effect of these parameters (agitation, aeration, temperature, inoculum ratio, pH etc.) and to find optimal conditions (Buchs, 2001). For modern-day applications (e.g. HTS platforms), different types of bioreactors are available, such as the different models of the so-called "slug bubble reactor" described by Terrier et al. (2007), which can deal with volumes up to 70 L and that was successfully tested for *Nicotiana tabacum* cell suspension cultures.

Of course, purchasing an out-of-scale bioreactor for our studies would not make sense, but fortunately the same concept is nowadays also available for small scale cultures (Anderlei et al., 2004; Samorski et al., 2005).

Cultures growing in shaking flasks, for example, can be monitored by the "respiration activity monitoring system" (RAMOS, HiTec Zang GMBH, Herzogenrath, Germany and Kühner, Birsfelden, Switzerland), which continously measures the oxygen transfer rate (OTR) and the carbon dioxide transfer rate (Anderlei et al., 2004).

On a smaller scale, the BioLector (commercialized by mp2-labs, Aachen, Germany) is an example of a culture system in a microtitration plate (MTP) that is able to carry out cell growth and fluorescence measurements under defined conditions of shaking (Samorski et al., 2005).

3 Conclusion and Perspectives

Isoprenoids, also referred to as terpenoids, represent the largest class of plant natural products and are implicated in nearly all the fundamental processes of plant growth, development and secondary metabolism, including isoprenylation of proteins. Higher plants synthesize their isoprenoids through two different routes, the cytosolic mevalonic acid (MVA) pathway and the plastidial 2-C-methyl-D-erythritol 4-phosphate (MEP) pathway. By contrast, the malaria parasite *Plasmodium falciparum*, as well as many pathogenic bacteria rely exclusively on the MEP pathway for the synthesis of their isoprenoids. As this pathway does not occur in mammals, it represents an attractive target for the design of antibiotics, antimalarial drugs and bleaching herbicides. Given the long periods necessary for the development and commercialization of new drugs, the fast rise of drug-resistance in pathogenic microbia and weeds poses a serious threat to human health and underlines the urgency to explore new ways for rapid identification of novel anti-infective and herbicidal compounds.

Isoprenylation of proteins, which has been recognized as a fundamental process in all eukaryotes, consists in the formation of a chemically stable thioether bond between a cysteine residue belonging to a carboxyterminal CaaX motif of a protein and a C_{15} (farnesyl) or a C_{20} (geranylgeranyl) isoprenyl chain. In the laboratory, an experimental system to visualize isoprenylation of proteins in living tobacco BY-2 (TBY-2) cells was available. This test system was based on a stably transformed TBY-2 cell line, expressing a dexamethasone-inducible GFP fused to the prenylable, C-terminal basic domain of the rice calmodulin CaM61, which naturally bears a CaaL geranylgeranylation motif. After induction, the resulting fusion protein (GFP-DB-CVIL) was predominantly targeted to the plasma membrane (PM).

The use of pathway-specific inhibitors of both isoprenoid biosynthetic pathways revealed that inhibition of the MEP pathway (by oxoclomazone OC and fosmidomycin Fos) as well as inhibition of the geranylgeranyltransferase type 1 (PGGT-1) shifted the localization of the GFP-BD-CVIL protein from the PM to the nucleus/nucleolus. By contrast, inhibition of the MVA pathway (by mevinolin) or protein farnesyltransferases did not affect the localization of the chimeric fusion protein. Chemical complementation assays with pathway-specific intermediates and isoprenols further confirmed that the MEP pathway mainly provided the isoprenoid precursors for the prenylation of the fusion protein (Gerber, 2005).

However, at the end of this previous study, different questions remained unsolved such as the chemical nature of the prenyl moiety of the GFP fusion protein and whether the effects that were observed after inhibition of the MEP pathway could be observed with other drugs interfering with this pathway.

The three major parts of the present work are the following:

I- Biological assay development (Figure 66)

II- Optimization of the assay to fit the requirements of image-based drug screening (Figure 67)

III- Image acquisition and analysis (Figure 68)

To address the above issues as well as to optimize this visualization system from a qualitative assay to a statistically trustable screening system, I generated a stably transformed cell line expressing a His-tagged version of the GFP-DB-CVIL fusion protein. In contrast to the initial GFP-DB-CVIL line, which consisted of a population of clones obtained without a selection step on solid medium, the new cell line was obtained after a simple cloning procedure.

In a first step, this new cell line was used in our laboratory to purify and analyze the tobacco prenylated GFP fusion protein, thereby demonstrating that it was strictly geranylgeranylated and carboxylmethylated *in vivo*.

Before extending our studies with this cell line, all major experiments with inhibitors of both isoprenoid biosynthetic pathways as well as the chemical complementation assays were repeated and the results confirmed the general observations made by Esther Gerber. Interestingly, during the course of this work, I could show that exogenous DX was able to reverse the inhibition induced by OC, but not that of DXR induced by Fos. It has also been demonstrated that addition of 5 µM GGol could overcome only inhibition effects triggered by both OC and Fos, but not those induced by inhibition of geranylgeranyltransferase PGGT-1. As a result, the chemical complementation with DX and GGol provided us with an elegant method to discriminate different inhibitor-induced effects.

In order to determine the impact of MVA derived prenyldiphosphates on the localization of the H6-GFP-DB-CVIL fusion protein, we tried to modulate the pool of endogenously available FPP by blocking several early steps of sterol biosynthesis including squalene synthase (by squalestatin SQ), squalene epoxidase and oxidosqualene cyclase. The corresponding inhibitors used were respectively squalestatin (SQ), Terbinafine (Tb) and Ro 48-8071 (Ro). Among these inhibitors, only SQ was shown to trigger a partial mislocalization of the fusion protein H6-GFP-DB-CVIL to the nucleus, an effect that was completely overcome by addition of DX or GGol, but not by squalene, suggesting some sensitivity of the protein prenyltransferase (implicated in the prenylation of the H6-GFP-DB-CVIL) to SQ. Clearly, further experiments will have to be conducted to confirm this assumption.

In this work, the bioassay was used for the first time to test novel drug candidates that were specifically designed on the basis of known inhibitors of DXS and DXR, the two first enzymes of the

MEP pathway. Whereas the DXS inhibitors tested so far were shown to be inefficient, all the members of Fos-derived prodrugs were able to shift the H6-GFP-DB-CVIL from the PM to the nucleus.
In order to prove that the present bioassay was not only able to serve as a qualitative approach for the identification of new drug candidates, but also as a statistical tool to compare performances of a drug candidate with other known inhibitors *in vivo*, I performed a quantitative analysis of the intracellular distribution of H6-GFP-DB-CVIL in response to different concentrations of the prodrugs. This was done by determining the ratios of inhibited to non-inhibited cells at a given concentration for six Fos-derived prodrugs. Interestingly, the best performing prodrugs in the bioassay with TBY-2 cells showed the same order of efficiency when tested on *Mycobacterium smegmatis* cells, suggesting that knowledge gained from plant cells might be transferred to other organisms. Nevertheless, keeping the potential of MEP pathway inhibitors as herbicides in mind, these results are very promising and set the course for the development of a chemical drug screen, with both biomedical and agricultural applications.

A major purpose of my thesis was to demonstrate the feasibility of establishing a medium to high-throughput compound screen on the basis of the initial protein prenylation assay. To address this issue, a systematic step-by-step protocol was developed, and each key-step for the development of a chemical drug screen was individually considered and if possible directly applied.
Clearly, the prerequisite for such a test system was the presence of a homogenous and highly fluorescent cell line, displaying high ratios of fluorescent to non-fluorescent cells. This cell line was obtained after a rigorous clonal selection process and successfully used to demonstrate the reproducibility of effects on single cells with a whole population of cells. An essential aspect and one of the novel contributions of this work was therefore the acquisition of images at low magnification, showing groups and sub-populations of cells. The advantage of such an approach is the fact that an image can be stored and used to give the relevant biological information that might just be overseen or misinterpreted by a microscope user at a given moment. With the software ImageJ, I could thus show that it was possible to detect and quantify cells displaying a mislocalization of the fusion protein by a rather simple image analysis approach, using the nucleus as a reference point.
One major challenge was, however, the detection of untreated cells, due to the fact that BY-2 cells are very diverse in shapes and sizes and grow in files of different sizes. In addition, because they are growing in a liquid medium, it is nearly impossible to avoid superimposed cells, whatever the dilution. This is clearly an unsolvable obstacle for image analysis softwares tested so far and even specific plug-ins for the detection of cellular features are adapted to more simple model systems such as bacterial, yeast or tissue cells. Perhaps a custom made algorithm might cope with this problem and resolve it, but this would need a bio-informatician working on this for a significant amount of time and many follow-up experiments would have to be performed. A possible solution to the problem of cell

shape heterogeneity might be the generation of protoplasts and their analysis by flux cytometry, but the necessary digestion of the cell wall would probably trigger stress responses biasing the observations.

Because of the unavailability of a suitable nuclear stain allowing counting of cells, I decided to generate a double-fluorescent cell line expressing a nuclear-targeted mRFP (NLS-mRFP) under the control of an estradiol-inducible promotor. With this cell line, I could demonstrate that there was no cross-induction of the GFP and mRFP expression by estradiol or dexamethasone and establish a time-scale for the estradiol-induced gene expression, which was of great importance for other approaches used in our laboratory such as the silencing of *DXR* and *CAS* genes in TBY-2 cells by an artificial micro-RNA-mediated strategy. The use of the nuclear-targeted, bright fluorescent mRFP allowed identifying and counting untreated cells at different magnifications and even in complex scenarios with superimposed cells.

In a next step, the whole initial bioassay was downscaled and adapted for the use of 96-well plates with a glass bottom. The first results as images obtained with the 96 well plates were very encouraging and a first proof of concept for the use of this high-density format with plant suspension cells in a fluorescence microscopic approach was achieved. As a first measure to improve the growth and imaging conditions, multi-well plates with square surfaces (microarray plates) were purchased. The square surface promises better aeration of the cultures and maximizes the surface for image acquisition. Of course, different parameters still have to be adapted, such as the optimal scanning speed and image acquisition settings to guarantee a satisfying throughput rate and exploitable data.
The automatization of the assay implies combination of automatic focusing routines, automatic stage movement and automatic imaging. Fortunately, basic software solutions for this kind of applications exist and first tests showed that the three processes can be handled. Of course, the automatic focusing remains the most critical point, as the cells will sediment after a certain period of time in the well.
The present work clearly demonstrated that an integrated approach using 96 well plates and automatic image acquisition and analysis will allow the use of the bioassay as a screening system for inhibitors of the MEP pathway and protein geranylgeranyltransferases. In addition, it will be possible to monitor potential toxic effects triggered by an inhibitor treatment. The use of different stains (cell-death and viability stains) should be of great interest in this context.

The availability of this bioassay will be of great use to address open questions and for many applications in agriculture and medicine. For instance, one can imagine applying this test to the search of compounds that interfere with the bio-activation of clomazone, which is P450-mediated or more generally the search of new herbicides. To elucidate mechanisms underlying the intracellular transport

of prenylated protein in TBY-2 cells is also an interesting topic. According to Esther Gerber (2005), the classical secretory pathway appeared not to be involved as a transit route of the GFP-DB-CVIL to the PM of TBY-2 cells. Interestingly, human KRAS4B shares several features with the GFP-DB-CVIL fusion protein (*e.g.* the polybasic domain and the CaaX-motif) but how both proteins are transported to the PM remains largely unknown. The use of the bioassay in combination with inhibitors of CaaX-processing and compounds interfering with the membrane anchorage of H6-GFP-DB-CVIL might be a promising strategy to investigate this aspect.

The bioassay can also be very useful to screen unknown chemical compounds. By testing unknown inhibitors provided by Dr. Bernard Weniger (data not shown), I made an interesting observation. Whereas none of the compounds was efficiently inducing a mislocalization of the fusion protein to the nucleus, several treatments triggered toxic effects. One compound in particular displayed an unusual phenotype, with barely detectable signals from the PM and nucleus; instead, the GFP fluorescence seemed to be trapped in the cytoplasm. Interestingly, this compound was identified as a prenylated anthracenoid, isolated from the stem bark of an african tree, and shown to have the highest activity in tests against leishmania, further validating the experimental system as a tool to detect cytotoxic effects. This could somehow indicate that the transport of H6-GFP-DB-CVIL might be mediated by protein-protein interactions, which are impaired by the prenylated compound. Several, prenyl-binding proteins are known, such as Rho-GDI or the delta-subunit of phosphodiesterase in animals, and similar proteins might be candidates for the transport of H6-GFP-DB-CVIL from the ER to its final cellular destination. The identification of possible interaction partners of H6-GFP-DB-CVIL as well as of compounds that interfere with its transport could therefore be of great interest to develop anti-oncogenic strategies.

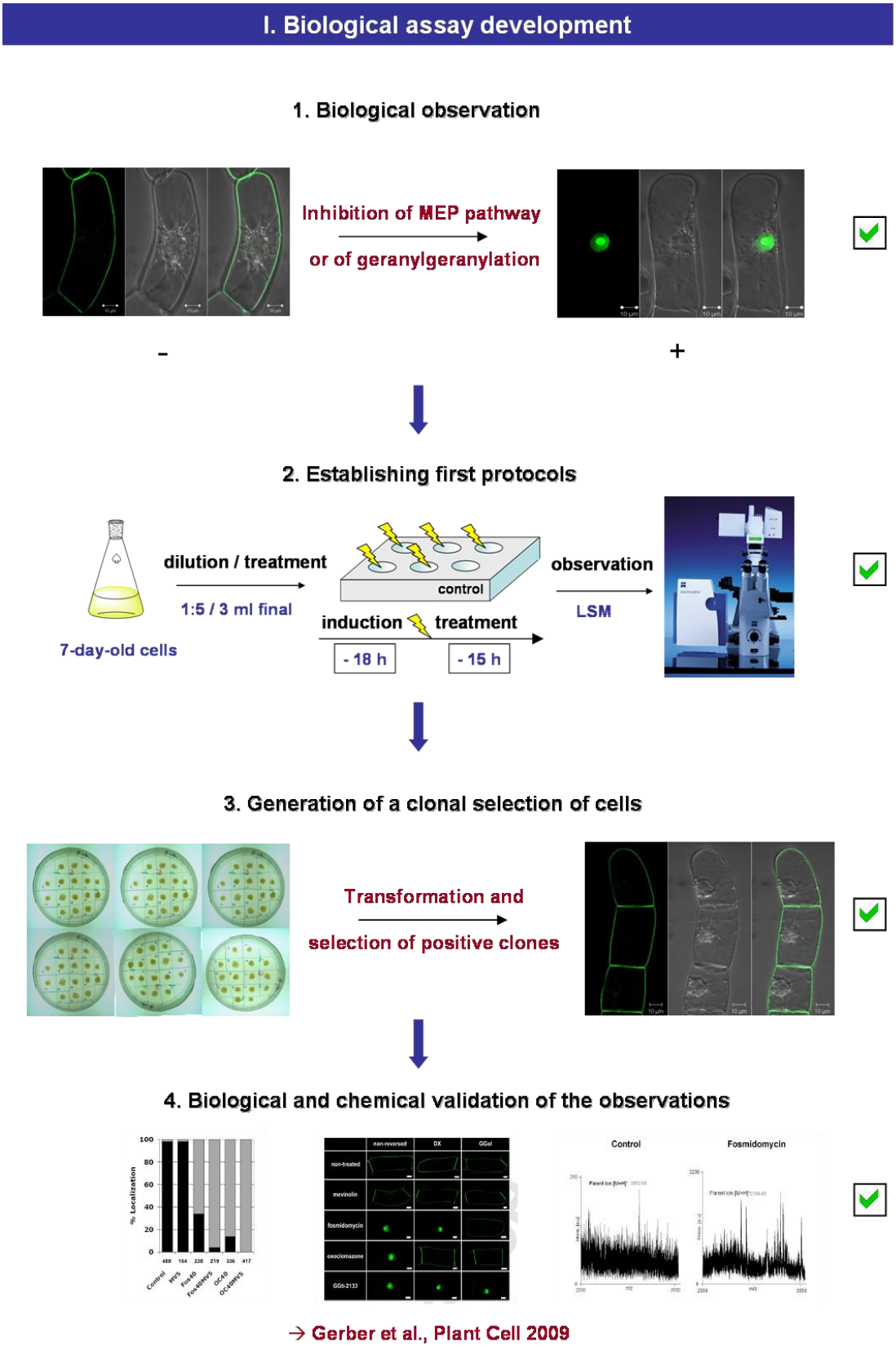

Figure 66. Biological assay development

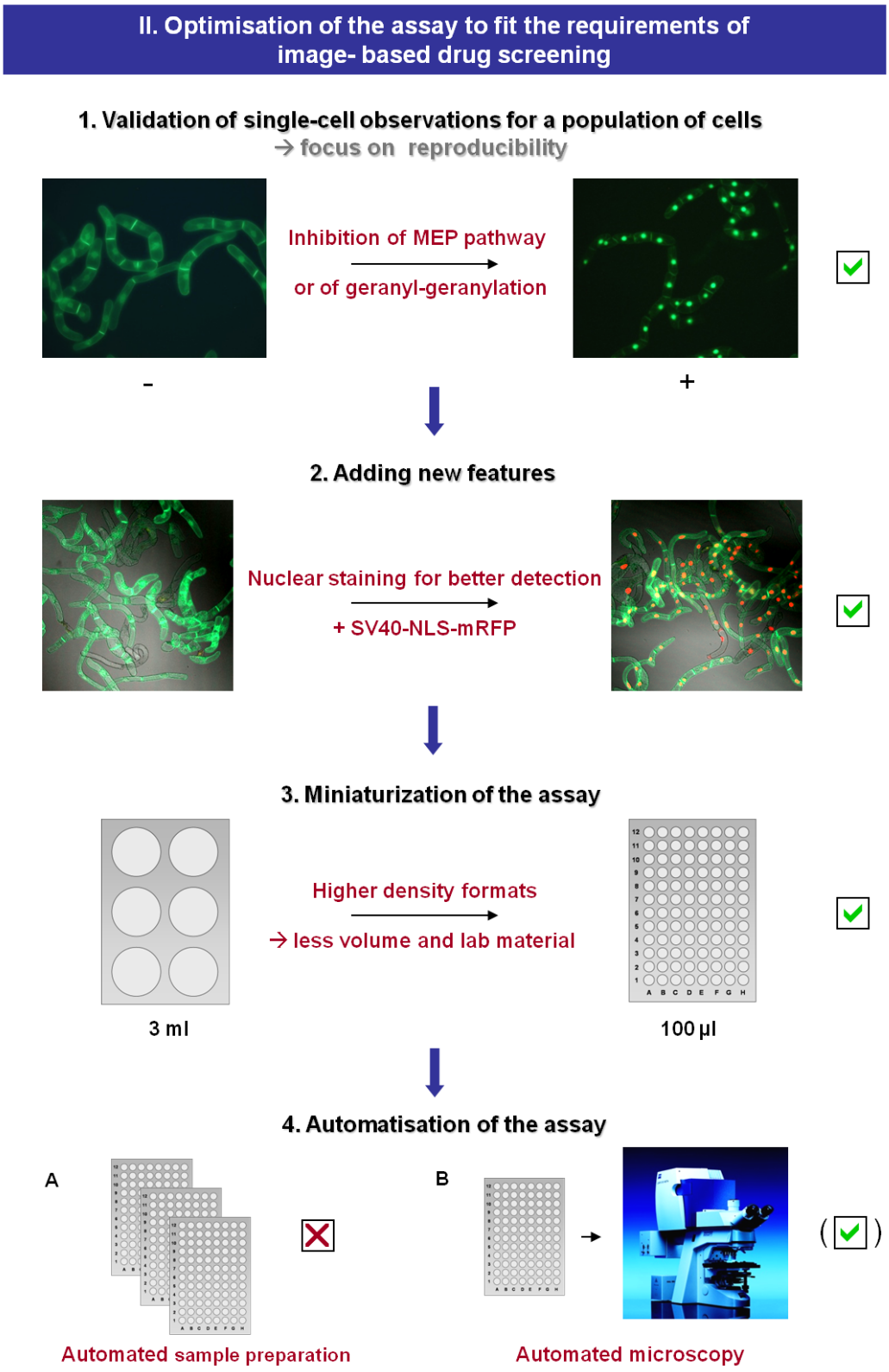

Figure 67. Optimization of the assay

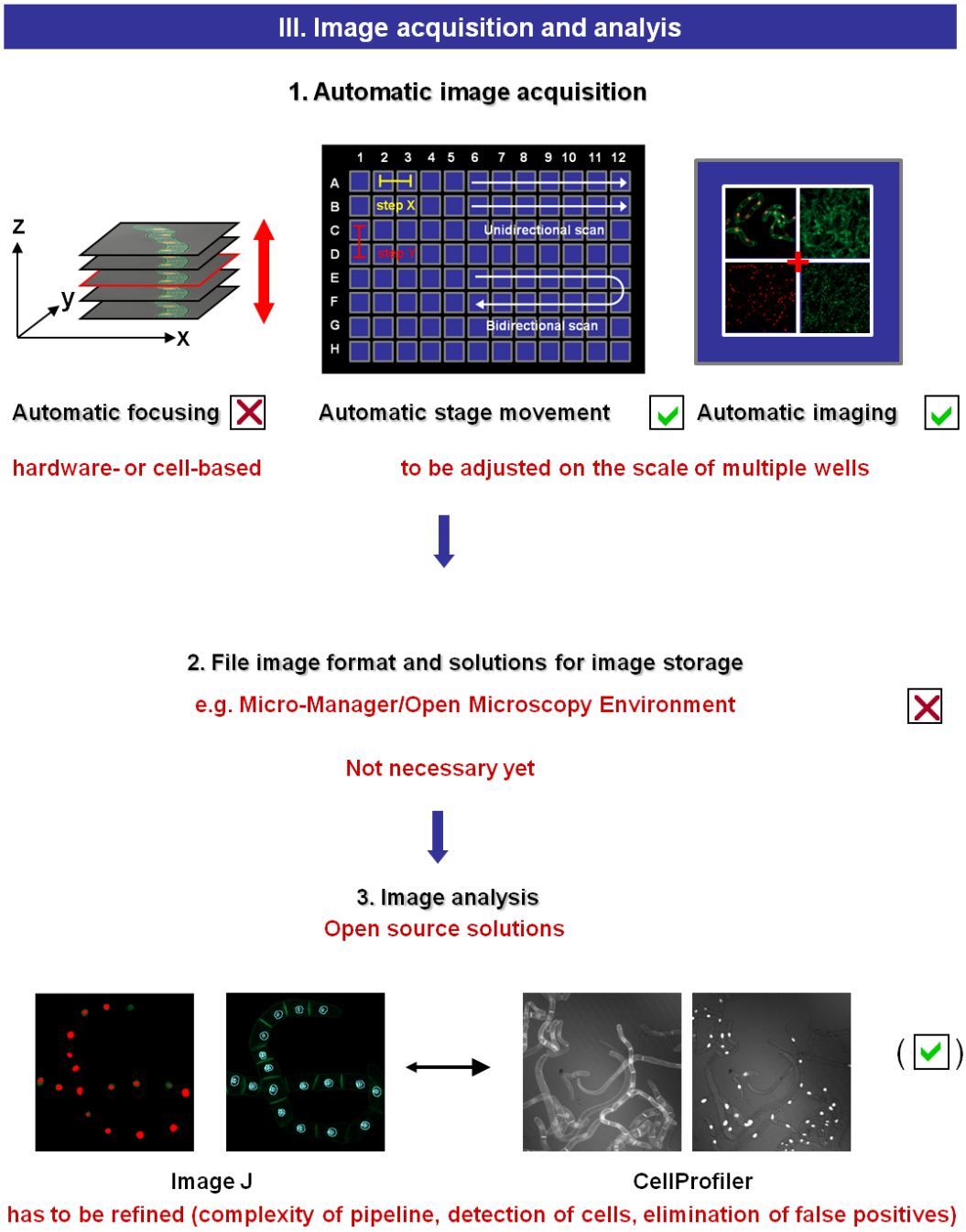

Figure 68. Image acquisition and analysis

4 Material and Methods

4.1 Instruments and software

4.1.1 Instruments

Instrument	Application	Brand
10 ml	Pipetting aid for up to ~30 ml	Drummond Scientific Co.
-20°C	Incubation and storage of samples at -20 – -25°C	Liebherr
Automatic TLC analyser	radioactice counter for TLC plates	Berthold
Bio-Photometer	Concentration measurement of RNA/DNA	Eppendorf
BK 15 with rotor Nr. 11133	cooled table-top centrifuge for Falcon tubes (50 ml)	Sigma
C10 platform shaker	agitation of TBY-2 cell cultures	New Brunswick Scientific
Capacitance Extender PLUS	Electroporation unit	Bio-RAD
Chemical hood	Chemical hood for general laboratory purposes	custom made
Cold room	Climatised room (4°C)	Eurovent
Acquisition Scanner GS800	Scanner for the acquisition of 2-D-Protein Gels	Bio-Rad
DXM1200	Epifluorescence Microscopy	Nikon
Fridge	Incubation and storage of samples at 4°C	Liebherr
Chemi-Smart 3000	Imaging of EtBr-stained agarose gels/ and fluorescent protein gels	Fisher BioBlock Scientific
Gene Pulser r II	Electroporation unit (transformation of Bacteria)	Bio-RAD
GFL 1803	Waterbath for incubations with integrated shaker platform	GFL
Heating plate	heating of liquids with integrated magnetic stearer	Fisher BioBlock Scientific
IFF 125 C ice machine	production of ice flakes	TOTALINE
Incubator	37°C incubator with shaking platform for growing liquid bacterial cultures	EHRET
Incubator	28°C incubator for growing agrobacterial colonies/TBY2 cultures on agar plates	Memmert
LaminAir HVR 2448	Laminar flow hood for culturing plant cells	Holten
LSM	Confocal Microscopy	Zeiss
Mastercycler Personal	Thermocycler for PCR amplification	Eppendorf
Microcol TDC80	Automated sample collector (Liquid chromatography)	GILSON
Minipuls 2	rotating pump for liquid chromatigraphy	GILSON
Mini-Spin	Table-top centrifuge for Eppendorf tubes	Eppendorf
Pipetman	Pipettes for handling volumes between 0.10 – 1000 µl	Eppendorf/Gilson
Plate reader	photometric analysis of samples	?
Polystat	Waterbath for incubations between RT and 95°C	Fisher BioBlock Scientific
PowerPac 200	Power supply for electrophoresis	Bio-Rad
Precisa 240 A	precision balance	Precisa
Protean 2/3	Chamber for separating protein samples by SDS-PAGE	Bio-Rad
Pulse Controller Plus	Electroporation unit	Bio-RAD
Scout II	analytical balance	OHAUS
Sprint	hplc machine	
Table centrifuge	Cooled table-top centrifuge for Eppendorf tubes	Eppendorf
Tri-Carb 2100 TR	Liquid scintillation analyser	PACKARD

Instrument	Application	Brand
Ultra Low - VIP Series	Incubation and storage of samples at -80°C	Sanyo
Vortex	vortex mixer	VEIP Scientific
WIDE MINI SUB CELL GT	Chamber for separating nucleic acids by agarose gel electrophoresis	Bio-Rad

Table 11: Overview of the instruments used in this study

4.1.2 Software, algorithms and databases

4.1.2.1 Software

Software	Version	Application	Developper
Adobe Photoshop	8.0	Program for editing graphics and images	Adobe Systems, San Jose (USA)
BioEdit	7.0.9	*In silico* manipulation and investigation of DNA and protein sequences	Tom Hall, Isis Biosciences, Carlsbad, CA (USA)
Biology Workbench	3.2	*In silico* manipulation and investigation of DNA and protein sequences	SDSC, San Diego (USA)
Endnote	9.0	Tool for managing bibliographic data	Thomson ISI Researchsoft, New York (USA)
Image J software	1.31	Program for editing graphics and images	Wayne Rasband, NIH (USA)
LSM Image Browser	4.2.0.121	Acquiring, analysing and processing of confocal images	Carl Zeiss AG, Jena (Germany)
Microsoft Office	2002	software package aiding in data analysis and supporting administrative work	Microsoft Corporation, Redmond (USA)
Nikon ACT-1	2.70	Acquiring and processing of pictures captured with the Nikon DXM1200 camera	Nikon Corporation, Tokyo (Japan)
Vector NTI	9.0	*In silico* manipulation and investigation of DNA and protein sequences	Invitrogen, Karlsruhe (Germany)

Table 12: List of all software packages and programs relevant to this study

4.1.2.2 Algorithms

Algorithm	Application	URL (*28.02.2011)	Reference/Developper
BioMath Calculators	T_m Calculations for Oligos	http://www.promega.com/biomath/calc11.htm	na.
BLAST at NCBI	**B**asic **L**ocal **A**lignment **S**earch **T**ool:collection of tools which allow to search nucleotide and protein databases of various organisms with different types of querys	http://blast.ncbi.nlm.nih.gov/Blast.cgi	Altschul et al. (1990)
Clustal W	ClustalW2 is a general purpose multiple sequence alignment program for DNA or proteins	http://www.ebi.ac.uk/clustalw2/index.html	Larkin et al. (2007), Higgins et al. (1994)
Clustal X	Clustal X is a windows interface for the ClustalW multiple sequence alignment program	http://www.clustal.org/	Larkin et al. (2007), Higgins et al. (1994)
Compute pI/MW	tool which allows the computation of the theoretical pI (isoelectric point) and Mw (molecular weight) for user entered sequences	http://www.expasy.org/tools/pi_tool.html	Gasteiger et al.(2003)
PrePS	Prenylation Prediction Suite	http://mendel.imp.ac.at/sat/PrePS/index.html	Maurer-Stroh and Eisenhaber (2005)
Prosite Motif Scan	Tool to scan an amino-acid sequence against PROSITE patterns and profiles	http://www.expasy.org/tools/scanprosite	Sigrist et al.(2002)
ProtScale	ProtScale allows you to compute and represent the profile produced by any amino acid scale on a selected protein – here: hydrophobicity/hydrophilicity scales	http://www.expasy.ch/tools/protscale.html	Kyte and Doolittle (1982)
Psort	Tool for protein subcellular localization prediction	http://psort.ims.u-tokyo.ac.jp/	Nakai and Kanehisa (1991)
Tmpred	program that makes a prediction of membrane-spanning regions and their orientation	http://www.ch.embnet.org/software/TMPRED_form.html	Hofmann and Stoffel (1993)
Translate tool	tool which allows the translation of a nucleotide (DNA/RNA) sequence to a protein sequence	http://www.expasy.org/tools/dna.html	Gasteiger et al. (2003)
WoLF PSORT	Tool for Protein Subcellular Localization Prediction	http://wolfpsort.org/	Horton et al. (2007)

Table 13: List of all algorithms relevant to this study

4.1.2.3 Databases

Database	Purpose	URL
Pfam	The Pfam database is a large collection of protein families, each represented by multiple sequence alignments and hidden Markov models (HMMs).	http://pfam.sanger.ac.uk/
Prosite	PROSITE consists of documentation entries describing protein domains, families and functional sites as well as associated patterns and profiles to identify them	http://www.expasy.org/prosite/
Swiss-Prot Protein knowledgebase	a curated protein sequence database which strives to provide a high level of annotation, a minimal level of redundancy and high level of integration with other databases	http://www.expasy.org/sprot/
NCBI Entrez	NCBI creates public databases, conducts research in computational biology, develops software tools for analyzing genome data, and disseminates biomedical information	http://www.ncbi.nlm.nih.gov/
TAIR (The Arabidopsis Information Resource)	The Arabidopsis Information Resource (TAIR) maintains a database of genetic and molecular biology data for the model higher plant *Arabidopsis thaliana*	http://www.arabidopsis.org/
TIGR	Collection of ESTs (expressed sequence tags) from a big variety of organisms - All plant species for which more than 1,000 ESTs or cDNA sequences are available and are included in this project	http://plantta.jcvi.org/index.shtml

Table 14: List of all databases relevant to this study

4.2 Enzymes, chemicals and consumable materials

4.2.1 Enzymes and Molecular Biology Kits

Enzymes and Molecular Biology Kits	Application	Supplier
5'-RACE System for Rapid Amplification of cDNA	Amplification of 5' - ends of mRNAs	GIBCO BRL - Division of Invitrogen Corporation (USA)
Dnase I (RNase-free)	RNA extraction protocol	Fermentas Corporation (Germany)
GeneRACER™ - Kit	RNA ligase-mediated rapid amplification of 5´ and 3´ cDNA ends (RLM-RACE)	Invitrogen Corporation (USA)
Go Taq Polymerase	Conventional PCR	Promega (USA)
NucleoBond® PC 100	Anion exchange columns for quick purification of nucleic acids	MACHEREY-NAGEL (Germany)
NucleoSpin® Extract II	PCR clean-up and gel extraction kit	MACHEREY-NAGEL (Germany)

NucleoSpin® Plasmid Quick Pure	Purification of highly pure plasmid DNA from bacterial cultures	MACHEREY-NAGEL (Germany)
Phusion Polymerase	High-Fidelity DNA Polymerase	Finnzymes (Sweden)
RNase-free Dnase Set	RNA extraction protocol	QIAGEN (The Netherlands)
RNasin RNase Inhibitor	inhibits RNase activity	Promega (USA)
Superscript™ III Reverse Transcriptase	system for the generation of first strand cDNA from mRNA	Invitrogen Corporation (USA)
T4 DNA ligase	Cloning /Construction of plasmids	Fermentas Corporation (Germany)
Taq Polymerase	Conventional PCR	Invitrogen Corporation (USA)
Terminal Deoxynucleotidyl Transferase - TdT (500 U)	TdT catalyzes the addition of nucleotides to the 3' terminus of a DNA molecule - used in RACE PCR	Fermentas Corporation (Germany)

Table 15: List of all the molecular biology kits and enzymes relevant to this study

Restriction endonucleases	T_m max activity (°C)	Buffer	Supplier
BamHI	37	REact 3	Gibco BRL
ClaI	37	REact 1 Buffer B+	Invitrogen Fermentas
EcoRI	37	REact 3	Gibco BRL
HindIII	37	REact 2	New England BioLabs
KpnI	37	NEBuffer 1 + 0.01% (w/v) BSA	New England BioLabs
NheI	37	REact 4	Invitrogen Fermentas
PvuII	37	REact 6	Gibco BRL
XbaI	37	REact 2	Gibco BRL
XhoI	37	REact 2	Gibco BRL

Table 16: List of all restriction endonucleases used in this study

4.2.2 Chemicals

If not indicated otherwise chemicals used during this thesis were provided by Sigma-Aldrich or Fluka.

4.2.3 Consumable Materials

DNA-Größenstandard:	New England Biolabs, Beverly
2-log DNA Ladder	(USA)
1 kb DNA Ladder	
Eppendorfgefäße Ambra	Eppendorf, Hamburg
Protein-Größenstandard Mark12™	Invitrogen, Karlsruhe
Prestained Protein Marker,	New England Biolabs, Beverly
Broad Range (6-175 kDa)	(USA)
QIAEX II Gel Extraction Kit	Qiagen, Hilden
QIAprep Spin Miniprep Kit	Qiagen, Hilden
Roti®-Quant Bradford-Reagenz	Roth, Karlsruhe

4.3 Living Material

4.3.1 Plant material

4.3.1.1 Tobacco cells

The tobacco *Nicotiana tabacum* L. Cv. Bright Yellow-2 (TBY-2) cell line used in this work was provided by Professor Toshiyuki Nagata (University of Tokyo, Japan). It was initially isolated by Kato et al. (1972) and is derived from calli induced from young plants (Nagata et al., 1992).
The cell suspension was maintained by subculturing the 7 days old cells (in stationary phase) as described in chapter 4.5.5.1.

4.3.1.2 *Arabidopsis thaliana*

Arabidopsis thaliana has over the years been established as a model plant for the study of the molecular biology and biochemistry of higher plants, which is due to its small genome size, mutant availability, a short generation cycle, and a size that allows growing many plants in parallel. In addition, sequencing of the *Arabidopsis* genome has been completed in the year 2000 (Arabidopsis Genome Initiative) and **T**he **A**rabidopsis **I**nformation **R**esource (TAIR) maintains a database of genetic and molecular biology data for this plant including the complete genome sequence along with gene structure, gene product information, metabolism, gene expression, DNA and seed stocks, genome maps, genetic and physical markers, publications, and information about the Arabidopsis research

community (source: http://www.arabidopsis.org/). Finally different approaches such as global analysis of transcripts or proteomic mapping are undertaken (Initiative, 2000; Bevan, 2002; Baerenfaller et al., 2008).

The cultivars used in the here described experiments were exclusively *Arabidopsis thaliana (L.) cv Columbia.*

Grains were sterilised by treating them with 1 ml of 70% ethanol containing 0,2% Twen and then washing them twice in 100% Ethanol before sowing them under sterile conditions on solid Murashige and Skoog medium (8 g/L Agar) supplemented with Sucrose at 2% and vitamines. The plates were wrapped with breathing tape (Urgopore) and put for 48 h at 4°C in the dark to allow stratification before exposing them to light in order to induce germination. The plants were grown under constant humidity and light conditions (long-day conditions after germination: 10 h light/21 °C) until they were harvested or used in experiments.

4.3.2 Bacteria

4.3.2.1 *Escherichia coli*

The *Escherichia coli* strain XL1-Blue was the standard strain used to amplify plasmid DNA in bacteria. Its properties allow blue-white colour screening for recombinant plasmids. The XL1-Blue genotype is as follows: *recA1, endA1, gyrA96, thi-1, hsdR17, supE44, relA1, lac* [F´ *proAB,lacI*^{q}*ΔM15,Tn10 (tet*^{r}*)*]. (Genes listed signify mutant alleles. Genes on the F´ episome, however, are wild type unless indicated otherwise).

Under normal conditions *E.coli* cells were grown at 37°C on Luria-Bertani cell medium (Table 17) supplemented with the suitable antibiotics. The XL1-Blue strain is tetracycline resistant and was used for preparation of chemical competent cells (4.5.2).

Luria Bertani medium for bacteria:	
Bacto-Tryptone	1%
Yeast Extract	0,50%
NaCl	1%
Pastagar B (1,5%)	1,50%
Adjust pH to 7 with NaOH; autoclave 20 min at 1 bar	

Table 17: Composition of the culture medium used for *Escherichia coli*

4.3.2.2 *Agrobacterium tumefaciens*

Agrobacterium tumefaciens is a phytopathogenic bacterium found in soils responsible for the so called Crown Gall disease in over 140 species of dicotyledonous plants, which is characterized by the formation of tumours. During infection by A. *tumefaciens*, a segment of DNA, the so called T-DNA (transferred DNA) which is flanked by short cis-acting elements (LB = left border; RB = right border) is transferred from the bacterium into the nuclear genome of the plant cell, a process which is exploited nowadays to efficiently transform plant cells with a desired gene (Zupan and Zambryski, 1995). Agrobacterium tumefaciens-mediated gene transfer is dependent on the expression products of the *vir* genes which normally reside within the borders of the T-DNA on the ti-Plasmid (tumor-inducing). But this two main components needed for succesful T-DNA transfer can also be located on different plasmids, which is the basis of "binary vector systems" (Hellens et al., 2000).

The LBA4404 strain used in this study (LBA4404.pBBR1MCS-5.virGN54D) disposes of a constitutive *virG* mutant gene on a compatible third plasmid – pAL4404 (ternary plasmid - which increases transformation frequencies and T-DNA transfer of a range of plant species compared to binary vector systems (Van der Fits et al., 2000). This strain was used to mediate transformation of tobacco BY2 cells (chapter 4.5.5.2).

The bacteria were grown on "yeast extract broth" (YEB) medium (Van Larebeke et al., 1974) (Table 18) at 25°C. The solid or liquid medium was supplemented with the suitable antibiotics: Rifampicin 20µg/ml (chromosomal marker) and gentamycin 40 µg/ml (Ti plasmid marker).

Yeast Extract Broth (YEB) medium:	
Gibco-beef extract	0,5 % (w/v)
Bacto-yeast extract	0,1 % (w/v)
Bacto-peptone	0,5 % (w/v)
Sucrose	0,5 % (w/v)
$MgSO_4$	0,048 % (w/v)
Adjust pH to 7,4 with NaOH; autoclave 20 min at 1 bar	

Table 18: Composition of the culture medium used for *Agrobacterium tumefaciens*

4.3.3 Antibiotics

Depending on the nature of the transformation experiment, plant and bacterial media were supplemented with one or more antibiotics (Table 19) to facilitate the selection of positive clones:

Antibiotics Abbreviation	Molecular Mass [g/Mol]	Solvant	Stock solution [mg/ml]	Storage conditions	Final Concentration [µg/ml]
Carbenicillin Carb	422,4 (disodium)	H_2O	500	- 20°C	500
Hygromycine B Hyg	527,5	H_2O	50	4°C	30
Ampicillin Amp	371,4 (sodium)	H_2O	100	-20°C	100
Kanamycin Kan	582,6 (sulfate)	H_2O	30	-20°C	30
Tetracycline Tet	444,4	EtOH	12,5	-20°C	12,5
Gentamycin Gen	477,6	H_2O	40	-20°C	40
Spectinomycin Spec	495,3 (di-hydrochloride)	H_2O	20	-20°C	20 (15)

Table 19: Antibiotics used to prepare selective culture media for plants and bacteria

4.4 Biochemical Methods

4.4.1 Protein extraction for BY-2 proteomics

Before starting the extraction, the BY-2 cells were collected in 2 ml Eppendorf or falcon tubes - depending on the volume of the assay – and were spinned down in a centrifuge using maximum speed. Directly after discarding the supernatant, the resulting pellet was frozen in liquid nitrogen. If the material was used for 2-D-gel electrophoresis, it was optionally washed several times in 1xPBS buffer before collecting the cells by filtration under vacuum (using glass fiber büchner with a porosity of 4).

Frozen material then was ground to a fine powder in a ball mill (Mikro-dismembranator S, B.Braun Biotech international, Melsungen Germany) at 3000 rpm for 2 min. The plant material, as well as the PFTE shaking flasks and the grinding balls were precooled in liquid nitrogen in order to avoid thawing of the plant material during the process.

For reasons of reproducibilty 300 mg of ground plant powder was dissolved in 1,7 ml of pre-cooled acetone with 10% TCA and 0,07% ß-mercapto-ethanol. The mixture then was vortexed vigorously for at least 30 seconds and the samples were precipitated ON at -20°C. The next day, the samples were centrifuged for 15 min at 4°C and maximum speed.

Protein and cell debris were washed two-three times by adding 1,8 ml washing buffer (acetone, 0,07% beta-mercaptoethanol, solution pre-cooled at -20°C) in order to remove any remaining TCA. Then the

supernatant was removed very carefully and between each washing step the pellet was vortexed for at least 30 seconds and if necessary a sterile metal spatule was used to dissolve it completely. Before centrifugation (15 min, 4°C, maximum speed), the solution was incubated for 1-2 h at -20°C. For the last washing step 80% acetone was used. The resulting pellet was then air-dried for 15 min.
Depending on the purpose of the protein extraction, two different follow-ip treatments were used.
For 1-D SDS PAGE, the pellets were dissolved in 200 µl of a Laemmli 2x buffer (62,5 mM Tris-HCl pH 6.8, 25% Glycerol, 2% SDS, add 10 µl betameracptoethanol to the sample for a final concentration of 5%). Then the samples were boiled for 3 min at 95°C and then cooled down very quickly again before going on to protein quantification. After quantification the samples were further diluted in Laemmlie buffer containing 0,01% bromophenol blue.
For subsequent analysis on a 2-D-SDS gel the pellet was dissolved in a special solubilisation buffer fitting the requirements of isoelectrofocusing (5-7 M urea, 2M thiourea, 4% CHAPS, Tris-HCl pH 8.5).

4.4.2 Protein quantification

The principle of this assay is based on the observation that the absorbance maximum for an acidic solution of Coomassie Brilliant Blue G-250 shifts from 465 nm to 595 nm when binding to a protein occurs. In this case, both, hydrophobic and ionic interactions stabilize the anionic form of the dye, causing a visible change in color, which can be measured with a light spectrophotometre.
By comparing the obtained values at 595 nm to a standard curve, the amount of protein could be determined. The concentrations of the original sample were in the following calculated taking into account the volume/sample and the dilution factors (Bradford, 1976).
The assay was performed according to the "Quick Start™ Bradford Protein Assay Instruction Manual-section: "microplate standard assay" (volume: 250 µL) available from Bio-Rad using bovine serum albumin as a standard.

4.4.3 SDS-PAGE

To seperate proteins according to their molecular weight SDS-Polyacryl-amid-gel-electrophorese according to the protocol of Laemmli (1970) was performed. As SDS is an anionic detergent that denatures secondary and non–disulfide–linked tertiary structures and applies a negative charge to each protein in proportion to its mass. This mass:charge ratio is uniform for most proteins. as a result, when an electric current is applied across the gel, the negatively-charged proteins migrate across the

gel towards the anode (+) and their distance of migration through the gel can be assumed to be directly related to the size of the protein (Shapiro et al., 1967; Weber et al., 1969; Laemmli, 1970).
A typical 1-D SDS PA-gel consists of two components. First of all, the low concentrated stacking gel (3-6%) with large pores and a pH 6.8, creating a thin starting zone of SDS-coated proteins and the higher concentrated resolving gel (usually 10 -20 %), which separates the proteins more or less according to their size. Larger proteins are retained by the small pores, whereas smaller molecules migrate quicker through the gel.
Protein concentration was estimated according to the protocol of Bradford (1976), with the Bio-Rad protein assay reagent (Bio-Rad) and bovine serum albumin as a standard. Vertical SDS-PAGE was performed as described by Laemmli (1970) using the Bio-Rad 2 minigel system.

4.5 General Techniques in Molecular Biology

4.5.1 Polymerase Chain Reaction (PCR)

Amplification of DNA fragments for sublconing reactions was carried out by means of a polymerase chain reaction (Mullis et al., 1986). The reaction was performed in an sterile PCR tube (Eppendorf) by mixing the following components:
10 x amplification buffer 2 µl, 50 mM $MgCl_2$ 0,6 µl, 10 mM solution of four dNTPs 0,5 µl, 5 µM forward primer 1 µl, 5 µM reverse primer 1 µl, thermostable DNA polymerase 1-5 units (Invitrogen), and adding template DNA and distilled H_2O to total volume 20 µl.
The amount of template DNA varies depending on its properties. The amplification reaction was performed in an Eppendorf Thermocycler with the following cycling parameters. Annealing temperatures as well as elongation times need to be adapted to suit the particular reaction conditions. In special cases PCRs with different salt concentration or by adding DMSO, which influences the secondary structures of the DNA have to be carried out before finding the optimal conditions.

Step	Time and Temperature	Repetitions/Cycles
Initial Denaturation	5 min at 95°C	1
Denaturation	30-60 sec at 95°C	20 – 35
Annealing	30-60 sec at 50-65°C	20 – 35
Extension	1 min/kbp at 72°C	20 – 35
Final extension	10 min at 72°C	1
Cooling	4°C	1

Table 20: Cycling Conditions for standard Polymerase Chain Reactions (PCR)
For fragments exceeding 1000 bp in size Phusion Flash Polymerase (Finnzymes) was used according to the manufacturer's recommendations. PCR products were purified by the kit "Nucleospin Extract II" (Macherey-Nagel).

4.5.2 Preparation of XL1-Blue competent cells

Two standard methods for the transformation of competent bacterial cells are widely used: The calcium chloride (Dagert and Ehrlich, 1979)and the electroporation method (Okamoto et al., 1997). During my studies only the calcium chloride method was used.
A glycerol stock of an XL1-blue strain containing no plasmids was thawn on ice and stroken out onto a LB plate containing 12,5 µg/ml tetracycline. The plate was incubated over night at 37°C until single colonies were visible. 3ml of LB medium (12,5 µg/ml) were inoculated sterily with a single colony and incubated for 12 h at 37°C under permanent shaking (200 rpm). 500 µl of this preculture were added to 50 ml of LB_{tet} medium and grown at 37°C until an $OD_{600\ nm}$ of 0,4-0,5 was reached (early log phase is optimal). Then the bacterial culture was transferred to a 50 ml Falcon^{TM} tube and pelleted by centrifugation for 10 min at 4500 rpm and 4°C. After discarding the supernatant the pellet was resuspended in 10 ml of sterile cold $CaCl_2$ solution ($CaCl_2$ 60 mM; PIPES 10 mM; glycerol 15 %; pH 7). After another centrifugation step (2500 rpm; 4°C; 10 min) the cells were resuspended in 10 ml of $CaCl_2$ solution and chilled on ice for 30 min before being centrifugated under the same conditions as above. The resulting pellet was resuspended in 0,5 – 1 ml of $CaCl_2$ solution to yield the final competent cell solution. The cells were then transferred to sterile cryo-tubes (0,65 ml) and frozen in liquid nitrogen before storing them at -80°C.

4.5.3 Transformation of *E.coli* chemical-competent cells

Calcium chloride treatment produces competent cells that will take up DNA following a heat shock step. There is a multitude of different protocols trying to optimize the yield of bacterial transformation (Tu et al., 2005). The following protocol describes the standard procedure from our laboratory:
One tube per transformation reaction to perform is taken from the -80°C stock and thawn on ice for 5-10 min before adding the DNA solution of interest (5 µl of ligation or 1 µl of plasmid mini preparation). The cells are incubated for 30 min on ice. The cells are then exposed to 42°C for 60-90 sec (heat shock).
Following the heat shock treatment, 300 µl of LB medium (without selective markers/antibiotics) are added in order to aid the bacterial cells' recovery prior to plating them on solid LB medium containing

the appropriate selective marker. Positive clones are picked the next day and transferred to 3 ml of LB medium with antibiotics and grown for 12 h at 37°C on an incubator-shaker before being analyzed.

4.5.4 Isolation of plasmid DNA from *Escherichia coli*

Isolation of plasmid DNA from *E. coli* is a routine method in research laboratories. The protocol involves SDS/alkaline lysis of the bacterial cells and was mainly performed using the NucleoSpin® Plasmid QuickPure kit from Machery-Nagel according to the user manual. This protocol is often referred to as a plasmid "mini-prep," and yields fairly clean DNA quickly and easily as the kits are especially designed for the rapid, small-scale preparation of pure plasmid DNA.

However the yield and quality of plasmid DNA depends also on other factors like the type of the growing media, the nature of the bacterial host, the plasmid type (size, copy number, selection marker etc.).

To obtain highly pure plasmid DNA, e.g. for the bombardement of BY-2 cells, alternatively a slightly modified protocol was used (1983).

An overnight culture of the transformed bacteria is pelleted for 1-2 min in a microcentrifugeand resuspended in 100 µl of GTE buffer (50 mM glucose, 25 mM Tris-HC1- pH 8, 10 mM EDTA - pH 8.0) by vigorous vortexing. After adding 200 µl of freshly prepared lysis buffer (0,2 N NaOH, 1 % SDS) the content of the tube is mixed by inversion. Now 150 µl of potassium acetate buffer (120 ml potassium acetate 5 M, 23 ml of glacial acetic acid, 57 ml H_2O, pH 4,8) are added and the tube is again mixed by inversion before being centrifugated for 30 min at 4°C at 11000 g .

The supernatant containing the cytosolic debris and the desired plasmid DNA is transferred to a new tube, mixed with 500 µl of isopropanol and again centrifugated under the same conditions as above. The resulting pellet is dried at room temperature and solubilized in 100 µl of RNAse A solution (0,1 mg/ml)

After 20 min of incubation at 37°c the supernatant is extracted with a Phenol/Chloroform/Isoamylalcohol (25/24/1) mix and centrifugated for 10 min at 11000 g.

The aqueous phase containing the nucleic acids is transferred to a new tube. The plasmid DNA is then precipitated by adding 100 µl of isopropanol and 10 µl of 3 M sodium acetate (pH 4,8) and centrifugating the mixture for 30 min at 11000g at 4°C. The pellet is dried at RT and resolubilized depending on ist size in 20 – 50 µl of H_2O or TE buffer (10 Tris/ 1EDTA, pH 8).

4.5.5 Stable transformation of BY-2 cells by agroinfection

4.5.5.1 TBY2 cell culture

A cell suspension of tobacco BY2 cells (*Nicotiana tabacum* cv Bright Yellow 2) was maintained by weekly subculture according to (Nagata et al., 1992), diluting 0,75 ml of 7 day old culture in 40 ml of fresh Murashige and Skoog medium (1962). The cells were then cultured at 27°C in the dark on a rotary shaker (154 rpm).

Product	Molecular weight [g/Mol]	Stock solution	weight/volume	Solvant	Recipe for 1 L
Murashige and Skoog (Basal salt mixture - 1L, M 0221 Duchefa)	-	-	-	-	**4,3 g**
Thiamine (Hydrochloride)	337,3	1000 x	20 mg/20ml	H_20	**1 ml of stock solution**
2,4-D (2,4-Dichlorophenoxyacetic acid)	221	500 x	1 mg/ml in EtOH	+ 9ml KOH (0,1 N)	**2 ml of stock solution**
KH_2PO_4	136,09	54x	20 g/L	H_20	**18,5 ml of stock solution**
Myo-Inositol	180,2	100x	10 g/L	H_20	**10 ml of stock sloution**
Sucrose	342,3	-	30 g	-	**30 g (3%)**
adjust pH to 5,8 with KOH; autoclave 20 min at 1 bar (for solid medium add 0,8 % Agar)					

Table 21: Composition of the modified Murashige and Skoog medium (MS) used for the subculturing of TBY-2 cells

Transformed cell lines were treated as the wt lines besides adding the suitable antibiotics to the culture medium.

4.5.5.2 TBY2 transformation protocol

The genes of interest were introduced into TBY2 cells by *Agrobacterium tumefaciens*-mediated transformation using the specially adapted LBA 4404 strain.

Therefore a single colony, harbouring the desired construct is used to inoculate 3 ml YEB in the presence of antibiotics and incubated at 28 °C for 24-48 hrs. Then 50 µl of this pre-culture are taken to inoculate 2 ml of fresh YEB (supplemented with the same antibiotics) and incubated overnight at 28° under permanent shaking.

The next day the bacteria cells are collected by centrifugation at 3500 rpm for 10 min and washed once with 2 ml of sterile 10 mM $MgSO_4$. The resulting pellet is resuspended in 400 µl 10 mM $MgSO_4$ supplemented with Acetosyringone to a final concentration of 200 µM (prepared in Ethanol) and incubated for 1h – 3h at room temperature.

Four ml of a 3-day-old TBY2 culture are incubated with 100-200 µl of the acetysyringone treated *Agrobacterium* cells. The suspension is co-cultivated in petri dishes (diameter: 6 cm) for 48 h at 27°C and washed 4 times with sterile TBY2-medium (3500 rpm for 5 min). After the last wash the needed antibiotics are added and the cells are plated onto solid TBY2 medium (with selection markers) and cultured for 3-6 weeks until calli appear which are transferred to new plates or to liquid medium in order to start clonal cultures to work with.

4.5.5.3 Re-selection of TBY2 calli from liquid medium

A big problem maintaining transformed TBY2 cell lines in liquid medium was the occuring loss of overall fluorescence or fluorescence intensity.

In order to restart new homogenous cell lines from an existing clonal liquid culture losing its fluorescence, several dilutions of the original cultures were made. The following dilution proved to give the best results as far as the numbers of appearing calli are concerned. 3 ml of a 7-day old TBY2 wt culture were 10 fold diluted in 27 ml of liquid TBY2- medium. In order to get a 500 fold dilution of the clonal culture 60 µl of the 7-day old fluorescent cell line (pTA-H6-GFP-DB-CVIL) were added and after homogenizing the solution, 7 ml were plated out on dishes containing TBY-2 solid medium (diameter: 12 cm), supplemented with the appropriate antibiotics. After 2-3 weeks the first calli should appear (25 – 100 calli). They are transferred to new plates and as soon as they reached more than 10 mm in diameter small liquid cultures were started by transferring and homogenizing half of the calli in 10 ml TBY-2 medium (supplemented with the appropriate antibiotics).

4.5.6 Preparation of *A. tumefaciens* chemical competent cells

The protocol used for competent cell preparation for heat shock transformation using $CaCl_2$ is derived from An et al.(1988).

An *A. tumefaciens* freezer stock is streaked out onto a YEB plate containing rifampicin (20 µg/ml) and gentamycin (40 µg/ml) and is incubated for 48 h at 28°C until separated colonies are visible.

In order to start a miniculture a single bacterial colony is inoculated in 10 ml using YEB medium supplemented with the appropriate antibiotics and incubated by shaking at 28°C for 48 h.

50 ml of YEB/Rif/Gen are inoculated with 0,5 – 1ml of the 10 ml culture and grown overnight under permanent shaking at 28°C until the OD_{600nm} reaches 0,6 – 0,8.

The cells are centrifugated for 10 min at 3000 g and 4°C and the pellet is resuspended in 1ml of pre-cooled $CaCl_2$ – solution. Finally the cells are aliquoted in sterile tubes (40 – 50 µl) and frozen in liquid N_2 before storing them at – 80°C.

4.5.7 Preparation of *A.tumefaciens* electro-competent cells

Agrobacterium tumefaciens strains are grown for 3days at 28°C on solid YEB medium containing the appropriate antibiotics. One colony is used start a pre-culture in 10 ml YEB medium (supplemented with antibiotics) which is incubated for 2 days at 28° and permanent shaking. 2ml of the pre-culture are used to inoculate 100 ml YEB medium and this culture is incubated at 28°C for about 12 hours until the OD_{600nm} reaches 1,0 – 1,2. The transformation competence of Agrobacterium cells is strongly associated with particular combinations of bacteria strains and plasmid-selection markers as well as the optimal phase of growth at which the competent cells are prepared for transformation (McCormac et al., 1998). Therefore the OD_{600nm} - values can vary depending on the strain used for transformation.

After reaching the right OD_{600nm} the cultures are transferred to Falcon tubes and chilled on ice for 20 min. After centrifugating the cells for 5 min at 4000 g and 4°C the resulting pellet is resuspended in 40 ml of ice-cold, sterile MilliQ- water. This step is repeated one more time before washing the cells 2 times in 25 ml 10 % Glycerol solution (4000 g, 5min, 4°C). Prior to the last centrifugation the pellet is resuspenden in 0,5 – 1ml of 10% Glycerol (ice-cold) before aliquoting the cells into sterile 0,65 ml Eppendorf tubes (40 µl) and storing them immediately at -80°C.

4.5.8 Transformation of *A.tumefaciens* chemical competent cells by heatshock

Approximately 1 µg of plasmid DNA is added to an aliquot of competent cells thawn on ice. After keeping the cells on ice for 5 min they are rapidly transferred to the -80 freezer or alternatively to liquid N_2 for 5 min before incubating them at 37°C for 5 min. 300 µl of YEB medium (without antibiotics) is added to each tube and the mixture is incubated for 3 h at 28°C and permanent shaking to allow the bacteria to recover. The recovered culture is plated onto YEB solid medium containing the appropriate antibiotics and incubated at 28°C.Transformed colonies should appear in 48-72 h.

4.5.9 Transformation of *A.tumefaciens* electro-competent cells by electroporation

1 µl (1-5 µg of DNA) of plasmid DNA is added to an aliquot of electro-competent *A.tumefaciens* cells thawn on ice and mixed.

The Mixture is transferred to a pre-cooled electroporation cuvette (Bio-Rad. 2ml) and the electroporation is carried out as recommended by the electroporators manufacturer (Bio-Rad: capacitance: 25 µF – Voltage: 1,44 – 2,4 kV – Resistance: 200 Ω - pulse length: 5 msec). Immediately after the electroporation 300 – 1000 µl of YEB medium are added and the cells are allowed to recover for 1 – 3 h at RT under gentle agitation. The cells are then spread on plates containing the appropriate antibiotics and incubated for 3-4 days at 28°C until first colonies appear.

4.5.10 Restriction of DNA fragments

Depending on the cloning strategies, single or double digestions with commercial available restriction enzymes (Roche, Fermentas, NEB) were performed.

For single digestions, approximately 200 ng of DNA is digested with 1-2 units of the relevant restriction enzyme (Roche, Biolabs, Fermentas) according to the manufacturers recommendations in a total volume of 10 µl. The mixture is incubated for 1 h at the optimum temperature of the specific enzyme.

For double digestions 200-500 ng of DNA are incubated with 1-2 units of the relevant restriction enzymes using the commercial buffer being optimal for the chosen restriction enzyme combination. Depending on the efficiency of the digestion reaction, samples are incubated for 2h or more (overnight) at the recommended temperature.

After digestion the samples are analyzed by DNA gel electrophoresis and the digested DNA is purified with the „Nucleospin Extract II“ kit from Macherey-Nagel.

4.5.11 Ligation of DNA fragments

In order to ligate a digested DNA fragment with the desired plasmid, the 20 µl ligation mixture containing 60-100 ng target DNA, 20-40 ng of plasmid DNA, 10 x ligation buffer and 1 unit of T4 DNA Ligase (Fermentas) is incubated overnight at 4°C.
The ligation product was in most of the cases directly used to transform chemically-competent *E.coli* cells by heat shock as described.

4.5.12 Cloning of blunt end DNAs into a sequencing vector using the Digestion – Ligation method (DIG-LIG)

This protocol was used to clone blunt end PCR products into a subcloning vector in order to verify the sequence of the amplified fragment.
It is taking advantage of the low SmaI working temperature which is close to the RT and its presence in the multiple cloning site (MCS) of most of the commercial cloning vectors, such as pBluescript. The MCS itsself is located in the LacZ coding sequence corresponding to wt beta-galactosidase and allows to select for positive clones by blue/white screening.
The 10 µl Digestion-ligation mixture, containing 1 µl plasmid DNA (~30 ng), target DNA (50-100 ng), 1 unit SmaI, 1 µl 10 x T4 ligase buffer, 1 µl T4 Ligase (Fermentas) is incubated overnight at RT. 5 µl of this dig-lig reaction are used to transform XL1-Blue competent cells as described and they are plated onto LB plates supplemented with 100 µg/ml Ampicilin. The transformed cells are grown in the presence of X-Galactosidase and IPTG. If the digestion-ligation reaction was successful, the bacterial colony will be white; if not, the colony will be blue.

4.5.13 Agarose Gel electrophoresis of DNA and RNA

This technique was used to seperate or to analyze DNA or RNA fragments. The electrophoresis is commonly performed on an agarose gel (0,8 – 2,5% in TAE buffer) and depending on the purpose of the Gel electrophoresis - visual analysis, quantification or isolation of a particular band – the concentration is chosen. A low percentage gel will show good separation (resolution) of large DNA fragments (5–10kb) and higher concentrated gel will show good resolution for small fragments (0.2–1kb).

Therefore 0,8 – 2,5 g Agarose ( ) are diluted in 100 ml of 1 x TAE buffer (40 mM Tris-acetate; 2 mM EDTA), heated in the microwave until the agarose is completely dissolved. Then the solution is cooled to room temperature and ethidium bromide, a DNA - intercalating reagent, which absorbs UV light and emits visible orange light, is added (10 µg/ml) before pouring the mixture into the gel chambers.
The samples are prepared with 5 x gel loading buffer (0,25% bromophenol blue ; 0,25% xylene cyanol ; 15% glycerol) and run at 90 V in 1 x TAE buffer next to a DNA size marker (Mass-Ruler, Bio-Rad). Bands are visualized under UV light and acquired with the Chemi-smart 3000 image acquisition system.

4.5.14 Glycerol stocks

In order to create a glycerol stock of a created or imported construct a single colony of the clone ispicked off a plate and grown overnight in the appropriate selectable liquid medium.
The next day 0,5 ml of the overnight culture are added to 80% sterile glycerol in a sterile screw cap microcentrifuge tube. Certain antibiotics, like tetracycline, should be removed first as they can display toxic effects over the time. This can be achieved by spinning down the culture and resuspending the cells in LB medium. After vortexing and adding all pertinent information on the tube the stock is frozen at -80°C.
To restart a culture the glycerol stock is briefly removed from -80°C and a small portion is scraped off the top of the frozen glycerol stock with a sterile metal inoculation loop and streaked onto a plate with the appropriate antibiotics.The tube is then rapidly returned to the -80°C freezer to avoid thawing as freeze thaw cycles will kill the clone.

4.5.15 Preparation of genomic DNA from bacteria

The pellet of a 50 ml over-night culture is gently mixed with 2,5 ml of alkaline solution (0,2 N NaOH, 2,5 % SDS) and incubated on ice for 30 min. Then 5ml of lysis solution (1,5 mg/ml lysozyme, 80 mM Tris-HCl, 10 mM EDTA, 1 % Glucose) are added and the content of the tube is mixed by inversion and incubated on ice for 5 min. After adding 3,75 ml of sodium acetate (3M, pH 4,8) the suspension is incubated on ice for 1 h before being centrifugated for 10 min at 8000 g. The supernatant is transferred to a new tube and the centrifugation step is repeated to get rid off the cellular debris.
In order to precipitate the DNA 2 volumes of 100% Ethanol are added and the tube is incubated at -20°C over-night and centrifugated for 20 min at 8000 rpm the next day. The resulting pellet is briefly dried and resuspended in 900 µl $T_{10}E_1$ and incubated on ice for several hours. After spinning the

solution for 10 min at 6000 g the supernatant is transferred to a new tube and is incubated for 15 min with 10µl RNase A (10 mg/ml). The DNA is then extracted by gently mixing the solution an equal amount of Phenol-Chloroform and transferring the upper, aqueous phase to a new tube after a spinning it at 10000 g for 10 min. A final precipitation step with 2 volumes 100% Ethanol is done before resuspending the air-dried pellet in an appropriate amount of $T_{10}E_1$. The purity of the DNA can be checked by electrophoresis or spectrophotometric analysis methods.

4.5.16 Isolation of total RNA from plant tissue

This protocol was used for total RNA extraction from *Arabidopsis thaliana* leaves as well as for *Nicotiana tabacum* BY2 cells.

After grinding the plant tissues in liquid nitrogen, 200 mg of the fine powder is transferred to a 2ml Eppendorf tube, where it is homogenized in 800 µl Trizol Reagent (Invitrogen) by vigorous vortexing and incubated on ice for 10-15 min (or alternatively 5 min on RT).

Then 800 µl of Chloroform/Isoamylalcohol (24/1) are added and the mixture is vortexed at least for 15 seconds before being chilled on ice for 10-15 min again. After centrifugation of the suspension for 15 min at 4°C and 12000 g the supernatant is transferred to a new 1,5 ml Eppendorf tube and the nucleic acids are precipitated by adding 1 ml of ice-cold Isopropanol. The mixture is incubated for 20 min at –20°C before being centrifugated for 30 min at 12000 g and 4°C. Now the supernatant is discarded carefully and the small pellet is washed with 500 µl 80% ethanol by centrifuging 12 min at 10000 g and 4°C. After discarding the supernatant the pellet is air-dried and resuspended in 20 – 50 µl of RNase-free water depending on its size. The concentration and purity of the RNA can be analyzed by spectrophotometric analysis (Table 22).

4.5.17 Reverse transcription

Before starting the synthesis of cDNA the extracted RNA should be treated with DNase I (Fermentas) in order to avoid DNA interference. The reaction is performed according to the manufacturers protocol, incubating 1 µg of RNA with 1µl RNase Out, 1µl 10 x buffer (+ $MgCl_2$) and 1 µl DNase I in a final volume of 10 µl for 30 min at 37°C. To stop the reaction 1 µl 25 mM EDTA was added and the mixture was incubated at 65°C for 10 min.

After incubating DNase I – treated RNA for 5min at 65°C with 1 µl Oligo-dt (15 tn) and 1µl dNTP-Mix (10 mM) the mixture is chilled for 1-2 min on ice before adding 4µl 5 x reaction buffer, 1µl 0,1 M

DTT, 1µl SuperScript III Reverse Transcriptase (Invitrogen). The reaction mixture is incubated at 50°C for 60 min, and at 70°C for 15 min. The synthesized cDNA can be used as the templates in PCR reactions.

4.5.18 Spectrophotometric analysis of nucleic acids

The concentrations of oligonucleotides, DNA and RNA were determined by absorption measurement in an Eppendorf spectrophotometer (BioPhotometer) according to the manufacturers' protocol. The measurements were performed at 230, 260 or 280 nm in special Eppendorf UVette® cuvettes. The extinction value at 260 nm allows an estimation of the concentration of nucleic acid in a sample, whereas the ratio between the values taken at 260 nm and 280 nm (A_{260}/A_{280}) and 230nm and 260 nm (A_{260}/A_{230}) provides an estimate of the purity of the nucleic acid. Nucleic acid is detected at 260 nm, whereas protein, salt and solvents are detected at 230 and 280 nm Good quality RNA should therefore have an OD 260/280 ratio of 1.8 to 2 and an OD 260/230 of 1.8 or greater indicating that extracted DNA/RNA is devoid of these contaminants.
To calculate the concentration of nucleic acid in the sample following equation can be used:

$[c] = OD_{260\ nm}$ x 40 µg/ml x dilution factor

Excitation wavelength and type of nucleic acid	amount of nucleic acid per 1 OD unit
1 A_{260} unit of double stranded DNA	50 µg
1 A_{260} unit single stranded DNA or RNA (>100 bases)	40 µg
1 A_{260} unit of single stranded DNA (less then 25 bases)	20 µg
1 A_{260} unit of single stranded DNA (30-80 bases)	30 µg

Table 22: Overview of the conversion factors used for DNA an RNA quantification

4.5.19 Particle bombardment of TBY2 cells

The standard vector used for transient transformation of TBY-2 cells was the pGFP-MRC vector, containing the coding sequence of the GFP protein.

4.5.19.1Preparation of the particles for bombardment

The Plasmid DNA was purified using the NucleoSpin® Plasmid QuickPure kit from Machery-Nagel according to the user manual. The protocol for precipitation of the plasmid DNA onto the M-17 tungsten particles (Bio-Rad: 1,1 µm diameter) is optimized for 2 shots per petri dish.
Therefore 1 mg (amount needed for one petri dish) of tungsten particles was resuspended by vigorous agitation in 1ml of 100% EtOH and incubated for 20 min at RT to allow the precipitation of the microprojectile beads on the bottom of the Eppendorf tube. After 2 min of centrifugation at 9.000 g and RT the supernatant was carefully removed and the beads were vacuum speed dried for several minutes.
After this procedure the tungsten particles were resuspended in 16,5 µl of 50% Glycerol (per mg of beads). Then 8 µl of DNA were added at a concentration of 1µg/µl. Now 33 µl of a calcium chloride solution (2 M) were added to the DNA/beads mixture. Finally 15 µl of Spermidine at a concentration of 2 M were mixed with the solution before vortexing the Eppendorf tube.
This mixture was allowed to stand for 20 min at RT prior to centrifugation for 30 sec at 350 g (1000 rpm in a small table centrifuge). After discarding the supernatant the beads were washed 2 times in 150 µl of 70% and 100% EtOH (30 sec at 350 g). This step was followed by vacuum speed drying for 5 min. To complete the pretreatment process the particles were resuspended in 14 µl of 100% EtOH which is sufficient to do 2 bombardments with the particle gun (7 µl each). It is recommended to use the pretreated microprojectile beads as soon as possible after preparation.

4.5.19.2 Preparation of the plant material for bombardment

For transient transformation of tobacco BY-2 cells a Particle Gun system was used (Particle Inflow Gun, Finer et al, 1992), which was optimized after Brown et al. (1994). Four days before doing the bombardment, 0,75 ml of a 7 day-old culture were diluted in 40 ml of MS-BY2 medium and grown under standard conditions (27°C, shaking at 120 rpm in the dark).
The day of the bombardment 3-5 ml of the cell culture were transferred under sterile conditions onto a Whatman paper (diameter 3 cm) using a buchner filter. The Whatman paper was then placed on top of a petri dish containing solid MS-BY2 medium (0,5 % Agar) and directly used for bombardment with the pretreated DNA-coated tungsten particles.

4.5.19.3 Bombardment and transient expression of desired proteins

Each petri dish containing the TBY-2 cells transferred on Whatman Paper received two bombardments by the particle gun. Normally at least two independent repetitions of the experiment were completed.
The settings used for the bombardment vary largely depending on the type of particle gun used and have to be adapted individually. For the particle gun used at the IBMP they were as follows: firing distance of the dish: 11 cm, pressure: 0,8 bar, opening time: 25 ms. After the first bombardment, the dish was turned 180° and the procedure was repeated.
Following particle gun treatment the samples were incubated for 16-20 h in the dark at 26°C to allow transient expression of the desired proteins.
The success of the bombardment was observed using a fluorescence microscope as described in the following section (4.5.20).

4.5.20 Microscopy

Cell imaging was performed using a LSM510 confocal laser scanning microscope equipped with an inverted Zeiss axiovert 100 M microscope (Carl Zeiss, Jena, Germany). For statistical observations, such as counting cells after various treatments, a 10x Zeiss objective ("Plan-Neofluar") was used. At confocal resolution, images were taken using a a 63x, 1.2 numerical aperture water immersion objective ("C-Apochromat"). In both cases, differential interference contrast (DIC) images were recorded.
Epifluorescence microscopy was performed using a Nikon E 800 fluorescence microscope equipped with a Nikon DXM1200 CCD high-resolution color camera (20x0,45 objective) and ACT-1 image software.
Images were processed with the latest version of the Zeiss LSM Image Browser software (Carl Zeiss, Jena, Germany) and exported as Tiff or JPEG files. Final image analysis and adjustments was performed using either Photoshop version 8.0 (Adobe Systems, San Jose, USA) or the Image J software version 1.31 (Wayne Rasband, NIH, USA; http://rsb.info.nih.gov/ij).

Fluorochrome	Purpose	Excitation peak (nm)	Emission peak (nm)	Laser (excitation)	Filter settings
DAPI (4',6-diamidino-2-phenylindole, dihydrochloride)	DNA staining (visualisation of nuclei)	364 (bound to DNA)	454 nm (bound to DNA)	Diode laser (405 nm)	"long pass" (475 nm)
Hoechst 33342	DNA staining (visualisation of nuclei)	350 (bound to DNA)	461 nm (bound to DNA)	Diode laser (405 nm)	"long pass" (475 nm)
Propidium Iodide	DNA staining (visualisation of dead cells)	535 nm (bound to DNA)	617 nm (bound to DNA)	Helium-Neon laser (543/633 nm)	„band pass“ (575-615nm)
Fluorescent Protein	**Purpose**	**Excitation peak (nm)**	**Emission peak (nm)**	**Laser (excitation)**	**Filter settings**
GFP (Green Fluorescent Protein)	intracellular localisation of fusion proteins	2 peaks: 395 nm /475 nm	509 nm	Argon laser (488 nm)	"band pass" (505-550nm)
mRFP (monomeric Red Fluorescent Protein)	intracellular localisation of fusion proteins	584 nm	605 nm	Helium-Neon laser (543/633 nm)	„band pass“ (575-615nm)

Table 23: Properties of the fluorochromes and fluorescent proteins used in this work

4.6 Bioinformatical Analysis

4.6.1 Molecular Biological Software

Two software packages (Vector NTI and BioEdit) and two free applications (Biology Workbench and NCBI ORF Finder) were used for the *in silico* manipulation of nucleic and protein sequences and the study of DNA and protein properties. Vector NTI software suite was used for the the analysis of DNA sequence chromatograms generated after DNA sequencing. Details on all software are listed in Table 12.

4.6.2 Algorithms and software for prediction

Several algorithms and software programs were used to analyze obtained nucleic acid and peptide sequences. An overview of the different programs used in this study is given in 4.1.2.1 and 4.1.2.2.

4.6.3 Database search

Different nucleic acid databases were consulted to retrieve sequence information from genomic clones, ESTs, mRNAs, cDNAs and translated proteins/polypeptides in order to design oligos for subsequent cloning purposes, semi-quantitative or RACE-PCRs.
The protein databases listed in table were consulted to analyze proteins and polypeptides in regard (see chapter 4.6.2).

4.6.4 Image acquisition, analysis and processing software

Agarose gel and SDS-PAGE pictures were captured with the Chemi-smart 3000 image acquisition system. Epifluorescence images were recorded and analyzed using Image J software, confocal microscopy images were acquired and analyzed with the latest version of the Zeiss LSM Image Browser program. All images were processed using Image J software and/or Adobe Photoshop. Illustrations were designed using Office 2002 PowerPoint or Adobe Illustrator CS version 11.0.0. Details concerning the used software are listed in Table 12. For specialised image analysis, ImageJ software was used.

5 References

Abdullah MA, Ali AM, Lajis NH, Marziah M, Sinskey AJ and Rha C (2005) Issues in Plant Cell Culture Engineering for Enhancement of Productivity. Developments in Chemical Engineering and Mineral Processing 13(5-6): 573-587.

Abe I, Rohmer M and Prestwich GD (1993) Enzymatic cyclization of squalene and oxidosqualene to sterols and triterpenes. Chemical Reviews 93: 2189-2206.

Abraham VC, Taylor DL and Haskins JR (2004) High content screening applied to large-scale cell biology. Trends Biotechnol 22(1): 15-22.

Abramoff MD, Magelhaes PJ and Ram SJ (2004) Image Processing with ImageJ. Biophotonics International 11(7): 36-42.

AbuMweis SS and Jones PJ (2008) Cholesterol-lowering effect of plant sterols. Curr Atheroscler Rep 10(6): 467-472.

Adam K-P, Thiel R and Zapp J (1999) Incorporation of 1-[1-^{13}C]Deoxy-D-xylulose in Chamomile Sesquiterpenes. Archives of Biochemistry and Biophysics 369(1): 127-132.

Adam KP, Thiel R, Zapp J and Becker H (1998) Involvement of the mevalonic acid pathway and the glyceraldehyde-pyruvate pathway in terpenoid biosynthesis of the liverworts *Ricciocarpos natans* and *Conocephalum conicum*. Arch Biochem Biophys 354(1): 181-187.

Adams RLP and Burdon RH (1985) Molecular Biology of DNA Methylation. New York: Springer Verlag.

Ai-Xia C, Yong-Gen L, Ying-Bo M, Shan L, Ling-Jian W and Xiao-Ya C (2007) Plant Terpenoids: Biosynthesis and Ecological Functions. Journal of Integrative Plant Biology 49(2): 179-186.

Albert A (1958) Chemical aspects of selective toxicity. Nature 182: 421-423.

Altschul SF, Gish W, Miller W, Myers EW and Lipman DJ (1990) Basic local alignment search tool. J Mol Biol 215(3): 403-410.

An G (1985) High efficiency transformation of cultured tobacco cells. Plant Physiol 79(2): 568-570.

An G, Ebert PR, Mitra A and Ha SB (1988) Binary Vectors In: Gelvin SB, Schilperoort RA, editors. Plant Molecular Biology Manual. Dordrecht: Kluwer Academic Publishers. pp. 1-19.

Anderlei T, Zang W, Papaspyrou M and Büchs J (2004) Online respiration activity measurement (OTR, CTR, RQ) in shake flasks. Biochem Eng J 17: 187-194.

Andrews M, Huizinga DH and Crowell DN (2010) The CaaX specificities of Arabidopsis protein prenyltransferases explain *era1* and *ggb* phenotypes. BMC Plant Biol 10: 118.

Aoyama T and Chua NH (1997) A glucocorticoid-mediated transcriptional induction system in transgenic plants. Plant J 11(3): 605-612.

Apolloni A, Prior IA, Lindsay M, Parton RG and Hancock JF (2000) H-ras but not K-ras traffics to the plasma membrane through the exocytic pathway. Mol Cell Biol 20(7): 2475-2487.

Araki N, Kusumi K, Masomoto K, Niwa Y and Iba K (2000) Temperature-sensitive *Arabidopis* mutant defective in 1-deoxy-D-xylulose-5-phosphate synthase within the plastid non-mevalonate pathway of isoprenoid biosynthesis. Physiol Plantarum 108: 19-24.

Argenta LC and Lopes NF (1991) Clomazone effects on pigment accumulation, photosynthetic and respiratory rates of greening soybean seedlings. R Bras Fisiol Veg 3: 69-74.

Argyrou A and Blanchard JS (2004) Kinetic and chemical mechanism of *Mycobacterium tuberculosis* 1-deoxy-D-xylulose-5-phosphate isomeroreductase. Biochemistry 43(14): 4375-4384.

Arigoni D, Sagner S, Latzel C, Eisenreich W, Bacher A and Zenk MH (1997) Terpenoid biosynthesis from 1-deoxy-D-xylulose in higher plants by intramolecular skeletal rearrangement. Proc Natl Acad Sci U S A 94(20): 10600-10605.

Astani A, Reichling J and Schnitzler P (2009) Comparative study on the antiviral activity of selected monoterpenes derived from essential oils. Phytother Res 24(5): 673-679.

Bach TJ (1986) Hydroxymethylglutaryl-CoA reductase, a key enzyme in phytosterol synthesis? Lipids 21(1): 82-88.

Bach TJ (1995) Some new aspects of isoprenoid biosynthesis in plants - A review. Lipids 30(3): 191-202.

Bach TJ and Lichtenthaler HK (1987) Plant growth regulation by mevinolin and other sterol biosynthesis inhibitors. In: Fuller G, Nes WD, editors. Ecology and metabolism of plant lipids 325 ed. Washington: American Chemical Society. pp. 109-139.

Bach TJ, Weber T and Motel A (1990) Some properties of enzymes involved in the biosynthesis and metabolism of 3-hydroxy-3-methylglutaryl-CoA in plants. Recent Advances in Phytochemistry 24: 1-82.

Baerenfaller K, Grossmann J, Grobei MA, Hull R, Hirsch-Hoffmann M, Yalovsky S, Zimmermann P, Grossniklaus U, Gruissem W and Baginsky S (2008) Genome-scale proteomics reveals *Arabidopsis thaliana* gene models and proteome dynamics. Science 320(5878): 938-941.

Bailey AM, Mahapatra S, Brennan PJ and Crick DC (2002) Identification, cloning, purification, and enzymatic characterization of *Mycobacterium tuberculosis* 1-deoxy-D-xylulose 5-phosphate synthase. Glycobiology 12(12): 813-820.

Baker CH, Matsuda SP, Liu DR and Corey EJ (1995) Molecular cloning of the human gene encoding lanosterol synthase from a liver cDNA library. Biochem Biophys Res Commun 213(1): 154-160.

Bansal VS and Vaidya S (1994) Characterization of two distinct allyl pyrophosphatase activities from rat liver microsomes. Arch Biochem Biophys 315(2): 393-399.

Banu NA, Hoque A, Watanabe-Sugimoto M, Matsuoka K, Nakamura Y, Shimoishi Y and Murata Y (2009) Proline and glycinebetaine induce antioxidant defense gene expression and suppress cell death in cultured tobacco cells under salt stress. J Plant Physiol 166(2): 146-156.

Barth O, Vogt S, Uhlemann R, Zschiesche W and Humbeck K (2009) Stress induced and nuclear localized HIPP26 from *Arabidopsis thaliana* interacts via its heavy metal associated domain with the drought stress related zinc finger transcription factor ATHB29. Plant Mol Biol 69(1-2): 213-226.

Baum B and Craig G (2004) RNAi in a postmodern, postgenomic era. Oncogene 23(51): 8336-8339.

Baumann NA, Sullivan DP, Ohvo-Rekila H, Simonot C, Pottekat A, Klaassen Z, Beh CT and Menon AK (2005) Transport of newly synthesized sterol to the sterol-enriched plasma membrane occurs via nonvesicular equilibration. Biochemistry 44(15): 5816-5826.

Baxter A, Fitzgerald BJ, Hutson JL, McCarthy AD, Motteram JM, Ross BC, Sapra M, Snowden MA, Watson NS, Williams RJ and et al. (1992) Squalestatin 1, a potent inhibitor of squalene synthase, which lowers serum cholesterol *in vivo*. J Biol Chem 267(17): 11705-11708.

Beato M (1989) Gene regulation by steroid hormones. Cell 56(3): 335-344.

Beck JG, Mathieu D, Loudet C, Buchoux S and Dufourc EJ (2007) Plant sterols in "rafts": a better way to regulate membrane thermal shocks. Faseb J 21(8): 1714-1723.

Begley M, Gahan CG, Kollas AK, Hintz M, Hill C, Jomaa H and Eberl M (2004) The interplay between classical and alternative isoprenoid biosynthesis controls gammadelta T cell bioactivity of *Listeria monocytogenes*. FEBS Lett 561(1-3): 99-104.

Belanger KD and Quatrano RS (2000) Polarity: the role of localized secretion. Curr Opin Plant Biol 3(1): 67-72.

Benveniste P (2004) Biosynthesis and accumulation of sterols. Annu Rev Plant Biol 55: 429-457.

Bergo MO, Ambroziak P, Gregory C, George A, Otto JC, Kim E, Nagase H, Casey PJ, Balmain A and Young SG (2002) Absence of the CAAX endoprotease Rce1: effects on cell growth and transformation. Mol Cell Biol 22(1): 171-181.

Bergstrom JD, Kurtz MM, Rew DJ, Amend AM, Karkas JD, Bostedor RG, Bansal VS, Dufresne C, VanMiddlesworth FL, Hensens OD and et al. (1993) Zaragozic acids: a family of fungal metabolites that are picomolar competitive inhibitors of squalene synthase. Proc Natl Acad Sci U S A 90(1): 80-84.

Bernardt R (2006) Cytochromes P450 as versatile biocatalysts. J Biotechnol 124: 128-145.

Betts JI and Baganz F (2006) Miniature bioreactors: current practices and future opportunities. Microb Cell Fact 5: 21.

Bevan M (2002) Genomics and plant cells: application of genomics strategies to *Arabidopsis* cell biology. Philos Trans R Soc Lond B Biol Sci 357(1422): 731-736.

Bick JA and Lange BM (2003) Metabolic cross talk between cytosolic and plastidial pathways of isoprenoid biosynthesis: unidirectional transport of intermediates across the chloroplast envelope membrane. Arch Biochem Biophys 415(2): 146-154.

Birnboim HC (1983) A rapid alkaline extraction method for the isolation of plasmid DNA. Methods Enzymol 100: 243-255.

Bloch K, Chaykin S, Phillips AH and De Waard A (1959) Mevalonic acid pyrophosphate and isopentenylpyrophosphate. J Biol Chem 234: 2595-2604.

Bohlmann J and Keeling CI (2008) Terpenoid biomaterials. Plant J 54(4): 656-669.

Bohlmann J, Meyer-Gauen G and Croteau R (1998) Plant terpenoid synthases: molecular biology and phylogenetic analysis. Proc Natl Acad Sci U S A 95(8): 4126-4133.

Bolte S, Talbot C, Boutte Y, Catrice O, Read ND and Satiat-Jeunemaitre B (2004) FM-dyes as experimental probes for dissecting vesicle trafficking in living plant cells. J Microsc 214(Pt 2): 159-173.

Bonetta D, Bayliss P, Sun S, Sage T and McCourt P (2000) Farnesylation is involved in meristem organization in *Arabidopsis*. Planta 211: 182-190.

Borner GH, Sherrier DJ, Weimar T, Michaelson LV, Hawkins ND, Macaskill A, Napier JA, Beale MH, Lilley KS and Dupree P (2005) Analysis of detergent-resistant membranes in *Arabidopsis*. Evidence for plasma membrane lipid rafts. Plant Physiol 137(1): 104-116.

Bos JL (1989) ras oncogenes in human cancer: a review. Cancer Res 49(17): 4682-4689.

Boucher Y and Doolittle WF (2000) The role of lateral gene transfer in the evolution of isoprenoid biosynthesis pathways. Mol Microbiol 37(4): 703-716.

Boulikas T (1993) Nuclear localization signals (NLS). Crit Rev Eukaryot Gene Expr 3(3): 193-227.

Boutte Y and Grebe M (2009) Cellular processes relying on sterol function in plants. Curr Opin Plant Biol 12(6): 705-713.

Bouvier F, Rahier A and Camara B (2005) Biogenesis, molecular regulation and function of plant isoprenoids. Prog Lipid Res 44(6): 357-429.

Bracha-Drori K, Shichrur K, Lubetzky TC and Yalovsky S (2008) Functional analysis of *Arabidopsis* post-prenylation CaaX processing enzymes and their function in subcellular protein targeting. Plant Physiol 148: 119-131.

Bracha K, Lavy M and Yalovsky S (2002) The *Arabidopsis* AtSTE24 is a CAAX protease with broad substrate specificity. J Biol Chem 277(33): 29856-29864.

Bradford MM (1976) A rapid and sensitive method for the quantitation of microgram quantities of protein utilizing the principle of protein-dye binding. Anal Biochem 72: 248-254.

Broers STJ (1994) Über die frühen Stufen von Isoprenoiden in *Escherichia coli* [PhD thesis]: ETH Zürich, Switzerland.

Brown A, Nemeria N, Yi J, Zhang D, Jordan WB, Machado RS, Guest JR and Jordan F (1997) 2-Oxo-3-alkynoic acids, universal mechanism-based inactivators of thiamin diphosphate-dependent decarboxylases: synthesis and evidence for potent inactivation of the pyruvate dehydrogenase multienzyme complex. Biochemistry 36(26): 8071-8081.

Brown AC and Parish T (2008) Dxr is essential in *Mycobacterium tuberculosis* and fosmidomycin resistance is due to a lack of uptake. BMC Microbiol 8: 78.

Brown AC, Eberl M, Crick DC, Jomaa H and Parish T (2010) The nonmevalonate pathway of isoprenoid biosynthesis in *Mycobacterium tuberculosis* is essential and transcriptionally regulated by Dxs. J Bacteriol 192(9): 2424-2433.

Buchs J (2001) Introduction to advantages and problems of shaken cultures. Biochem Eng J 7(2): 91-98.

Buckingham J (2004) Dictionary of Natural Products, Web Version. Chapman and Hall, London.

Budziszewski GJ, Lewis SP, Glover LW, Reineke J, Jones G, Ziemnik LS, Lonowski J, Nyfeler B, Aux G, Zhou Q, McElver J, Patton DA, Martienssen R, Grossniklaus U, Ma H, Law M and Levin JZ (2001) *Arabidopsis* genes essential for seedling viability: isolation of insertional mutants and molecular cloning. Genetics 159(4): 1765-1778.

Buetow L, Brown AC, Parish T and Hunter WN (2007) The structure of *Mycobacteria* 2*C*-methyl-D-erythritol-2,4-cyclodiphosphate synthase, an essential enzyme, provides a platform for drug discovery. BMC Struct Biol 7: 68.

Buhaescu I and Izzedine H (2007) Mevalonate pathway: A review of clinical and therapeutical implications. Clinical Biochemistry 40(9-10): 575-584.

Burnett P, Robertson JK, Palmer JM, Ryan RR, Dubin AE and Zivin RA (2003) Fluorescence imaging of electrically stimulated cells. J Biomol Screen 8(6): 660-667.

Busquets A, Keim V, Closa M, del Arco A, Boronat A, Arro M and Ferrer A (2008) *Arabidopsis thaliana* contains a single gene encoding squalene synthase. Plant Mol Biol 67(1-2): 25-36.

Caldelari D, Sternberg H, Rodríguez-Concepción M, Gruissem W and Yalovsky S (2001) Efficient prenylation by a plant geranylgeranyltransferase-I requires a functional CaaL box motif and a proximal polybasic domain. Plant Physiol 126: 1416-1429.

Campbell RE, Tour O, Palmer AE, Steinbach PA, Baird GS, Zacharias DA and Tsien RY (2002) A monomeric red fluorescent protein. Proc Natl Acad Sci U S A 99(12): 7877-7882.

Campos N, Rodríguez-Concepción M, Seemann M, Rohmer M and Boronat A (2001) Identification of gcpE as a novel gene of the 2-*C*-methyl-D-erythritol 4-phosphate pathway for isoprenoid biosynthesis in *Escherichia coli*. FEBS Lett 488(3): 170-173.

Cane DE (1999) Isoprenoid biosynthesis overview. In: Barton SD, Nakanishi K, Meth-Cohn O, editors. Comprehensive natural products chemistry: isoprenoids including carotenoids and steroids. Oxford: Elsevier Science. pp. 1-12.

Cane DE, Rossi T, Tillman AM and Pachlatko JP (1981) Stereochemichal studies of isoprenoid biosynthesis: Biosynthesis of pentelenolactone from [U-$^{13}C_6$]glucose and [6-$^{2}H_2$]glucose. J Am Chem Soc 103: 1838-1843.

Carpenter AE (2007a) Software opens the door to quantitative imaging. Nat Methods 4(2): 120-121.

Carpenter AE (2007b) Image-based chemical screening. Nat Chem Biol 3(8): 461-465.

Carpenter AE and Sabatini DM (2004) Systematic genome-wide screens of gene function. Nat Rev Genet 5(1): 11-22.

Carretero-Paulet L, Ahumada I, Cunillera N, Rodríguez-Concepción M, Ferrer A, Boronat A and Campos N (2002) Expression and molecular analysis of the Arabidopsis *DXR* gene encoding 1-deoxy-D-xylulose 5-phosphate reductoisomerase, the first committed enzyme of the 2-*C*-methyl-D-erythritol 4-phosphate pathway. Plant Physiol 129(4): 1581-1591.

Cassera MB, Merino EF, Peres VJ, Kimura EA, Wunderlich G and Katzin AM (2007) Effect of fosmidomycin on metabolic and transcript profiles of the methylerythritol phosphate pathway in *Plasmodium falciparum*. Mem Inst Oswaldo Cruz 102(3): 377-383.

Cavalier-Smith T (1999) Principles of protein and lipid targeting in secondary symbiogenesis: Euglenoid, dinoflagellate, and sporozoan plastid origins and the eukaryote family tree. J Eukaryot Microbiol 46(4): 347-366.

Chang JH, Konz MJ, Aly EA, Sticker RE, Wilson KR, Krog NE and Dickinson PE (1987) 3-Isoxazolidinones and related compounds a new class of herbicides. In: Baker DR, Fenyes JG, Moberg WK, Cross B, editors. Synthesis and Chemistry of Agrochemicals - ACS symposium Series 355. Washington: American Chemical Society. pp. 10-23.

Chappell J (1995) The Biochemistry and Molecular Biology of Isoprenoid Metabolism. Plant Physiol 107(1): 1-6.

Chappell J (2002) The genetics and molecular genetics of terpene and sterol origami. Curr Opin Plant Biol 5(2): 151-157.

Chappell J, Wolf F, Proulx J, Cuellar R and Saunders C (1995) Is the Reaction Catalyzed by 3-Hydroxy-3-Methylglutaryl Coenzyme A Reductase a Rate-Limiting Step for Isoprenoid Biosynthesis in Plants? Plant Physiol 109(4): 1337-1343.

Chary SN, Bultema RL, Packard CE and Crowell DN (2002) Prenylcysteine alpha-carboxyl methyltransferase expression and function in *Arabidopsis thaliana*. Plant J 32: 735-747.

Chemler JA, Yan Y and Koffas MA (2006) Biosynthesis of isoprenoids, polyunsaturated fatty acids and flavonoids in *Saccharomyces cerevisiae*. Microb Cell Fact 5: 20.

Chen Y (1999) Selective inhibition of ras-transformed cell growth by a novel fatty acid-based chloromethyl ketone designed to target Ras endoprotease. Ann N Y Acad Sci 886: 103-108.

Chiu W, Niwa Y, Zeng W, Hirano T, Kobayashi H and Sheen J (1996) Engineered GFP as a vital reporter in plants. Curr Biol 6(3): 325-330.

Choy E, Chiu VK, Silletti J, Feoktistov M, Morimoto T, Michaelson D, Ivanov IE and Philips MR (1999) Endomembrane trafficking of ras: the CAAX motif targets proteins to the ER and Golgi. Cell 98(1): 69-80.

Christian AE, Byun HS, Zhong N, Wanunu M, Marti T, Furer A, Diederich F, Bittman R and Rothblat GH (1999) Comparison of the capacity of beta-cyclodextrin derivatives and cyclophanes to shuttle cholesterol between cells and serum lipoproteins. J Lipid Res 40(8): 1475-1482.

Christianson DW (2006) Structural biology and chemistry of the terpenoid cyclases. Chem Rev 106(8): 3412-3442.

Christman JK (2002) 5-Azacytidine and 5-aza-2'-deoxycytidine as inhibitors of DNA methylation: Mechanistic studies and their implications for cancer therapy. Oncogene 21(35): 5483-5495.

Chung MC, Ferreira EI, Santos JL, Giarolla J, Rando DG, Almeida AE, Bosquesi PL, Menegon RF and Blau L (2008) Prodrugs for the treatment of neglected diseases. Molecules 13(3): 616-677.

Clarke S (1992) Protein isoprenylation and methylation at carboxy-terminal cysteine residues. Annu Rev Biochem 61: 355-386.

Cokol M, Nair R and Rost B (2000) Finding nuclear localization signals. EMBO Rep 1(5): 411-415.

Colman-Lerner A, Gordon A, Serra E, Chin T, Resnekov O, Endy D, Pesce CG and Brent R (2005) Regulated cell-to-cell variation in a cell-fate decision system. Nature 437(7059): 699-706.

Connolly JD and Hill RA (1991) Dictionary of Terpenoids. London: Chapman and Hall.

Cordoba E, Salmi M and Leon P (2009) Unravelling the regulatory mechanisms that modulate the MEP pathway in higher plants. J Exp Bot 60(10): 2933-2943.

Corey EJ, Matsuda SP and Bartel B (1993) Isolation of an *Arabidopsis thaliana* gene encoding cycloartenol synthase by functional expression in a yeast mutant lacking lanosterol synthase by the use of a chromatographic screen. Proc Natl Acad Sci U S A 90(24): 11628-11632.

Corey EJ, Matsuda SP, Baker CH, Ting AY and Cheng H (1996) Molecular cloning of a *Schizosaccharomyces pombe* cDNA encoding lanosterol synthase and investigation of conserved tryptophan residues. Biochem Biophys Res Commun 219(2): 327-331.

Courdavault V, Burlat V, St-Pierre B and Giglioli-Guivarc'h N (2009) Proteins prenylated by type I protein geranylgeranyltransferase act positively on the jasmonate signalling pathway triggering the biosynthesis of monoterpene indole alkaloids in *Catharanthus roseus*. Plant Cell Rep 28(1): 83-93.

Cox AD, Garcia AM, Westwick JK, Kowalczyk JJ, Lewis MD, Brenner DA and Der CJ (1994) The CAAX peptidomimetic compound B581 specifically blocks farnesylated, but not geranylgeranylated or myristylated, oncogenic ras signaling and transformation. J Biol Chem 269(30): 19203-19206.

Crane CM, Kaiser J, Ramsden NL, Lauw S, Rohdich F, Eisenreich W, Hunter WN, Bacher A and Diederich F (2006) Fluorescent inhibitors for IspF, an enzyme in the non-mevalonate pathway for isoprenoid biosynthesis and a potential target for antimalarial therapy. Angew Chem Int Ed Engl 45(7): 1069-1074.

Croteau R (1987) Biosynthesis and catabolism of monoterpenoids. Chem Rev 87: 929-954.

Croteau R, Kutchan T and Lewis N (2000) Natural products (secondary metabolites), Biochemistry and Molecular Biology of Plants. In: Buchanan B, Gruissem W, Jones R, editors. Biochemistry and Molecular Biology of Plants. Rockville, MD: American Society of Plant Biologists. pp. 1250-1268.

Crowell DN (2000) Functional implications of protein isoprenylation in plants. Prog Lipid Res 39: 393-408.

Crowell DN and Kennedy M (2001) Identification and functional expression in yeast of a prenylcysteine alpha-carboxyl methyltransferase gene from *Arabidopsis thaliana*. Plant Mol Biol 45(4): 469-476.

Crowell DN and Huizinga DH (2009) Protein isoprenylation: the fat of the matter. Trends in Plant Science 14(3): 163-170.

Cunillera N, Boronat A and Ferrer A (1997) The *Arabidopsis thaliana FPS1* gene generates a novel mRNA that encodes a mitochondrial farnesyl-diphosphate synthase isoform. J Biol Chem 272(24): 15381-15388.

Cunillera N, Arro M, Delourme D, Karst F, Boronat A and Ferrer A (1996) *Arabidopsis thaliana* contains two differentially expressed farnesyl-diphosphate synthase genes. J Biol Chem 271(13): 7774-7780.

Cutler S, Ghassemian M, Bonetta D, Cooney S and McCourt P (1996) A protein farnesyl transferase involved in abscisic acid signal transduction in *Arabidopsis*. Science 273: 1239-1241.

Dagert M and Ehrlich SD (1979) Prolonged incubation in calcium chloride improves the competence of *Escherichia coli* cells. Gene 6(1): 23-28.

De Wilde C, Van Houdt H, De Buck S, Angenon G, De Jaeger G and Depicker A (2000) Plants as bioreactors for protein production: avoiding the problem of transgene silencing. Plant Mol Biol 43(2-3): 347-359.

Deem AK, Bultema RL and Crowell DN (2006) Prenylcysteine methylesterase in *Arabidopsis thaliana*. Gene 380(2): 159-166.

Degenhardt J, Gershenzon J, Baldwin IT and Kessler A (2003) Attracting friends to feast on foes: engineering terpene emission to make crop plants more attractive to herbivore enemies. Curr Opin Biotechnol 14(2): 169-176.

Devon TK and Scott AI (1972) Handbook of Naturally Occuring Compounds. New York: Academic Press.

Dewick PM (2002) The biosynthesis of C5-C25 terpenoid compounds. Nat Prod Rep 19(2): 181-222.

Dhiman RK, Schaeffer ML, Bailey AM, Testa CA, Scherman H and Crick DC (2005) 1-Deoxy-D-xylulose 5-phosphate reductoisomerase (IspC) from *Mycobacterium tuberculosis*: towards understanding mycobacterial resistance to fosmidomycin. J Bacteriol 187(24): 8395-8402.

Dhonukshe P, Mathur J, Hulskamp M and Gadella TW, Jr. (2005) Microtubule plus-ends reveal essential links between intracellular polarization and localized modulation of endocytosis during division-plane establishment in plant cells. BMC Biol 3: 11.

Dingwall C and Laskey RA (1991) Nuclear targeting sequences--a consensus? Trends Biochem Sci 16(12): 478-481.

Dingwall C and Laskey R (1992) The nuclear membrane. Science 258(5084): 942-947.

Disch A, Hemmerlin A, Bach TJ and Rohmer M (1998a) Mevalonate-derived isopentenyl diphosphate is the biosynthetic precursor of ubiquinone prenyl side chain in tobacco BY-2 cells. Biochem J 331 (Pt 2): 615-621.

Disch A, Schwender J, Muller C, Lichtenthaler HK and Rohmer M (1998b) Distribution of the mevalonate and glyceraldehyde phosphate/pyruvate pathways for isoprenoid biosynthesis in

unicellular algae and the cyanobacterium *Synechocystis* PCC 6714. Biochem J 333 (Pt 2): 381-388.

Dohi K, Nishikiori M, Tamai A, Ishikawa M, Meshi T and Mori M (2006) Inducible virus-mediated expression of a foreign protein in suspension-cultured plant cells. Arch Virol 151(6): 1075-1084.

Dondorp AM, Yeung S, White L, Nguon C, Day NP, Socheat D and von Seidlein L (2010) Artemisinin resistance: current status and scenarios for containment. Nat Rev Microbiol 8(4): 272-280.

Dong A, Xin H, Yu Y, Sun C, Cao K and Shen WH (2002) The subcellular localization of an unusual rice calmodulin isoform, OsCaM61, depends on its prenylation status. Plant Mol Biol 48(3): 203-210.

Down RE, Ford L, Bedford SJ, Gatehouse LN, Newell C, Gatehouse JA and Gatehouse AMR (2001) Influence of plant development and environment on transgene expression in potato and consequences for insect resistance. Transgenic Research 10(3): 223-236.

Downward J (2003) Targeting RAS signalling pathways in cancer therapy. Nat Rev Cancer 3(1): 11-22.

Dudareva N, Andersson S, Orlova I, Gatto N, Reichelt M, Rhodes D, Boland W and Gershenzon J (2005) The nonmevalonate pathway supports both monoterpene and sesquiterpene formation in snapdragon flowers. Proc Natl Acad Sci U S A 102(3): 933-938.

Duetz WA, Ruedi L, Hermann R, O'Connor K, Buchs J and Witholt B (2000) Methods for intense aeration, growth, storage, and replication of bacterial strains in microtiter plates. Appl Environ Microbiol 66(6): 2641-2646.

Dufourc EJ (2008) The role of phytosterols in plant adaptation to temperature. Plant Signal Behav 3(2): 133-134.

Dufresne C, Wilson KE, Singh SB, Zink DL, Bergstrom JD, Rew D, Polishook JD, Meinz M, Huang L, Silverman KC and et al. (1993) Zaragozic acids D and D2: potent inhibitors of squalene synthase and of Ras farnesyl-protein transferase. J Nat Prod 56(11): 1923-1929.

Duke SO and Paul RN (1986) Effects of dimethazone (FMC 57020) on chloroplast development. I. Ultrastructural effects in cowpea (*Vigna unguiculata* L.) primary leaves. Pesticide Biochemistry and Physiology 25: 1-10.

Duke SO and Kenyon WH (1986) Effects of dimethazone (FMC 57020) on chloroplast development. II. Pigment synthesis and photosynthetic function in cowpea (*Vigna unguiculata* L.) primary leaves. Pesticide Biochemistry and Physiology 25: 11-17.

Duke SO, Kenyon WH and Paul RN (1985) FMC 57020 effects on chloroplast development in pitted morningglory (*Ipomea lacunose*) cotyledons. Weed Sci 33 786-794.

Dunn JJ, Krippl B, Bernstein KE, Westphal H and Studier FW (1988) Targeting bacteriophage T7 RNA polymerase to the mammalian cell nucleus. Gene 68(2): 259-266.

Dunn KW and Wang E (2000) Optical aberrations and objective choice in multicolor confocal microscopy. Biotechniques 28(3): 542-544, 546, 548-550.

Duvold T, Cali P, Bravo JM and Rohmer M (1997) Incorporation of 2-*C*-methyl-D-erythritol, a putative isoprenoid precursor in the mevalonate-independent pathway, into ubiquinone and menaquinone of *Escherichia coli*. Tetrahedron Lett 38: 6181-6184.

Dykema PE, Sipes PR, Marie A, Biermann BJ, Crowell DN and Randall SK (1999) A new class of proteins capable of binding transition metals. Plant Mol Biol 41(1): 139-150.

Eberhardt NL and Rilling HC (1975) Prenyltransferase from *Saccharomyces cerevisiae*. Purification to homogeneity and molecular properties. J Biol Chem 250(3): 863-866.

Edwards PA and Ericsson J (1999) Sterols and isoprenoids: signaling molecules derived from the cholesterol biosynthetic pathway. Annu Rev Biochem 68: 157-185.

Eggert US, Kiger AA, Richter C, Perlman ZE, Perrimon N, Mitchison TJ and Field CM (2004) Parallel chemical genetic and genome-wide RNAi screens identify cytokinesis inhibitors and targets. PLoS Biol 2(12): e379.

Eisenreich W, Rohdich F and Bacher A (2001) Deoxyxylulose phosphate pathway to terpenoids. Trends Plant Sci 6(2): 78-84.

Eisenreich W, Bacher A, Arigoni D and Rohdich F (2004) Biosynthesis of isoprenoids via the non-mevalonate pathway. Cell Mol Life Sci 61(12): 1401-1426.

ElNaggar SF, Creekmore RW, Schocken MJ, Rosen RT and Robinson RA (1992) Metabolism of clomazone herbicide in soybean. J Agric Food Chem 40: 880-883.

Elowitz MB, Levine AJ, Siggia ED and Swain PS (2002) Stochastic gene expression in a single cell. Science 297(5584): 1183-1186.

Enfissi EM, Fraser PD, Lois LM, Boronat A, Schuch W and Bramley PM (2005) Metabolic engineering of the mevalonate and non-mevalonate isopentenyl diphosphate-forming pathways for the production of health-promoting isoprenoids in tomato. Plant Biotechnol J 3(1): 17-27.

Enjuto M, Lumbreras V, Marin C and Boronat A (1995) Expression of the *Arabidopsis* HMG2 gene, encoding 3-hydroxy-3-methylglutaryl coenzyme A reductase, is restricted to meristematic and floral tissues. Plant Cell 7(5): 517-527.

Enjuto M, Balcells L, Campos N, Caelles C, Arró M and Boronat A (1994) *Arabidopsis thaliana* contains two differentially expressed 3-hydroxy-3-methylglutaryl-CoA reductase genes, which encode microsomal forms of the enzyme. Proc Natl Acad Sci U S A 91(3): 927-931.

Eoh H, Narayanasamy P, Brown AC, Parish T, Brennan PJ and Crick DC (2009) Expression and characterization of soluble 4-diphosphocytidyl-2-*C*-methyl-D-erythritol kinase from bacterial pathogens. Chem Biol 16(12): 1230-1239.

Eoh H, Brown AC, Buetow L, Hunter WN, Parish T, Kaur D, Brennan PJ and Crick DC (2007) Characterization of the *Mycobacterium tuberculosis* 4-diphosphocytidyl-2-*C*-methyl-D-erythritol synthase: potential for drug development. J Bacteriol 189(24): 8922-8927.

Estévez JM, Cantero A, Reindl A, Reichler S and León P (2001) 1-Deoxy-D-xylulose-5-phosphate synthase, a limiting enzyme for plastidic isoprenoid biosynthesis in plants. J Biol Chem 276(25): 22901-22909.

Estévez JM, Cantero A, Romero C, Kawaide H, Jiménez LF, Kuzuyama T, Seto H, Kamiya Y and León P (2000) Analysis of the expression of *CLA1*, a gene that encodes the 1-deoxyxylulose 5-phosphate synthase of the 2-*C*-methyl-D-erythritol-4-phosphate pathway in Arabidopsis. Plant Physiol 124(1): 95-104.

Ettmayer P, Amidon GL, Clement B and Testa B (2004) Lessons learned from marketed and investigational prodrugs. J Med Chem 47(10): 2393-2404.

Eubanks LM and Poulter CD (2003) *Rhodobacter capsulatus* 1-deoxy-D-xylulose 5-phosphate synthase: steady-state kinetics and substrate binding. Biochemistry 42(4): 1140-1149.

Fahrenkrog B and Aebi U (2003) The nuclear pore complex: nucleocytoplasmic transport and beyond. Nat Rev Mol Cell Biol 4(10): 757-766.

Feldherr CM, Kallenbach E and Schultz N (1984) Movement of a karyophilic protein through the nuclear pores of oocytes. J Cell Biol 99(6): 2216-2222.

Fellermeier M, Kis K, Sagner S, Maier U, Bacher A and Zenk MH (1999) Cell-free conversion of 1-deoxy-D-xylulose 5-phosphate and 2-C-methyl-D-erythritol 4-phosphate into β-carotene in higher plants and its inhibition by fosmidomycin. Tetrahedron Lett 40: 2743-2746.

Fenech M (2005) *In vitro* micronucleus technique to predict chemosensitivity. Methods Mol Med 111: 3-32.

Ferhatoglu Y and Barrett M (2006) Studies of clomazone mode of action. Pesticide Biochemistry and Physiology 85(1): 7-14.

Ferhatoglu Y, Avdiushko S and Barrett M (2005) The basis for the safening of clomazone by phorate insecticide in cotton and inhibitors of cytochrome P450s. Pesticide Biochemistry and Physiology 81: 59-70.

Finnegan EJ, Brettell RI and Dennis ES (1993) The role of DNA methylation in the regulation of plant gene expression. Exs 64: 218-261.

Finnegan EJ, Genger RK, Peacock WJ and Dennis ES (1998) DNA Methylation in Plants. Annu Rev Plant Physiol Plant Mol Biol 49: 223-247.

Fischer AJ, Bayer DE, Carriere MD, Ateh CM and Yim KO (2000) Mechanisms of resistance to bispyribac-sodium in an *Echinochloa phyllopogon* accession. Pesticide Biochemistry and Physiology 68: 156-165.

Fischer U, Kuhlmann M, Pecinka A, Schmidt R and Mette MF (2008) Local DNA features affect RNA-directed transcriptional gene silencing and DNA methylation. Plant J 53(1): 1-10.

Fisk TL, Lundberg BE, Guest JL, Ray S, Barrett TJ, Holland B, Stamey K, Angulo FJ and Farley MM (2005) Invasive infection with multidrug-resistant *Salmonella enterica* serotype typhimurium definitive type 104 among HIV-infected adults. Clin Infect Dis 40(7): 1016-1021.

Fitzpatrick TB, Amrhein N, Kappes B, Macheroux P, Tews I and Raschle T (2007) Two independent routes of de novo vitamin B6 biosynthesis: not that different after all. Biochem J 407(1): 1-13.

Flesch G and Rohmer M (1988) Prokaryotic hopanoids: the biosynthesis of the bacteriohopane skeleton. Formation of isoprenic units from two distinct acetate pools and a novel type of carbon/carbon linkage between a triterpene and D-ribose. Eur J Biochem 175(2): 405-411.

Flores-Sánchez IJ, Ortega-López J, del Carmen Montes-Horcasitas M and Ramos-Valdivia AC (2002) Biosynthesis of sterols and triterpenes in cell suspension cultures of *Uncaria tomentosa*. Plant Cell Physiol 43(12): 1502-1509.

Flournoy DS and Frey PA (1989) Inactivation of the pyruvate dehydrogenase complex of *Escherichia coli* by fluoropyruvate. Biochemistry 28(25): 9594-9602.

FMC corporation APG, Philadelphia PA (2001) Command 3ME label.

Fontana A, Kelly MT, Prasad JD and Anderson RJ (2001) Evidence for the biosynthesis of squalene *via* the methylerythritol phosphate pathway in a *Streptomyces* sp. obtained from a marine sediment. J Org Chem 66: 6202-6206.

Foster LJ, de Hoog CL, Zhang Y, Zhang Y, Xie X, Mootha VK and Mann M (2006) A mammalian organelle map by protein correlation profiling. Cell 125(1): 187-199.

Fox SJ (2006) A History of High-Throughput Screening for Drug Discovery: A Special Report Summarizing Six Comprehensive Industry Studies in the Years 1998-2005. Moraga, CA.

Francis KE and Spiker S (2005) Identification of *Arabidopsis thaliana* transformants without selection reveals a high occurrence of silenced T-DNA integrations. Plant J 41(3): 464-477.

Freeman MR and Solomon KR (2004) Cholesterol and prostate cancer. J Cell Biochem 91(1): 54-69.

Freiberg C, Wieland B, Spaltmann F, Ehlert K, Brotz H and Labischinski H (2001) Identification of novel essential *Escherichia coli* genes conserved among pathogenic bacteria. J Mol Microbiol Biotechnol 3(3): 483-489.

Furfine ES, Leban JJ, Landavazo A, Moomaw JF and Casey PJ (1995) Protein farnesyltransferase: kinetics of farnesyl pyrophosphate binding and product release. Biochemistry 34(20): 6857-6862.

Gabrielsen M, Kaiser J, Rohdich F, Eisenreich W, Laupitz R, Bacher A, Bond CS and Hunter WN (2006) The crystal structure of a plant 2*C*-methyl-D-erythritol 4-phosphate cytidylyltransferase exhibits a distinct quaternary structure compared to bacterial homologues and a possible role in feedback regulation for cytidine monophosphate. Febs J 273(5): 1065-1073.

Galichet A and Gruissem W (2003) Protein farnesylation in plants-conserved mechanisms but different targets. Curr Opin Plant Biol 6: 530-535.

Galichet A and Gruissem W (2006) Developmentally controlled farnesylation modulates AtNAP1;1 function in cell proliferation and cell expansion during *Arabidopsis* leaf development. Plant Physiol 142(4): 1412-1426.

Galichet A, Hoyerová K, Kamínek M and Gruissem W (2008) Farnesylation directs AtIPT3 subcellular localization and modulates cytokinin biosynthesis in *Arabidopsis*. Plant Physiol 146(3): 1155-1164.

Ganjewala D, Kumar S and Luthra R (2009) An Account of Cloned Genes of Methyl-erythritol-4-phosphate Pathway of Isoprenoid Biosynthesis in Plants. Curr Issues Mol Biol 11 (Suppl 1): i35-45.

Garcia AM, Rowell C, Ackermann K, Kowalczyk JJ and Lewis MD (1993) Peptidomimetic inhibitors of Ras farnesylation and function in whole cells. J Biol Chem 268(25): 18415-18418.

Gardner MJ, Hall N, Fung E, White O, Berriman M, Hyman RW, Carlton JM, Pain A, Nelson KE, Bowman S, Paulsen IT, James K, Eisen JA, Rutherford K, Salzberg SL, Craig A, Kyes S, Chan MS, Nene V, Shallom SJ, Suh B, Peterson J, Angiuoli S, Pertea M, Allen J, Selengut J, Haft D, Mather MW, Vaidya AB, Martin DM, Fairlamb AH, Fraunholz MJ, Roos DS, Ralph SA, McFadden GI, Cummings LM, Subramanian GM, Mungall C, Venter JC, Carucci DJ, Hoffman SL, Newbold C, Davis RW, Fraser CM and Barrell B (2002) Genome sequence of the human malaria parasite *Plasmodium falciparum*. Nature 419(6906): 498-511.

Gardner RG, Shan H, Matsuda SP and Hampton RY (2001) An oxysterol-derived positive signal for 3-hydroxy- 3-methylglutaryl-CoA reductase degradation in yeast. J Biol Chem 276(12): 8681-8694.

Gasteiger E, Gattiker A, Hoogland C, Ivanyi I, Appel RD and Bairoch A (2003) ExPASy: The proteomics server for in-depth protein knowledge and analysis. Nucleic Acids Res 31(13): 3784-3788.

Gatz C (1997) Chemical Control of Gene Expression. Annu Rev Plant Physiol Plant Mol Biol 48: 89-108.

Gatz C, Frohberg C and Wendenburg R (1992) Stringent repression and homogeneous de-repression by tetracycline of a modified CaMV 35S promoter in intact transgenic tobacco plants. Plant J 2(3): 397-404.

Gavin AC, Aloy P, Grandi P, Krause R, Boesche M, Marzioch M, Rau C, Jensen LJ, Bastuck S, Dumpelfeld B, Edelmann A, Heurtier MA, Hoffman V, Hoefert C, Klein K, Hudak M, Michon AM, Schelder M, Schirle M, Remor M, Rudi T, Hooper S, Bauer A, Bouwmeester T, Casari G, Drewes G, Neubauer G, Rick JM, Kuster B, Bork P, Russell RB and Superti-Furga G (2006) Proteome survey reveals modularity of the yeast cell machinery. Nature 440(7084): 631-636.

Geelen DN and Inze DG (2001) A bright future for the bright yellow-2 cell culture. Plant Physiol 127(4): 1375-1379.

Georgiev M, Pavlov A and Ilieva M (2004) Rosmarinic acid production by *Lavandula vera* MM cell suspension: the effect of temperature. . Biotechnol Lett 26: 855-856.

Georgiev M, Pavlov A and Ilieva M (2006) Selection of high rosmarinic acid producing *Lavandula vera* MM cell lines. Process Biochemistry 41(9): 2068-2071.

Georgiev MI, Weber J and Maciuk A (2009) Bioprocessing of plant cell cultures for mass production of targeted compounds. Appl Microbiol Biotechnol 83(5): 809-823.

Gerber E (2005) Localisation cellulaire de protéines fluorescentes isoprénylables dans les cellules de tabac BY-2. [Thèse doctorale]. Strasbourg: Université Louis Pasteur (ULP).

Gerber E, Hemmerlin A, Hartmann M, Heintz D, Hartmann MA, Mutterer J, Rodriguez-Concepcion M, Boronat A, Van Dorsselaer A, Rohmer M, Crowell DN and Bach TJ (2009) The plastidial 2-*C*-methyl-D-erythritol 4-phosphate pathway provides the isoprenyl moiety for protein geranylgeranylation in tobacco BY-2 cells. Plant Cell 21(1): 285-300.

Gershenzon J and Kreis W (1999) Biochemistry of terpenoids: Monoterpenes, sesquiterpenes, diterpenes, sterols, cardiac glycosides and steroid saponins. Annual Plant Reviews: Biochemistry of Plant Secondary Metabolism. Wink, M. ed: Sheffield Academic Press. pp. 222-299.

Gershenzon J and Dudareva N (2007) The function of terpene natural products in the natural world. Nat Chem Biol 3(7): 408-414.

Gibbs JB, Pompliano DL, Mosser SD, Rands E, Lingham RB, Singh SB, Scolnick EM, Kohl NE and Oliff A (1993) Selective inhibition of farnesyl-protein transferase blocks ras processing in vivo. J Biol Chem 268(11): 7617-7620.

Giuliano KA, Haskins JR and Taylor DL (2003) Advances in high content screening for drug discovery. Assay Drug Dev Technol 1(4): 565-577.

Giuliano KA, DeBiasio RL, Dunlay RT, Gough A, Volosky JM and Zock J (1997) High-Content Screening: a new approach to easing key bottlenecks in the drug discovery process. J Biomol Screen 2: 249-259.

Glasby JS (1982) Encyclopedia of the Terpenoids. Chichester, England: John Wiley and Sons.

Goldstein JL and Brown MS (1990) Regulation of the mevalonate pathway. Nature 343(6257): 425-430.

Goodwin JS, Drake KR, Rogers C, Wright L, Lippincott-Schwartz J, Philips MR and Kenworthy AK (2005) Depalmitoylated Ras traffics to and from the Golgi complex via a nonvesicular pathway. J Cell Biol 170(2): 261-272.

Gordon A, Colman-Lerner A, Chin TE, Benjamin KR, Yu RC and Brent R (2007) Single-cell quantification of molecules and rates using open-source microscope-based cytometry. Nat Methods 4(2): 175-181.

Görlich D and Kutay U (1999) Transport between the cell nucleus and the cytoplasm. Annu Rev Cell Dev Biol 15: 607-660.

Görlich D, Prehn S, Laskey RA and Hartmann E (1994) Isolation of a protein that is essential for the first step of nuclear protein import. Cell 79(5): 767-778.

Görlich D, Kostka S, Kraft R, Dingwall C, Laskey RA, Hartmann E and Prehn S (1995) Two different subunits of importin cooperate to recognize nuclear localization signals and bind them to the nuclear envelope. Curr Biol 5(4): 383-392.

Grabinska K and Palamarczyk G (2002) Dolichol biosynthesis in the yeast *Saccharomyces cerevisiae*: an insight into the regulatory role of farnesyl diphosphate synthase. FEMS Yeast Res 2(3): 259-265.

Grebe M, Xu J, Mobius W, Ueda T, Nakano A, Geuze HJ, Rook MB and Scheres B (2003) *Arabidopsis* sterol endocytosis involves actin-mediated trafficking via ARA6-positive early endosomes. Curr Biol 13(16): 1378-1387.

Guevara-Garciá A, San Román C, Arroyo A, Cortés ME, de la Luz Gutiérrez-Nava M and León P (2005) Characterization of the Arabidopsis *clb6* mutant illustrates the importance of posttranscriptional regulation of the methyl-D-erythritol 4-phosphate pathway. Plant Cell 17(2): 628-643.

Guo DA, Venkatramesh M and Nes WD (1995) Developmental regulation of sterol biosynthesis in *Zea mays*. Lipids 30(3): 203-219.

Gururaja TL, Goff D, Kinoshita T, Goldstein E, Yung S, McLaughlin J, Pali E, Huang J, Singh R, Daniel-Issakani S, Hitoshi Y, Cooper RD and Payan DG (2006) R-253 disrupts microtubule networks in multiple tumor cell lines. Clin Cancer Res 12(12): 3831-3842.

Guy RK (2000) Inhibition of sonic hedgehog autoprocessing in cultured mammalian cells by sterol deprivation. Proc Natl Acad Sci U S A 97(13): 7307-7312.

Haemers T, Wiesner J, Poecke SV, Goeman J, Henschker D, Beck E, Jomaa H and Calenbergh SV (2006) Synthesis of [alpha]-substituted fosmidomycin analogues as highly potent *Plasmodium falciparum* growth inhibitors. Bioorganic & Medicinal Chemistry Letters 16(7): 1888-1891.

Hahn FM, Eubanks LM, Testa CA, Blagg BS, Baker JA and Poulter CD (2001) 1-Deoxy-D-xylulose 5-phosphate synthase, the gene product of open reading frame (ORF) 2816 and ORF 2895 in *Rhodobacter capsulatus*. J Bacteriol 183(1): 1-11.

Hall MN, Craik C and Hiraoka Y (1990) Homeodomain of yeast repressor alpha 2 contains a nuclear localization signal. Proc Natl Acad Sci U S A 87(18): 6954-6958.

Halpin C (2005) Gene stacking in transgenic plants--the challenge for 21st century plant biotechnology. Plant Biotechnol J 3(2): 141-155.

Han HK and Amidon GL (2000) Targeted prodrug design to optimize drug delivery. AAPS PharmSci 2(1): E6.

Hancock JF (2003) Ras proteins: different signals from different locations. Nat Rev Mol Cell Biol 4(5): 373-384.

Hancock JF (2006) Lipid rafts: contentious only from simplistic standpoints. Nat Rev Mol Cell Biol 7(6): 456-462.

Hancock JF, Paterson H and Marshall CJ (1990) A polybasic domain or palmitoylation is required in addition to the CAAX motif to localize p21ras to the plasma membrane. Cell 63(1): 133-139.

Hancock JF, Magee AI, Childs JE and Marshall CJ (1989) All ras proteins are polyisoprenylated but only some are palmitoylated. Cell 57(7): 1167-1177.

Hancock JF, Cadwallader KA, Paterson H and Marshall CJ (1991) A CAAX or a CAAL motif and a second signal are sufficient for plasma membrane targeting of RAS proteins. EMBO J 10(13): 4033-4039.

Harborne JB (1990) Role of secondary metabolites in chemical defence mechanisms in plants. Ciba Found Symp 154: 126-134; discussion 135-129.

Harker M and Bramley PM (1999) Expression of prokaryotic 1-deoxy-D-xylulose-5-phosphatases in *Escherichia coli* increases carotenoid and ubiquinone biosynthesis. FEBS Lett 448(1): 115-119.

Harker M, Hellyer A, Clayton JC, Duvoix A, Lanot A and Safford R (2003) Co-ordinate regulation of sterol biosynthesis enzyme activity during accumulation of sterols in developing rape and tobacco seed. Planta 216(4): 707-715.

Hartmann MA (1998) Plant sterols and the membrane environment. Trends Plant Sci 3: 170-175.

Hartmann MA and Benveniste P (1987) Plant membrane sterols: isolation, identification and biosynthesis. Methods Enzymol 148:: 632-650.

Hartmann MA and Bach TJ (2001) Incorporation of all-*trans*-farnesol into sterols and ubiquinone in *Nicotiana tabacum* L. cv Bright Yellow-2 cell cultures. Tetrahedron Lett 42: 655-657.

Hartmann MA, Wentzinger L, Hemmerlin A and Bach TJ (2000) Metabolism of farnesyl diphosphate in tobacco BY-2 cells treated with squalestatin. Biochem Soc Trans 28(6): 794-796.

Hasunuma T, Takeno S, Hayashi S, Sendai M, Bamba T, Yoshimura S, Tomizawa K, Fukusaki E and Miyake C (2008) Overexpression of 1-Deoxy-D-xylulose-5-phosphate reductoisomerase gene in chloroplast contributes to increment of isoprenoid production. J Biosci Bioeng 105(5): 518-526.

Hellens R, Mullineaux P and Klee H (2000) Technical Focus: a guide to *Agrobacterium* binary Ti vectors. Trends Plant Sci 5(10): 446-451.

Hemmerlin A and Bach TJ (1998) Effects of mevinolin on cell cycle progression and viability of tobacco BY-2 cells. Plant J 14: 65-74.

Hemmerlin A and Bach TJ (2000) Farnesol-induced cell death and stimulation of 3-hydroxy-3-methylglutaryl-coenzyme A reductase activity in tobacco cv bright yellow-2 cells. Plant Physiol 123(4): 1257-1268.

Hemmerlin A, Fischt I and Bach TJ (2000) Differential interaction of branch-specific inhibitors of isoprenoid biosynthesis with cell cycle progression in tobacco BY-2 cells. Physiol Plant 110: 343-350.

Hemmerlin A, Hoeffler JF, Meyer O, Tritsch D, Kagan IA, Grosdemange-Billiard C, Rohmer M and Bach TJ (2003) Cross-talk between the cytosolic mevalonate and the plastidial methylerythritol phosphate pathways in tobacco bright yellow-2 cells. J Biol Chem 278(29): 26666-26676.

Hemmerlin A, Tritsch D, Hartmann M, Pacaud K, Hoeffler JF, van Dorsselaer A, Rohmer M and Bach TJ (2006) A cytosolic Arabidopsis D-xylulose kinase catalyzes the phosphorylation of 1-deoxy-D-xylulose into a precursor of the plastidial isoprenoid pathway. Plant Physiol 142(2): 441-457.

Hemmerlin A, Gerber E, Feldtrauer JF, Wentzinger L, Hartmann MA, Tritsch D, Hoeffler JF, Rohmer M and Bach TJ (2004) A review of tobacco BY-2 cells as an excellent system to study the synthesis and function of sterols and other isoprenoids. Lipids 39(8): 723-735.

Hemmi K, Takeno H, Hashimoto M and Kamiya T (1982) Studies on phosphonic acid antibiotics. IV. Synthesis and antibacterial activity of analogs of 3-(N-acetyl-N-hydroxyamino)-propylphosphonic acid (FR-900098). Chem Pharm Bull (Tokyo) 30(1): 111-118.

Hermann R, Lehmann M and Buchs J (2003) Characterization of gas-liquid mass transfer phenomena in microtiter plates. Biotechnol Bioeng 81(2): 178-186.

Herz S, Wungsintaweekul J, Schuhr CA, Hecht S, Luttgen H, Sagner S, Fellermeier M, Eisenreich W, Zenk MH, Bacher A and Rohdich F (2000) Biosynthesis of terpenoids: YgbB protein converts 4-diphosphocytidyl-2*C*-methyl-D-erythritol 2-phosphate to 2*C*-methyl-D-erythritol 2,4-cyclodiphosphate. Proc Natl Acad Sci U S A 97(6): 2486-2490.

Hess FD (2000) Light-dependent herbicides - an overview. Weed Sci 48: 160-170.

Hey SJ, Powers SJ, Beale MH, Hawkins ND, Ward JL and Halford NG (2006) Enhanced seed phytosterol accumulation through expression of a modified HMG-CoA reductase. Plant Biotechnol J 4(2): 219-229.

Hicks GR, Smith HM, Shieh M and Raikhel NV (1995) Three classes of nuclear import signals bind to plant nuclei. Plant Physiol 107(4): 1055-1058.

Higgins DG (1994) CLUSTAL V: multiple alignment of DNA and protein sequences. Methods Mol Biol 25: 307-318.

Himmeldirk K, Kennedy IA, Hill RE, Sayer BG and Spencer ID (1996) Biosynthesis of vitamins B_1 and B_6 in *E.coli*: concurrent incorporation of 1-deoxy-D-xylulose into thiamin (B_1) and pyridoxol (B_6). Chem Commun 10: 1187-1188.

Hinson DD, Chambliss KL, Toth MJ, Tanaka RD and Gibson KM (1997) Post-translational regulation of mevalonate kinase by intermediates of the cholesterol and nonsterol isoprene biosynthetic pathways. J Lipid Res 38(11): 2216-2223.

Hoeffler JF, Tritsch D, Grosdemange-Billiard C and Rohmer M (2002) Isoprenoid biosynthesis *via* the methylerythritol phosphate pathway. Mechanistic investigations of the 1-deoxy-D-xylulose 5-phosphate reductoisomerase. Eur J Biochem 269(18): 4446-4457.

Hoffman AF and Garippa RJ (2007) A pharmaceutical company user's perspective on the potential of high content screening in drug discovery. Methods Mol Biol 356: 19-31.

Hofmann K and Stoffel W (1993) TMbase - A database of membrane spanning proteins segments. Biol Chem Hoppe-Seyler 374: 166.

Hood JK and Silver PA (1998) Cse1p is required for export of Srp1p/importin-alpha from the nucleus in *Saccharomyces cerevisiae*. J Biol Chem 273(52): 35142-35146.

Horton P, Park KJ, Obayashi T, Fujita N, Harada H, Adams-Collier CJ and Nakai K (2007) WoLF PSORT: protein localization predictor. Nucleic Acids Res 35(Web Server issue): W585-587.

Houston JG, Banks MN, Binnie A, Brenner S, O'Connell J and Petrillo EW (2008) Case study: impact of technology investment on lead discovery at Bristol-Myers Squibb, 1998-2006. Drug Discov Today 13(1-2): 44-51.

Hsieh MH, Chang CY, Hsu SJ and Chen JJ (2008) Chloroplast localization of methylerythritol 4-phosphate pathway enzymes and regulation of mitochondrial genes in *ispD* and *ispE* albino mutants in Arabidopsis. Plant Mol Biol 66(6): 663-673.

Hughes TR, Marton MJ, Jones AR, Roberts CJ, Stoughton R, Armour CD, Bennett HA, Coffey E, Dai H, He YD, Kidd MJ, King AM, Meyer MR, Slade D, Lum PY, Stepaniants SB, Shoemaker DD, Gachotte D, Chakraburtty K, Simon J, Bard M and Friend SH (2000) Functional discovery via a compendium of expression profiles. Cell 102(1): 109-126.

Huizinga DH, Omosegbon O, Omery B and Crowell DN (2008) Isoprenylcysteine methylation and demethylation regulate abscisic acid signaling in *Arabidopsis*. Plant Cell 20(10): 2714-2728.

Hunter WN (2007) The non-mevalonate pathway of isoprenoid precursor biosynthesis. J Biol Chem 282(30): 21573-21577.

Iglesias VA, Moscone EA, Papp I, Neuhuber F, Michalowski S, Phelan T, Spiker S, Matzke M and Matzke AJ (1997) Molecular and cytogenetic analyses of stably and unstably expressed transgene loci in tobacco. Plant Cell 9(8): 1251-1264.

Initiative AG (2000) Analysis of the genome sequence of the flowering plant *Arabidopsis thaliana*. Nature 408(6814): 796-815.

Jans DA, Xiao CY and Lam MH (2000) Nuclear targeting signal recognition: a key control point in nuclear transport? Bioessays 22(6): 532-544.

Jeffrey FM, Rajagopal A, Malloy CR and Sherry AD (1991) ^{13}C-NMR: a simple yet comprehensive method for analysis of intermediary metabolism. Trends Biochem Sci 16(1): 5-10.

Jeong SY, Rose A, Joseph J, Dasso M and Meier I (2005) Plant-specific mitotic targeting of RanGAP requires a functional WPP domain. Plant J 42(2): 270-282.

Johnson CD, Chary SN, Chernoff EA, Zeng Q, Running MP and Crowell DN (2005) Protein geranylgeranyltransferase I is involved in specific aspects of abscisic acid and auxin signaling in *Arabidopsis*. Plant Physiol 139 (722-733).

Jomaa H, Wiesner J, Sanderbrand S, Altincicek B, Weidemeyer C, Hintz M, Turbachova I, Eberl M, Zeidler J, Lichtenthaler HK, Soldati D and Beck E (1999) Inhibitors of the nonmevalonate pathway of isoprenoid biosynthesis as antimalarial drugs. Science 285(5433): 1573-1576.

Jordan DL, Bollich PK, Burns AB and Walker DM (1998) Rice (*Oryza sativa*) response to clomazone. Weed Sci 46: 374-380.

Julliard JH and Douce R (1991) Biosynthesis of the thiazole moiety of thiamin (vitamin B1) in higher plant chloroplasts. Proc Natl Acad Sci U S A 88(6): 2042-2045.

Kaiser J, Yassin M, Prakash S, Safi N, Agami M, Lauw S, Ostrozhenkova E, Bacher A, Rohdich F, Eisenreich W, Safi J and Golan-Goldhirsh A (2007) Anti-malarial drug targets: screening for inhibitors of 2*C*-methyl-D-erythritol 4-phosphate synthase (IspC protein) in Mediterranean plants. Phytomedicine 14(4): 242-249.

Kajita S, Matsui C, Syono K, Suzuki M and Nagata T (1980) Fine structure of fusion bodies formed between pea root nodule and tobacco mesophyll protoplasts. Zeitschrift für Pflanzenphysiologie 97: 233-240.

Kalderon D, Roberts BL, Richardson WD and Smith AE (1984a) A short amino acid sequence able to specify nuclear location. Cell 39(3 Pt 2): 499-509.

Kalderon D, Richardson WD, Markham AF and Smith AE (1984b) Sequence requirements for nuclear location of simian virus 40 large-T antigen. Nature 311(5981): 33-38.

Kamuro Y, Kawai T and Kakiuchi T (1991) Herbicidal methods and compositions comprising fosmidomycin. In: States U, editor.

Karpen HE, Bukowski JT, Hughes T, Gratton JP, Sessa WC and Gailani MR (2001) The sonic hedgehog receptor patched associates with caveolin-1 in cholesterol-rich microdomains of the plasma membrane. J Biol Chem 276(22): 19503-19511.

Kasahara H, Hanada A, Kuzuyama T, Takagi M, Kamiya Y and Yamaguchi S (2002) Contribution of the mevalonate and methylerythritol phosphate pathways to the biosynthesis of gibberellins in *Arabidopsis*. J Biol Chem 277(47): 45188-45194.

Kaspera R and Croteau R (2006) Cytochrome P450 oxygenases of taxol biosynthesis. Phytochem Rev 5: 433-444.

Kato K, Matsumoto T, Koiwai S, Mizusaki S, Nishida K, Nogushi M and Tamaki E (1972) Liquid suspension culture of tobaco cells. In: Terui G, editor. Fermentation Technology Today. Osaka: Society of Fermentation Technology. pp. 689-695.

Keminer O and Peters R (1999) Permeability of single nuclear pores. Biophys J 77(1): 217-228.

Kieran PM, MacLoughlin PF and Malone DM (1997) Plant cell suspension cultures: some engineering considerations. Journal of Biotechnology 59(1-2): 39-52.

Kierszniowska S, Seiwert B and Schulze WX (2009) Definition of *Arabidopsis* sterol-rich membrane microdomains by differential treatment with methyl-beta-cyclodextrin and quantitative proteomics. Mol Cell Proteomics 8(4): 612-623.

Kim BR, Kim SU and Chang YJ (2005) Differential expression of three 1-deoxy-D-xylulose-5-phosphate synthase genes in rice. Biotechnol Lett 27(14): 997-1001.

Kim SM, Kuzuyama T, Chang YJ, Song KS and Kim SU (2006) Identification of class 2 1-deoxy-D-xylulose 5-phosphate synthase and 1-deoxy-D-xylulose 5-phosphate reductoisomerase genes from *Ginkgo biloba* and their transcription in embryo culture with respect to ginkgolide biosynthesis. Planta Med 72(3): 234-240.

Kim SM, Kuzuyama T, Kobayashi A, Sando T, Chang YJ and Kim SU (2008) 1-Hydroxy-2-methyl-2-(*E*)-butenyl 4-diphosphate reductase (IDS) is encoded by multicopy genes in gymnosperms *Ginkgo biloba* and *Pinus taeda*. Planta 227(2): 287-298.

Kim YB, Kim SM, Kang MK, Kuzuyama T, Lee JK, Park SC, Shin SC and Kim SU (2009) Regulation of resin acid synthesis in *Pinus densiflora* by differential transcription of genes encoding multiple 1-deoxy-D-xylulose 5-phosphate synthase and 1-hydroxy-2-methyl-2-(*E*)-butenyl 4-diphosphate reductase genes. Tree Physiol 29(5): 737-749.

Kirby J and Keasling JD (2009) Biosynthesis of plant isoprenoids: perspectives for microbial engineering. Annu Rev Plant Biol 60: 335-355.

Kirby J, Nishimoto M, Park JG, Withers ST, Nowroozi F, Behrendt D, Rutledge EJ, Fortman JL, Johnson HE, Anderson JV and Keasling JD (2010) Cloning of casbene and neocembrene synthases from *Euphorbiaceae* plants and expression in *Saccharomyces cerevisiae*. Phytochemistry 71(13): 1466-1473.

Klein TM, Harper EC, Svab Z, Sanford JC, Fromm ME and Maliga P (1988) Stable genetic transformation of intact *Nicotiana* cells by the particle bombardment process. Proc Natl Acad Sci U S A 85(22): 8502-8505.

Klumpp M, Boettcher A, Becker D, Meder G, Blank J, Leder L, Forstner M, Ottl J and Mayr LM (2006) Readout technologies for highly miniaturized kinase assays applicable to high-throughput screening in a 1536-well format. J Biomol Screen 11(6): 617-633.

Köhler S, Delwiche CF, Denny PW, Tilney LG, Webster P, Wilson RJ, Palmer JD and Roos DS (1997) A plastid of probable green algal origin in Apicomplexan parasites. Science 275(5305): 1485-1489.

Köhne S, Neumann K, Pühler A and Broer I (1998) The heat-treatment induced reduction of the *pat* gene encoded herbicide resistance in *Nicotiana tabacum* is influenced by the transgene sequence. J Plant Phsyiol 153: 631-642.

Kokwaro G (2009) Ongoing challenges in the management of malaria. Malar J 8 Suppl 1: S2.

Kola I and Landis J (2004) Can the pharmaceutical industry reduce attrition rates? Nat Rev Drug Discov 3(8): 711-715.

Konstantinopoulos PA, Karamouzis MV and Papavassiliou AG (2007) Post-translational modifications and regulation of the RAS superfamily of GTPases as anticancer targets. Nat Rev Drug Discov 6(7): 541-555.

Koppisch AT, Fox DT, Blagg BS and Poulter CD (2002) *E. coli* MEP synthase: steady-state kinetic analysis and substrate binding. Biochemistry 41(1): 236-243.

Kosugi S, Hasebe M, Matsumura N, Takashima H, Miyamoto-Sato E, Tomita M and Yanagawa H (2009) Six classes of nuclear localization signals specific to different binding grooves of importin alpha. J Biol Chem 284(1): 478-485.

Kovarik A and Fojtova M (1999) Estimation of viable cell count after fluorescein diacetate staining using phosphorimager analysis. Biotechniques 27(4): 685, 688.

Kuemmerle HP, Murakawa T and De Santis F (1987) Pharmacokinetic evaluation of fosmidomycin, a new phosphonic acid antibiotic. Chemioterapia 6(2): 113-119.

Kumagai-Sano F, Hayashi T, Sano T and Hasezawa S (2006) Cell cycle synchronization of tobacco BY-2 cells. Nat Protoc 1(6): 2621-2627.

Kuntz L, Tritsch D, Grosdemange-Billiard C, Hemmerlin A, Willem A, Bach TJ and Rohmer M (2005) Isoprenoid biosynthesis as a target for antibacterial and antiparasitic drugs: phosphonohydroxamic acids as inhibitors of deoxyxylulose phosphate reducto-isomerase. Biochem J 386(Pt 1): 127-135.

Kuroda Y, Okuhara M, Goto T, Okamoto M, Terano H, Kohsaka M, Aoki H and Imanaka H (1980) Studies on new phosphonic acid antibiotics. IV. Structure determination of FR-33289, FR-31564 and FR-32863. J Antibiot (Tokyo) 33(1): 29-35.

Kurz T, Geffken D and Wackendorff C (2003) Hydroxyurea analogues of Fosmidomycin. Z Naturforsch 58b: 106-110.

Kurz T, Schluter K, Kaula U, Bergmann B, Walter RD and Geffken D (2006) Synthesis and antimalarial activity of chain substituted pivaloyloxymethyl ester analogues of Fosmidomycin and FR900098. Bioorg Med Chem 14(15): 5121-5135.

Kutay U, Bischoff FR, Kostka S, Kraft R and Gorlich D (1997) Export of importin alpha from the nucleus is mediated by a specific nuclear transport factor. Cell 90(6): 1061-1071.

Kuthanova A, Fischer L, Nick P and Opatrny Z (2008) Cell cycle phase-specific death response of tobacco BY-2 cell line to cadmium treatment. Plant Cell Environ 31(11): 1634-1643.

Kuzuyama T (2002) Mevalonate and nonmevalonate pathways for the biosynthesis of isoprene units. Biosci Biotechnol Biochem 66(8): 1619-1627.

Kuzuyama T, Shimizu T, Takahashi S and Seto H (1998) Fosmidomycin, a specific inhibitor of 1-deoxy-D-xylulose 5-phosphate reductoisomerase in the nonmevalonate pathway for terpenoid biosynthesis. Tetrahedron Letters 39(43): 7913-7916.

Kuzuyama T, Takagi M, Takahashi S and Seto H (2000a) Cloning and characterization of 1-deoxy-D-xylulose 5-phosphate synthase from *Streptomyces* sp. Strain CL190, which uses both the mevalonate and nonmevalonate pathways for isopentenyl diphosphate biosynthesis. J Bacteriol 182(4): 891-897.

Kuzuyama T, Takahashi S, Takagi M and Seto H (2000b) Characterization of 1-deoxy-D-xylulose 5-phosphate reductoisomerase, an enzyme involved in isopentenyl diphosphate biosynthesis, and identification of its catalytic amino acid residues. J Biol Chem 275(26): 19928-19932.

Kuzuyama T, Takagi M, Kaneda K, Dairi T and Seto H (2000c) Formation of 4-(cytidine 5'-diphospho)-2-*C*-methyl-D-erythritol from 2-*C*-methyl-D-erythritol 4-phosphate by 2-*C*-methyl-D-erythritol 4-phosphate cytidylyltransferase, a new enzyme in the nonmevalonate pathway. Tetrahedron Lett 41: 703-706.

Kyte J and Doolittle RF (1982) A simple method for displaying the hydropathic character of a protein. J Mol Biol 157(1): 105-132.

LaCasse EC and Lefebvre YA (1995) Nuclear localization signals overlap DNA- or RNA-binding domains in nucleic acid-binding proteins. Nucleic Acids Res 23(10): 1647-1656.

Lamango NS (2005) Liver prenylated methylated protein methyl esterase is an organophosphate-sensitive enzyme. J Biochem Mol Toxicol 19(5): 347-357.

Lamprecht MR, Sabatini DM and Carpenter AE (2007) CellProfiler™: free, versatile software for automated biological image analysis. Biotechniques 42(1): 71-75.

Lang P, Yeow K, Nichols A and Scheer A (2006) Cellular imaging in drug discovery. Nat Rev Drug Discov 5(4): 343-356.

Lange A, Mills RE, Lange CJ, Stewart M, Devine SE and Corbett AH (2007) Classical nuclear localization signals: definition, function, and interaction with importin alpha. J Biol Chem 282(8): 5101-5105.

Lange BM and Croteau R (1999) Isoprenoid biosynthesis via a mevalonate-independent pathway in plants: cloning and heterologous expression of 1-deoxy-D-xylulose-5-phosphate reductoisomerase from peppermint. Arch Biochem Biophys 365(1): 170-174.

Lange BM and Ghassemian M (2003) Genome organization in *Arabidopsis thaliana*: a survey for genes involved in isoprenoid and chlorophyll metabolism. Plant Mol Biol 51(6): 925-948.

Lange BM, Wildung MR, McCaskill D and Croteau R (1998) A family of transketolases that directs isoprenoid biosynthesis via a mevalonate-independent pathway. Proc Natl Acad Sci U S A 95(5): 2100-2104.

Larkin MA, Blackshields G, Brown NP, Chenna R, McGettigan PA, McWilliam H, Valentin F, Wallace IM, Wilm A, Lopez R, Thompson JD, Gibson TJ and Higgins DG (2007) Clustal W and Clustal X version 2.0. Bioinformatics 23(21): 2947-2948.

Lassner MW, Jones A, Daubert S and Comai L (1991) Targeting of T7 RNA polymerase to tobacco nuclei mediated by an SV40 nuclear location signal. Plant Mol Biol 17(2): 229-234.

Laule O, Furholz A, Chang HS, Zhu T, Wang X, Heifetz PB, Gruissem W and Lange M (2003) Crosstalk between cytosolic and plastidial pathways of isoprenoid biosynthesis in *Arabidopsis thaliana*. Proc Natl Acad Sci U S A 100(11): 6866-6871.

Launholt D, Merkle T, Houben A, Schulz A and Grasser KD (2006) *Arabidopsis* chromatin-associated HMGA and HMGB use different nuclear targeting signals and display highly dynamic localization within the nucleus. Plant Cell 18(11): 2904-2918.

Lauw S, Illarionova V, Bacher A, Rohdich F and Eisenreich W (2008) Biosynthesis of isoprenoids: studies on the mechanism of 2*C*-methyl-D-erythritol-4-phosphate synthase. Febs J 275(16): 4060-4073.

Learned RM and Connolly EL (1997) Light modulates the spatial patterns of 3-hydroxy-3-methylglutaryl coenzyme A reductase gene expression in *Arabidopsis thaliana*. Plant J 11(3): 499-511.

Lee SJ, Matsuura Y, Liu SM and Stewart M (2005) Structural basis for nuclear import complex dissociation by RanGTP. Nature 435(7042): 693-696.

Lee YJ, Kim DH, Kim YW and Hwang I (2001) Identification of a signal that distinguishes between the chloroplast outer envelope membrane and the endomembrane system in vivo. Plant Cell 13(10): 2175-2190.

Lefebvre B, Furt F, Hartmann MA, Michaelson LV, Carde JP, Sargueil-Boiron F, Rossignol M, Napier JA, Cullimore J, Bessoule JJ and Mongrand S (2007) Characterization of lipid rafts from *Medicago truncatula* root plasma membranes: a proteomic study reveals the presence of a raft-associated redox system. Plant Physiol 144(1): 402-418.

Leivar P, González VM, Castel S, Trelease RN, López-Iglesias C, Arró M, Boronat A, Campos N, Ferrer A and Fernàndez-Busquets X (2005) Subcellular localization of Arabidopsis 3-hydroxy-3-methylglutaryl-coenzyme A reductase. Plant Physiol 137(1): 57-69.

Lell B, Ruangweerayut R, Wiesner J, Missinou MA, Schindler A, Baranek T, Hintz M, Hutchinson D, Jomaa H and Kremsner PG (2003) Fosmidomycin, a novel chemotherapeutic agent for malaria. Antimicrob Agents Chemother 47(2): 735-738.

Lemichez E, Wu Y, Sanchez JP, Mettouchi A, Mathur J and Chua NH (2001) Inactivation of AtRac1 by abscisic acid is essential for stomatal closure. Genes Dev 15: 1808-1816.

Lenhart A, Weihofen WA, A.E.W. P and Schulz GE (2002) Crystal Structure of a Squalene Cyclase in Complex with the Potential Anticholesteremic Drug Ro48-8071. Chem Biol 9(5): 639-645.

Levenson RM, Mansfield JR, Tsien RY, Olson ES and Wang L (2005) Multiplexing fluorescent agents with multispectral imaging: microscopy and in-vivo examples. AACR Meeting Abstracts 2005(1): 906-d-907.

Levsky JM and Singer RH (2003) Gene expression and the myth of the average cell. Trends Cell Biol 13(1): 4-6.

Levy SB and Marshall B (2004) Antibacterial resistance worldwide: causes, challenges and responses. Nat Med 10(12 Suppl): S122-129.

Li H, Shen JJ, Zheng ZL, Lin Y and Yang Z (2001) The Rop GTPase switch controls multiple developmental processes in *Arabidopsis*. Plant Physiol 126: 670-684.

Li J, Nagpal P, Vitart V, McMorris TC and Chory J (1996) A role for brassinosteroids in light-dependent development of *Arabidopsis*. Science 272(5260): 398-401.

Liao JK and Laufs U (2005) Pleiotropic effects of statins. Annu Rev Pharmacol Toxicol 45: 89-118.

Lichtenthaler HK (1999) The 1-Deoxy-D-Xylulose-5-Phosphate Pathway of Isoprenoid Biosynthesis in Plants. Annu Rev Plant Physiol Plant Mol Biol 50: 47-65.

Lichtenthaler HK, Rohmer M and Schwender J (1997a) Two independent biochemical pathways for isopentenyl diphosphate and isoprenoid biosynthesis in higher plants. Physiol Plantarum 101: 643-652.

Lichtenthaler HK, Schwender J, Disch A and Rohmer M (1997b) Biosynthesis of isoprenoids in higher plant chloroplasts proceeds via a mevalonate-independent pathway. FEBS Lett 400(3): 271-274.

Lieber A, Kiessling U and Strauss M (1989) High level gene expression in mammalian cells by a nuclear T7-phase RNA polymerase. Nucleic Acids Res 17(21): 8485-8493.

Liederer BM and Borchardt RT (2006) Enzymes involved in the bioconversion of ester-based prodrugs. J Pharm Sci 95(6): 1177-1195.

Lim L and McFadden GI (2010) The evolution, metabolism and functions of the apicoplast. Philos Trans R Soc Lond B Biol Sci 365(1541): 749-763.

Liron Y, Paran Y, Zatorsky NG, Geiger B and Kam Z (2006) Laser autofocusing system for high-resolution cell biological imaging. J Microsc 221(Pt 2): 145-151.

Liu SY, Shocken M and Rosazza JPN (1996) Microbial transformations of clomazone. J Agric Food Chem 44(313-319).

Livermore DM (2003) The threat from the pink corner. Ann Med 35(4): 226-234.

Lois LM, Rodríguez-Concepción M, Gallego F, Campos N and Boronat A (2000) Carotenoid biosynthesis during tomato fruit development: regulatory role of 1-deoxy-D-xylulose 5-phosphate synthase. Plant J 22(6): 503-513.

Lois LM, Campos N, Putra SR, Danielsen K, Rohmer M and Boronat A (1998) Cloning and characterization of a gene from *Escherichia coli* encoding a transketolase-like enzyme that catalyzes the synthesis of D-1-deoxyxylulose 5-phosphate, a common precursor for isoprenoid, thiamin, and pyridoxol biosynthesis. Proc Natl Acad Sci U S A 95(5): 2105-2110.

Loraine AE, Yalovsky S, Fabry S and Gruissem W (1996) Tomato Rab1A homologs as molecular tools for studying rab geranylgeranyl transferase in plant cells. Plant Physiol 110: 1337-1347.

Lowe PN and Perham RN (1984) Bromopyruvate as an active-site-directed inhibitor of the pyruvate dehydrogenase multienzyme complex from *Escherichia coli*. Biochemistry 23(1): 91-97.

Lüttgen H, Rohdich F, Herz S, Wungsintaweekul J, Hecht S, Schuhr CA, Fellermeier M, Sagner S, Zenk MH, Bacher A and Eisenreich W (2000) Biosynthesis of terpenoids: YchB protein of *Escherichia coli* phosphorylates the 2-hydroxy group of 4-diphosphocytidyl-2*C*-methyl-D-erythritol. Proc Natl Acad Sci U S A 97(3): 1062-1067.

Lutzov M, Beyer P and Kleining H (1990) The herbicide Command does not inhibit the prenyl diphosphate-forming enzymes in plastids. Z Naturforsch 45 856-858.

Lynen F, Eggerer H, Henning U and Kessel I (1958) Farnesyl-pyrophosphate und 3-Methyl-Δ^3-butenyl-1-pyrophosphate, die biologischen Vorstufen des Squalens. Angew Chemie 70: 738-742.

Mac Sweeney A, Lange R, Fernandes RPM, Schulz H, Dale GE, Douangamath A, Proteau PJ and Oefner C (2005) The Crystal Structure of *E. coli* 1-Deoxy-D-xylulose-5-phosphate Reductoisomerase in a Ternary Complex with the Antimalarial Compound Fosmidomycin and NADPH Reveals a Tight-binding Closed Enzyme Conformation. Journal of Molecular Biology 345(1): 115-127.

Magyar Z, De Veylder L, Atanassova A, Bakó L, Inzé D and Bögre L (2005) The role of the *Arabidopsis* E2FB transcription factor in regulating auxin-dependent cell division. Plant Cell 17(9): 2527-2541.

Mahmoud SS and Croteau RB (2001) Metabolic engineering of essential oil yield and composition in mint by altering expression of deoxyxylulose phosphate reductoisomerase and menthofuran synthase. Proc Natl Acad Sci U S A 98(15): 8915-8920.

Malumbres M and Barbacid M (2003) RAS oncogenes: the first 30 years. Nat Rev Cancer 3(6): 459-465.

Mandel MA, Feldmann KA, Herrera-Estrella L, Rocha-Sosa M and León P (1996) CLA1, a novel gene required for chloroplast development, is highly conserved in evolution. Plant J 9(5): 649-658.

Mansfield JR, Gossage KW, Hoyt CC and Levenson RM (2005) Autofluorescence removal, multiplexing, and automated analysis methods for in-vivo fluorescence imaging. J Biomed Opt 10(4): 41207.

Maréchal E and Cesbron-Delauw MF (2001) The apicoplast: a new member of the plastid family. Trends Plant Sci 6(5): 200-205.

Martin VJ, Pitera DJ, Withers ST, Newman JD and Keasling JD (2003) Engineering a mevalonate pathway in *Escherichia coli* for production of terpenoids. Nat Biotechnol 21(7): 796-802.

Masferrer A, Arró M, Manzano D, Schaller H, Fernández-Busquets X, Moncaleán P, Fernández B, Cunillera N, Boronat A and Ferrer A (2002) Overexpression of *Arabidopsis thaliana* farnesyl diphosphate synthase (FPS1S) in transgenic *Arabidopsis* induces a cell death/senescence-like response and reduced cytokinin levels. Plant J 30(2): 123-132.

Mathema B, Kurepina NE, Bifani PJ and Kreiswirth BN (2006) Molecular epidemiology of tuberculosis: current insights. Clin Microbiol Rev 19(4): 658-685.

Matsuura Y and Stewart M (2005) Nup50/Npap60 function in nuclear protein import complex disassembly and importin recycling. EMBO J 24(21): 3681-3689.

Matz MV, Fradkov AF, Labas YA, Savitsky AP, Zaraisky AG, Markelov ML and Lukyanov SA (1999) Fluorescent proteins from nonbioluminescent Anthozoa species. Nat Biotechnol 17(10): 969-973.

Matzke M, Aufsatz W, Kanno T, Daxinger L, Papp I, Mette MF and Matzke AJ (2004) Genetic analysis of RNA-mediated transcriptional gene silencing. Biochim Biophys Acta 1677(1-3): 129-141.

Mau CJD and Croteau R (2006) Cytochrome P450 oxygenases of monoterpene metabolism. Phytochem Rev 5: 373-383.

Maurer-Stroh S and Eisenhaber F (2005) Refinement and prediction of protein prenylation motifs. Genome Biol 6(6): R55.

Maurer-Stroh S, Washietl S and Eisenhaber F (2003a) Protein prenyltransferases. Genome Biol 4(4):212.

Maurer-Stroh S, Washietl S and Eisenhaber F (2003b) Protein prenyltransferases: anchor size, pseudogenes and parasites. Biol Chem 384(7): 977-989.

Maury J, Asadollahi MA, Moller K, Clark A and Nielsen J (2005) Microbial isoprenoid production: an example of green chemistry through metabolic engineering. Adv Biochem Eng Biotechnol 100: 19-51.

Mayr LM and Fuerst P (2008) The future of high-throughput screening. J Biomol Screen 13(6): 443-448.

McCaskill D and Croteau R (1993) Procedures for the isolation and quantification of the intermediates of the mevalonic acid pathway. Anal Biochem 215(1): 142-149.

McCormac AC, Elliott MC and Chen DF (1998) A simple method for the production of highly competent cells of *Agrobacterium* for transformation via electroporation. Mol Biotechnol 9(2): 155-159.

McGarvey DJ and Croteau R (1995) Terpenoid metabolism. Plant Cell 7(7): 1015-1026.

Meder D and Simons K (2005) Cell biology. Ras on the roundabout. Science 307(5716): 1731-1733.

Meigs TE and Simoni RD (1997) Farnesol as a regulator of HMG-CoA reductase degradation: characterization and role of farnesyl pyrophosphatase. Arch Biochem Biophys 345(1): 1-9.

Meng L, Ziv M and Lemaux PG (2006) Nature of stress and transgene locus influences transgene expression stability in barley. Plant Mol Biol 62(1-2): 15-28.

Menon-Rudolph S, Nishikawa S, Zeng X and Jordan F (1992) Rate of Decarboxylation, Monitored via the Key Enzyme-Bound Enamine, of Conjugated &-Keto Acids by Pyruvamide Activated Pyruvate Decarboxylase Is Kinetically Competent with Turnover. J Am ChemSoc 114(26): 10110-10112.

Meyer P, Linn F, Heidmann I, Meyer H, Niedenhof I and Saedler H (1992) Endogenous and environmental factors influence 35S promoter methylation of a maize *A1* gene construct in transgenic petunia and its colour phenotype. Mol Gen Genet 231(3): 345-352.

Miller B, Heuser T and Zimmer W (2000) Functional involvement of a deoxy-D-xylulose 5-phosphate reductoisomerase gene harboring locus of *Synechococcus leopoliensis* in isoprenoid biosynthesis. FEBS Lett 481(3): 221-226.

Miller B, Oschinski C and Zimmer W (2001) First isolation of an isoprene synthase gene from poplar and successful expression of the gene in *Escherichia coli*. Planta 213(3): 483-487.

Miller LH, Baruch DI, Marsh K and Doumbo OK (2002) The pathogenic basis of malaria. Nature 415(6872): 673-679.

Minami A, Fujiwara M, Furuto A, Fukao Y, Yamashita T, Kamo M, Kawamura Y and Uemura M (2009) Alterations in detergent-resistant plasma membrane microdomains in *Arabidopsis thaliana* during cold acclimation. Plant Cell Physiol 50(2): 341-359.

Mine Y, Kamimura T, Nonoyama S, Nishida M, Goto S and Kuwahara S (1980) *In vitro* and *in vivo* antibacterial activities of FR-31564, a new phosphonic acid antibiotic. J Antibiot (Tokyo) 33(1): 36-43.

Mitchinson DA (2005) Drug resistance in tuberculosis. Eur Respir J 25(2): 376-379.

Miyawaki A, Nagai T and Mizuno H (2005) Engineering fluorescent proteins. Adv Biochem Eng Biotechnol 95: 1-15.

Moede T, Leibiger B, Pour HG, Berggren P and Leibiger IB (1999) Identification of a nuclear localization signal, RRMKWKK, in the homeodomain transcription factor PDX-1. FEBS Lett 461(3): 229-234.

Moffat J and Sabatini DM (2006) Building mammalian signalling pathways with RNAi screens. Nat Rev Mol Cell Biol 7(3): 177-187.

Mongrand S, Morel J, Laroche J, Claverol S, Carde JP, Hartmann MA, Bonneu M, Simon-Plas F, Lessire R and Bessoule JJ (2004) Lipid rafts in higher plant cells: purification and characterization of Triton X-100-insoluble microdomains from tobacco plasma membrane. J Biol Chem 279(35): 36277-36286.

Morand OH, Aebi JD, Dehmlow H, Ji YH, Gains N, Lengsfeld H and Himber J (1997) Ro 48-8071, a new 2,3-oxidosqualene:lanosterol cyclase inhibitor lowering plasma cholesterol in hamsters, squirrel monkeys, and minipigs: comparison to simvastatin. J Lipid Res 38(2): 373-390.

Moreau P, Hartmann MA, Perret AM, Sturbois-Balcerzak B and Cassagne C (1998) Transport of sterols to the plasma membrane of leek seedlings. Plant Physiol 117(3): 931-937.

Morel J, Claverol S, Mongrand S, Furt F, Fromentin J, Bessoule JJ, Blein JP and Simon-Plas F (2006) Proteomics of plant detergent-resistant membranes. Mol Cell Proteomics 5(8): 1396-1411.

Mouritsen OG and Zuckermann MJ (2004) What's so special about cholesterol? Lipids 39(11): 1101-1113.

Mueller-Fahrnow A and Egner U (1999) Ligand-binding domain of estrogen receptors. Curr Opin Biotechnol 10(6): 550-556.

Müller C, Schwender J, Zeidler J and Lichtenthaler HK (2000) Properties and inhibition of the first two enzymes of the non-mevalonate pathway of isoprenoid biosynthesis. Biochem Soc Trans 28: 792-793.

Müller E, Lörz H and Lütticke S (1996) Variability of transgene expression in clonal cell lines of wheat. Plant Science 114(1): 71-82.

Mullis K, Faloona F, Scharf S, Saiki R, Horn G and Erlich H (1986) Specific enzymatic amplification of DNA *in vitro*: the polymerase chain reaction. Cold Spring Harb Symp Quant Biol 51 Pt 1: 263-273.

Musser JM (1995) Antimicrobial agent resistance in mycobacteria: molecular genetic insights. Clin Microbiol Rev 8(4): 496-514.

Nagata N, Suzuki M, Yoshida S and Muranaka T (2002) Mevalonic acid partially restores chloroplast and etioplast development in *Arabidopsis* lacking the non-mevalonate pathway. Planta 216(2): 345-350.

Nagata T, Nemoto Y and Hasezawa S (1992) Tobacco BY-2 cell line as the "HeLa" cell in the cell biology of higher plants. Int Rev Cytol 132: 1-30.

Nagata T, Sakamoto K and Shimizu T (2009) TOBACCO BY-2 CELLS: THE PRESENT AND BEYOND. In Vitro Cellular and Developmental Biology - Plant 40(2): 163-166.

Nah J, Song SJ and Back K (2001) Partial characterization of farnesyl and geranylgeranyl diphosphatases induced in rice seedlings by UV-C irradiation. Plant Cell Physiol 42(8): 864-867.

Nair R and Rost B (2005) Mimicking cellular sorting improves prediction of subcellular localization. J Mol Biol 348(1): 85-100.

Nair R and Rost B (2008) Protein subcellular localization prediction using artificial intelligence technology. Methods Mol Biol 484: 435-463.

Nair R, Carter P and Rost B (2003) NLSdb: database of nuclear localization signals. Nucleic Acids Res 31(1): 397-399.

Nakai K and Kanehisa M (1991) Expert system for predicting protein localization sites in gram-negative bacteria. Proteins 11(2): 95-110.

Neumann K, Droge-Laser W, Kohne S and Broer I (1997) Heat treatment results in a loss of transgene-encoded activities in several tobacco lines. Plant Physiol 115(3): 939-947.

Nocarova E and Fischer L (2009) Cloning of transgenic tobacco BY-2 cells; an efficient method to analyse and reduce high natural heterogeneity of transgene expression. BMC Plant Biol 9: 44.

Norman MA, Liebl RA and Widholm JM (1990a) Site of clomazone action in tolerant-soybean and susceptible-cotton photomixotrophic cell suspension cultures. Plant Physiol 94(2): 704-709.

Norman MA, Liebl RA and Widholm JM (1990b) Site of Clomazone Action in Tolerant-Soybean and Susceptible-Cotton Photomixotrophic Cell Suspension Cultures. Plant Physiol 94(2): 704-709.

Norman MA, Liebl RA and Widholm JM (1990c) Uptake and Metabolism of Clomazone in Tolerant-Soybean and Susceptible-Cotton Photomixotrophic Cell Suspension Cultures. Plant Physiol 92(3): 777-784.

Ohyama K, Suzuki M, Kikuchi J, Saito K and Muranaka T (2009) Dual biosynthetic pathways to phytosterol via cycloartenol and lanosterol in *Arabidopsis*. Proc Natl Acad Sci U S A 106(3): 725-730.

Okada K, Saito T, Nakagawa T, Kawamukai M and Kamiya Y (2000) Five geranylgeranyl diphosphate synthases expressed in different organs are localized into three subcellular compartments in *Arabidopsis*. Plant Physiol 122(4): 1045-1056.

Okamoto A, Kosugi A, Koizumi Y, Yanagida F and Udaka S (1997) High efficiency transformation of Bacillus brevis by electroporation. Biosci Biotechnol Biochem 61(1): 202-203.

Olliaro P and Wells TN (2009) The global portfolio of new antimalarial medicines under development. Clin Pharmacol Ther 85(6): 584-595.

Ormerod MG, Sun XM, Brown D, Snowden RT and Cohen GM (1993) Quantification of apoptosis and necrosis by flow cytometry. Acta Oncol 32(4): 417-424.

Ortmann R, Wiesner J, Reichenberg A, Henschker D, Beck E, Jomaa H and Schlitzer M (2005) Alkoxycarbonyloxyethyl ester prodrugs of FR900098 with improved in vivo antimalarial activity. Arch Pharm (Weinheim) 338(7): 305-314.

Osuna MD, Vidotto F, Fischer AJ, Bayer DE, De Prado R and Ferrero A (2002) Cross-resistance to bispyribac-sodium and bensulfuron-methyl in *Echinichloa phyllopogon* and *Cyperus difformis*. Pesticide Biochemistry and Physiology 73: 9-17.

Ozawa R, Arimura G, Takabayashi J, Shimoda T and Nishioka T (2000) Involvement of jasmonate- and salicylate-related signaling pathways for the production of specific herbivore-induced volatiles in plants. Plant Cell Physiol 41(4): 391-398.

Page JE, Hause G, Raschke M, Gao W, Schmidt J, Zenk MH and Kutchan TM (2004) Functional analysis of the final steps of the 1-deoxy-D-xylulose 5-phosphate (DXP) pathway to isoprenoids in plants using virus-induced gene silencing. Plant Physiol 134(4): 1401-1413.

Paradise EM, Kirby J, Chan R and Keasling JD (2008) Redirection of flux through the FPP branch-point in *Saccharomyces cerevisiae* by down-regulating squalene synthase. Biotechnol Bioeng 100(2): 371-378.

Parish CA, Smrcka AV and Rando RR (1995) Functional significance of beta gamma-subunit carboxymethylation for the activation of phospholipase C and phosphoinositide 3-kinase. Biochemistry 34(23): 7722-7727.

Paschold A, Halitschke R and Baldwin IT (2006) Using 'mute' plants to translate volatile signals. Plant J 45(2): 275-291.

Patel DV, Schmidt RJ, Biller SA, Gordon EM, Robinson SS and Manne V (1995) Farnesyl diphosphate-based inhibitors of Ras farnesyl protein transferase. J Med Chem 38(15): 2906-2921.

Pedraza JM and van Oudenaarden A (2005) Noise propagation in gene networks. Science 307(5717): 1965-1969.

Pei ZM, Ghassemian M, Kwak CM, McCourt P and Schroeder JI (1998) Role of farnesyltransferase in ABA regulation of guard cell anion channels and plant water loss. Science 282: 287-290.

Perlman ZE, Slack MD, Feng Y, Mitchison TJ, Wu LF and Altschuler SJ (2004) Multidimensional drug profiling by automated microscopy. Science 306(5699): 1194-1198.

Peskan T and Oelmuller R (2000) Heterotrimeric G-protein beta-subunit is localized in the plasma membrane and nuclei of tobacco leaves. Plant Mol Biol 42(6): 915-922.

Pethe K, Swenson DL, Alonso S, Anderson J, Wang C and Russell DG (2004) Isolation of *Mycobacterium tuberculosis* mutants defective in the arrest of phagosome maturation. Proc Natl Acad Sci U S A 101(37): 13642-13647.

Phillips MA, Walter MH, Ralph SG, Dabrowska P, Luck K, Uros EM, Boland W, Strack D, Rodríguez-Concepción M, Bohlmann J and Gershenzon J (2007) Functional identification and differential expression of 1-deoxy-D-xylulose 5-phosphate synthase in induced terpenoid resin formation of Norway spruce (*Picea abies*). Plant Mol Biol 65(3): 243-257.

Picard D (1993) Steroid-binding domains for regulating the functions of heterologous proteins in cis. Trends Cell Biol 3(8): 278-280.

Pichersky E and Gershenzon J (2002) The formation and function of plant volatiles: perfumes for pollinator attraction and defense. Curr Opin Plant Biol 5(3): 237-243.

Piel J, Donath J, Bandemer K and Boland W (1998) Mevalonate-independent biosynthesis of terpenoid volatiles in plants: induced and constitutive emission of volatiles. Angew Chemie Int Ed Eng 37: 2478-2481.

Prasher DC, Eckenrode VK, Ward WW, Prendergast FG and Cormier MJ (1992) Primary structure of the *Aequorea victoria* green-fluorescent protein. Gene 111(2): 229-233.

Prendergast FG and Mann KG (1978) Chemical and physical properties of aequorin and the green fluorescent protein isolated from *Aequorea forskalea*. Biochemistry 17(17): 3448-3453.

Pritchard JB, French JE, Davis BJ and Haseman JK (2003) The role of transgenic mouse models in carcinogen identification. Environ Health Perspect 111(4): 444-454.

Procopiou PA, Bailey EJ, Bamford MJ, Craven AP, Dymock BW, Houston JG, Hutson JL, Kirk BE, McCarthy AD, Sareen M and et al. (1994) The squalestatins: novel inhibitors of squalene synthase. Enzyme inhibitory activities and in vivo evaluation of C1-modified analogues. J Med Chem 37(20): 3274-3281.

Pröls F and Meyer P (1992) The methylation patterns of chromosomal integration regions influence gene activity of transferred DNA in *Petunia hybrida*. Plant J 2(4): 465-475.

Proteau PJ (2004) 1-Deoxy-D-xylulose 5-phosphate reductoisomerase: an overview. Bioorg Chem 32(6): 483-493.

Pucci MJ (2006) Use of genomics to select antibacterial targets. Biochemical Pharmacology 71(7): 1066-1072.

Qian D, Zhou D, Ju R, Cramer CL and Yang Z (1996) Protein farnesyltransferase in plants: Molecular characterization and involvement in cell cycle control. Plant Cell 8: 2381-2394.

Querol J, Rodríguez-Concepción M, Boronat A and Imperial S (2001) Essential role of residue H49 for activity of *Escherichia coli* 1-deoxy-D-xylulose 5-phosphate synthase, the enzyme catalyzing the first step of the 2-*C*-methyl-D-erythritol 4-phosphate pathway for isoprenoid synthesis. Biochem Biophys Res Commun 289(1): 155-160.

Querol J, Campos N, Imperial S, Boronat A and Rodríguez-Concepción M (2002) Functional analysis of the *Arabidopsis thaliana* GCPE protein involved in plastid isoprenoid biosynthesis. FEBS Lett 514(2-3): 343-346.

Radu A, Blobel G and Moore MS (1995) Identification of a protein complex that is required for nuclear protein import and mediates docking of import substrate to distinct nucleoporins. Proc Natl Acad Sci U S A 92(5): 1769-1773.

Raikhel N (1992) Nuclear Targeting in Plants. . Plant Physiol 100(4): 1627-1632.

Ramsden NL, Buetow L, Dawson A, Kemp LA, Ulaganathan V, Brenk R, Klebe G and Hunter WN (2008) A Structure-Based Approach to Ligand Discovery for 2*C*-Methyl-D-Erythritol-2,4-cyclodiphosphate Synthase: A Target for Antimicrobial Therapy. J Med Chem 52: 2531-2542.

Randall SK, Marshall MS and Crowell DN (1993) Protein isoprenylation in suspension-cultured tobacco cells. Plant Cell 5(4): 433-442.

Raschke M, Fellermeier M and Zenk MH (2004) A high-performance liquid chromatography method for the analysis of intermediates of the deoxyxylulose phosphate pathway. Anal Biochem 335(2): 235-243.

Raser JM and O'Shea EK (2004) Control of stochasticity in eukaryotic gene expression. Science 304(5678): 1811-1814.

Rautio J, Kumpulainen H, Heimbach T, Oliyai R, Oh D, Jarvinen T and Savolainen J (2008) Prodrugs: design and clinical applications. Nat Rev Drug Discov 7(3): 255-270.

Re EB, Jones D and Learned RM (1995) Co-expression of native and introduced genes reveals cryptic regulation of HMG CoA reductase expression in Arabidopsis. Plant J 7(5): 771-784.

Reuter K, Sanderbrand S, Jomaa H, Wiesner J, Steinbrecher I, Beck E, Hintz M, Klebe G and Stubbs MT (2002) Crystal structure of 1-deoxy-D-xylulose-5-phosphate reductoisomerase, a crucial enzyme in the non-mevalonate pathway of isoprenoid biosynthesis. J Biol Chem 277(7): 5378-5384.

Richards GR, Smith AJ, Parry F, Platts A, Chan GK, Leveridge M, Kerby JE and Simpson PB (2006) A morphology- and kinetics-based cascade for human neural cell high content screening. Assay Drug Dev Technol 4(2): 143-152.

Ro DK, Paradise EM, Ouellet M, Fisher KJ, Newman KL, Ndungu JM, Ho KA, Eachus RA, Ham TS, Kirby J, Chang MC, Withers ST, Shiba Y, Sarpong R and Keasling JD (2006) Production of the antimalarial drug precursor artemisinic acid in engineered yeast. Nature 440(7086): 940-943.

Robbins J, Dilworth SM, Laskey RA and Dingwall C (1991) Two interdependent basic domains in nucleoplasmin nuclear targeting sequence: identification of a class of bipartite nuclear targeting sequence. Cell 64(3): 615-623.

Roche Y, Gerbeau-Pissot P, Buhot B, Thomas D, Bonneau L, Gresti J, Mongrand S, Perrier-Cornet JM and Simon-Plas F (2008) Depletion of phytosterols from the plant plasma membrane provides evidence for disruption of lipid rafts. Faseb J 22(11): 3980-3991.

Rodrigues Goulart H, Kimura EA, Peres VJ, Couto AS, Aquino Duarte FA and Katzin AM (2004) Terpenes Arrest Parasite Development and Inhibit Biosynthesis of Isoprenoids in *Plasmodium falciparum*. Antimicrob Agents Chemother 48(7): 2502-2509.

Rodríguez-Concepción M (2004) The MEP pathway: a new target for the development of herbicides, antibiotics and antimalarial drugs. Curr Pharm Des 10(19): 2391-2400.

Rodríguez-Concepción M (2006) Early steps in isoprenoid biosynthesis: Multilevel regulation of the supply of common precursors in plant cells. Phytochemistry Reviews 5: 1-15.

Rodríguez-Concepción M and Boronat A (2002) Elucidation of the methylerythritol phosphate pathway for isoprenoid biosynthesis in bacteria and plastids. A metabolic milestone achieved through genomics. Plant Physiol 130(3): 1079-1089.

Rodríguez-Concepción M, Yalovsky S, Zik M, Fromm H and Gruissem W (1999) The prenylation status of a novel plant calmodulin directs plasma membrane or nuclear localization of the protein. EMBO J 18: 1996-2007.

Rodríguez-Concepción M, Toledo-Ortiz G, Yalovsky S, Caldelari D and Gruissem W (2000) Carboxyl-methylation of prenylated calmodulin CaM53 is required for efficient plasma membrane targeting of the protein. Plant J 24: 775-784.

Rodríguez-Concepción M, Ahumada I, Diez-Juez E, Sauret-Güeto S, Lois LM, Gallego F, Carretero-Paulet L, Campos N and Boronat A (2001) 1-Deoxy-D-xylulose 5-phosphate reductoisomerase and plastid isoprenoid biosynthesis during tomato fruit ripening. Plant J 27(3): 213-222.

Roerdink JBTM and Meijster A (2001) The watershed transform: definitions, algorithms and parallelization strategies. Fundam Inform 41: 187-228.

Rohdich F, Bacher A and Eisenreich W (2005) Isoprenoid biosynthetic pathways as anti-infective drug targets. Biochem Soc Trans 33(Pt 4): 785-791.

Rohdich F, Wungsintaweekul J, Fellermeier M, Sagner S, Herz S, Kis K, Eisenreich W, Bacher A and Zenk MH (1999) Cytidine 5'-triphosphate-dependent biosynthesis of isoprenoids: YgbP protein of *Escherichia coli* catalyzes the formation of 4-diphosphocytidyl-2-*C*-methylerythritol. Proc Natl Acad Sci U S A 96(21): 11758-11763.

Rohdich F, Hecht S, Gartner K, Adam P, Krieger C, Amslinger S, Arigoni D, Bacher A and Eisenreich W (2002) Studies on the nonmevalonate terpene biosynthetic pathway: metabolic role of IspH (LytB) protein. Proc Natl Acad Sci U S A 99(3): 1158-1163.

Rohdich F, Wungsintaweekul J, Luttgen H, Fischer M, Eisenreich W, Schuhr CA, Fellermeier M, Schramek N, Zenk MH and Bacher A (2000) Biosynthesis of terpenoids: 4-diphosphocytidyl-2-*C*-methyl-D-erythritol kinase from tomato. Proc Natl Acad Sci U S A 97(15): 8251-8256.

Rohmer M (1999) The discovery of a mevalonate-independent pathway for isoprenoid biosynthesis in bacteria, algae and higher plants. Nat Prod Rep 16(5): 565-574.

Rohmer M (2003) Mevalonate-independent methylerythritol phosphate pathway for isoprenoid biosynthesis. Elucidation and distribution. Pure Appl Chem 75(2-3): 375-387.

Rohmer M, Knani M, Simonin P, Sutter B and Sahm H (1993) Isoprenoid biosynthesis in bacteria: a novel pathway for the early steps leading to isopentenyl diphosphate. Biochem J 295 (Pt 2): 517-524.

Rohmer M, Seemann M, Horbach S, Bringer-Meyer S and Sahm H (1996) Glyceraldehyde 3-phosphate and pyruvate as precursors of isoprenic units in an alternative non-mevalonate pathway for terpenoid biosynthesis. J Am Chem Soc 118: 2564-2566.

Rose A and Meier I (2001) A domain unique to plant RanGAP is responsible for its targeting to the plant nuclear rim. Proc Natl Acad Sci U S A 98(26): 15377-15382.

Roskoski R, Jr. (2003) Protein prenylation: a pivotal posttranslational process. Biochem Biophys Res Commun 303(1): 1-7.

Rothblat GH, de la Llera-Moya M, Atger V, Kellner-Weibel G, Williams DL and Phillips MC (1999) Cell cholesterol efflux: integration of old and new observations provides new insights. J Lipid Res 40(5): 781-796.

Rout MP, Aitchison JD, Suprapto A, Hjertaas K, Zhao Y and Chait BT (2000) The yeast nuclear pore complex: composition, architecture, and transport mechanism. J Cell Biol 148(4): 635-651.

Rual JF, Venkatesan K, Hao T, Hirozane-Kishikawa T, Dricot A, Li N, Berriz GF, Gibbons FD, Dreze M, Ayivi-Guedehoussou N, Klitgord N, Simon C, Boxem M, Milstein S, Rosenberg J, Goldberg DS, Zhang LV, Wong SL, Franklin G, Li S, Albala JS, Lim J, Fraughton C, Llamosas E, Cevik S, Bex C, Lamesch P, Sikorski RS, Vandenhaute J, Zoghbi HY, Smolyar A, Bosak S, Sequerra R, Doucette-Stamm L, Cusick ME, Hill DE, Roth FP and Vidal M (2005) Towards a proteome-scale map of the human protein-protein interaction network. Nature 437(7062): 1173-1178.

Ruiz-Santaella JP, Heredia A and Prado RD (2006) Basis of selectivity of cyhalofop-butyl in *Oryza sativa* L. Planta 223(2): 191-199.

Running MP, Fletcher JC and Meyerowitz EM (1998) The WIGGUM gene is required for proper regulation of floral meristem size in *Arabidopsis*. Development 125: 2545-2553.

Running MP, Lavy M, Sternberg H, Galichet A, Gruissem W, Hake S, Ori N and Yalovsky S (2004) Enlarged meristems and delayed growth in *plp* mutants result from lack of CaaX prenyltransferases. Proc Natl Acad Sci U S A 101: 7815-7820.

Ruzicka L (1953) The isoprene rule and the biogenesis of terpenic compounds. Experientia 9(10): 357-367.

Ryder NS (1992) Terbinafine: mode of action and properties of the squalene epoxidase inhibition. Br J Dermatol 126 Suppl 39: 2-7.

Sacchettini JC and Poulter CD (1997) Creating isoprenoid diversity. Science 277(5333): 1788-1789.

Sagami H, Morita Y and Ogura K (1994) Purification and properties of geranylgeranyl-diphosphate synthase from bovine brain. J Biol Chem 269(32): 20561-20566.

Sakamoto Y, Furukawa S, Ogihara H and Yamasaki M (2003) Fosmidomycin resistance in adenylate cyclase deficient (*cya*) mutants of *Escherichia coli*. Biosci Biotechnol Biochem 67(9): 2030-2033.

Sallaud C, Rontein D, Onillon S, Jabès F, Duffé P, Giacalone C, Thoraval S, Escoffier C, Herbette G, Leonhardt N, Causse M and Tissier A (2009) A novel pathway for sesquiterpene biosynthesis from Z,Z-farnesyl pyrophosphate in the wild tomato *Solanum habrochaites*. Plant Cell 21(1): 301-317.

Samorski M, Muller-Newen G and Büchs J (2005) Quasi-continuous combined scattered light and fluorescence measurements: a novel measurement technique for shaken microtiter plates. Biotechnol Bioeng 92: 61-68

Sanclemente T, Marques-Lopes I, Fajó-Pascual M, Cofán M, Jarauta E, Ros E, Puzo J and García-Otín AL (2009) A moderate intake of phytosterols from habitual diet affects cholesterol metabolism. J Physiol Biochem 65(4): 397-404.

Sandman G and Boger P (1986) Interference of dimethazone with formation of terpenoid compounds. Z Naturforsch 41(729-732).

Sandman G and Boger P (1987) Interconversion of prenyl pyrophosphates and subsequent reactions in the presence of FMC 57020. Z Naturforsch 42: 803-807.

Santos A, Ortiz de Solórzano C, Vaquero JJ, Pena JM, Malpica N and del Pozo F (1997) Evaluation of autofocus functions in molecular cytogenetic analysis. J Microsc 188(Pt 3): 264-272.

Sauret-Güeto S, Ramos-Valdivia A, Ibánez E, Boronat A and Rodríguez-Concepción M (2003) Identification of lethal mutations in *Escherichia coli* genes encoding enzymes of the methylerythritol phosphate pathway. Biochem Biophys Res Commun 307(2): 408-415.

Sauret-Güeto S, Uros EM, Ibánez E, Boronat A and Rodríguez-Concepcíon M (2006) A mutant pyruvate dehydrogenase E1 subunit allows survival of *Escherichia coli* strains defective in 1-deoxy-D-xylulose 5-phosphate synthase. FEBS Lett 580(3): 736-740.

Schaeffer A, Bronner R, Benveniste P and Schaller H (2001) The ratio of campesterol to sitosterol that modulates growth in *Arabidopsis* is controlled by STEROL METHYLTRANSFERASE 2;1. Plant J 25(6): 605-615.

Schafer WR and Rine J (1992) Protein prenylation: genes, enzymes, targets and functions. Annu Rev Genet 30: 209-237.

Schaller H (2003) The role of sterols in plant growth and development. Prog Lipid Res 42(3): 163-175.

Schaller H (2004) New aspects of sterol biosynthesis in growth and development of higher plants. Plant Physiol Biochem 42(6): 465-476.

Schaller H, Grausem B, Benveniste P, Chye ML, Tan CT, Song YH and Chua NH (1995) Expression of the Hevea brasiliensis (H.B.K.) Mull. Arg. 3-Hydroxy-3-Methylglutaryl-Coenzyme A Reductase 1 in Tobacco Results in Sterol Overproduction. Plant Physiol 109(3): 761-770.

Schlüter K, Walter RD, Bergmann B and Kurz T (2006) Arylmethyl substituted derivatives of Fosmidomycin: Synthesis and antimalarial activity. European Journal of Medicinal Chemistry 41(12): 1385-1397.

Schmitt F, Oakeley EJ and Jost JP (1997) Antibiotics induce genome-wide hypermethylation in cultured *Nicotiana tabacum* plants. J Biol Chem 272(3): 1534-1540.

Schubert D, Lechtenberg B, Forsbach A, Gils M, Bahadur S and Schmidt R (2004) Silencing in *Arabidopsis* T-DNA transformants: the predominant role of a gene-specific RNA sensing mechanism versus position effects. Plant Cell 16(10): 2561-2572.

Schuler I, Milon A, Nakatani Y, Ourisson G, Albrecht AM, Benveniste P and Hartman MA (1991) Differential effects of plant sterols on water permeability and on acyl chain ordering of soybean phosphatidylcholine bilayers. Proc Natl Acad Sci U S A 88(16): 6926-6930.

Schwab R, Ossowski S, Riester M, Warthmann N and Weigel D (2006) Highly specific gene silencing by artificial microRNAs in Arabidopsis. Plant Cell 18(5): 1121-1133.

Schwab W, Davidovich-Rikanati R and Lewinsohn E (2008) Biosynthesis of plant-derived flavor compounds. Plant J 54(4): 712-732.

Schwarz MK (1994) Terpen-Biosynthese in *Gingko biloba*: Eine überraschende Geschichte [PhD thesis]: ETH Zürich, Switzerland.

Schwarz MK and Arigoni D (1999) Ginkgolide biosynthesis. In: Barton SD, Nakanishi K, Meth-Cohn O, Cane DE, editors. Comprehensive natural products chemistry. Amsterdam: Elsevier. pp. 367-401.

Schwender J, Seemann M, Lichtenthaler HK and Rohmer M (1996) Biosynthesis of isoprenoids (carotenoids, sterols, prenyl side-chains of chlorophylls and plastoquinone) via a novel pyruvate/glyceraldehyde 3-phosphate non-mevalonate pathway in the green alga *Scenedesmus obliquus*. Biochem J 316 (Pt 1): 73-80.

Schwender J, Müller C, Zeidler J and Lichtenthaler HK (1999) Cloning and heterologous expression of a cDNA encoding 1-deoxy-D-xylulose-5-phosphate reductoisomerase of *Arabidopsis thaliana*. FEBS Lett 455(1-2): 140-144.

Schwender J, Zeidler J, Groner R, Müller C, Focke M, Braun S, Lichtenthaler FW and Lichtenthaler HK (1997) Incorporation of 1-deoxy-D-xylulose into isoprene and phytol by higher plants and algae. FEBS Lett 414(1): 129-134.

Scragg AH (1995) The problems associated with high biomass levels in plant cell suspensions. Plant Cell, Tissue and Organ Culture 42(2): 163-170.

Sebti SM (2005) Protein farnesylation: implications for normal physiology, malignant transformation, and cancer therapy. Cancer Cell 7(4): 297-300.

Seetang-Nun Y, Sharkey TD and Suvachittanont W (2008) Molecular cloning and characterization of two cDNAs encoding 1-deoxy-D-xylulose 5-phosphate reductoisomerase from *Hevea brasiliensis*. J Plant Physiol 165(9): 991-1002.

Shen W, Wei Y, Dauk M, Tan Y, Taylor DC, Selvaraj G and Zou J (2006) Involvement of a glycerol-3-phosphate dehydrogenase in modulating the NADH/NAD+ ratio provides evidence of a mitochondrial glycerol-3-phosphate shuttle in *Arabidopsis*. Plant Cell 18(2): 422-441.

Shigi Y (1989) Inhibition of bacterial isoprenoid synthesis by fosmidomycin, a phosphonic acid-containing antibiotic. J Antimicrob Chemother 24(2): 131-145.

Shimomura O, Johnson FH and Saiga Y (1962) Extraction, purification and properties of aequorin, a bioluminescent protein from the luminous hydromedusan, *Aequorea*. J Cell Comp Physiol 59: 223-239.

Shipton CA, Parmryd I, Swiezewska E, Andersson B and Dallner G (1995) Isoprenylation of plant proteins *in vivo*. Isoprenylated proteins are abundant in the mitochondria and nuclei of spinach. J Biol Chem 270(2): 566-572.

Shuttleworth A and Johnson SD (2009) A key role for floral scent in a wasp-pollination system in *Eucomis* (Hyacinthaceae). Ann Bot 103(5): 715-725.

Sigrist CJ, Cerutti L, Hulo N, Gattiker A, Falquet L, Pagni M, Bairoch A and Bucher P (2002) PROSITE: a documented database using patterns and profiles as motif descriptors. Brief Bioinform 3(3): 265-274.

Silber K, Heidler P, Kurz T and Klebe G (2005) AFMoC enhances predictivity of 3D QSAR: a case study with DOXP-reductoisomerase. J Med Chem 48(10): 3547-3563.

Silvius JR, Bhagatji P, Leventis R and Terrone D (2006) K-ras4B and prenylated proteins lacking "second signals" associate dynamically with cellular membranes. Mol Biol Cell 17(1): 192-202.

Simmen U and Gisi U (1995) Effects of seed treatment with SAN 789F, a homopropargylamine fungicide, on germination and contents of squalene and sterols of wheat seedlings Pestic Biochem Physiol 52: 25-32.

Simons K and Ikonen E (1997) Functional rafts in cell membranes. Nature 387(6633): 569-572.

Simons K and Toomre D (2000) Lipid rafts and signal transduction. Nat Rev Mol Cell Biol 1(1): 31-39.

Skorupinska-Tudek K, Poznanski J, Wojcik J, Bienkowski T, Szostkiewicz I, Zelman-Femiak M, Bajda A, Chojnacki T, Olszowska O, Grunler J, Meyer O, Rohmer M, Danikiewicz W and Swiezewska E (2008) Contribution of the mevalonate and methylerythritol phosphate pathways to the biosynthesis of dolichols in plants. J Biol Chem 283(30): 21024-21035.

Smith C and Eisenstein M (2005) Automated imaging: data as far as the eye can see (Technology Feature). Nature Methods 2: 547 - 555.

Smith MG, Jona G, Ptacek J, Devgan G, Zhu H, Zhu X and Snyder M (2005) Global analysis of protein function using protein microarrays. Mech Ageing Dev 126(1): 171-175.

Soltis DA, McMahon G, Caplan SL, Dudas DA, Chamberlin HA, Vattay A, Dottavio D, Rucker ML, Engstrom RG, Cornell-Kennon SA and Boettcher BR (1995) Expression, purification, and characterization of the human squalene synthase: use of yeast and baculoviral systems. Arch Biochem Biophys 316(2): 713-723.

Sorek N, Poraty L, Sternberg H, Bar E, Lewinsohn E and Yalovsky S (2007) Activation Status-Coupled Transient S Acylation Determines Membrane Partitioning of a Plant Rho-Related GTPase. Mol Cell Biol 27(6): 2144-2154.

Sorokin AV, Kim ER and Ovchinnikov LP (2007) Nucleocytoplasmic transport of proteins. Biochemistry (Mosc) 72(13): 1439-1457.

Sprenger GA, Schorken U, Wiegert T, Grolle S, de Graaf AA, Taylor SV, Begley TP, Bringer-Meyer S and Sahm H (1997) Identification of a thiamin-dependent synthase in *Escherichia coli* required for the formation of the 1-deoxy-D-xylulose 5-phosphate precursor to isoprenoids, thiamin, and pyridoxol. Proc Natl Acad Sci U S A 94(24): 12857-12862.

Stade K, Ford CS, Guthrie C and Weis K (1997) Exportin 1 (Crm1p) is an essential nuclear export factor. Cell 90(6): 1041-1050.

Starkuviene V and Pepperkok R (2007) The potential of high-content high-throughput microscopy in drug discovery. Br J Pharmacol 152(1): 62-71.

Starkuviene V, Pepperkok R and Erfle H (2007) Transfected cell microarrays: an efficient tool for high-throughput functional analysis. Expert Rev Proteomics 4(4): 479-489.

Steinbacher S, Kaiser J, Eisenreich W, Huber R, Bacher A and Rohdich F (2003) Structural basis of fosmidomycin action revealed by the complex with 2-*C*-methyl-D-erythritol 4-phosphate synthase (IspC). Implications for the catalytic mechanism and anti-malaria drug development. J Biol Chem 278(20): 18401-18407.

Stella VJ (2007) A case for prodrugs. In: Stella VJ, Borchardt RT, Hageman MJ, Oliyai R, Maag H et al., editors. Prodrugs: Challenges and Rewards. New York: Springer.

Stewart M, Baker RP, Bayliss R, Clayton L, Grant RP, Littlewood T and Matsuura Y (2001) Molecular mechanism of translocation through nuclear pore complexes during nuclear protein import. FEBS Lett 498(2-3): 145-149.

Suh KN, Kain KC and Keystone JS (2004) Malaria. CMAJ 170(11): 1693-1702.

Suzuki M and Muranaka T (2007) Molecular genetics of plant sterol backbone synthesis. Lipids 42(1): 47-54.

Suzuki M, Nakagawa S, Kamide Y, Kobayashi K, Ohyama K, Hashinokuchi H, Kiuchi R, Saito K, Muranaka T and Nagata N (2009) Complete blockage of the mevalonate pathway results in male gametophyte lethality. J Exp Bot 60(7): 2055-2064.

Suzuki N, Yamaguchi Y, Koizumi N and Sano H (2002) Functional characterization of a heavy metal binding protein CdI19 from *Arabidopsis*. Plant J 32(2): 165-173.

Swiezewskaa E and Danikiewiczb W (2005) Polyisoprenoids: Structure, biosynthesis and function. Prog Lipid Res 44: 235-258.

Takagi M, Kuzuyama T, Kaneda K, Watanabe H, Dairi T and Seto H (2000) Studies on the nonmevalonate pathway: formation of 2-*C*-methyl-D-erythritol 2,4-cyclodiposphate from 2-phospho-4-(cytidine 5'-diphospho)-2-*C*-methyl-D-erythritol. Tetrahedron Lett 41: 3395-3398.

Takahashi S and Koyama T (2006) Structure and function of cis-prenyl chain elongating enzymes. Chem Rec 6(4): 194-205.

Takahashi S, Kuzuyama T, Watanabe H and Seto H (1998) A 1-deoxy-D-xylulose 5-phosphate reductoisomerase catalyzing the formation of 2-*C*-methyl-D-erythritol 4-phosphate in an alternative nonmevalonate pathway for terpenoid biosynthesis. Proc Natl Acad Sci U S A 95(17): 9879-9884.

Takenoya M, Ohtaki A, Noguchi K, Endo K, Sasaki Y, Ohsawa K, Yajima S and Yohda M (2010) Crystal structure of 1-deoxy-D-xylulose 5-phosphate reductoisomerase from the hyperthermophile *Thermotoga maritima* for insights into the coordination of conformational changes and an inhibitor binding. J Struct Biol 170(3): 532-539.

Tamaru Y, Ui S, Murashima K, Kosugi A, Chan H, Doi RH and Liu B (2002) Formation of Protoplasts from Cultured Tobacco Cells and *Arabidopsis thaliana* by the Action of Cellulosomes and Pectate Lyase from *Clostridium cellulovorans*. Appl Environ Microbiol 68(5): 2614-2618.

Tambasco-Studart M, Titiz O, Raschle T, Forster G, Amrhein N and Fitzpatrick TB (2005) Vitamin B6 biosynthesis in higher plants. Proc Natl Acad Sci U S A 102(38): 13687-13692.

Tan EW and Rando RR (1992) Identification of an isoprenylated cysteine methyl ester hydrolase activity in bovine rod outer segment membranes. Biochemistry 31: 5572-5578.

Tanaka M, Bateman R, Rauh D, Vaisberg E, Ramachandani S, Zhang C, Hansen KC, Burlingame AL, Trautman JK, Shokat KM and Adams CL (2005) An unbiased cell morphology-based screen for new, biologically active small molecules. PLoS Biol 3(5): e128.

Ten Hoopen HJG, Vinke JL, Moreno PRH, Verpoorte R and Heijnen JJ (2002) Influence of temperature on growth and ajmalicine production by *Catharanthus roseus* suspension cultures. Enzyme Microb Technol 30: 56-65

TenBrook PL and Tjeerdema RS (2006) Biotransformation of clomazone in rice (*Oryza sativa*) and early watergrass (*Echinochloa oryzoides*). Pesticide Biochemistry and Physiology 85: 38-45.

Terjung S, Walter T, Seitz A, Neumann B, Pepperkok R and Ellenberg J (2010) High-throughput microscopy using live mammalian cells. Cold Spring Harb Protoc: pdb top84.

Terrier B, Courtois D, Henault N, Cuvier A, Bastin M, Aknin A, Dubreuil J and Petiard V (2007) Two new disposable bioreactors for plant cell culture: The wave and undertow bioreactor and the slug bubble bioreactor. Biotechnol Bioeng 96(5): 914-923.

Thai L, Rush JS, Maul JE, Devarenne T, Rodgers DL, Chappell J and Waechter CJ (1999) Farnesol is utilized for isoprenoid biosynthesis in plant cells via farnesyl pyrophosphate formed by successive monophosphorylation reactions. Proc Natl Acad Sci U S A 96(23): 13080-13085.

Thayer AM (2005) Fighting Malaria. Chem Eng News 83: 69-82.

Thelin A, Peterson E, Hutson JL, McCarthy AD, Ericsson J and Dallner G (1994) Effect of squalestatin 1 on the biosynthesis of the mevalonate pathway lipids. Biochim Biophys Acta 1215(3): 245-249.

Tholl D (2006) Terpene synthases and the regulation, diversity and biological roles of terpene metabolism. Curr Opin Plant Biol 9(3): 297-304.

Tice RR (1988) The cytogenetic evaluation of in vivo genotoxic and cytotoxic activity using rodent somatic cells. Cell Biol Toxicol 4(4): 475-486.

Tinland B, Koukolikova-Nicola Z, Hall MN and Hohn B (1992) The T-DNA-linked VirD2 protein contains two distinct functional nuclear localization signals. Proc Natl Acad Sci U S A 89(16): 7442-7446.

Tovar-Méndez A, Miernyk JA and Randall DD (2003) Regulation of pyruvate dehydrogenase complex activity in plant cells. Eur J Biochem 270(6): 1043-1049.

Trias J, Jarlier V and Benz R (1992) Porins in the cell wall of mycobacteria. Science 258(5087): 1479-1481.

Tsien RY (1998) The green fluorescent protein. Annu Rev Biochem 67: 509-544.

Tu Z, He G, Li KX, Chen MJ, Chang J, Chen L, Yao K, Liu DP, Ye H, Shi J and Wu X (2005) An improved system for competent cell preparation and high efficiency plasmid transformation using different *Escherichia coli* strains. Electronic Journal of Biotechnology 8 (1)(April 15).

Uetz P and Hughes RE (2000) Systematic and large-scale two-hybrid screens. Curr Opin Microbiol 3(3): 303-308.

Van der Fits L, Deakin EA, Hoge JH and Memelink J (2000) The ternary transformation system: constitutive *virG* on a compatible plasmid dramatically increases *Agrobacterium*-mediated plant transformation. Plant Mol Biol 43(4): 495-502.

Van Dessel GA, De Busser HM and Lagrou AR (2001) On the occurence of multiple isoprenylated cysteine methyl ester hydrolase activities in bovine adrenal medulla. Biochem Biophys res Commun 284: 50-56.

van Gisbergen PA, Esseling-Ozdoba A and Vos JW (2008) Microinjecting FM4-64 validates it as a marker of the endocytic pathway in plants. J Microsc 231(2): 284-290.

Van Larebeke N, Engler G, Holsters M, Van den Elsacker S, Zaenen I, Schilperoort RA and Schell J (1974) Large plasmid in *Agrobacterium tumefaciens* essential for crown gall-inducing ability. Nature 252(5479): 169-170.

van Leeuwen W, Ruttink T, Borst-Vrenssen AW, van der Plas LH and van der Krol AR (2001) Characterization of position-induced spatial and temporal regulation of transgene promoter activity in plants. J Exp Bot 52(358): 949-959.

Vasudevan A, Qian Y, Vogt A, Blaskovich MA, Ohkanda J, Sebti SM and Hamilton AD (1999) Potent, highly selective, and non-thiol inhibitors of protein geranylgeranyltransferase-I. J Med Chem 42(8): 1333-1340.

Vaucheret H, Palauqui JC, Elmayan T and Moffatt B (1995) Molecular and genetic analysis of nitrite reductase co-suppression in transgenic tobacco plants. Mol Gen Genet 248(3): 311-317.

Veillard NR and Mach F (2002) Statins: the new aspirin? Cell Mol Life Sci 59(11): 1771-1786.

Vencill WK (2002) Herbicide Handbook. Lawrence, KS: Weed Science Society of America.

Vencill WK, Hatzios KK and Wilson HP (1990) Absorption, translocation and metabolism of ^{14}C-clomazone in soybean (*Glycine max*) and three *Amaranthus* weed species. J Plant Growth Regul 9: 127-132.

Verkhusha VV and Lukyanov KA (2004) The molecular properties and applications of Anthozoa fluorescent proteins and chromoproteins. Nat Biotechnol 22(3): 289-296.

Verpoorte R and Memelink J (2002) Engineering secondary metabolite production in plants. Curr Opin Biotechnol 13(2): 181-187.

Vögeli U and Chappell J (1988) Induction of sesquiterpene cyclase and suppression of squalene synthetase activities in plant cell cultures treated with fungal elicitor. Plant Physiol 88(4): 1291-1296.

Vollmar F, Hacker C, Zahedi RP, Sickmann A, Ewald A, Scheer U and Dabauvalle MC (2009) Assembly of nuclear pore complexes mediated by major vault protein. J Cell Sci 122(Pt 6): 780-786.

Voynova NE, Rios SE and Miziorko HM (2004) *Staphylococcus aureus* mevalonate kinase: isolation and characterization of an enzyme of the isoprenoid biosynthetic pathway. J Bacteriol 186(1): 61-67.

Wallach O (1914) Terpene und Campher: Zusammenfassung eigener Untersuchungen auf dem Gebiet der alicyclischen Kohlenstoffverbindungen. Leipzig: Veit.

Walter MH, Fester T and Strack D (2000) Arbuscular mycorrhizal fungi induce the non-mevalonate methylerythritol phosphate pathway of isoprenoid biosynthesis correlated with accumulation of the 'yellow pigment' and other apocarotenoids. Plant J 21(6): 571-578.

Walter MH, Hans J and Strack D (2002) Two distantly related genes encoding 1-deoxy-D-xylulose 5-phosphate synthases: differential regulation in shoots and apocarotenoid-accumulating mycorrhizal roots. Plant J 31(3): 243-254.

Wang G and Deschenes RJ (2006) Plasma membrane localization of Ras requires class C Vps proteins and functional mitochondria in *Saccharomyces cerevisiae*. Mol Cell Biol 26(8): 3243-3255.

Warfield TR, Carlson DB, Bellmann SK and Guscar HL (1985) Weed control in soybeans using command. Weed Sci Abstr 25: 105.

Watson P, Jones AT and Stephens DJ (2005) Intracellular trafficking pathways and drug delivery: fluorescence imaging of living and fixed cells. Adv Drug Deliv Rev 57(1): 43-61.

Weimer MR, Balke NE and Buhler DD (1992) Herbicide clomazone does not inhibit *in vitro* geranylgeranyl synthesis from mevalonate. Plant Physiol 98(2): 427-432.

Wentzinger LF, Bach TJ and Hartmann MA (2002) Inhibition of squalene synthase and squalene epoxidase in tobacco cells triggers an up-regulation of 3-hydroxy-3-methylglutaryl coenzyme a reductase. Plant Physiol 130(1): 334-346.

WHO WHO (2009) Global tuberculosis control - epidemiology, strategy, financing: WHO Report 2009.

Whyte DB, Kirschmeier P, Hockenberry TN, Nunez-Oliva I, James L, Catino JJ, Bishop WR and Pai JK (1997) K- and N-Ras are geranylgeranylated in cells treated with farnesyl protein transferase inhibitors. J Biol Chem 272(22): 14459-14464.

Widholm JM (1972) The use of fluorescein diacetate and phenosafranine for determining viability of cultured plant cells. Stain Technol 47(4): 189-194.

Wiesner J, Borrmann S and Jomaa H (2003) Fosmidomycin for the treatment of malaria. Parasitol Res 90 Suppl 2: S71-76.

Wilding EI, Brown JR, Bryant AP, Chalker AF, Holmes DJ, Ingraham KA, Iordanescu S, So CY, Rosenberg M and Gwynn MN (2000) Identification, evolution, and essentiality of the mevalonate pathway for isopentenyl diphosphate biosynthesis in gram-positive cocci. J Bacteriol 182(15): 4319-4327.

Wille A, Zimmermann P, Vranova E, Furholz A, Laule O, Bleuler S, Hennig L, Prelic A, von Rohr P, Thiele L, Zitzler E, Gruissem W and Buhlmann P (2004) Sparse graphical Gaussian modeling of the isoprenoid gene network in *Arabidopsis thaliana*. Genome Biol 5(11): R92.

Wilson CJ, Si Y, Thompsons CM, Smellie A, Ashwell MA, Liu JF, Ye P, Yohannes D and Ng SC (2006) Identification of a small molecule that induces mitotic arrest using a simplified high-content screening assay and data analysis method. J Biomol Screen 11(1): 21-28.

Wilson RJ, Denny PW, Preiser PR, Rangachari K, Roberts K, Roy A, Whyte A, Strath M, Moore DJ, Moore PW and Williamson DH (1996) Complete gene map of the plastid-like DNA of the malaria parasite *Plasmodium falciparum*. J Mol Biol 261(2): 155-172.

Winter-Vann AM, Baron RA, Wong W, dela Cruz J, York JD, Gooden DM, Bergo MO, Young SG, Toone EJ and Casey PJ (2005) A small-molecule inhibitor of isoprenylcysteine carboxyl methyltransferase with antitumor activity in cancer cells. Proc Natl Acad Sci U S A 102(12): 4336-4341.

Withers ST, Gottlieb SS, Lieu B, Newman JD and Keasling JD (2007) Identification of isopentenol biosynthetic genes from *Bacillus subtilis* by a screening method based on isoprenoid precursor toxicity. Appl Environ Microbiol 73(19): 6277-6283.

Wolfertz M, Sharkey TD, Boland W and Kuhnemann F (2004) Rapid regulation of the methylerythritol 4-phosphate pathway during isoprene synthesis. Plant Physiol 135(4): 1939-1945.

Wouters FS, Verveer PJ and Bastiaens PI (2001) Imaging biochemistry inside cells. Trends Cell Biol 11(5): 203-211.

Woyengo TA, Ramprasath VR and Jones PJ (2009) Anticancer effects of phytosterols. Eur J Clin Nutr 63(7): 813-820.

Wu CC, Reilly JF, Young WG, Morrison JH and Bloom FE (2004) High-throughput morphometric analysis of individual neurons. Cereb Cortex 14(5): 543-554.

Wyatt RE, Ainley WM, Nagao RT, Conner TW and Key JL (1993) Expression of the *Arabidopsis AtAux2-11* auxin-responsive gene in transgenic plants. Plant Mol Biol 22 731-749.

Xiang S, Usunow G, Lange G, Busch M and Tong L (2007) Crystal structure of 1-deoxy-D-xylulose 5-phosphate synthase, a crucial enzyme for isoprenoids biosynthesis. J Biol Chem 282(4): 2676-2682.

Xiao C, Xin H, Dong A, Sun C and Cao K (1999) A novel calmodulin-like protein gene in rice which has an unusual prolonged C-terminal sequence carrying a putative prenylation site. DNA Res 6(3): 179-181.

Xiao CY and Jans DA (1998) An engineered site for protein kinase C flanking the SV40 large T-antigen NLS confers phorbol ester-inducible nuclear import. FEBS Lett 436(3): 313-317.

Yajima S, Nonaka T, Kuzuyama T, Seto H and Ohsawa K (2002) Crystal structure of 1-deoxy-D-xylulose 5-phosphate reductoisomerase complexed with cofactors: implications of a flexible loop movement upon substrate binding. J Biochem 131(3): 313-317.

Yajima S, Hara K, Sanders JM, Yin F, Ohsawa K, Wiesner J, Jomaa H and Oldfield E (2004) Crystallographic structures of two bisphosphonate:1-deoxyxylulose-5-phosphate reductoisomerase complexes. J Am Chem Soc 126(35): 10824-10825.

Yalovsky S, Loraine AE and Gruissem W (1996) Specific prenylation of tomato Rab proteins by geranylgeranyl type-II transferase requires a conserved cysteine-cysteine motif. Plant Physiol 110: 1349-1359.

Yalovsky S, Rodríguez-Concepción M and Gruissem W (1999) Lipid modification of proteins-slipping in and out of membranes. Trends Plant Sci 4: 429-438.

Yalovsky S, Kulukian A, Rodríguez-Concepción M, Young CA and Gruissem W (2000) Functional requirement of plant farnesyltransferase during development in *Arabidopsis*. Plant Cell 12: 1267-1278.

Yalovsky S, Trueblood CE, Callan KL, Narita JO, Jenkins SM, Rine J and Gruissem W (1997) Plant farnesyltransferase can restore yeast Ras signaling and mating. Mol Cell Biol 17(4): 1986-1994.

Yang Z, Cramer CL and Watson JC (1993) Protein farnesyltransferase in plants. Molecular cloning and expression of a homolog of the beta subunit from the garden pea. Plant Physiol 101: 667-674.

Yasuor H, TenBrook PL, Tjeerdema RS and Fischer AJ (2008) Responses to clomazone and 5-ketoclomazone by *Echinochloa phyllopogon* resistant to multiple herbicides in Californian rice fields. Pest Manag Sci 64(10): 1031-1039.

Yasuor H, Zou W, Tolstikov VV, Tjeerdema RS and Fischer AJ (2010) Differential oxidative metabolism and 5-ketoclomazone accumulation are involved in *Echinochloa phyllopogon* resistance to clomazone. Plant Physiol 153(1): 319-326.

Yates PJ, Haughan PA, Lenton JR and L.J. G (1991) Effects of terbinafine on growth, squalene and steryl ester content of celery cell suspension culture. Pestic Biochem Phys 40: 221-226.

Yin X and Proteau PJ (2003) Characterization of native and histidine-tagged deoxyxylulose 5-phosphate reductoisomerase from the cyanobacterium *Synechocystis sp.* PCC6803. Biochim Biophys Acta 1652(1): 75-81.

Yokota A and Sasajima K (1984) Formation of 1-deoxy-D-Threo-pentulose and 1-deoxy-L-threo pentulose by cell free extracts of microorganisms. Agric Biol Chem 48: 149-158.

Yokota A and Sasajima K (1986) Formation of 1-deoxy-ketose by pyruvate dehydrogenase and acetoin dehydrogenase. Agric Biol Chem 50: 2517-2524.

Young SG, Ambroziak P, Kim E and Clarke S (2000) Postprenylation protein processing: CXXX (CaaX) endoproteases and isoprenylcysteine carboxyl methyltransferase. In: Tamanoi F, Sigman DS, editors. Protein Lipidation. San Diego: Academic Press. pp. 153-213.

Yuan YJ, Ge ZQ, Li JC, Wu JC, Hu ZD and (2002) Differentiation of apoptotic and necrotic cells in suspension cultures of *Taxus cuspidata* by the combined use of fluorescent dying and histochemical staining methods. Biotechnol Lett 24: 71-76.

Yun MS, Yogo Y, Miura R, Yasamue Y and Fischer AJ (2005) Cytochrome P-450 monooxygenase activity in herbicide-resistant and -susceptible late watergrass (*Echinochloa phyllopogon*). Pesticide Biochemistry and Physiology 83: 107-114.

Zeidler J, Lichtenthaler HK, May HU and Lichtenthaler FW (1997) Is isoprene emitted by plants synthesized via the novel isopentenyl pyrophosphate pathway ? Z Naturforsch Teil C 53: 15-23.

Zeidler J, Schwender J, Mueller C and Lichtenthaler HK (2000) The non-mevalonate isoprenoid biosynthesis of plants as a test system for drugs against malaria and pathogenic bacteria. Biochem Soc Trans 28(6): 796-798.

Zeidler J, Schwender J, Müller C, Wiesner J, Weidemeyer C, Beck E, Jomaa H and Lichtenthaler HK (1998) Inhibition of the non-mevalonate 1-deoxy-D-xylulose-5-phosphate pathway of plant isoprenoid biosynthesis by fosmidomycin. Z Naturforsch Teil C 53: 980-986.

Zhang FL and Casey PJ (1996) Protein prenylation: molecular mechanisms and functional consequences. Annu Rev Biochem 65: 241-269.

Zhang H, Ohyama K, Boudet J, Chen Z, Yang J, Zhang M, Muranaka T, Maurel C, Zhu JK and Gong Z (2008) Dolichol biosynthesis and its effects on the unfolded protein response and abiotic stress resistance in *Arabidopsis*. Plant Cell 20(7): 1879-1898.

Zhang J, Campbell RE, Ting AY and Tsien RY (2002) Creating new fluorescent probes for cell biology. Nat Rev Mol Cell Biol 3(12): 906-918.

Zhang L, Tschantz WR and Casey PJ (1997) Isolation and characterization of a prenylcysteine lyase from bovine brain. J Biol Chem 272(37): 23354-23359.

Zheng W (2006) Quantitative HTS. Screening 7: 14-16.

Zhou D and White RH (1991) Early steps of isoprenoid biosynthesis in *Escherichia coli*. Biochem J 273 (Pt 3): 627-634.

Zhu JK, Bressan RA and Hasegawa PM (1993) Isoprenylation of the plant molecular chaperone ANJ1 facilitates membrane association and function at high temperature. Proc Natl Acad Sci U S A 90: 8557-8561.

Zhu XF, Suzuki K, Saito T, Okada K, Tanaka K, Nakagawa T, Matsuda H and Kawamukai M (1997) Geranylgeranyl pyrophosphate synthase encoded by the newly isolated gene *GGPS6* from *Arabidopsis thaliana* is localized in mitochondria. Plant Mol Biol 35(3): 331-341.

Zidovetzki R and Levitan I (2007) Use of cyclodextrins to manipulate plasma membrane cholesterol content: evidence, misconceptions and control strategies. Biochim Biophys Acta 1768(6): 1311-1324.

Zignol M, Hosseini MS, Wright A, Weezenbeek CL, Nunn P, Watt CJ, Williams BG and Dye C (2006) Global incidence of multidrug-resistant tuberculosis. J Infect Dis 194(4): 479-485.

Zimmermann P, Hirsch-Hoffmann M, Hennig L and Gruissem W (2004) GENEVESTIGATOR. *Arabidopsis* microarray database and analysis toolbox. Plant Physiol 136(1): 2621-2632.

Zimmermann T (2005) Spectral imaging and linear unmixing in light microscopy.; Rietdorf J, editor. Heidelberg: Springer.

Zimmermann T, Rietdorf J and Pepperkok R (2003) Spectral imaging and its applications in live cell microscopy. FEBS Lett 546(1): 87-92.

Zuo J and Chua NH (2000) Chemical-inducible systems for regulated expression of plant genes. Curr Opin Biotechnol 11(2): 146-151.

Zuo J, Niu QW and Chua NH (2000) Technical advance: An estrogen receptor-based transactivator XVE mediates highly inducible gene expression in transgenic plants. Plant J 24(2): 265-273.

Zupan JR and Zambryski P (1995) Transfer of T-DNA from *Agrobacterium* to the plant cell. Plant Physiol 107(4): 1041-1047.

Acknowledgements

In the first place, I would like to thank Prof. Dr. Thomas J. Bach for giving me the opportunity to work in the highly interesting field of isoprenoid research and for his continous support throughout my thesis.

Besides my advisor, I would like to thank the rest of my thesis committee: Prof. Francis Karst, PD Dr. Michael H. Walter, Dr. Benoît St.-Pierre, Prof. Rüdiger Hell and Prof. Michel Rohmer for their interest in my work and their readiness to read and evaluate my PhD thesis, as well as their insightful comments and hard questions.

I am grateful to all the members of the Bach and Rohmer groups with whom I interacted during my thesis, who helped and supported my work, especially Dr. Denis Tritsch and Mme. Magalie Parisse.

It is also noteworthy to mention those members of Hubert Schaller's and Danièle Werck's groups who helped me in different situations either with their actions or good advice. Thank you very much.

I also greatly appreciate the financial support of the Région Alsace.

I would also like to thank Prof. Jacques-Henry Weil for always having an open door, and for welcoming me with a smile on his face for a little chat in his office. It was always a great pleasure talking to him about science and topics beyond.

Furthermore, I would like to thank those employees of the IBMP who managed the facilities I used during my research and contributed significantly to the success of my thesis.

My special thanks belong to Dr. Marie-Andrée Hartmann for helping me get through difficult times, and for all the emotional support, entertainment, and caring she provided. I cannot thank her and her husband John enough for their unselfish assistance in correcting the grammar in this thesis.

I am also very grateful for my pleasant and helpful colleagues (and friends) Dr. Elisabet Gas and Dr. Dimitri Heintz who are responsible for some of the best times I had during my stay in Strasbourg, and who provided a stimulating environment to learn and work in. I will never forget our trip to Japan.

I wish to thank my family and close friends for always believing in me, as well as for their encouragement and ongoing support, without which I could not have started a career in science.

Last but by no means least I would like to thank my girlfriend Nadine for her constant support, love and patience.

6 Summary

In our laboratory, we have recently established an *in vivo* visualization system for the geranylgeranylation of proteins, based on a stably transformed tobacco BY-2 cell line (Gerber et al., 2009). This line expresses a dexamethasone-inducible GFP fused to the prenylable, C-terminal basic domain of the rice calmodulin CaM61, which naturally bears a CaaL geranylgeranylation motif (GFP-BD-CVIL). The use of pathway-specific inhibitors revealed that inhibition of the MEP pathway as well as inhibition of geranylgeranyltransferase type 1 (PGGT-1) shifted the localization of the GFP-BD-CVIL protein from the membrane to the nucleus/nucleolus. In contrast, inhibiting the MVA pathway did not affect the localization. Chemical complementation assays with pathway-specific intermediates further confirmed that the geranylgeranyl diphosphate precursor for the isoprenylation of the GFP-DB-CVIL fusion protein is predominantly delivered by the MEP pathway, thus providing us with a versatile bioassay that allows to screen for inhibitors of the MEP pathway, which could have significance for the development of pharmaceutical compounds (antibiotics, antimalarial drugs...) and bleaching herbicides.
During the present work, this test system has succesfully been used to check novel herbicide and drugs, and to study the impact of inhibitors of sterol biosynthesis and post prenylation reactions on the localization of the geranylgeranylable fusion protein.
In order to optimize this visualization system from a more qualitative assay to a statistically trustable high-throughput screening system, the existing GFP-BD-CVIL cell line was further transformed with an estradiol-inducible vector, driving the expression of a RFP protein, C-terminally fused to a NLS (nuclear localisation signal). This new strategy allows quantifying the total number of viable cells *versus* the number of inhibited cells after various treatments. Coupled to a semi-automatic counting system (based on the freely available image processing software ImageJ), it also reduces both the time of image analysis and the risk of user-generated bias to a minimum. Moreover, there is no cross-induction of gene expression by dexamethasone (GFP-BD-CVIL) and estradiol (NLS-RFP), an important prerequisite for studies beyond attempts of establishing such a high-throughput test system. Finally, the assay was adapted to the use of 96-well glass-bottom plates and provided us with an inexpensive, visual system to screen for potential inhibitors of the MEP pathway.

Dans notre laboratoire, nous avons récemment mis au point un système permettant de visualiser la géranylgéranylation des protéines *in vivo*, en utilisant une lignée cellulaire de tabac BY-2 transformée (Gerber et al., 2009). Cette lignée exprime une protéine GFP inductible par la déxaméthasone et fusionnée en C-terminal avec le domaine basique de la calmoduline de riz CaM61, qui porte un motif CaaL de géranylgéranylation (GFP-BD-CVIL). L'inhibition de la voie du MEP et de la géranylgéranyl-transférase de type 1 (PGGT-1) par des inhibiteurs spécifiques se traduit par une délocalisation de la protéine GFP-BD-CVIL de la membrane plasmique au noyau et nucléole. Par contre, l'inhibition de la voie du MVA n'affecte pas la localisation de la protéine. Des essais de complémentation chimique avec des intermédiaires biosynthétiques ont confirmé que les précurseurs du GGPP, pour l'isoprénylation de la protéine de fusion, sont fournis essentiellement par la voie du MEP, nous permettant ainsi de disposer d'un test biologique pour le criblage d'inhibiteurs spécifiques de cette voie, susceptibles d'avoir des applications en pharmacie et en agriculture, tels que des antibiotiques, des agents anti-paludisme ou des herbicides.
Dans la présente étude, ce test a été utilisé avec succès pour examiner l'efficacité de nouveaux herbicides et étudier les effets d'inbibiteurs de la biosynthèse des stérols et des réactions de post-prénylation sur la localisation de la protéine de fusion géranylgéranylable.
Dans le but d'optimiser ce système de visualisation et le transformer en un système de criblage fiable, la lignée cellulaire exprimant la protéine GFP-BD-CVIL a été retransformée avec un vecteur inductible par l'estradiol, contrôlant l'expression d'une protéine RFP fusionnée, en C-terminal avec une séquence NLS ("*nuclear localization signal*"). Cette nouvelle stratégie permet de quantifier le nombre total de cellules viables dans une population de cellules traitée par différents inhibiteurs. Couplée à un système semi-automatique de comptage (basé sur le logiciel ImageJ), elle réduit à la fois le temps d'analyse et le risque de biais générés par l'utilisateur. De plus, il n'y a aucune induction croisée de l'expression des gènes par la déxaméthasone (GFP-BD-CVIL) et l'estradiol (RFP-NLS), une condition préalable indispensable pour l'utilisation ultérieure de ce test à plus grande échelle. Finalement, le test a été adapté pour l'utilisation de plaques de verre à 96 puits, ce qui permet d'établir un système de criblage à grande échelle et bon marché, pour la recherche d'inhibiteurs potentiels de la voie du MEP.